ALFAKHOURI, LARA, Ph. D. Design, Synthesis and Biological Evaluation of GPR55 Agonists and Resorcylic Acid Lactone-based Analogues as TAK-1 Inhibitors. (2015) Directed by Dr. Mitchell Croatt. 189 pp.

GPR55 is a potential target for treating various illnesses. Inhibition of this membrane-bound G protein-coupled receptor may potentially alleviate inflammatory and neuropathic pain and treat osteoporosis and cancer. Radiolabelling of a potent and selective ligand will aid in establishing the physiological roles and pharmacology of the receptor. High throughput screening presented a hit that was used to design, based on a constructed homology model, and synthesize various analogues. The structure activity relationships inferred from the tested analogues will help in refinement of the homology model and design future analogues.

(5*Z*)-7-Oxozeanol and related analogues were isolated and screened to explore their activity as TAK-1 inhibitors. Seven analogues were synthesized and eight natural products isolated that examined the role that different areas of the molecule contribute to TAK-1 inhibition. A novel nonaromatic difluoro-derivative was synthesized that had similar potency compared to the lead. This is the first example of a nonaromatic compound in this class to have TAK-1 inhibition. Covalent docking for the isolated and synthesized analogues was carried out and found a strong correlation between the observed activities and the calculated binding.

DESIGN, SYNTHESIS AND BIOLOGICAL EVALUATION OF GPR55 AGONISTS AND RESORCYLIC ACID LACTONE-BASED ANALOGUES AS TAK-1 INHIBITORS

by

Lara Alfakhouri

A Dissertation Submitted to
the Faculty of the Graduate School at
The University of North Carolina at Greensboro
in Partial Fulfillment
of the Requirements for the Degree
Doctor of Philosophy

Greensboro
2015

Approved by

_____

Committee Chair

APPROVAL PAGE

This dissertation, written by Lara Alfakhouri, has been approved by the following committee of the Faculty of The Graduate School at the University of North Carolina at Greensboro

Committee Chair _____

Mitchell Croatt

Committee Members _____

Patricia Reggio

_____

Nicholas Oberlies

_____

Kimberly Petersen

_____

Date of Acceptance by Committee

_____

Date of Final Oral Examination

TABLE OF CONTENTS

Page

LIST OF ABBREVIATIONS

Å	angstrom
δ	chemical shift in parts per million downfield from tetramethylsilane
°C	degrees Celsius
µ	micro
Ar	aromatic
aq	aqueous
calcd	calculated
COSY	correlation spectroscopy
DMAP	4-(dimethylamino)pyridine
DMF	*N*,*N*-dimethylformamide
DMSO	dimethyl sulfoxide
equiv.	equivalent
ESI	electrospray ionization
EtOAc	ethyl acetate
GPCR	G protein-coupled receptor
HF	Hartree–Fock
HMBC	heteronuclear multiple bond correlation
HPLC	high performance liquid chromatography
HRMS	high-resolution mass spectrometry
HSQC	heteronuclear single quantum correlation

Hz	hertz
L	liter
M^+	parent molecular ion
m/z	mass-to-charge ratio
MeOH	methanol
mL	milliliter
mmol	millimole
mol	mole
NBS	*N*-bromosuccinimide
NMR	nuclear magnetic resonance
Ph	phenyl
ppm	part(s) per million
rt	room temperature
SAR	structure–activity relationship
tert	tertiary
TAK-1	transforming growth factor-beta-activated kinase 1
THF	tetrahydrofuran
TLC	thin layer chromatography
UV	ultraviolet
v/v	volume per unit volume
Vis	visible

Selectfluor®	1-chloromethyl-4-fluoro-1,4-diazoniabicyclo[2.2.2]octane bis(tetrafluoroborate)

CHAPTER I

DESIGN, SYNTHESIS AND BIOLOGICAL EVALUATION OF GPR55 AGONISTS

1.1 Introduction

GPR55 is a G protein-coupled receptor that has been recently deorphanized. The membrane-bound receptor is highly expressed in the brain, particularly in striatum.[1] It is also found on cell surfaces of other tissues and cells such as bone marrow,[2] neutrophils[3] and spleen.[4] It has been established so far that GPR55 is a potential target for treating pain,[5] osteoporosis[2] and cancer.[6]

In adjuvant-induced inflammation and partial nerve ligation pain models, GPR55 knockout mice developed neither inflammatory nor neuropathic mechanical hyperplasia. Such findings present this receptor as a potential target for treating both inflammatory and neuropathic pain.[5] The knockout mice also revealed a role of GPR55 in regulating osteoclasts' number and function based on the finding that the number of inactive osteoclasts was higher compared to wild type mice.[2] A recent study revealed high expression of GPR55 in myenteric colonic neurons and the involvement of the receptor in colonic motility, thus adding to its already established medical applications, the potential of treating illnesses linked to colon motility.[7] Furthermore, Lysophosphatidyl inositol (LPI, **1.1**, Figure 1.1), which is the endogenous ligand of GPR55, was demonstrated to induce wound healing of human lung endothelial cells and inhibit platelet aggregation.[8]

Figure 1.1 Chemical structures of LPI (**1.1**), CID1792197 (**1.2**), CID1172084 (**1.3**) and CID2440433 (**1.4**).

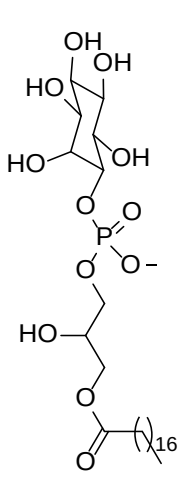

LPI, (**1.1)**

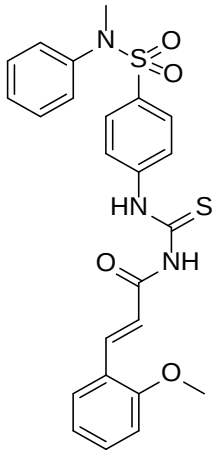

CID1792197, (**1.2)**
EC_{50}: 0.11 μM

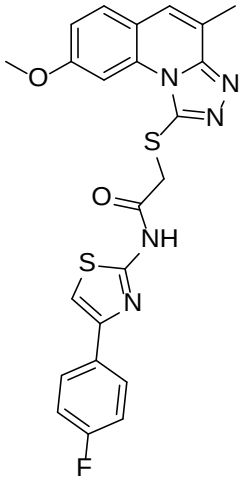

CID1172084, (**1.3)**
EC_{50}: 0.16 μM

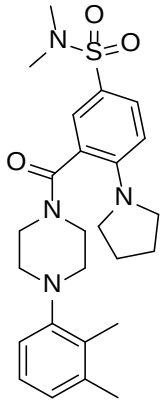

CID2440433, (**1.4)**
EC_{50}: 0.26 μM

The role of GPR55 in cancer proliferation has been recently well-established to be proliferative rather than anti-proliferative.6 Not only it was detected in various cancer cell lines such as breast, brain, skin6, and prostate9 but also discovered in a number of clinical isolates from cancer patients.6 Furthermore, it has been shown that GPR55 activation stimulates angiogenesis10 and migration9 which explains the correlation of GPR55 expression with cancer aggressiveness. The preceding findings present GPR55 as an intriguing target for singular treatment of cancer. Its sole use will minimize the side effects accompanying the trivial adjuvant therapies used, which necessitates halting cancer proliferation, angiogenesis and migration combined for successful cancer eradication.

Initial *in vitro* screening classified GPR55 as a cannabinoid receptor due to similarities with cannabinoid receptors CB_1 and CB_2.[11] Yet the variant cannabinoid

ligands exert either different or mainly opposite pharmacology when bound to GPR55. AM251 (**1.5**) (Figure 1.2) for instance, which is a CB_1 antagonist, strongly activates GPR55.[12] Another example is the CB_1 and CB_2 agonist CP55940[13] (**1.6**) (Figure 1.2) which acts as an antagonist when bound to GPR55. In addition, the results obtained for the same ligand tested may vary depending on the assay employed and the cell type. For example, Rimonabant (**1.7**) (Figure 1.2) is reported as an agonist[14] and an antagonist[15] for GPR55 using β Arrestin2-GFP assay and ERK1/2 kinase assay, respectively. The unpredicted activity for some of the cannabinoid ligands and the unexplainable dual activity can be better understood with radiolabeling. Binding assays for a radiolabeled potent ligand will provide a proof of pairing and affinity of the ligand with the artificially expressed receptor in cell lines and specify the activity of antagonists.[16] Also, these assays will help in defining a concise classification and understanding of the physiological and pharmacological roles of this receptor.

Figure 1.2 Chemical Structures of AM251 (**1.5**), CP55940 (**1.6**), Rimonabant (**1.7**).

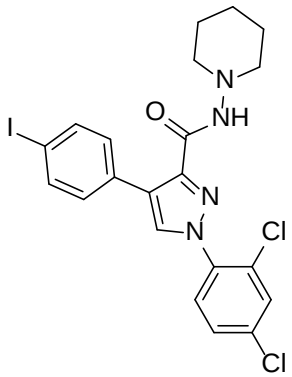

AM251, (**1.5**)

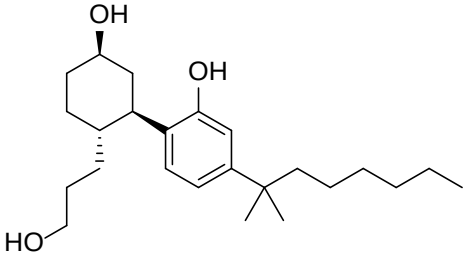

CP55940, (**1.6**)

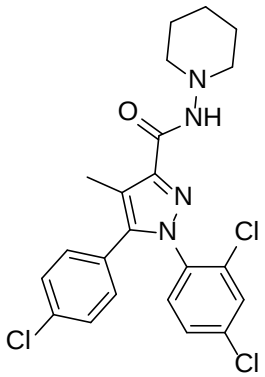

Rimonabant (**1.7**)

1.2 Results and Discussion

LPI (**1.1**) (Figure 1.1) is not the best candidate to be labeled for studying the receptor due to its lack of selectivity to GPR55. The need for such a selective and potent ligand prompted high throughput screening which was conducted by the Sanford-Burnham screening center. Out of approximately 290,000 different compounds tested, three chemically distinct compounds, namely CID1792197 (**1.2**), CID1172084 (**1.3**), and CID2440433 (**1.4**) (Figure 1.1), were identified as potent agonists of GPR55 with EC_{50}'s of 0.11, 0.16 and 0.26 μM, respectively. An added value to the moderate potency of these ligands is their selectivity for GPR55 over other cannabinoid receptors, > 30 μM activity of CB_1, CB_2 and the closely related atypical cannabinoid receptor GPR35, which renders them as appropriate leads to develop probes for studying GPR55.

GPR55 is among the majority of G-protein coupled receptors waiting to be crystallized. Attempting to explain the experimental pharmacological behavior of a receptor that has not been crystallized is achievable via homology modeling. The homology model of GPR55 was designed and constructed using the Beta-2 adrenergic receptor as a template. Contrary to class A GPCRs, where the binding pocket is oriented horizontally,[17] The GPR55 active site, R*, model shows the binding pocket as a deep vertical channel reaching down to residue N7.46 which constitutes the end of the binding pocket. Yet, the horizontal character of the space near the EC loops was retained. When compounds **1.1**-**1.4** were docked in the binding pocket, the primary interactions were between the most negative electrostatic region and residue K2.60 which is the only charged residue in the proposed GPR55 binding site (Figure 1.3). Indeed, K2.60A

mutation led to no detected response upon ligand binding indicating its importance in GPR55 activation and signal transduction.

Figure 1.3 LPI **1.1**; CID1792197 **1.2**, CID1172084 **1.3**, and CID2440433 **1.4** - GPR55 R* complexes.

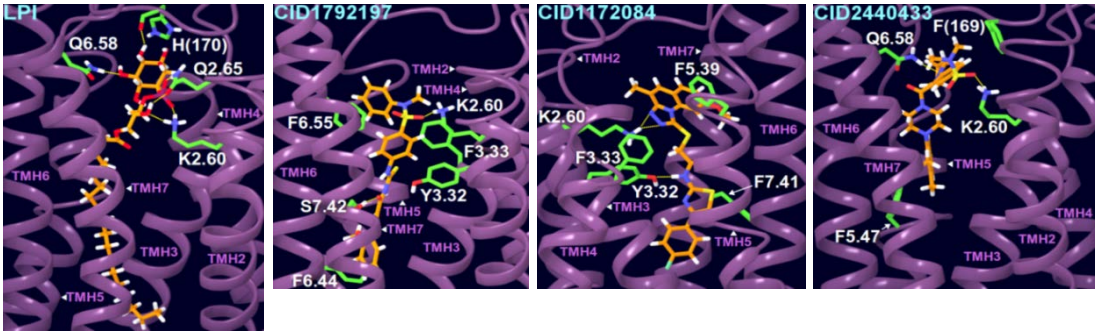

For developing a nano molar-potent ligand, CID1792197 (**1.2**) was chosen as a lead for having the lowest EC_{50} amongst the screened compounds. Modifications of the lead (**1.2**) were targeted at the two termini. The narrowness of the vertical pore of the binding pocket, depicted in the GPR55 R* model and supported by the diminished activity of CID1172084 (**1.3**) upon methylating the amide nitrogen, discouraged carrying modifications that will alter the size of the lead core.

The choice of structural modifications at the two termini aimed towards enhancing solubility, eliminating the Michael acceptor functionality and most importantly exploring additional interactions as depicted when docking the proposed ligands in the GPR55 R* model. (Table 1.1) shows the initially proposed ligands.

Table 1.1 Structures of Proposed Analogues **1.8-1.16.**

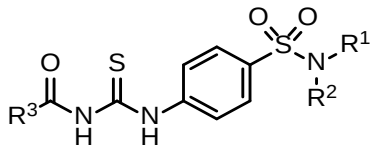

Structure	R^3	$-NR^1R^2$	Structure	R^3	$-NR^1R^2$
1.2	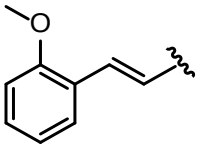	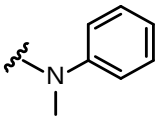	**1.8**	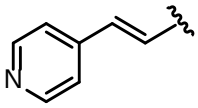	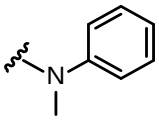
1.9	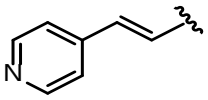	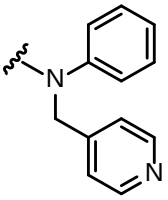	**1.10**	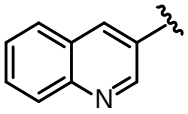	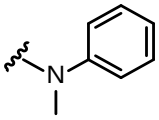
1.11	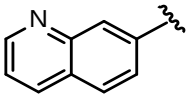	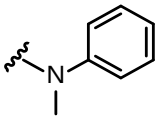	**1.12**	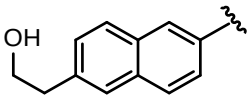	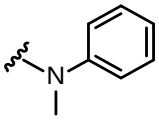

Structure	R^3	$-NR^1R^2$	Structure	R^3	$-NR^1R^2$
1.13	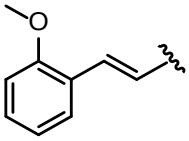	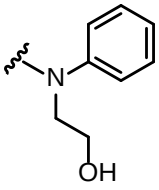	**1.14**	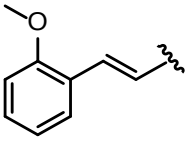	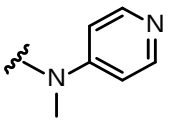

1.15 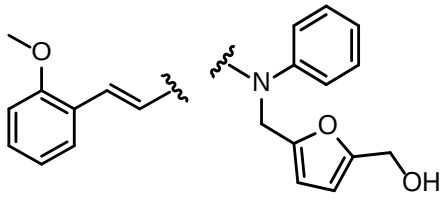 **1.16** 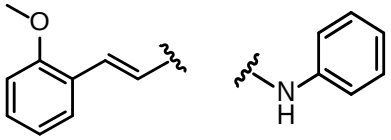

To study the effect of enhancing solubility, the anisole moiety in the parent compound **1.2** was proposed to be replaced with a pyridine, **1.11**. In Analogues **1.13**, **1.11**, and **1.12**, the anisole acryloyl was quinolone, isoquinoline or naphthalene rings, respectively. The purpose of this substitution was to remove the Michael acceptor yet keeping the same spatial arrangement between the carbonyl and the left end aromaticity. Modeling of the naphthalene analogue **1.12** indicated additional H bond interactions of the hydroxyethyl moiety with two different residues at helices 6 and 7 of GPR55 R* model.

Synthesis and biological evaluation of analogues **1.13-1.16** was aimed to explore the effect of the varying substituents attached to the sulfonamide nitrogen. Interactions in the horizontal binding pocket near the extracellular loops, where those substituents resided when docked in the homology model, included hydrogen bonding for compounds **1.13**, **1.14** and **1.15** and aromatic pi-pi stacking for **1.14**.[18] The EC_{50}'s of the synthesized proposed analogues directed later modifications to further explore the structure-activity relationships.

The proposed synthetic scheme presented a feasible way of introducing the substituents separately followed by joining the two termini in a single step (Scheme 1.1).

The various sulfonamides were prepared by substituting the chloride in *p*-nitro sulfonyl chloride (**1.17**) with the proper amine.[19] The resulting *p*-nitro sulfonamide was reduced into the corresponding amine through catalytic hydrogenation.[20]

Scheme 1.1 Retrosynthetic Scheme of GPR55 Agonists

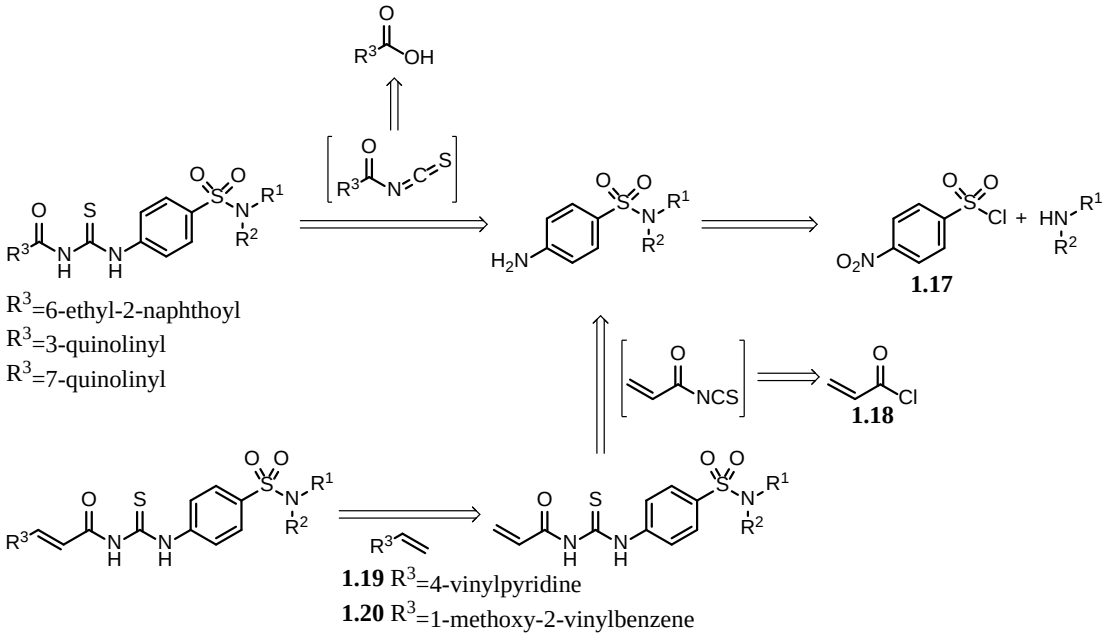

For analogues having the quinoline **1.10**, isoquinoline **1.11** or naphthalene rings **1.12**, the *p*-amino sulfonamide was coupled with the 10-membered aromatic isothiocyanate intermediate, prepared *in situ* by reacting the acyl chloride with potassium isothiocyanate, to give rise to the target GPR55 proposed analogue.[21] As for analogues with the pyridinyl acrylamide **1.8**-**1.9** and methoxyphenyl acrylamide **1.13**-**1.16**, the synthesis was envisioned by first coupling the *p*-amino sulfonamide with acryloyl isothiocyanate, prepared *in situ* by reacting acryloyl chloride **1.18** with potassium

isothiocyanate, followed by Grubbs cross-metathesis with either 2-vinylpyridine **1.19** or 1-methoxy-2-vinylbenzene **1.20**.

1.2.1 Synthesis of the alkylphenyl amine precursors 1.21-1.33

The majority of the amine precursors were commercially available, while the ones which were not accessible were synthesized through reductive amination[22] (Scheme 1.2). Aniline (**1.23**) was reacted with the different aldehydes **1.21-1.22, 1.28-1.30** to give the corresponding imine which was reduced into the target secondary amines using $NaHB_4$.[22] Initially, in the case of isonicotinaldehyde (**1.21**) and 5-(hydroxymethyl)furan-2-carbaldehyde (**1.22**), the resulting imines **1.24-1.25** were purified. For secondary amines **1.31-1.33**, the imine intermediates were reacted with the reducing agent without being isolated.

Scheme 1.2 Synthetic scheme for synthesis of alkyl phenyl amines **1.21-1.33**. Reagents and conditions: (a) aniline (**1.23**) ethanol, 80 °C (28-56%); (b) i) $NaBH_4$, MeOH ii) HCl (52-72%); (c) i) ethanol, 80 °C ii) $NaBH_4$, MeOH iii) HCl (34-96%).

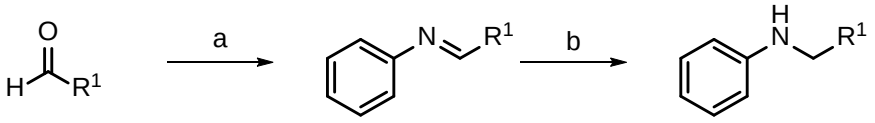

1.21 R^1=4'-pyridine **1.24** R^1=4'-pyridine **1.26** R^1=4'-pyridine
1.22 R^1=(2'CH_2OH)furan **1.25** R^1=(2'CH_2OH)furan **1.27** R^1=(2'CH_2OH)furan

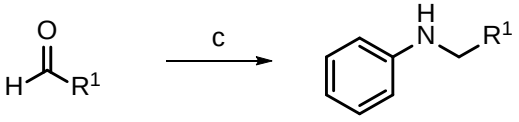

1.28 R^1=2'-phenol **1.31** R^1=2'-phenol
1.29 R^1=3'-phenol **1.32** R^1=3'-phenol
1.30 R^1=4'-phenol **1.33** R^1=4'-phenol

1.2.2 Synthesis of 6-(2-((*tert*-butyldimethylsilyl)oxy)methyl)-2-naphthoic acid 1.40 and 6-(2-((*tert*-butyldimethylsilyl)oxy)ethyl)-2-naphthoic acid 1.41

Precursors for of the variant substituents at the left termini of the lead were commercially available except for 6-(2-hydroxyethyl)-2-naphthoic acid or its protected version. Thus, it was prepared in lab starting with the commercially available methyl 6-bromo-2-naphthoate (**1.34**) (Scheme 1.3). Attempts to reduce the ester **1.34** to the corresponding aldehyde **1.36**, using DIBAL-H[23] in a one pot reaction, were not successful despite the efforts of maintaining the temperature of the mixture at -78 °C throughout the entire reaction time. The only product observed following quenching the reaction at variant times was the alcohol **1.35**. A 24 hour reaction time of **1.34** with 1.2 equivalents of the reducing reagent did not result in complete conversion to the corresponding alcohol **1.35**. Thus, the number of equivalents of DIBAL-H used was increased to 3 to ensure full conversion. The resulting alcohol was initially reoxidized using MnO_2 in $CHCl_3$ to give the corresponding aldehyde **1.36.**[24] The low yields recovered upon the use of the aforementioned conditions, in particular when scaling up the reaction, necessitated the use of the alternative Swern oxidation conditions. The use of DMSO and oxalyl chloride followed by Et_3N significantly enhanced the yields of oxidizing the alcohol **1.35** to the aldehyde **1.36**. A Witting reaction, using triphenylphosphonium iodide, was conducted to prepare 2-bromo-6-vinylnaphthalene **1.37** thus adding an extra carbon to the aldehyde **1.36**.[25] Hydroboration/oxidation of **1.37** gave the anti-Markovnikov alcohol **1.38**.[26] Protection of the alcohol **1.38** was done, using TBSCl in basic conditions,[27] prior to conversion into the corresponding carboxylic acid

1.42. Conversion of the aryl bromide **1.40** into the corresponding carboxylic acid **1.42** was achieved by lithium-halogen exchange using *n*-butyl lithium followed by purging the mixture with CO_2 gas.[28] The structurally similar precursor **1.35** was also protected and converted to the carboxylic acid **1.41** to investigate further the effect of the side chain length on activity.

Scheme 1.3 Synthesis of 6-(2-((*tert*-butyldimethylsilyl)oxy)methyl)-2-naphthoic acid (**1.41**)and 6-(2-((*tert*-butyldimethylsilyl)oxy)ethyl)-2-naphthoic acid (**1.42**). Reagents and conditions: (a) i) 3 eq. DIBAL-H, THF, - 40 °C ii) $NH_4Cl_{(aq)}$ (90%); (b) MnO_2, $CHCl_3$ (47%); (c) i) oxalyl chloride, DMSO ii) Et_3N (60%); (d) Ph_3PCH_3I, NaH, THF (65%); (e) i) BH_3-THF, THF ii) NaOH, H_2O_2 (77%); (f) TBSCl, DMAP, Et_3N (54-84%); (g) i) *n*BuLi, THF ii) CO_2 iii) H_3O^+ (42%).

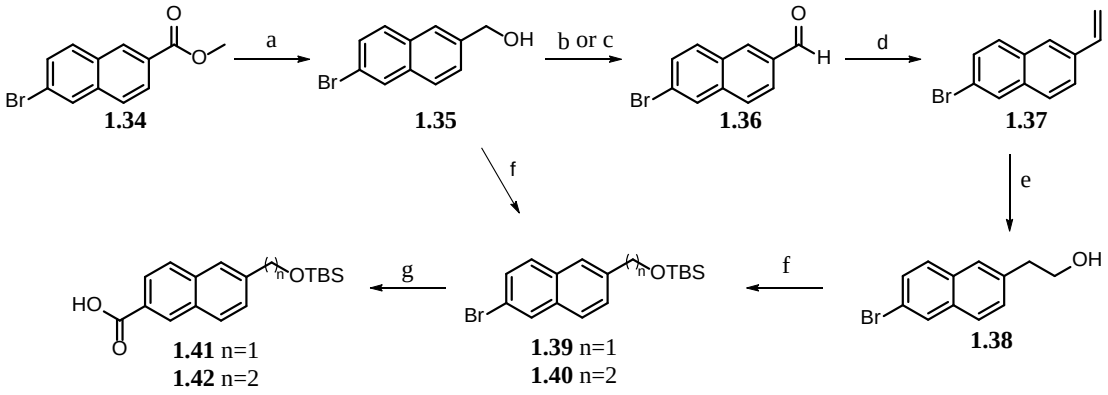

The discouraging lengthy and low yield method for synthesizing 6-(2-hydroxyethyl)-2-naphthoic acid prompted the search for an alternative more feasible method (Scheme 1.4). Prior to substituting the bromine in the bromo ester **1.34** with a hydroxyethyl, it was hydrolyzed to the corresponding carboxylic acid 5-(hydroxymethyl)furan-2-carbaldehyde (**1.43**) using KOH in methanol. Initially the carboxylic acid (**1.43**) was treated with more than two equivalents of *n*BuLi followed by ethylene oxide and a Lewis acid. Analysis of

the crude reaction mixture indicated that the sole product, detected by ^{1}H NMR, was the dehalogenated acid **1.45**. The use of NaH to deprotonate the carboxylic acid prior to lithium-halogen exchange by *n*BuLi proved to be successful. Mass analysis of the crude mixture indicated the formation of the intended product; however, a similar result was not achieved upon scaling up the reaction under the aforementioned conditions. Development of the method is still undergoing to ensure applicability on large-scale reactions.

Scheme 1.4 Attempted synthesis of 6-(2-hydroxyethyl)-2-naphthoic acid (**1.44**). Reagents and conditions: (a) 3 eq. KOH, MeOH, 40 °C, 48 hours (56%); (b) i) *n*-BuLi, THF (0.1 M), -78 °C; ii) ethylene oxide; iii. $BF_3.Et_2O$, -78 °C to rt; (c) i) 1.2 eq. NaH, THF (0.1M) ii) *n*BuLi, -78 °C, 3 hr; iii) ethylene oxide; iv) $BF_3.Et_2O$.

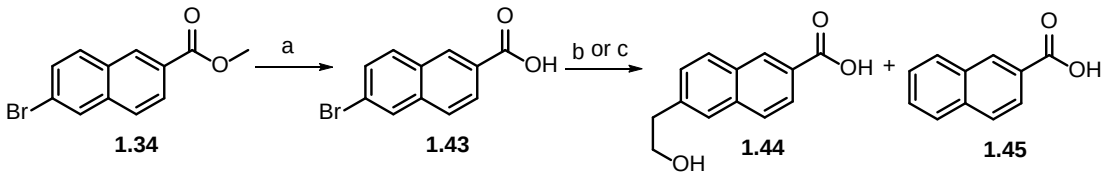

1.2.3 Synthesis of *p*-nitro and *p*-aminobenzene sulfonamides 1.46-1.69

Upon the availability of the primary or secondary amines, they were reacted with *p*-nitro sulfonyl chloride (**1.17**) in basic conditions to give the corresponding *p*-nitro sulfonamides[19] **1.46-1.57** (Scheme 1.5). Pd-catalyzed hydrogenation was used to reduce the nitro group into the corresponding aniline **1.58-1.69**.[20]

Scheme 1.5 Synthesis of *p*-nitro and *p*-amino benzene sulfonamides. Reagents and conditions: (a) R^1R^2NH, pyridine, CH_2Cl_2 (5-91%); (b) Pd/C, H_2, MeOH (12-92%).

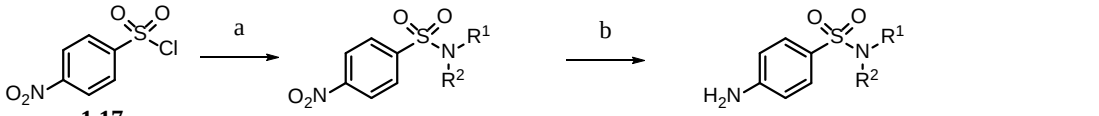

1.17

1.46 R^1=Ph, R^2=CH_3
1.47 R^1=Ph, R^2=CH_2CH_2OH
1.48 R^1=Ph, R^2=CH_2(4-pyridinyl)
1.49 R^1=Ph, R^2=CH_2(('-CH_2OH)Furyl)
1.50 R^1=Ph, R^2=H
1.51 R^1=CH_3, R^2=4-pyridinyl
1.52 R^1=Ph, R^2=CH_2(2-phenol)
1.53 R^1=Ph, R^2=CH_2(3-phenol)
1.54 R^1=Ph, R^2=CH_2(4-phenol)
1.55 R^1=H, R^2=3-propyl-1*H*-indole
1.56 R^1=H, R^2=CH_2CH_2OH
1.57 R^1=H, R^2=$CH_2CHOHCH_2OH$

1.58 R^1=Ph, R^2=CH_3
1.59 R^1=Ph, R^2=CH_2CH_2OH
1.60 R^1=Ph, R^2=CH_2(4-pyridinyl)
1.61 R^1=Ph, R^2=CH_2((5-CH_2OH)furyl)
1.62 R^1=Ph, R^2=H
1.63 R^1=CH_3, R^2=4-pyridinyl
1.64 R^1=Ph, R^2=CH_2(2-phenol)
1.65 R^1=Ph, R^2=CH_2(3-phenol)
1.66 R^1=Ph, R^2=CH_2(4-phenol)
1.67 R^1=H, R^2=3-propyl-1*H*-indole
1.68 R^1=H, R^2=CH_2CH_2OH
1.69 R^1=H, R^2=$CH_2CHOHCH_2OH$

1.2.4 Attempted synthesis of compounds 1.2 and 1.8 via cross metathesis

As proposed, methoxyphenyl acrylamide **1.2** and pyridinyl acrylamide **1.8** analogues were approached via cross metathesis of carbamothioylacrylamide intermediate **1.70** with 2-vinylpyridine (**1.17**) or 1-methoxy-2-vinylbenzene (**1.16**), respectively (Scheme 1.6). Unfortunately, polymers of **1.16** and **1.17** were the sole products formed as deducted by ^{1}H NMR analysis.

Scheme 1.6 Attempted synthesis of compounds **1.2** and **1.8** via cross metathesis. Reagents and conditions: (a) i) KSCN, CH_3CN, -10 °C to rt, 3 hours; ii) **1.58** (47%); (b) 2-vinylpyridine (**1.16**) or 1-methoxy-2-vinylbenzene (**1.17**), Hoveyda-Grubbs Catalyst, CH_2Cl_2.

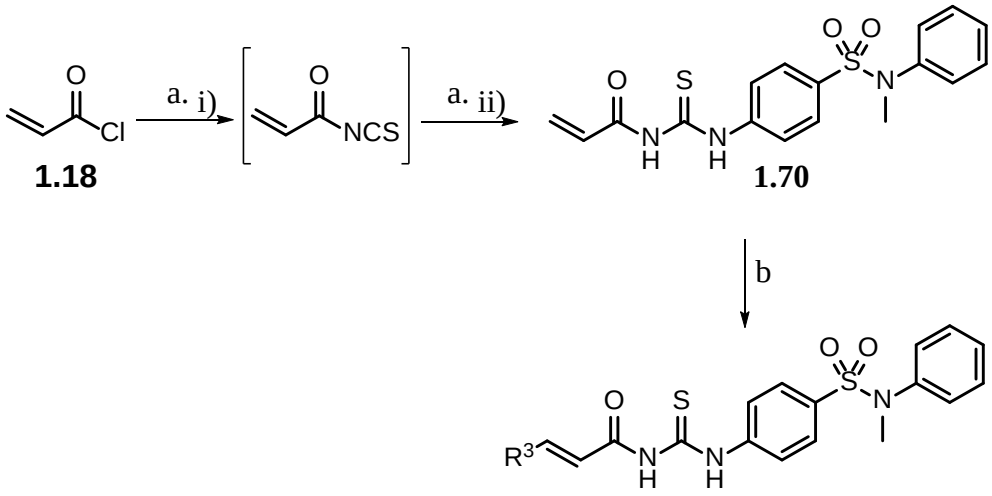

1.2.5 Synthesis of analogues 1.2, 1.10-1.13 and 1.71-1.83

Analogues **1.10** and **1.8** were prepared by coupling of the isothiocyante intermediate, derived from the commercially available carboxylic acids, with the synthesized aniline **1.58** (Scheme 1.7). This success geared the preparation of pyridinyl acrylamide and methoxyphenyl acrylamide analogues towards following the aforstated method. Thus, the commercially available carboxylic acids; 2-methoxyphenylacrylic acid **1.71**, quinoline-3-carboxylic acid **1.72**, quinoline-7-carboxylic acid **1.73** and the synthesized 6-(2-((*tert*-butyldimethylsilyl)oxy)methyl)-2-naphthoic acid **1.38** and 6-(2-((*tert*-butyldimethylsilyl)oxy)ethyl)-2-naphthoic acid **1.39** were converted into the more active acyl chlorides by refluxing with thionyl chloride. The resultant acyl chlorides were

converted into the isothiocyanate intermediates, *in situ*, using potassium thiocyante.[21] The crude intermediates were reacted with the prepared *p*-amino sulfonamides to give the target analogues (Scheme 1.7).

Scheme 1.7 Synthesis of analogues **1.2**, **1.10**-**1.13** and **1.75**-**1.87.** Reagents and conditions: (a) $SOCl_2$, 80 °C, 3 hrs; (b) i) KSCN, CH_3CN, -10 °C – r.t., 3 hrs; ii) 24 hrs (6-65%).

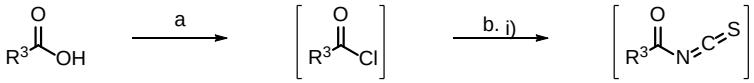

1.41 R^3=6-(2-((*tert*-butyldimethylsilyl)oxy)methyl)-2-naphthoyl
1.42 R^3=6-(2-((*tert*-butyldimethylsilyl)oxy)ethyl)-2-naphthoyl
1.71 R^3=2-(2'-methoxy)phenyl acrylyl
1.72 R^3=3-quinolinyl
1.73 R^3=7-quinolinyl

b. ii) **1.57-1.68,**

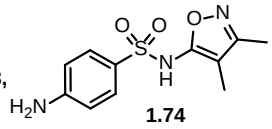

1.74

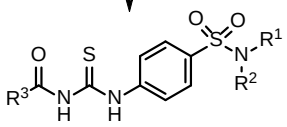

1.2 R^1=Ph, R^2=CH_3, R^3=2-(2'-methoxy)phenylacrylyl
1.10 R^1=Ph, R^2=CH_3, R^3=3-quinolinyl
1.11 R^1=Ph, R^2=CH_3, R^3=7-quinolinyl
1.12 R^1=Ph, R^2=CH_3, R^3=6-(2-((*tert*-butyldimethylsilyl)oxy)ethyl)-2-naphthoyl
1.13 R^1=Ph, R^2=CH_2CH_2OH, R^3=2-(2'-methoxy)phenyl acrylyl
1.11 R^1=CH_3, R^2=4-Pyridinyl, R^3=2-(2'-methoxy)phenyl acrylyl
1.15 R^1=Ph, R^2=CH_2((5'-CH_2OH)furyl), R^3=2-(2'-methoxy)phenyl acrylyl
1.16 R^1=Ph, R^2=H, R^3=2-(2'-methoxy)phenyl acrylyl
1.75 R^1=Ph, R^2=CH_3, R^3=6-(2-((*tert*-butyldimethylsilyl)oxy)methyl)-2-naphthoyl
1.76 R^1=Ph, R^2=CH_2CH_2OH, R^3=7-quinolinyl
1.77 R^1=Ph, R^2=CH_2(4-pyridinyl), R^3=2-(2'-methoxy)phenyl acrylyl
1.78 R^1=Ph, R^2=CH_2((5'-CH_2OH)furyl), R^3=7-quinolinyl
1.79 R^1=Ph, R^2=CH_2(2-phenol), R^3=2-(2'-methoxy)phenyl acrylyl
1.80 R^1=Ph, R^2=CH_2(3-phenol), R^3=2-(2'-methoxy)phenyl acrylyl
1.81 R^1=Ph, R^2=CH_2(4-phenol), R^3=2-(2'-methoxy)phenyl acrylyl
1.82 R^1=H, R^2=3-propyl-1*H*-indole, R^3=2-(2'-methoxy)phenyl acrylyl
1.83 R^1=H, R^2=CH_2CH_2OH, R^3=2-(2'-methoxy)phenyl acrylyl
1.84 R^1=H, R^2=$CH_2CHOHCH_2OH$, R^3=2-(2'-methoxy)phenyl acrylyl
1.85 R^1=H, R^2=3,4,-dimethylisoxazoyl, R^3=2-(2'-methoxy)phenyl acrylyl
1.86 R^1=Ph, R^2=CH_2(4-pyridinyl), R^3=7-quinolinyl
1.87 R^1=Ph, R^2=CH_2(4-phenol), R^3=7-quinolinyl

Efforts to synthesize analogue **1.8** using the procedure presented in Scheme 1.7 were not successful. Table 1.2 summarizes the alterations of the method that were attempted. To address the insolubility of the acyl chloride in CH_3CN, which was believed to arise from the interaction of the hydrochloric acid byproduct with the pyridine basic nitrogen, bases such as triethylamine (Entry 1) and dimethylaminopyridine (Entry 2) were added. None of the bases used helped in solubilizing the intermediate acyl chloride nor resulted in formation of the target product as deduced from TLC analysis. Another approach was the use of different solvents; namely dimethylformamide (Entry 3) and dimethyl sulfoxide (Entry 4) which aided in dissolving the acyl chloride however did not result in product formation.

Table 1.2 Conditions for Synthesis of Compound **1.8.**

Entry	Solvent	Base	Reaction time	Result
1	CH_3CN	Et_3N	4 hours	No reaction
2	CH_3CN	DMAP	overnight	No reaction
3	DMF	N/A	overnight	No reaction
4	DMSO	N/A	overnight	No reaction

To decrease the possibility of pyridinium salt formation, an alternative electrophilic intermediate was prepared (Scheme 1.8). A base was used in the process of creating the acid anhydride which theoretically would help in competing with the pyridinyl nitrogen for the produced HCl. Similar to the acyl chloride, the anhydride was not purified yet the success of its formation was confirmed by thin layer chromatography. Nevertheless, no product was detected after reacting it with potassium thiocyanate.

Scheme 1.8 Attempts for synthesis of compound **1.8.** Reagents and conditions: (a) $(CH_3)_3CCOCl$, Et_3N, THF; (b) KSCN, CH_3CN.

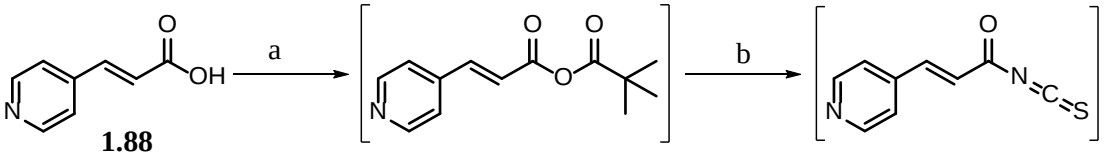

1.3 Biological Assay Results

The synthesized final compounds were tested for activation of GPR55 using a *β*-Arrestin assay except for the indole analogue **1.82** due to decomposition during purification using column chromatography. The stable and strong binding of *β*-Arrestin, labeled with green fluorescent protein, with GPCRs allow an accurate and reproducible read out of the activation response.[29] The EC_{50}'s are summarized in Figure1.4. The synthesized parent ligand activity when retested was significantly decreased (7.0 μM) in comparison to the reported activity (0.11 μM) of the same ligand that was prepared by another lab. This may indicate that the activities of the synthesized ligands herein are significantly more potent than the IC_{50}'s indicate. Despite the difference between the two

reported absolute activities of the parent ligand, considerable structure-activity relationship can be inferred from the relative activities of the synthesized ligands and this will drive future design towards the synthesis of the target single digit nM-active ligand.

Figure 1.4 Biological data for synthesized potential GPR55 agonists.

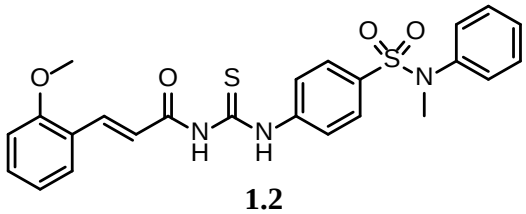

1.2

EC_{50} = 7.0 μM

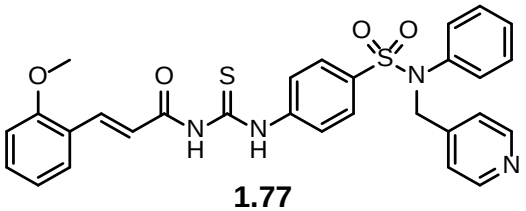

1.77

EC_{50} = 0.33 μM

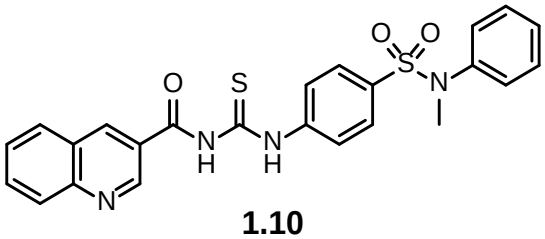

1.10

EC_{50} = ~30 μM

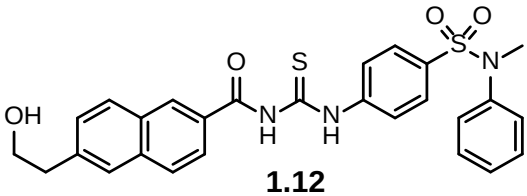

1.12

EC_{50} = 0.29 μM

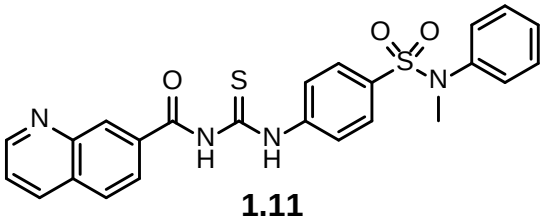

1.11

EC_{50} = 1.0 μM

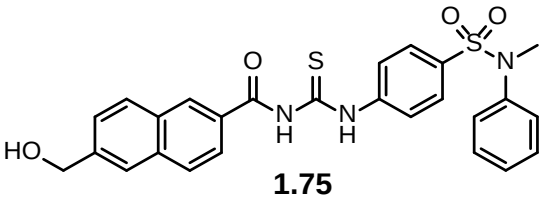

1.75

EC_{50} = 3.9 μM

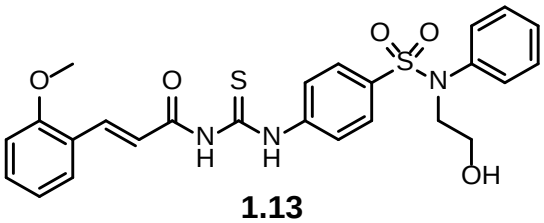

1.13

EC_{50} = 0.71 μM

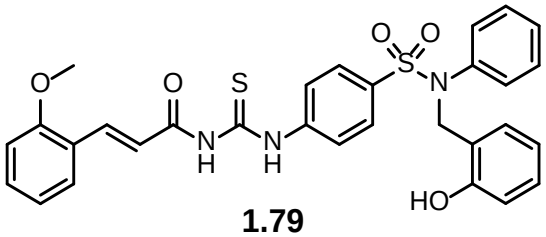

1.79

EC_{50} = 2.2 μM

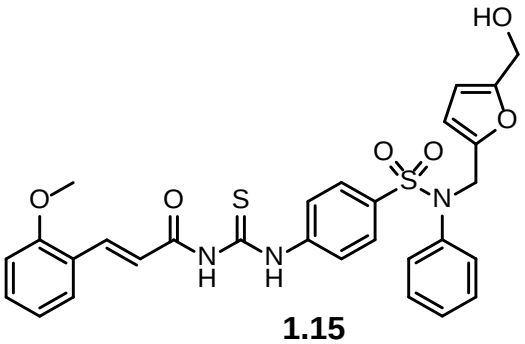

1.15

EC_{50} = 0.12 μM

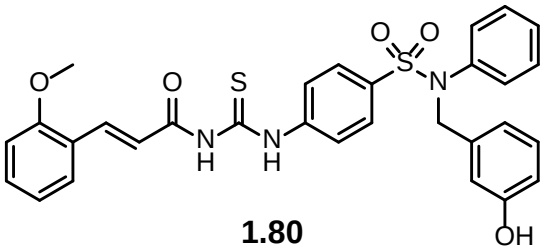

1.80

EC_{50} = 1.5 μM

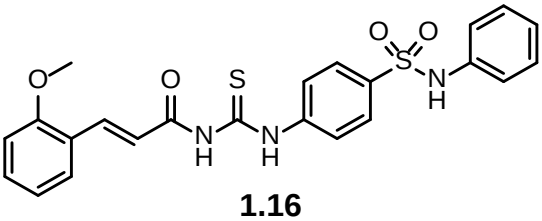

1.16

EC_{50} = 0.60 μM

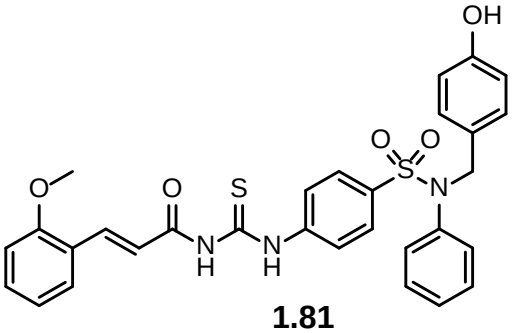

1.81

EC_{50} = 0.48 μM

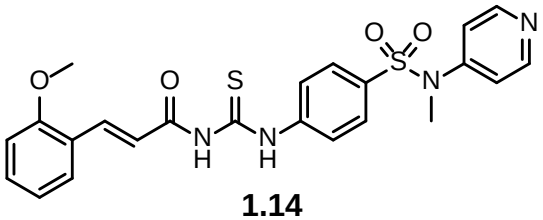

1.14

EC_{50} = 0.50 μM

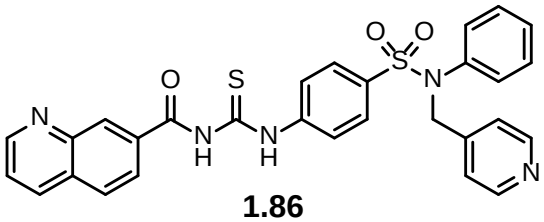

1.86

EC_{50} = 0.46 μM

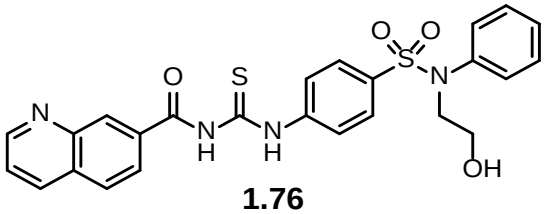

1.76

EC_{50} = 0.22 μM

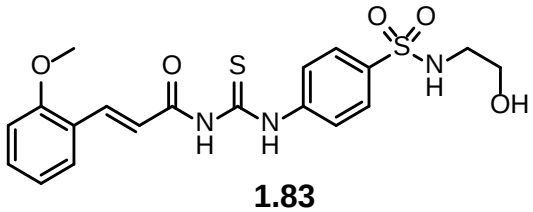

1.83

EC_{50} = > 30 μM

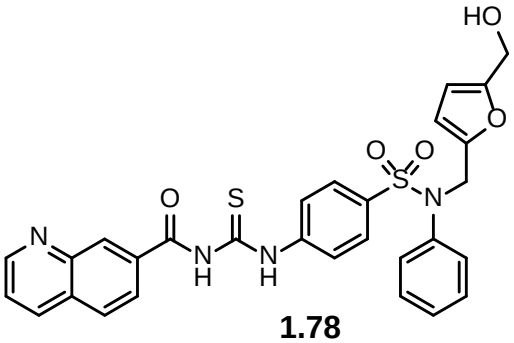

1.78

EC_{50} = 0.50 μM

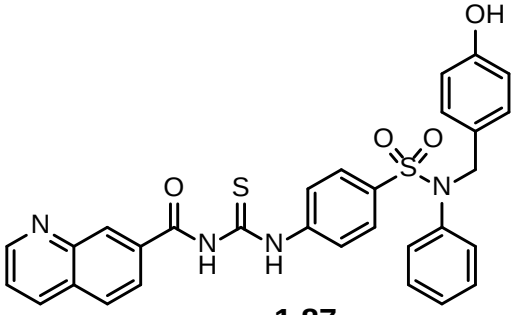

1.87

EC_{50} = 0.14 μM

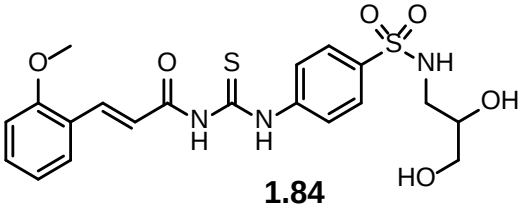

1.84

EC_{50} = > 30 μM

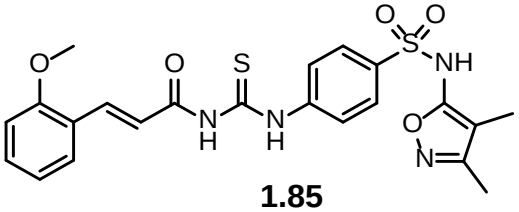

1.85

EC_{50} = > 30 μM

For analogues having the 2-methoxyphenyl acryloyl moiety **1.10**, **1.73**, **1.75-1.77**, **1.79-1.81**, it is crucial for the pharmacophore to have an aromatic phenyl ring as one of the substituents of the sulfonamide's nitrogen; removing the phenyl ring diminished the activity. Such an effect can be inferred from the loss of activity when the sulfonamide phenyl substituent in compound **1.10** was replaced with hydrogen in compound **1.79**. Even replacing the phenyl **1.13** with another aromatic bioisostere; namely 3,4-dimethylisoxazole **1.78**, led to the same result as when removing the ring. Although, the aforementioned substituent leads to solubility enhancement, the change of distribution and overall electron density of the isoxazole π-system relative to the phenyl counterpart may play a major contributing factor to disturbing the *pi-pi* stacking with the nearby interacting residue in the extracellular horizontal part of the binding pocket.

Among all of the proposed and synthesized analogues, compound **1.12**, which has a phenyl and a 2'-hydroxyfuran substituents on the sulfonamide nitrogen, showed the best activity with an EC_{50} of 0.12 μM. When compared to **1.10**, the rigidity caused by the aromatic furan thus positioning the hydroxymethyl in proximity to a hydrogen bond donor or acceptor in the horizontal part of the binding pocket can be considered a contributing factor in the nearly 6-fold increase in activity. This legitimate assumption has driven the choice of making a phenol isostere of the hydroxymethylfuran. To further explore the effect of the hydroxyl position in the phenol substituent relative to the methylene, *ortho* **1.79**, *meta* **1.80** and *para* **1.81** analogues were prepared. The *para*-phenol analogue **1.81** was the most active compared to the *ortho* **1.79** and *meta* **1.80**, yet

it was 4-fold less active than **1.15** suggesting that the furan oxygen may play a part in providing additional interactions with the receptor.

Replacing the 2-methoxyphenyl acryloyl moiety in **1.2** with 3-quinoline and 7-isoquinoline showed immense difference in activity. The former analogue **1.7** was inactive while the 7-quinoline structural isomer **1.10** was moderately active with an EC_{50} of 1.0 μM. Such a difference indicates that the nitrogen position in the 10-membered heteroaromatic ring is crucial for its interaction with the binding pocket. The 2-methoxyphenyl acryloyl, in analogues showing activities better than 1.0 μM, was substituted with 7-isoquinoline to synergize the relative increase in activity by the two termini's most active substitution. Nevertheless, the outcome of such combinations did not follow the same pattern. For some, there was an increase in activity when the 2-methoxyphenyl acryloyl was substituted with 7-quinoline as seen when comparing **1.81** to **1.86**, while a decrease in activity for the most potent analogue **1.12** was noticed.

The expected increase in activity in analogue **1.8** was confirmed by the experimental moderate activity. As designed, a side chain length of 2 carbons is needed for the hydroxyl to reach deep in the base of the binding pocket for its target interaction. This can be confirmed by the order of magnitude decrease in activity when shortening the side chain by one carbon as in analogue **1.84**. Future analogues bearing the hydroxyethylnaphthyl group are to be synthesized to enhance the potency further.

1.4 Experimental

Unless otherwise stated, all reactions were carried out under an atmosphere of dry nitrogen in oven-dried glassware. Indicated reaction temperatures refer to those of the

reaction bath, while room temperature (rt) is noted as 25 °C. All solvents and reagents were obtained from commercial sources and were used as received. Analytical thin layer chromatography (TLC) was performed on silica gel 60 F254 precoated plates (0.25 mm) from Merck. Visualization was accomplished by irradiation under a 254 nm UV lamp. Silicycle silica gel 230−400 (particle size 40−63 μm) mesh was used for all flash column chromatography. If needed, products were purified by reverse phase chromatography, which was performed using a Varian purification system employing a Phenomenex Gemini-NX, (5 μm, C18, 110A, AX. 250 × 21.20 mm). The mobile phase was a mixture of acetonitrile and H_2O containing 0.1% formic acid. ^{1}H NMR spectra were recorded on a Jeol ECA 500 MHz spectrometer or a Jeol ECS 400 MHz spectrometer in the solvent indicated. All ^{1}H NMR experiments were run at 17 °C except for DMSO-d_6 solvent that was run at 25 °C. Chemical shifts are reported in δ units, parts per million (ppm) downfield of TMS, and were measured relative to the signals for chloroform (7.26 ppm), methanol (3.31 ppm), acetone (2.05 ppm) and dimethyl sulfoxide (2.50 ppm). All ^{13}C NMR spectra were reported in ppm relative to the signals for chloroform (77 ppm), methanol (49 ppm), acetone (29.8 ppm) and dimethyl sulfoxide (39.5 ppm) with ^{1}H decoupled observation. Data for ^{1}H NMR are reported as follows: chemical shift (δ ppm), multiplicity (s = singlet, d = doublet, t = triplet, q = quartet, quint = quintet, sext = sextet, sept = septet, oct = octet, m = multiplet), integration and coupling constant (Hz), whereas ^{13}C NMR analyses were reported in terms of chemical shift and number of equivalent carbons if more than one. High resolution mass spectrometry data (HRMS) were performed on a Thermo Fisher Scientific UPLC/LTQ Orbitrap XL system.

1.4.1 General procedure A for synthesis of secondary amines (1.24-1.25).

Step 1: Synthesis of Imines **1.21-1.22**.[30] Aniline (**1.23**) (1 eq.) and the aldehyde **1.21-1.22** (1 eq.) were dissolved in dry ethanol (0.5 M) and the resulting mixture heated under reflux for 3 hrs. The solution was cooled to room temperature and the solvent removed under reduced pressure. Purification of the product was done via recrystallization using an appropriate mixture of solvents where enough volume of the more polar solvent was added to dissolve the crude mixture and the less polar solvent was added until reaching the saturation point.

(*E*)-*N*-Phenyl-1-(pyridin-4-yl)methanimine (1.24).[22] The crude product was recrystallized using a mixture of ethyl acetate and hexane. Yield (0.936 g, 28%). ^{1}H NMR matched that previously reported.[22]

^{1}H NMR (500 MHz, Acetone-d_6): δ 8.73 (dd, *J* = 1.7, 4.3 Hz, 2H; Ar-H), 8.64 (s, 1H; CH), 7.84 (dd, *J* = 1.7, 4.3 Hz, 2H; Ar-H), 7.42 (dd, *J* = 1.7, 6.6 Hz, 2 H; Ar-H), 7.26-7.30 (m, 3H; Ar-H).

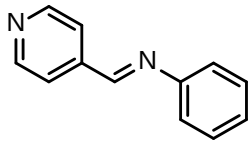

Figure 1.5 ^{1}H NMR spectrum of compound **1.24** [500 MHz, Acetone-d_6].

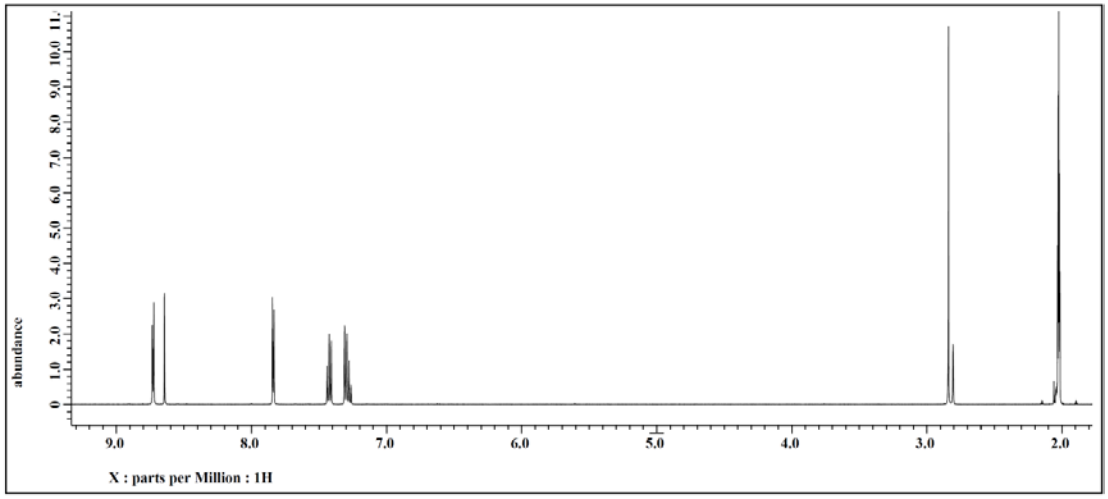

(*E*)-(5-((Phenylimino)methyl)furan-2-yl)methanol (1.25). The crude product was recrystallized using a mixture of dichloromethane and hexane. Yield (0.47 g, 56%).

^{1}H NMR (500 MHz, Acetone-d_6): δ 8.33 (s, 1H, N=CH), 7.37 (m, 2H; Ar-H), 7.20 (m, 3H; Ar-H), 7.00 (d, *J* = 3.3 Hz, Ar-H), 6.48 (d, *J* = 3.4 Hz, Ar-H), 4.61 (s, 1H, O-CH_2), 4.60 (s, 1H, O-CH_2).

^{13}C NMR (125 MHz, Acetone-d_6): δ 159.3, 152.0, 147.9, 129.2 (2C), 125.9 (2C), 120.9 (2C), 117.3, 109.3, 56.6.

HRMS (ESI, m/z): Calculated for $C_{12}H_{12}NO_2$ $[M + H]^+$ 202.0863; found 202.0855 (3.7 ppm).

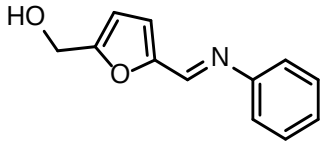

Figure 1.6 ^{1}H and ^{13}C NMR spectra of compound **1.25** [500 MHz for ^{1}H and 125 MHz for ^{13}C, Acetone-d_6].

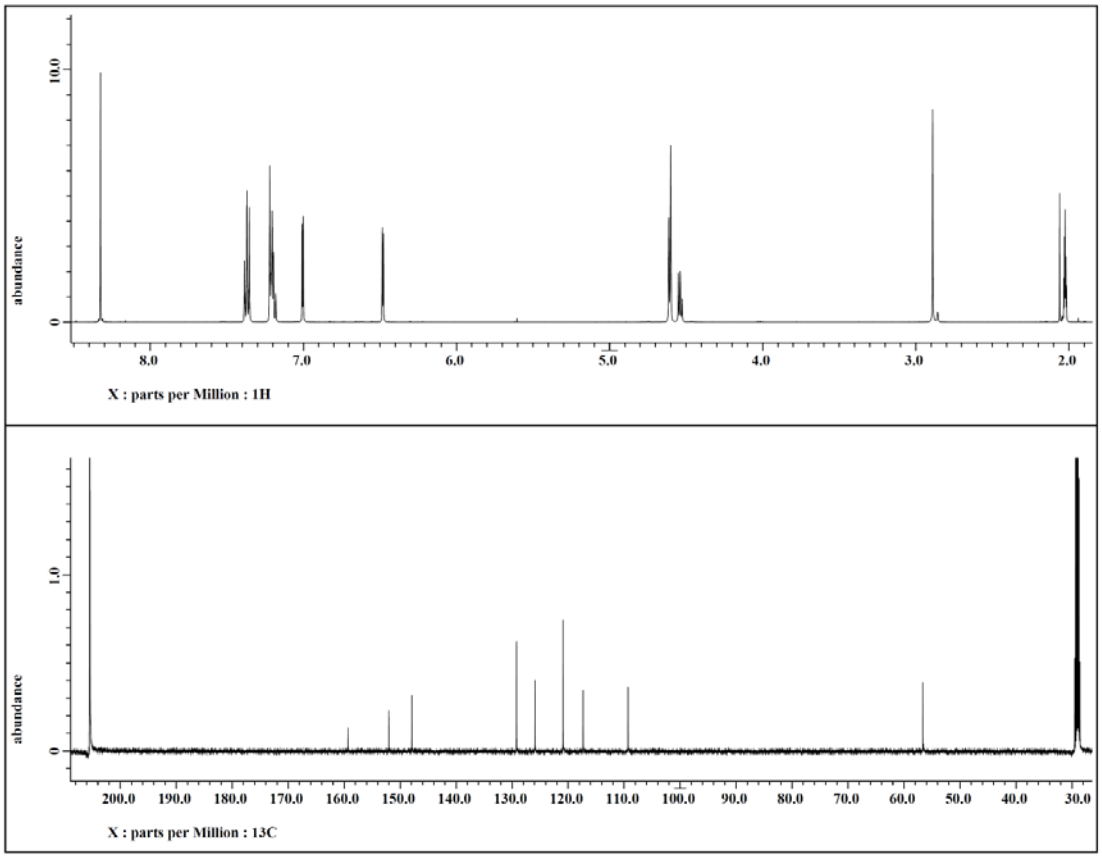

Step 2: Reduction of Imines **1.26-1.27**.[22] The imine **1.24-1.25** (1 eq.) was dissolved in MeOH (0.5 M). $NaBH_4$ (5 eq.) was added portion-wise and the mixture stirred for 24 hours at room temperature. It was acidified to a pH of 3 using HCl (50 % v/v) followed by increasing the pH to 9 using NaOH (2 M). The product was extracted using dichloromethane. The organic layer was dried over $MgSO_4$, filtered and concentrated under reduced pressure. Purification of the product was done via recrystallization using flash column chromatography or an appropriate mixture of solvents where enough

volume of the more polar solvent was added to dissolve the crude mixture and the less polar solvent was added until reaching the saturation point.

***N*-(Pyridin-4-ylmethyl)aniline (1.26)**. The crude product was recrystallized using a mixture of dichloromethane and hexane. Yield (0.786 g, 52%). ^{1}H NMR matched that previously reported.[22]

^{1}H NMR (500 MHz, Acetone-d_6): δ 8.46 (dd, *J* = 1.7, 4.6 Hz, 2H; Ar-H), 7.33 (dd, *J* = 1.7, 4.6 Hz, 2H; Ar-H), 7.04 (dd, *J* = 1.7, 6.6 Hz, 2H; Ar-H), 6.54-6.59 (m, 3H; Ar-H), 4.39 (d, *J* = 5.7 Hz, 2H, CH_2).

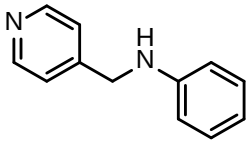

Figure 1.7 ^{1}H NMR spectrum of compound **1.26** [500 MHz, Acetone-d_6].

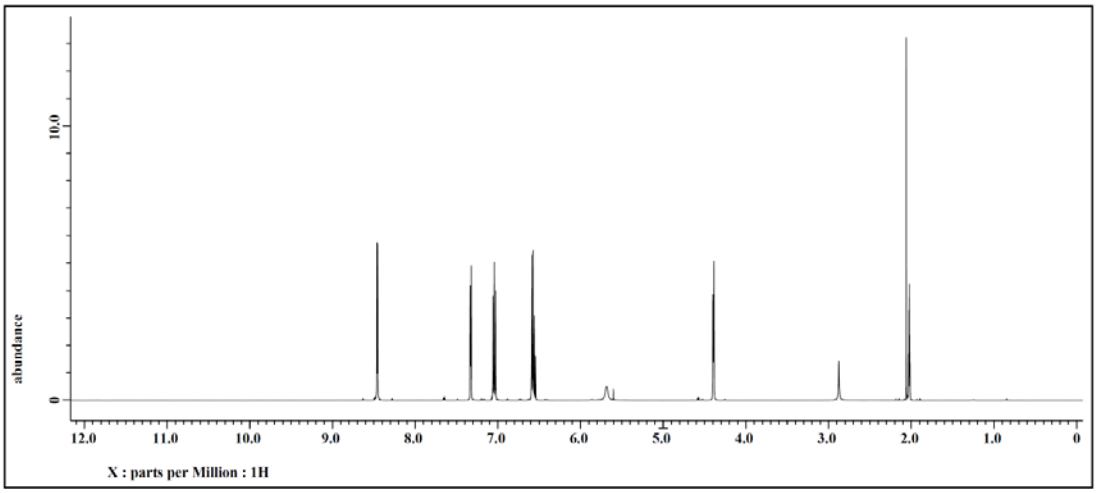

(5-((Phenylamino)methyl)furan-2-yl)methanol (1.27). The crude product was purified using flash column chromatography over silica gel. It eluted with ethyl acetate and hexane (0.2:1, v/v). Yield (0.514 g, 72%).

^{1}H NMR (500 MHz, Acetone-d_6): δ 7.07 (dd, *J* = 7.2, 8.6 Hz, 2H, Ar-H), 6.68 (dd, *J* = 1.2, 8.6 Hz, 2H, Ar-H), 6.58 (d, *J* = 7.2 Hz, Ar-H), 6.16 (d, *J* = 3.2 Hz, 1H, Fu-H), 6.15 (d, *J* = 3.2 Hz, 1H, Fu-H), 5.28 (bs, 1H; N-H), 4.44 (d, *J* = 5.7 Hz, 2H; O-CH_2), 4.25 (d, *J* = 5.7 Hz, 2H; N-CH_2), 4.21 (t, *J* = 6.0 Hz, 1H; O-H).

^{13}C NMR (125 MHz, Acetone-d_6): δ 154.8, 153.0, 148.6, 128.9 (2C), 116.8, 112.7 (2C), 107.6, 107.4, 56.5, 40.7.

HRMS (ESI, m/z): Calculated for $C_{12}H_{14}NO_2$ $[M + H]^+$ 204.1019; found 204.1014 (2.5 ppm).

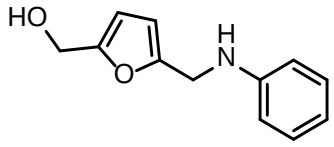

Figure 1.8 ^{1}H and ^{13}C NMR spectra of compound **1.27** [500 MHz for ^{1}H and 125 MHz for ^{13}C, Acetone-d_6]

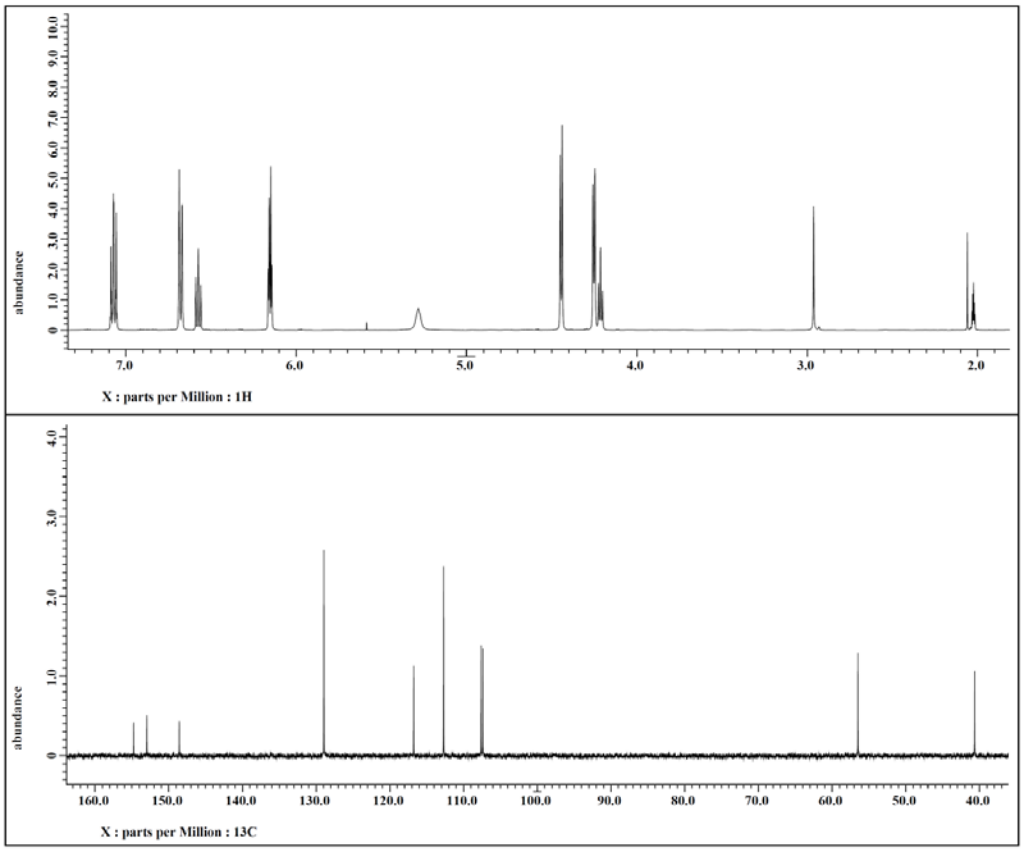

1.4.2 General procedure B for synthesis of secondary amines (1.31-1.34).

Aniline **1.20** (1 eq.) and the aldehyde **1.25-1.27** (1 eq.) were dissolved in dry ethanol (0.8 M) and the resulting mixture heated under reflux for 3 hrs. The solution was cooled to room temperature, $NaBH_4$ (5 eq.) added portion-wise and the mixture stirred for an hour. It was diluted with H_2O and extracted with ethyl acetate. The organic layer was dried over $MgSO_4$, filtered and concentrated. Purification of the crude product was accomplished via recrystallization using an appropriate mixture of solvents where enough

volume of the more polar solvent was added to dissolve the crude mixture and the less polar solvent was added until reaching the saturation point.

2-((Phenylamino)methyl)phenol (1.31). The crude product was via recrystallization using a mixture of ethyl acetate and hexane. Yield (0.359 g, 96%). ^{1}H NMR matched that previously reported.[31]

^{1}H NMR (400 MHz, Chloroform-d_3): δ 8.44 (bs, 1H; O-H), 7.26-7.20 (m, 3H; Ar-H), 7.16 (d. *J* = 6.9 Hz, 1H; Ar-H), 6.94-6.84 (m, 5H; Ar-H), 4.41 (s, 2H, N-CH_2), 3.95 (bs, 1H; N-H). ^{1}H NMR matched that previously reported.[31]

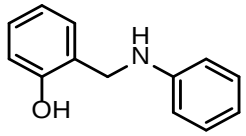

Figure 1.9 ^{1}H NMR spectrum of compound **1.31** [400 MHz, Chloroform-d_3].

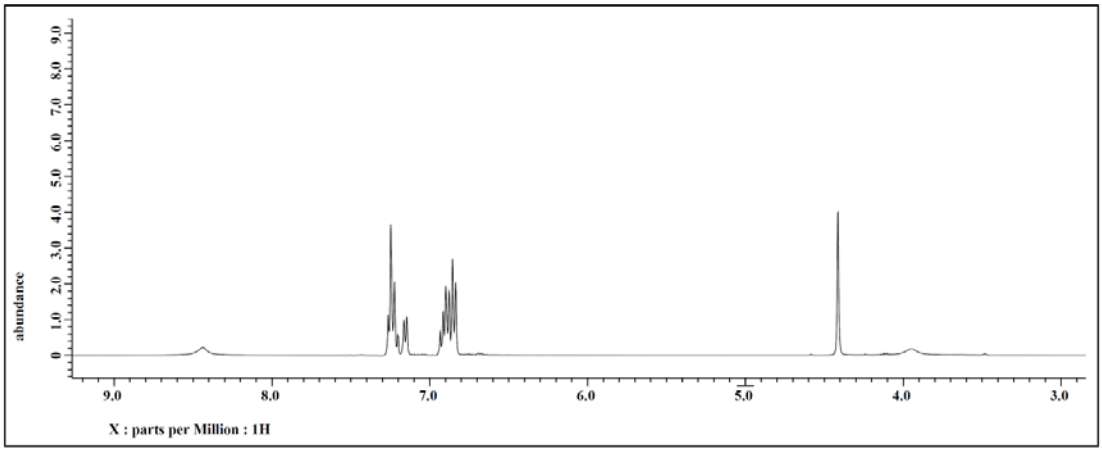

3-((Phenylamino)methyl)phenol (1.32). The crude product was purified via recrystallization using a mixture of ethyl acetate and hexane. Yield (0.116 g, 36%). ^{1}H NMR matched that previously reported.[32]

^{1}H NMR (400 MHz, Methanol-d_4): δ 7.08 (t, *J* = 7.8 Hz, 1H; Ar-H), 7.03 (t, *J* = 8.0 Hz, 2H; Ar-H), 8.24 (m, 2H; Ar-H), 6.62-6.53 (m, 4H; Ar-H), 4.20 (s, 2H, N-CH_2).

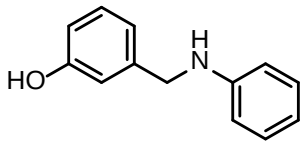

Figure 1.10 ^{1}H NMR spectrum of compound **1.32** [400 MHz, Methanol-d_4]

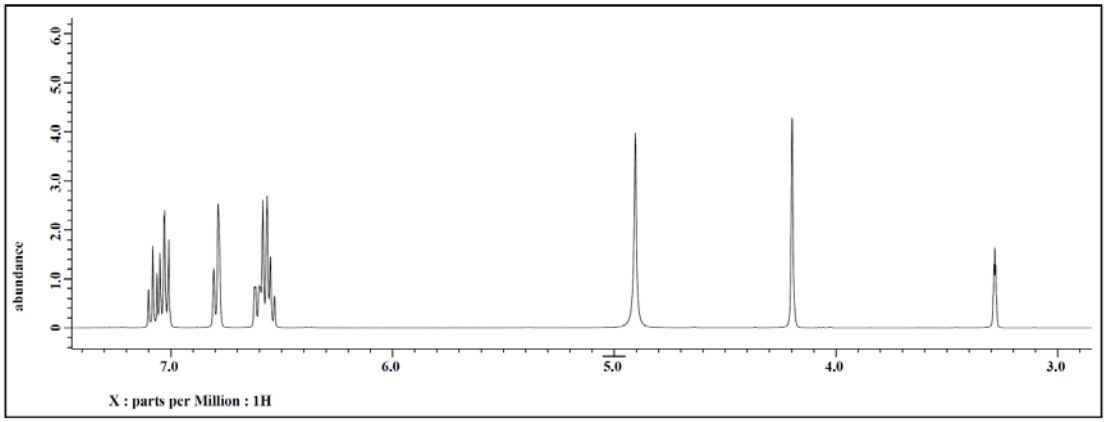

4-((Phenylamino)methyl)phenol (1.33). The crude product was purified via recrystallization using a mixture of ethyl acetate and hexane. Yield (110 mg, 34%). ^{1}H NMR matched that previously reported.[33]

^{1}H NMR (500 MHz, Chloroform-d_3): δ 7.24 (d, *J* = 8.6 Hz, 2H; Ar-H), 7.17 (dd, *J* = 7.5, 8.6 Hz, 2H, Ar-H), 6.80 (d, *J* = 8.6 Hz, 2H; Ar-H), 6.72 (t, *J* = 7.5 Hz, 1H; Ar-H), 6.63 (d, *J* = 8.6 Hz, 2H; Ar-H), 4.24 (s, 2H; N-CH_2). ^{1}H NMR matched that previously reported.[33]

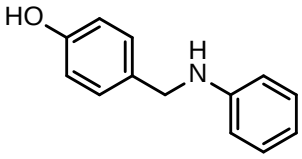

Figure 1.11 ^{1}H NMR spectrum of compound **1.33** [500 MHz, Methanol-d_4]

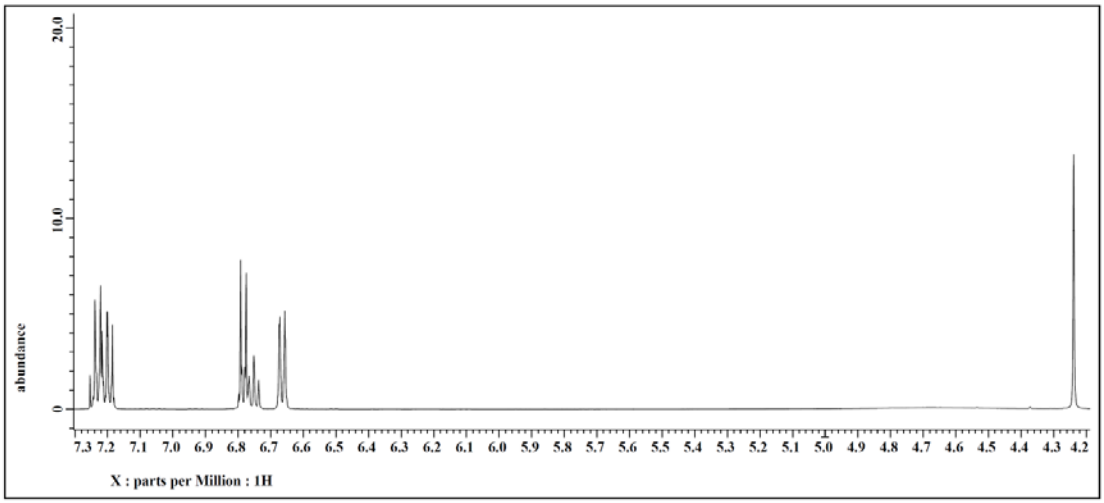

1.4.3 General Procedure for the synthesis of *p*-nitro sulfonamides (1.46-1.57).

A suspension of *p*-nitrobenzenesulfonyl chloride **1.17** (1.1 eq.), in CH_2Cl_2 (0.6 M), was added to a solution of the amine (1 eq.) and pyridine (2 eq.) in CH_2Cl_2 (0.9 M) and the mixture stirred for 24 hours. It was diluted with CH_2Cl_2 and extracted with 1M HCl and 10% $NaHCO_3$. The organic layer was dried and the solvent evaporated. Purification was done via flash column chromatography or recrystallization using an appropriate solvent or a mixture of solvents where enough volume of the more polar solvent was added to dissolve the crude mixture and the less polar solvent was added until reaching the saturation point.

***N*-Methyl-4-nitro-*N*-phenylbenzenesulfonamide (1.46)**. The crude product was purified via recrystallization using a mixture of ethyl acetate and hexane. Yield (0.677 g, 26%). ^{1}H NMR matched that previously reported.[34]

^{1}H NMR (500 MHz, Acetone-d_6): δ 8.39 (d, *J* = 8.6 Hz, 2H; Ar-H), 7.80 (d, *J* = 8.6 Hz, 2H; Ar-H), 7.35-7.29 (m, 3H; Ar-H), 7.14 (d, *J* = 8.0 Hz, 2H; Ar-H), 3.25 (s, 3H; N-CH_3).

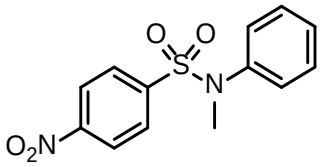

Figure 1.12 ^{1}H NMR spectrum of compound **1.46** [500 MHz, Acetone-d_6].

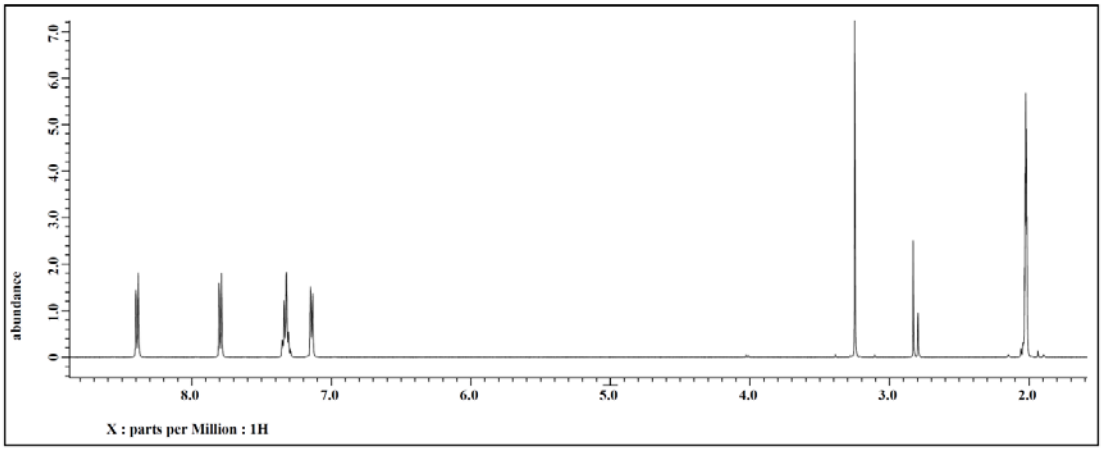

***N*-(2-Hydroxyethyl)-4-nitro-*N*-phenylbenzenesulfonamide (1.47)**. The crude product was purified via recrystallization using ethyl acetate. Yield (0.147 g, 10%).

^{1}H NMR (500 MHz, Acetone-d_6): δ 8.38 (dd, *J* = 2.3, 9.2 Hz, 2H; Ar-H), 7.88 (d, *J* = 9.2 Hz, 2H; Ar-H), 7.35-7.32 (m, 3H; Ar-H), 7.14 (dd, *J* = 2.3, 6.9 Hz, 2H; Ar-H), 3.91 (t, *J* = 5.7 Hz, 1H; O-H), 3.77 (t, *J* = 6.3 Hz, 2H; N-CH_2), 3.54 (q, *J* = 5.7 Hz, 2H; O-CH_2).

^{13}C NMR (125 MHz, Acetone-d_6): δ 150.3, 144.4, 139.1, 129.3 (2C), 129.2 (2C), 129.1(2C), 128.4 (2C), 124.3, 59.4, 53.6.

HRMS (ESI, m/z): Calculated for $C_{14}H_{15}N_2O_5S$ $[M + H]^+$ 323.0696; found 323.0691 (1.6 ppm).

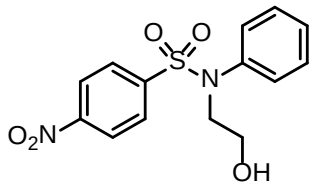

Figure 1.13 ^{1}H and ^{13}C NMR spectra of compound **1.47** [500 MHz for ^{1}H and 125 MHz for ^{13}C, Acetone-d_6].

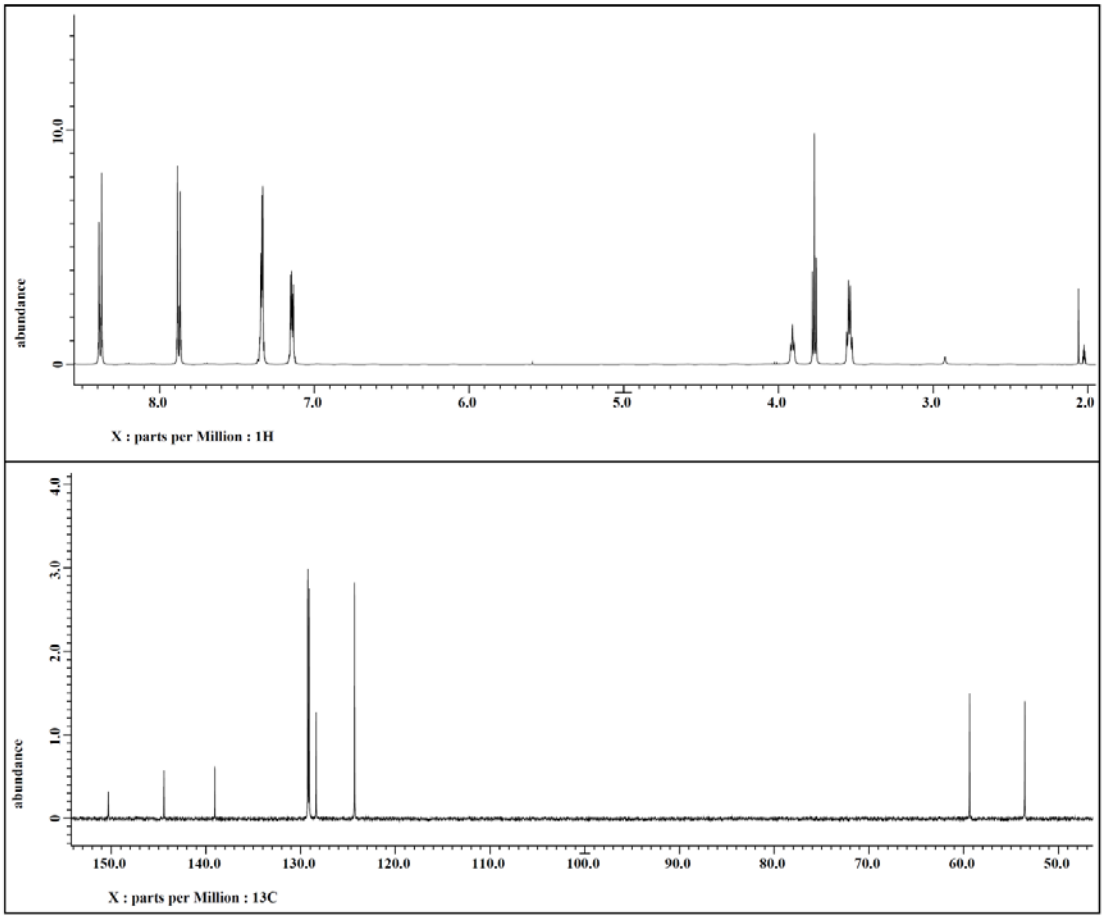

4-Nitro-*N*-phenyl-*N*-(pyridin-4-ylmethyl)benzenesulfonamide (1.48). The crude product was purified via recrystallization using ethyl acetate. Yield (0.193 g, 38%).

^{1}H NMR (500 MHz, Acetone-d_6): δ 8.45 (d, *J* = 6.3 Hz, 2H; Ar-H), 8.43 (d, *J* = 9.2 Hz, 2H; Ar-H), 7.94 (d, *J* = 8.6 Hz, 2H; Ar-H), δ 7.31 (d, *J* = 6.3 Hz, 2H; Ar-H), 7.29-7.25 (m, 3H, Ar-H), 7.17-7.15 (m, 2H, Ar-H), 4.96 (s, 2H, N-CH_2).

^{13}C NMR (125 MHz, Acetone-d_6): δ 150.6, 149.9 (2C), 145.3, 143.7, 138.5, 129.3 (2C), 129.2 (2C), 128.8 (2C), 128.4, 124.5 (2C), 123.0 (2C), 53.6.

HRMS (ESI, m/z): Calculated for $C_{18}H_{16}N_3O_4S$ $[M + H]^+$ 370.0856; found 370.0844 (3.3 ppm).

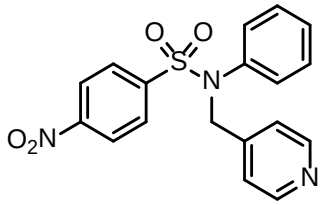

Figure 1.14 ^{1}H and ^{13}C NMR spectra of compound **1.48** [500 MHz for ^{1}H and 125 MHz for ^{13}C, Acetone-d_6].

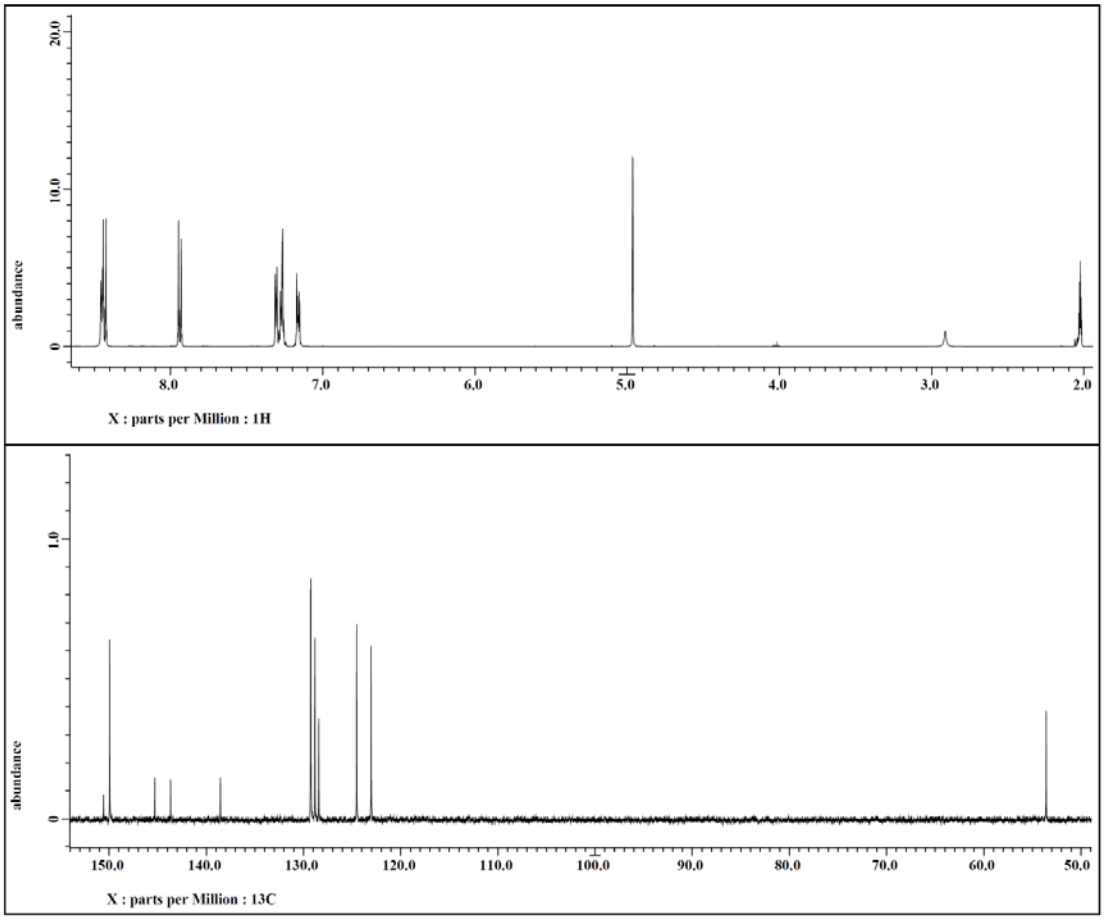

***N*-((5-(Hydroxymethyl)furan-2-yl)methyl)-4-nitro-*N*-phenylbenzenesulfonamide (1.49)**. The crude product was purified via recrystallization using a mixture of ethyl acetate in hexane. Yield (9.3 mg, 5%).

^{1}H NMR (500 MHz, Acetone-d_6): δ 8.38 (dd, *J* = 2.3, 8.6 Hz, 2H; Ar-H), 7.89 (dd, *J* = 2.3, 8.6 Hz, 2H, Ar-H), 7.31-7.26 (m, 3H; Ar-H), 7.05 (dd, *J* = 2.3, 8.0 Hz, 2H; Ar-H), 6.06 (d, *J* = 2.9 Hz, 1H; Fu-H), 6.03 (d, *J* = 2.9 Hz, 1H; Fu-H), 4.88 (s, 2H; N-CH_2), 4.36 (d, *J* = 5.7 Hz, 2H; N-CH_2), 4.21 (t, *J* = 5.7 Hz, 1H; O-H).

^{13}C NMR (125 MHz, Acetone-d_6): δ 156.1, 150.3, 148.6, 144.7, 138.7, 129.3 (2C), 129.2 (2C), 129.1 (4C), 128.5, 124.3 (2C), 110.7, 107.5, 56.3, 48.2.

HRMS (ESI, m/z): Calculated for $C_{18}H_{17}N_2O_6S$ $[M + H]^+$ 389.0802; found 389.0794 (2.0 ppm).

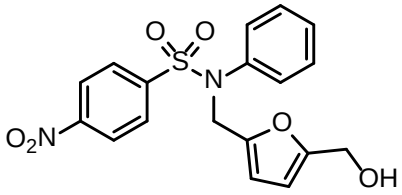

Figure 1.15 ^{1}H and ^{13}C NMR spectra of compound **1.49** [500 MHz for ^{1}H and 125 MHz for ^{13}C, Acetone-d_6].

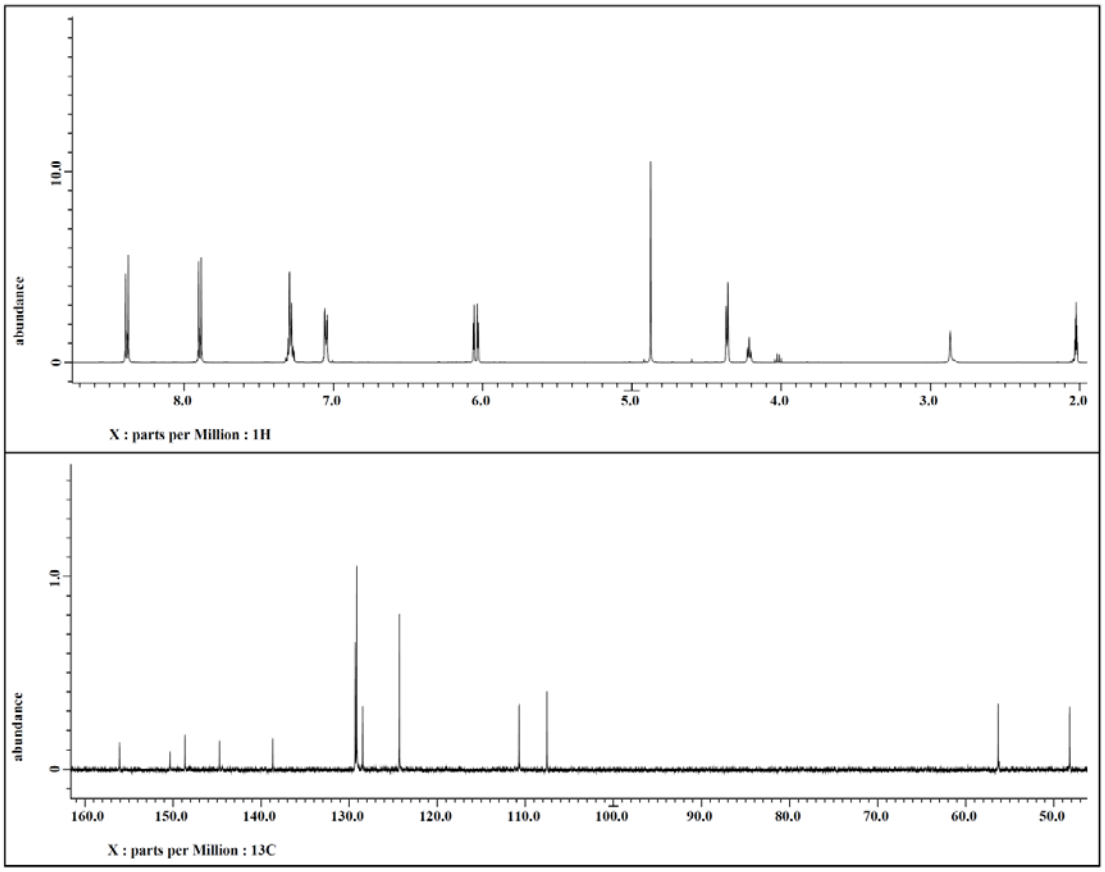

4-Nitro-*N*-phenylbenzenesulfonamide (1.50). The crude product was purified via recrystallization was done using ethyl acetate. Yield (68 mg, 5%). ^{1}H NMR matched that previously reported.[34]

^{1}H NMR (500 MHz, Acetone-d_6): δ 9.29 (s, 1H; NH), 8.35 (dd, *J* = 2.3, 8.6 Hz, 2H; Ar-H), 8.02 (dd, *J* = 2.3, 8.6 Hz, 2H; Ar-H), 7.28-7.24 (m, 2H; Ar-H), 7.21-7.19 (m, 2H; Ar-H), 7.12 (tt, *J* = 1.2, 7.5 Hz, 1H; Ar-H). ^{1}H NMR matched that previously reported.[34]

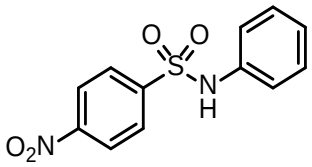

Figure 1.16 ^{1}H NMR spectrum of compound **1.50** [500 MHz, Acetone-d_6].

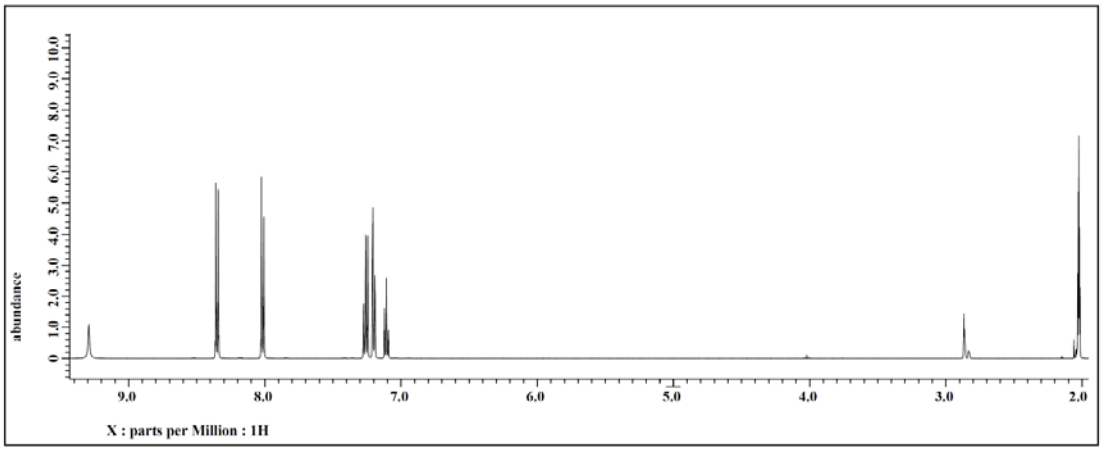

***N*-Methyl-4-nitro-*N*-(pyridin-4-yl)benzenesulfonamide (1.51)**. The crude product was purified via flash column chromatography. It eluted with ethyl acetate and hexane (0.75:1, v/v). Yield (0.366 g, 34%).

^{1}H NMR (500 MHz, Acetone-d_6): δ 8.49 (dd, *J* = 1.7, 4.6 Hz, 2H; Ar-H), 8.40 (dd, *J* = 2.3, 9.2 Hz, 2H; Ar-H), 7.90 (dd, *J* = 2.3, 9.2 Hz, 2H; Ar-H), 7.27 (dd, *J* = 1.7, 4.6 Hz, 2H; Ar-H), 3.34 (s, 3H; N-CH_2).

^{13}C NMR (125 MHz, Acetone-d_6): δ 150.8 (2C), 148.3, 141.93, 141.92, 129.1 (2C), 124.6 (2C), 118.6 (2C), 36.5.

HRMS (ESI, m/z): Calculated for $C_{12}H_{12}N_3O_4S$ $[M + H]^+$ 294.0543; found 294.0539 (1.4 ppm).

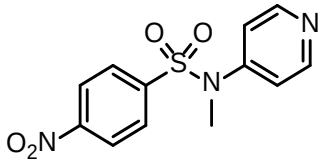

Figure 1.17 ^{1}H and ^{13}C NMR spectra of compound **1.51** [500 MHz for ^{1}H and 125 MHz for ^{13}C, Acetone-d_6].

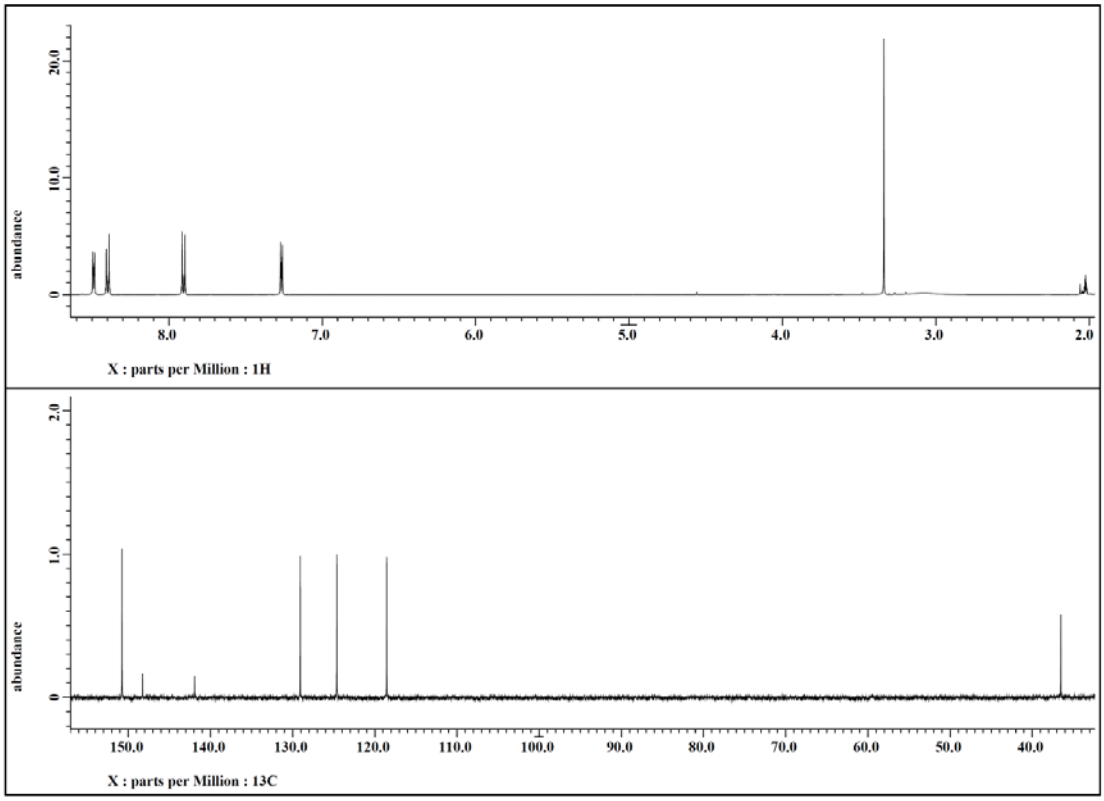

***N*-(2-Hydroxybenzyl)-4-nitro-*N*-phenylbenzenesulfonamide (1.52)**. The crude product was purified via recrystallization using a mixture of ethyl acetate and hexane. Yield (175 mg, 91%).

^{1}H NMR (400 MHz, Chloroform-d_3): δ 8.35 (d, J = 8.7 Hz, 2H; Ar-H), 7.88 (d, J = 8.7 Hz, 2H; Ar-H), 7.32-7.24 (m, 3H; Ar-H), δ 7.15 (dt, J_d = 1.8 Hz, J_t = 7.3 Hz, 1H; Ar-H), 6.95 (dd, J = 1.8, 8.0 Hz, 2H; Ar-H), 6.72 (dt, J_t = 1.8 Hz, J_d = 7.8 Hz, 1H; Ar-H), 6.68 (t, J = 7.8 Hz, 1H; Ar-H), 4.76 (s, 2H; N-CH_2).

^{13}C NMR (100 MHz, Acetone-d_6): δ 155.8, 151.1, 145.0, 139.7, 130.8, 129.9 (2C), 129.7 (2C), 129.6 (2C), 129.6, 128.8, 125.1, 122.7, 120.3, 115.9, 49.9.

HRMS (ESI, m/z): Calculated for $C_{19}H_{17}N_2O_5S$ $[M + H]^+$ 385.0853; found 385.0845 (2.0 ppm).

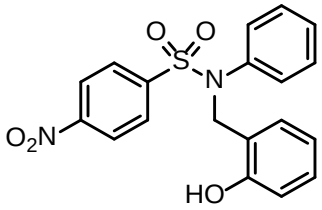

Figure 1.18 ^{1}H and ^{13}C NMR spectra of compound **1.52** [400 MHz for ^{1}H, Chloroform-d_3 and 100 MHz for ^{13}C, Acetone-d_6].

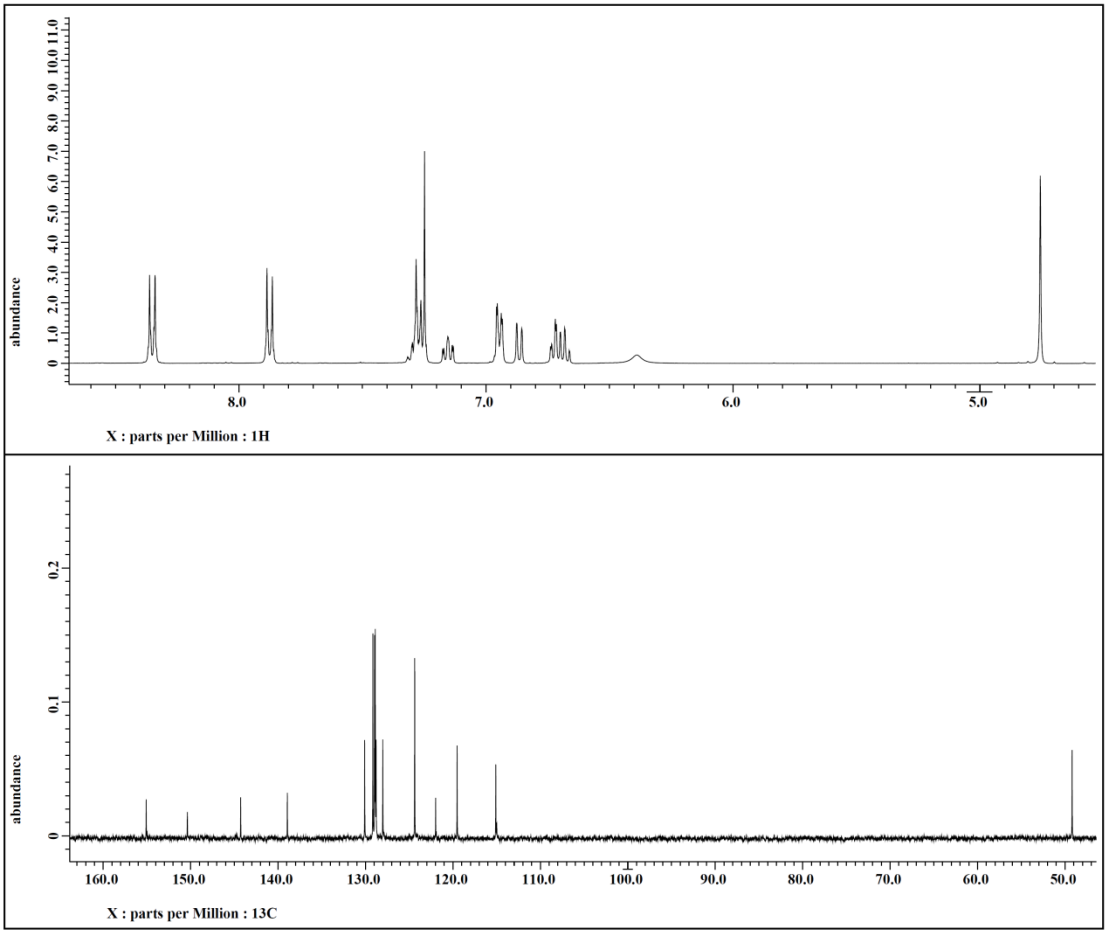

***N*-(3-Hydroxybenzyl)-4-nitro-*N*-phenylbenzenesulfonamide (1.53)**. The crude product was purified via recrystallization using a mixture of ethyl acetate and hexane. Yield (260 mg, 67%).

^{1}H NMR (500 MHz, DMSO-d_6) δ. 9.35 (bs, 1H; Ar-OH), 8.38 (d, *J* = 8.6 Hz, 2H; Ar-H), 7.87 (d, *J* = 8.6 Hz, 2H; Ar-H), 7.27-7.21 (m, 3H; Ar-H), 7.05 (d, *J* = 7.5 Hz, 2H; Ar-H), 7.00 (dd, *J* = 7.5, 8.0 Hz, 1H; Ar-H), 6.68 (s, 1H; Ar-H), 6.60 (d, *J* = 7.5 Hz, 1H; Ar-H), 6.56 (d, *J* = 8.0 Hz, 1H; Ar-H), 4.73 (s, 2H; N-CH_2).

^{13}C NMR (125 MHz, DMSO-d_6) δ. 157.9, 150.5, 143.8, 138.6, 137.7, 129.9, 129.6 (2C), 129.5 (2C), 129.1 (2C), 128.6, 125.2 (2C), 119.2, 115.4, 115.1, 54.4.

HRMS (ESI, m/z): calculated for $C_{19}H_{17}N_2O_5S$ $[M + H]^+$ 385.0853; found 385.0843 (2.5 ppm).

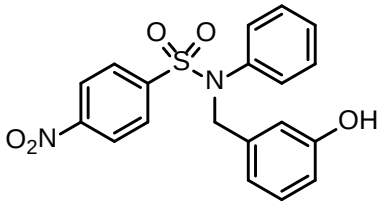

Figure 1.19 ^{1}H and ^{13}C NMR spectra of compound **1.53** [500 MHz for ^{1}H and 125 MHz for ^{13}C, DMSO-d_6].

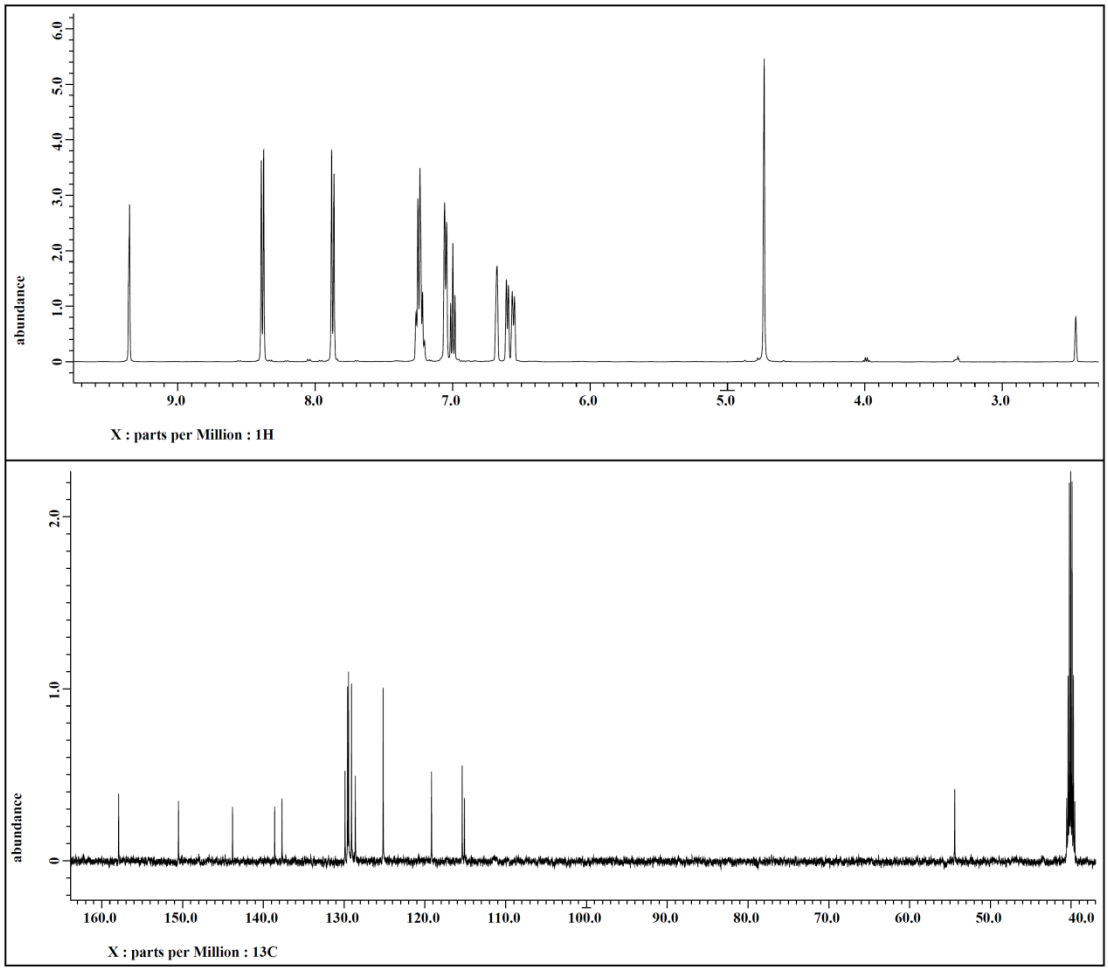

***N*-(4-Hydroxybenzyl)-4-nitro-*N*-phenylbenzenesulfonamide (1.54)**. Purification was done via flash column chromatography using ethyl acetate in hexane (0.2:1 % v/v). Yield (106 mg, 45%).

^{1}H NMR (500 MHz, Methanol-d_4): δ 8.38 (d, *J* = 9.2 Hz, 2H; Ar-H), 7.86 (d, *J* = 9.2 Hz, 2H; Ar-H), 7.22-7.21 (m, 3H; Ar-H), 6.99 (d, *J* = 8.6 Hz, 2H; Ar-H), 6.95-6.93 (m, 2H; Ar-H), 6.59 (d, *J* = 8.6 Hz, 2H; Ar-H), 4.71 (s, 2H; N-CH_2).

^{13}C NMR (125 MHz, Methanol-d_4) δ 156.9, 150.3, 144.3, 138.3, 129.9 (2C), 129.1 (2C), 128.8 (2C), 128.7 (2C), 128.0, 126.3, 124.0 (2C), 114.8 (2C), 54.3.

HRMS (ESI, m/z): Calculated for $C_{19}H_{17}N_2O_5S$ $[M + H]^+$ 385.0853; found 385.0845 (2.0 ppm).

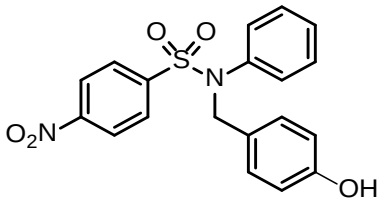

Figure 1.20 ^{1}H and ^{13}C NMR spectra of compound **1.54** [500 MHz for ^{1}H and 125 MHz for ^{13}C, Methanol-d_4].

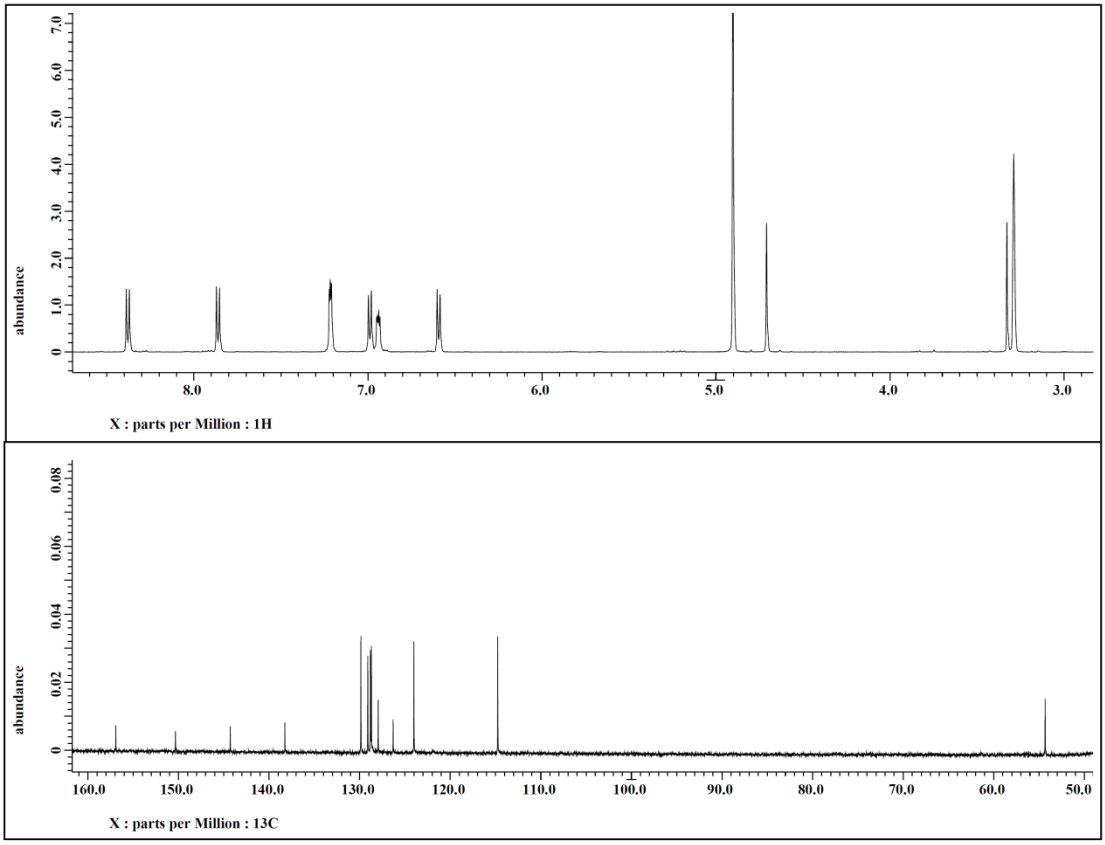

***N*-(2-(1*H*-Indol-3-yl)ethyl)-4-nitrobenzenesulfonamide (1.55)**. The crude product was purified via flash column chromatography over silica gel. It eluted using ethyl acetate in hexane (0.25:1 % v/v). Yield (38 mg, 45%).

^{1}H NMR (400 MHz, Chloroform-d_3): δ 8.10 (dd, *J* = 2.3, 9.2 Hz, 2H; Ar-H), 8.02 (bs, 1H; Indole-NH), 7.75 (dd, *J* = 2.3, 9.2 Hz, 2H; Ar-H), 7.31 (d, *J* = 8.6 Hz, 2H; Ar-H), 7.16 (t, *J* = 7.5 Hz, 1H; Ar-H), 7.02 (d, *J* = 6.9 Hz, 1H; Ar-H), 6.99-6.98 (m, 1H; Ar-H), 4.46 (t, *J* = 5.7 Hz, 1H; SO_2N-H), 3.35 (q, *J* = 6.3 Hz, 2H; N-CH_2), 2.96 (t, *J* = 6.3 Hz, 2H; Ar-CH_2).

^{13}C NMR (100 MHz, Chloroform-d_3): δ 149.7, 145.3, 136.5, 128.0 (2C), 126.6, 124.0 (2C), 122.7, 122.7, 119.8, 118.4, 11.5, 111.2, 43.1, 25.6.

HRMS (ESI, m/z): Calculated for $C_{16}H_{16}N_3O_4S$ $[M + H]^+$ 346.0856; found 346.0851 (1.5 ppm).

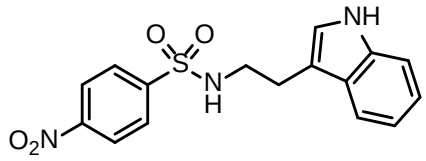

Figure 1.21 ^{1}H and ^{13}C NMR spectra of compound **1.55** [400 MHz for ^{1}H and 100 MHz for ^{13}C, Chloroform-d_3].

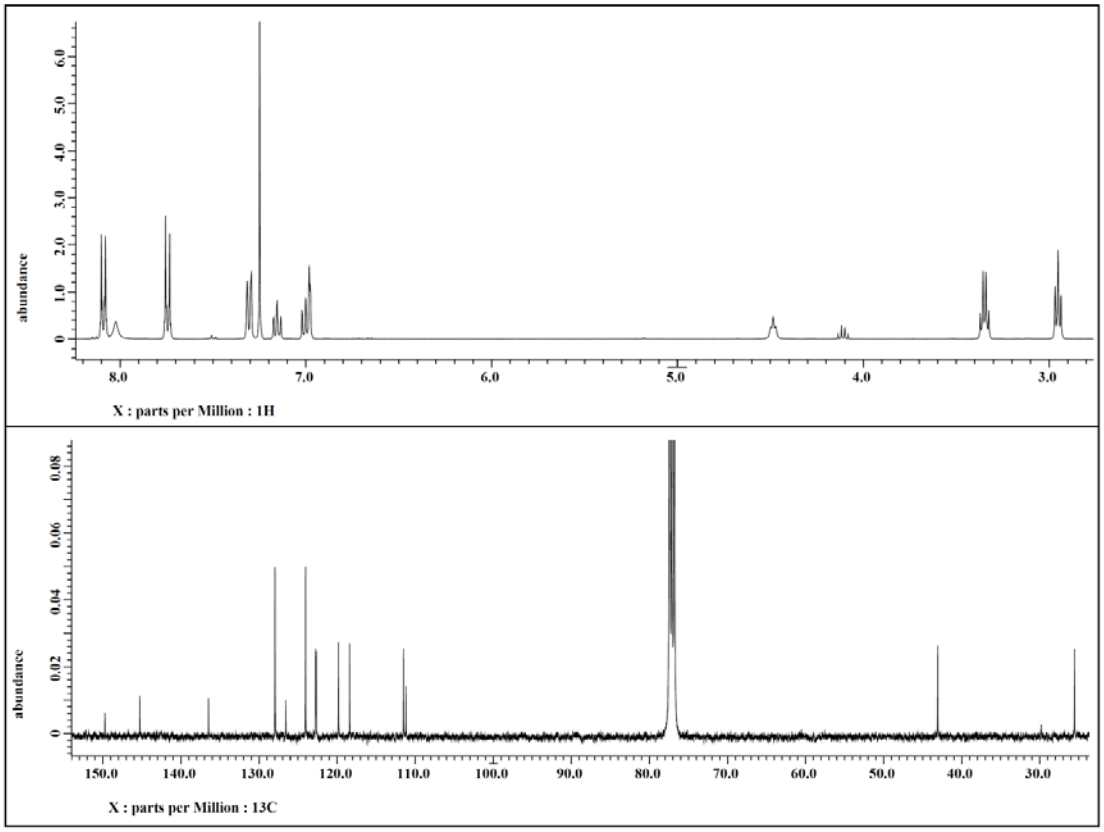

***N*-(2-Hydroxyethyl)-4-nitrobenzenesulfonamide (1.56)**. Purification was done via recrystallization using a mixture of ethyl acetate and hexane. Yield (658 mg, 54%).

^{1}H NMR (500 MHz, Methanol-d_4): δ 8.39 (d, *J* = 8.6 Hz, 2H; Ar-H), 8.08 (d, *J* = 8.6 Hz, 2H; Ar-H), 3.52 (t, *J* = 5.7 Hz, 2H; O-CH_2), 3.00 (t, *J* = 5.7 Hz, 2H; N-CH_2).

^{13}C NMR (125 MHz, Methanol-d_4) δ 150.0, 146.6, 128.1 (2C), 124.1 (2C), 60.5, 45.0.

HRMS (ESI, m/z): Calculated for $C_8H_{11}N_2O_5S$ $[M + H]^+$ 247.0383; found 247.0379 (1.7 ppm).

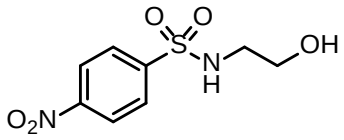

Figure 1.22 ^{1}H and ^{13}C NMR spectra of compound **1.56** [500 MHz for ^{1}H and 125 MHz for ^{13}C, Methanol-d_4].

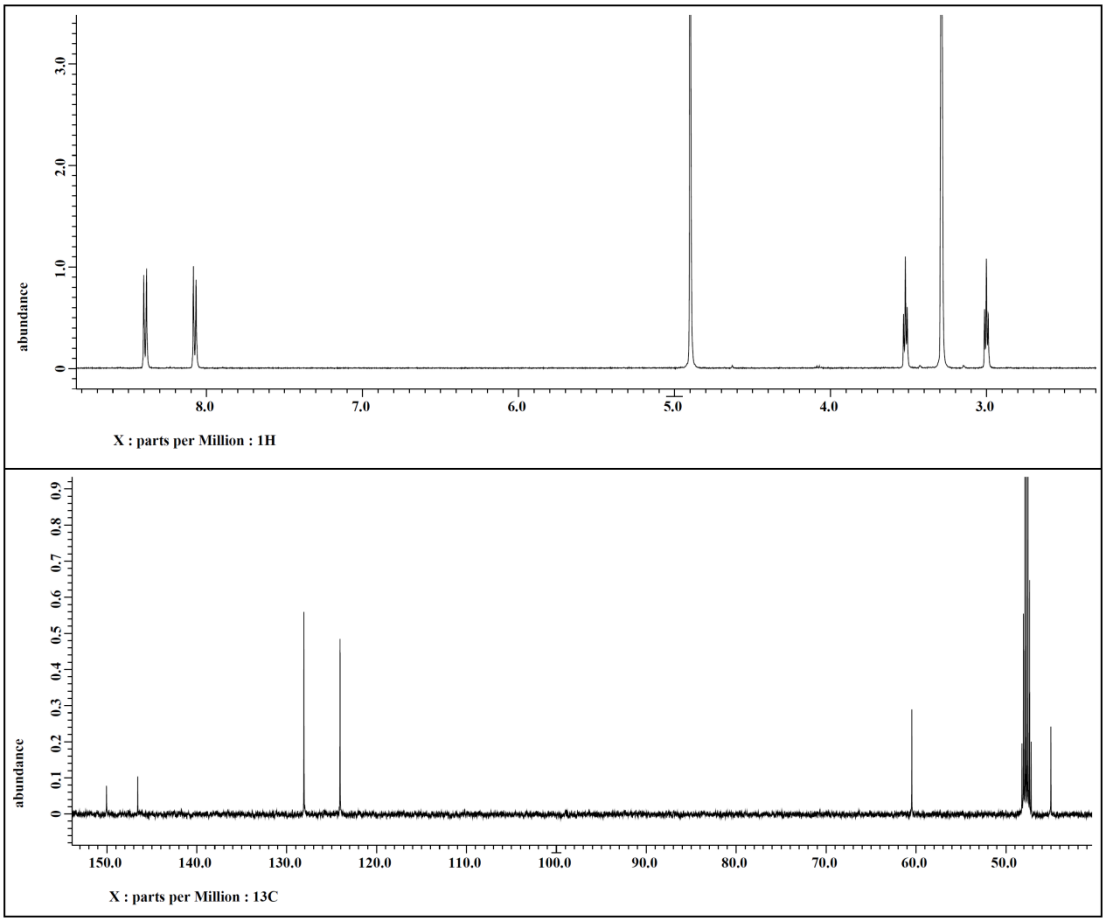

***N*-(2,3-Dihydroxypropyl)-4-nitrobenzenesulfonamide (1.57)**. The crude product was purified via flash column chromatography over silica gel. It eluted using 70% ethyl acetate in hexane. Yield (69 mg, 45%). ^{1}H NMR matched that previously reported.[35]

^{1}H NMR (500 MHz, Methanol-d_4): δ 8.39 (d, *J* = 8.6 Hz, 2H; Ar-H), 8.08 (d, *J* = 8.6 Hz, 2H; Ar-H), 3.60 (p, *J* = 5.2 Hz, 1H; O-CH) 3.47-3.41 (m, 2H; O-CH_2), 3.07 (dd, *J* = 5.2, 13.2 Hz, 1H; N-CH_2), 2.86 (dd, *J* = 6.9, 13.2 Hz, 1H; N-CH_2).

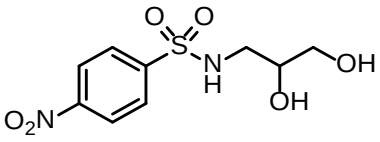

Figure 1.23 ^{1}H NMR spectrum of compound **1.57** [500 MHz, Methanol-d_4].

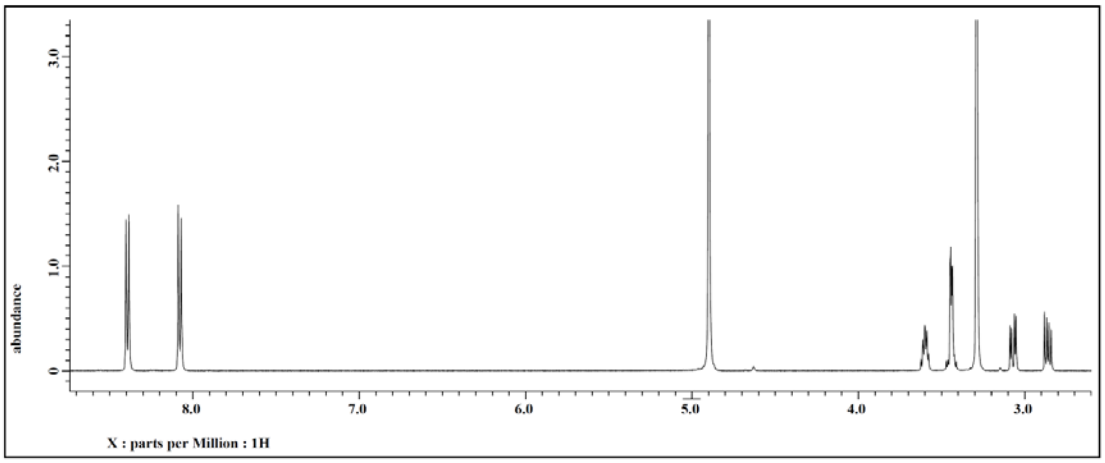

1.4.4 General procedure for the synthesis of *p*-amino sulfonamides (1.58-1.69).

Nitro-substituted benzenesulfonamide **1.46-1.57** was dissolved in MeOH (0.1 M) and hydrogenated (1 bar-H_2) over 50% w/w palladium on charcoal. The mixture was filtered through a pad of celite and the solvent was evaporated under reduced pressure.

Purification was done via flash column chromatography or recrystallized using an appropriate solvent or mixture of solvents where enough volume of the more polar solvent was added to dissolve the crude mixture and the less polar solvent was added until reaching the saturation point.[36]

4-Amino-*N*-methyl-*N*-phenylbenzenesulfonamide (1.58). The crude product was purified via recrystallization using MeOH. Yield (210 mg, 12%). ^{1}H NMR matched that previously reported.[34]

^{1}H NMR (500 MHz, Acetone-d_6) δ 7.29 (d, *J* = 7.5 Hz, 1H; Ar-H), 7.27 (d, *J* = 6.9 Hz, 1H; Ar-H), 7.23-7.20 (m, 1H, Ar-H), 7.16 (d, *J* = 8.6 Hz, 2H; Ar-H), 7.12 (dd, *J* = 1.7, 7.5 Hz, 2H; Ar-H), 6.65 (d, *J* = 8.6 Hz, 2H; Ar-H), 5.53 (bs, 1H; N-H_2), 3.08 (s, 3H, N-CH_3).

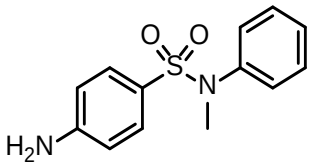

Figure 1.24 ^{1}H NMR spectrum of compound **1.58** [500 MHz, Acetone-d_6].

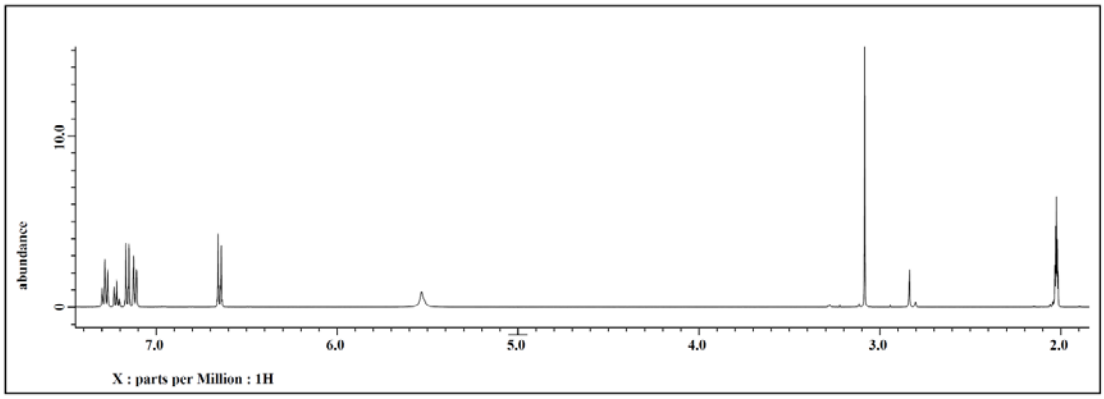

4-Amino-*N*-(2-hydroxyethyl)-*N*-phenylbenzenesulfonamide (1.59). The crude product was purified via recrystallization using a mixture of ethyl acetate and hexane. Yield (236 mg, 52%).

^{1}H NMR (400 MHz, Chloroform-d_3): δ 8.01 (d, *J* = 8.7 Hz, 2H; Ar-H), 7.79 (d, *J* = 8.7 Hz, 2H; Ar-H), 7.35-7.34 (m, 3H; Ar-H), 7.11-7.09 (m, 2H; Ar-H), 3.77 (t, *J* = 5.5 Hz, 2H; O-CH_2), 3.69 (t, *J* = 5.5 Hz, 2H; O-CH_2).

^{13}C NMR (100 MHz, Chloroform-d_3): 154.3, 140.6, 139.0, 129.6 (2C), 129.02 (2C), 129.00 (2C), 128.7, 123.6 (2C), 60.5, 53.8.

HRMS (ESI, m/z): Calculated for $C_{14}H_{16}N_2O_3S$ $[M + H]^+$ 293.0954; found 293.0946 (2.9 ppm).

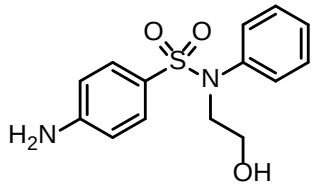

Figure 1.25 ^{1}H and ^{13}C NMR spectra of compound **1.59** [400 MHz for ^{1}H and 100 MHz for ^{13}C, Chloroform-d_3].

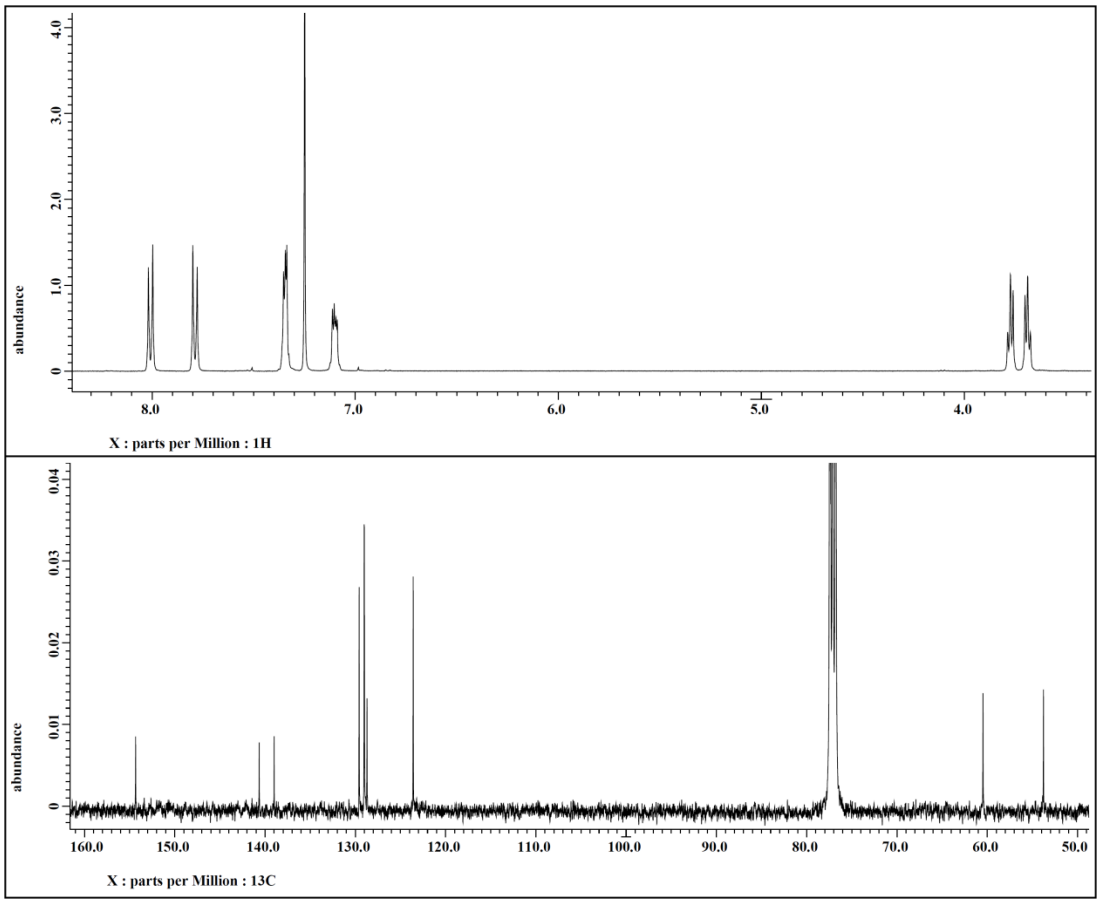

4-Amino-*N*-phenyl-*N*-(pyridin-4-ylmethyl)benzenesulfonamide (1.60). The crude product was purified via recrystallization using ethyl acetate. Yield (71 mg, 32%).

^{1}H NMR (500 MHz, Acetone-d_6): δ 8.42 (dd, *J* = 1.7, 4.6 Hz, 2H; Ar-H), 7.32-7.30 (m, 4H; Ar-H), 7.24-7.20 (m, 2H; Ar-H), 7.19-7.16 (m, 1H; Ar-H), 7.16-7.12 (m, *J* = 2H; Ar-H), 6.71 (dd, *J* = 2.3, 8.6 Hz, 2H; Ar-H), 5.62 (bs, 1H; N-H_2), 4.81 (s, 2H; N-CH_2).

^{13}C NMR (125 MHz, Acetone-d_6): δ 153.2, 149.8 (2C), 146.3, 139.9, 129.8 (2C), 128.7 (2C), 128.6 (2C), 127.5, 124.0, 123.1 (2C), 113.1, 52.8.

HRMS (ESI, m/z): calculated for $C_{18}H_{18}N_3O_2S$ $[M + H]^+$ 340.1114; found 340.1104 (3.0 ppm).

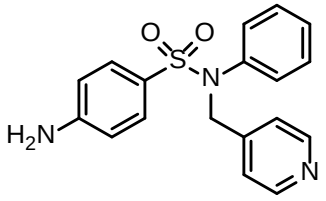

Figure 1.26 ^{1}H and ^{13}C NMR spectra of compound **1.60** [500 MHz for ^{1}H and 125 MHz for ^{13}C, Acetone-d_3].

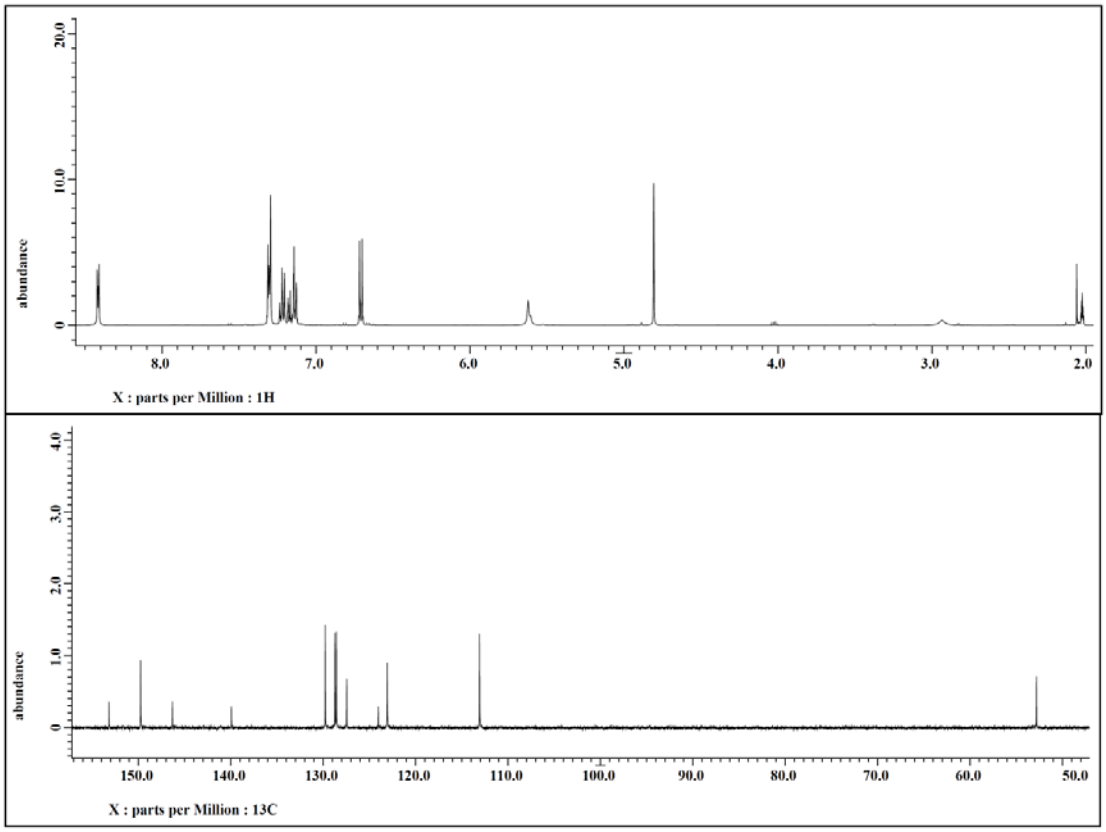

4-Amino-*N*-((5-(hydroxymethyl)furan-2-yl)methyl)-*N*-phenylbenzenesulfonamide (1.61). The crude product was purified via flash column chromatography. It eluted using ethyl acetate in hexane (0.4:1 % v/v). Yield (253 mg, 50%).

^{1}H NMR (400 MHz, Chloroform-d_3): δ 7.37 (d, *J* = 8.7 Hz, 2H; Ar-H), 7.25-7.22 (m, 3H; Ar-H), 7.02-6.99 (m, 2H; Ar-H), δ 6.60 (d, *J* = 8.7 Hz, 2H; Ar-H), 6.07 (d, *J* = 3.2 Hz, 1H; Ar-H), 5.99 (d, *J* = 3.2 Hz, 1H; Ar-H), 4.69 (s, 2H; O-CH_2), 4.44 (s, 2H; N-CH_2).

^{13}C NMR (125 MHz, Acetone-d_6): δ 155.5, 153.0, 149.4, 139.8, 129.8 (2C), 128.9 (2C), 128.6 (2C), 127.6, 124.6, 113.1 (2C), 110.0, 107.6, 56.4, 47.4.

HRMS (ESI, m/z): Calculated for $C_{18}H_{19}N_2O_4S$ $[M + H]^+$ 359.1060; found 359.1056 (1.1 ppm).

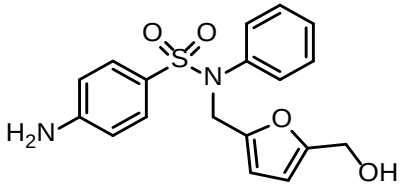

Figure 1.27 ^{1}H and ^{13}C NMR spectra of compound **1.61** [400 MHz for ^{1}H, Chloroform-d_3 and 125 MHz for ^{13}C, Acetone-d_3].

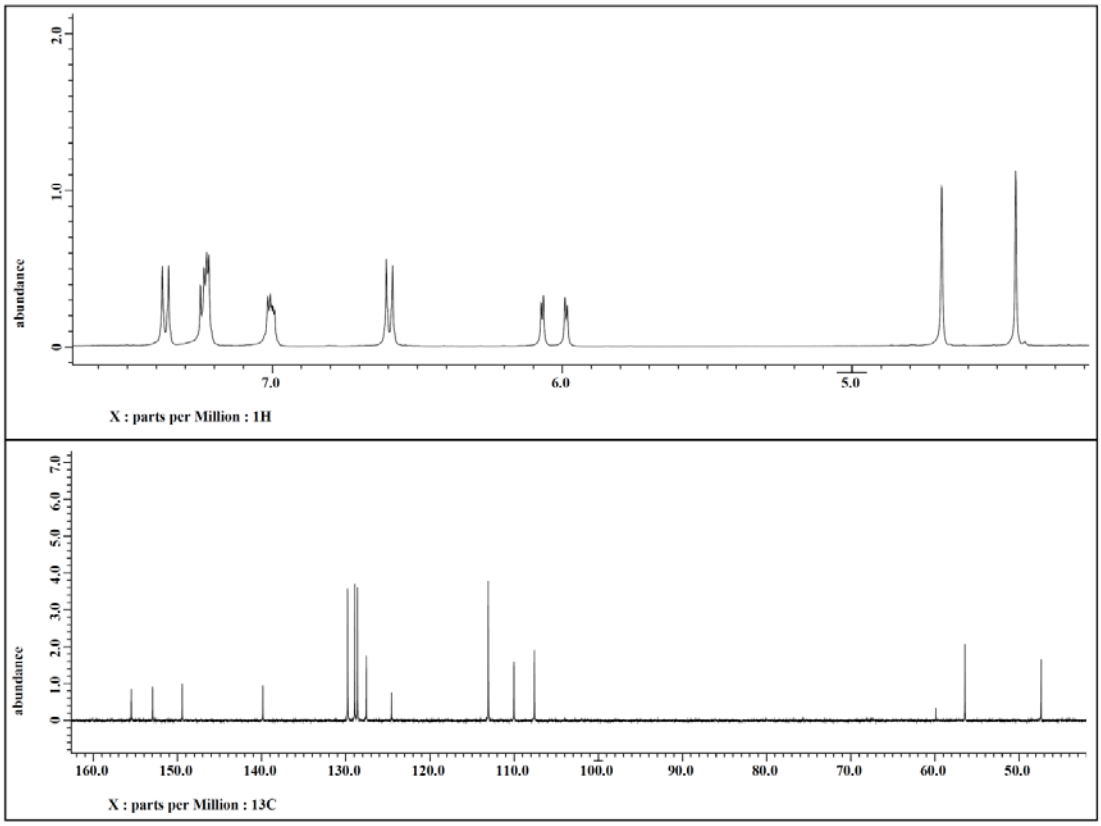

4-Amino-*N*-phenylbenzenesulfonamide (1.62). The crude product was purified via recrystallization using methanol. Yield (82 mg, 18%). ^{1}H NMR matched that previously reported.[34]

^{1}H NMR (500 MHz, Acetone-d_6): δ 8.63 (bs, 1H; Ar-NH_2), 7.44 (dd, *J* = 2.3, 8.6 Hz, 2H; Ar-H), 7.21-7.16 (m, 4H; Ar-H), 6.99 (tt, *J* = 1.7, 6.9 Hz, 1H; Ar-H), 6.62 (dd, *J* = 2.3, 8.6, 2H; Ar-H), 5.45 (bs, 1H; SO_2-NH).

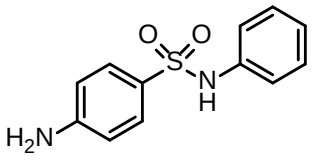

Figure 1.28 ^{1}H NMR spectrum of compound **1.62** [500 MHz, Acetone-d_3].

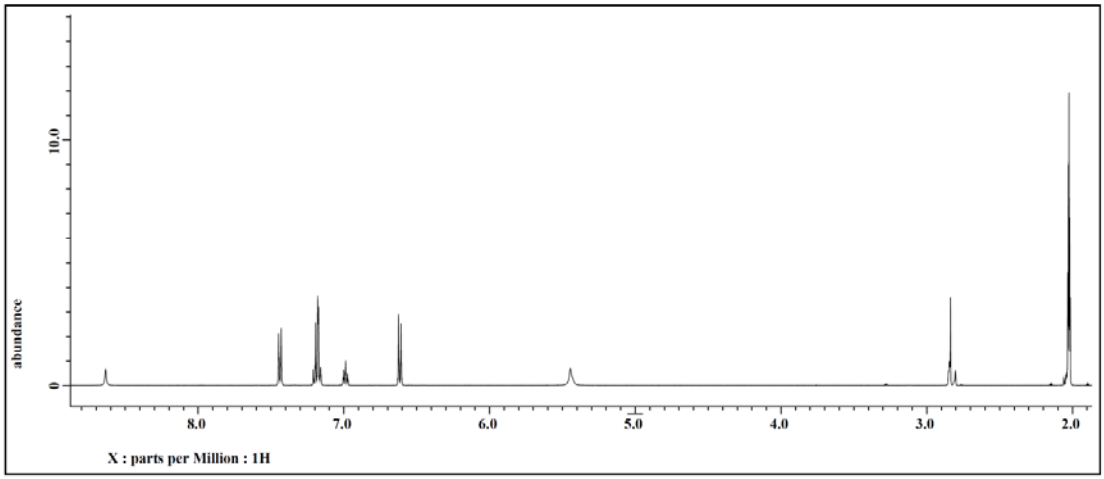

4-Amino-*N*-methyl-*N*-(pyridin-4-yl)benzenesulfonamide (1.63). Yield (0.107g, 73%).

^{1}H NMR (500 MHz, Acetone-d_3): δ 8.42 (dd, *J* = 1.7, 4.6 Hz, 2H; Ar-H), 7.29 (d, *J* = 2.3, 8.6 Hz, 2H; Ar-H), 7.25 (dd, *J* = 1.7, 4.6 Hz, 2H; Ar-H), 6.66 (d, *J* = 1.7, 8.6 Hz, 2H; Ar-H), 5.65 (d, *J* = 6.3 Hz, 1H; N-H_2), 3.20 (s, 3H; N-CH_3).

^{13}C NMR (125 MHz, Acetone-d_6): δ 153.5, 150.2 (2C), 149.3, 129.5 (2C), 122.5, 117.4 (2C), 113.1, 113.0, 113.0 (2C), 35.7.

HRMS (ESI, m/z): Calculated for $C_{12}H_{14}N_3O_2S$ $[M + H]^+$ 264.0801; found 264.0794 (2.7 ppm).

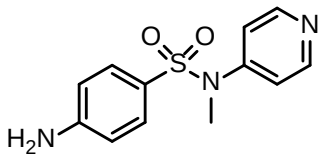

Figure 1.29 ^{1}H and ^{13}C NMR spectra of compound **1.63** [500 MHz for ^{1}H and 125 MHz for ^{13}C, Acetone-d_3].

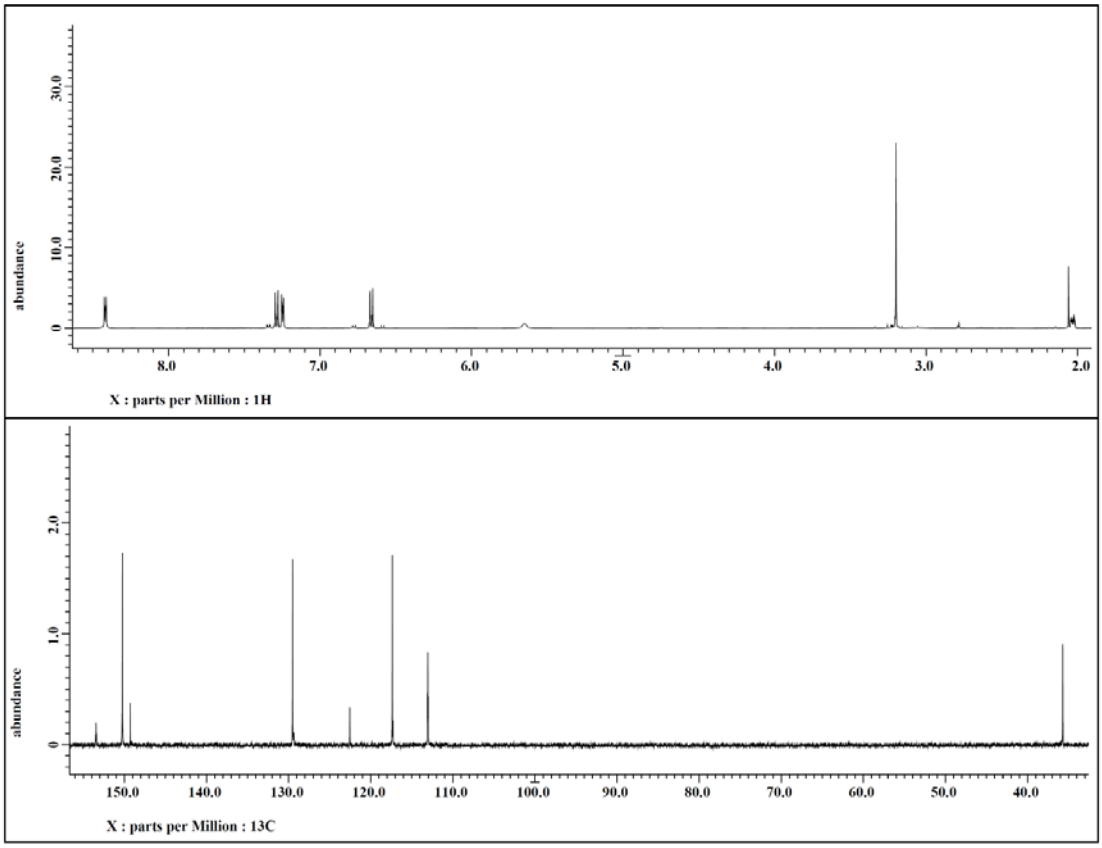

4-Amino-*N*-(2-hydroxybenzyl)-*N*-phenylbenzenesulfonamide (1.64). Purification was done via flash column chromatography using 30% ethyl acetate in hexane. Yield (70 mg, 76%).

^{1}H NMR (400 MHz, Methanol-d_4) δ 7.27 (d, J = 8.7 Hz, 2H; Ar-H), 7.19-7.13 (m, 4H; Ar-H), 7.02 (dd, J = 1.8, 7.8 Hz, 2H; Ar-H), 6.93 (dt, J_d =1.8 Hz, J_t = 7.8 Hz, 2H; Ar-H), 6.66-6.59 (m, 4H; Ar-H), 4.72 (s, 2H; N-CH_2).

^{13}C NMR (100 MHz, Acetonitrile-d_3) δ: 155.0, 152.8, 139.6, 130.2, 129.8 (2C), 129.0, 128.7 (2C), 128.6 (2C), 127.7, 124.1, 122.2, 119.8, 115.4, 113.2 (2C), 49.0.

HRMS (ESI, m/z): Calculated for $C_{19}H_{19}N_2O_3S$ $[M + H]^+$ 355.1111; found 355.1102 (2.5 ppm).

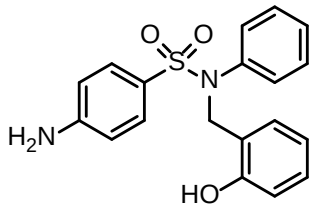

Figure 1.30 ^{1}H and ^{13}C NMR spectra of compound **1.64** [400 MHz for ^{1}H, Methanol-d_4 and 100 MHz for ^{13}C, Acetonitrile-d_3].

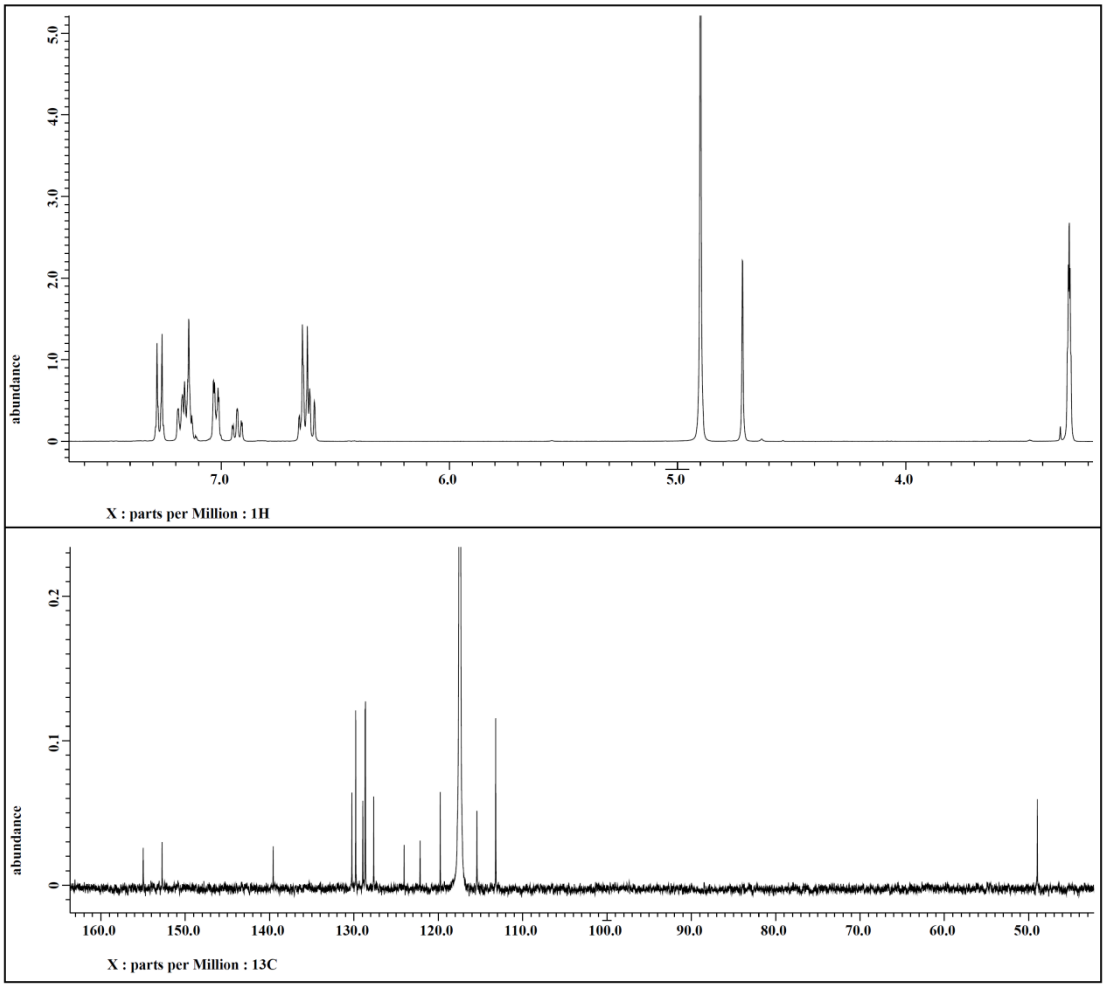

4-Amino-*N*-(3-hydroxybenzyl)-*N*-phenylbenzenesulfonamide (1.65). Purification was done via flash column chromatography using 30% ethyl acetate in hexane. Yield (63 mg, 68%).

^{1}H NMR (400 MHz, Methanol-d_4): δ 7.27 (d, *J* = 8.7 Hz, 2H; Ar-H), 7.19-7.13 (m, 3H; Ar-H), 7.00-6.94 (m, 3H; Ar-H), 6.69 (s, 1H; Ar-H), 6.63 (m, 3H; Ar-H), 6.55 (dd, *J* = 1.8, 7.8 Hz, 1H; Ar-H), 4.6 (s, 1H; N-CH_2).

^{13}C NMR (125 MHz, Acetone-d_6): δ 157.1, 153.2, 139.5, 138.0, 129.5 (2C), 128.9 (2C), 128.9 (2C), 128.3, 127.3, 123.8, 119.4, 115.0, 114.0, 112.9, 53.9.

HRMS (ESI, m/z): Calculated for $C_{19}H_{19}N_2O_3S$ $[M + H]^+$ 355.1111; found 355.1096 (4.2 ppm).

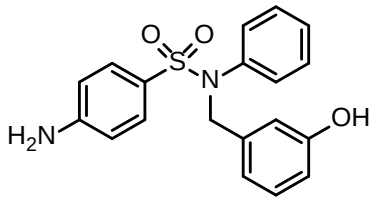

Figure 1.31 ^{1}H and ^{13}C NMR spectra of compound **1.65** [400 MHz for ^{1}H, Methanol-d_4 and 125 MHz for ^{13}C, Acetone-d_6].

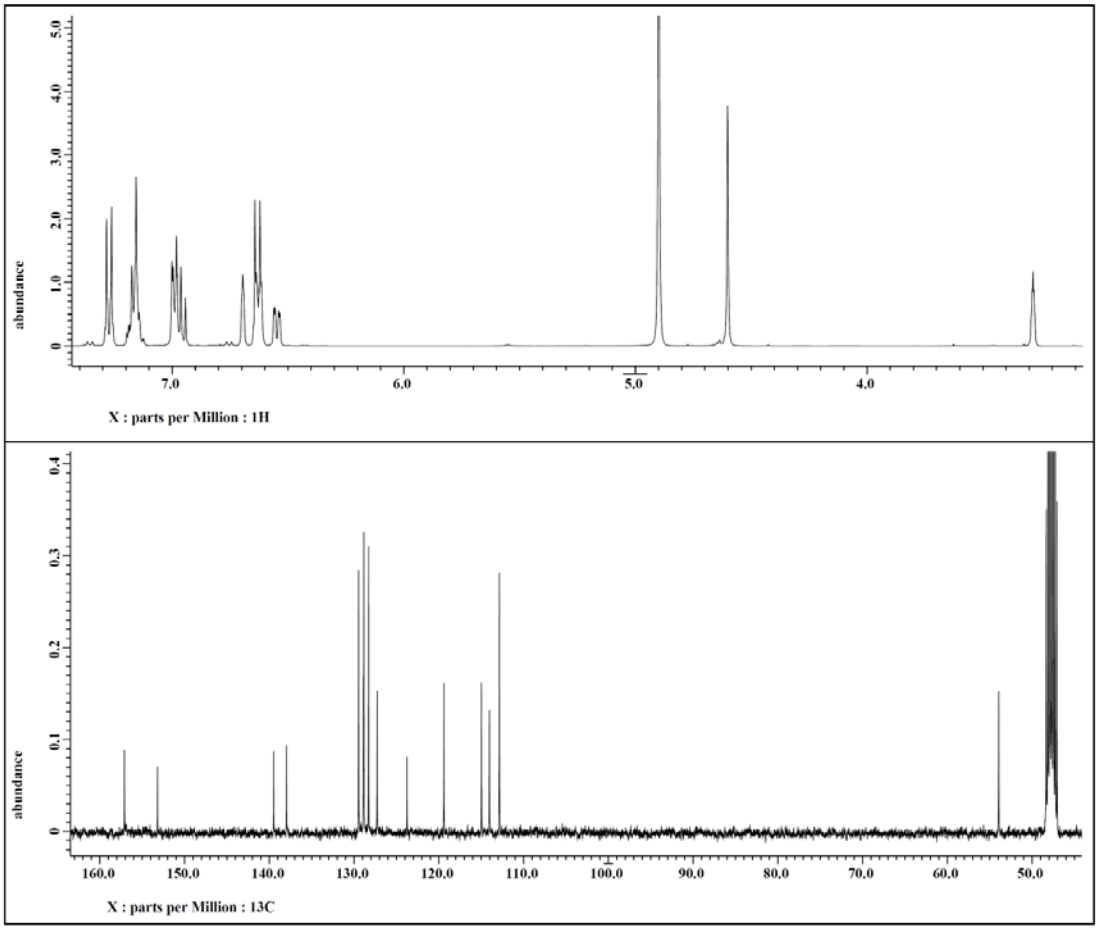

4-Amino-*N*-(4-hydroxybenzyl)-*N*-phenylbenzenesulfonamide (1.66). Purification was done via flash column chromatography using 30% ethyl acetate in hexane. Yield (35.5 mg, 47%).

^{1}H NMR (400 MHz, Acetonitrile-d_3): δ 7.29 (d, *J* = 8.7 Hz, 2H; Ar-H), 7.22-7.15 (m, 3H; Ar-H), 7.02-6.97 (m, 4H; Ar-H), 6.83 (s, 1H; Ar-OH), 6.64 (d, *J* = 8.7 Hz, 2H; Ar-H), 6.60 (d, *J* = 8.2 Hz, 2H; Ar-H), 4.85 (bs, 2H; Ar-NH_2), 4.57 (s, 2H; N-CH_2).

^{13}C NMR (100 MHz, Acetonitrile-d_3): δ 156.3, 152.6, 139.6, 129.9 (2C), 129.7 (2C), 129.0 (2C), 128.6 (2C), 127.7, 127.5, 124.7, 115.0 (2C), 113.2 (2C), 53.3.

HRMS (ESI, m/z): Calculated for $C_{19}H_{19}N_2O_3S$ $[M + H]^+$ 355.1111; found 355.1108 (0.8 ppm).

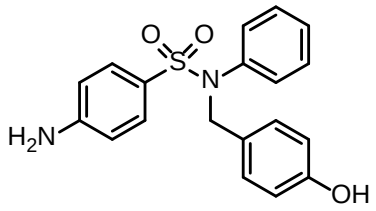

Figure 1.32 ^{1}H and ^{13}C NMR spectra of compound **1.66** [400 MHz for ^{1}H and 100 MHz for ^{13}C, Acetonitrile-d_3].

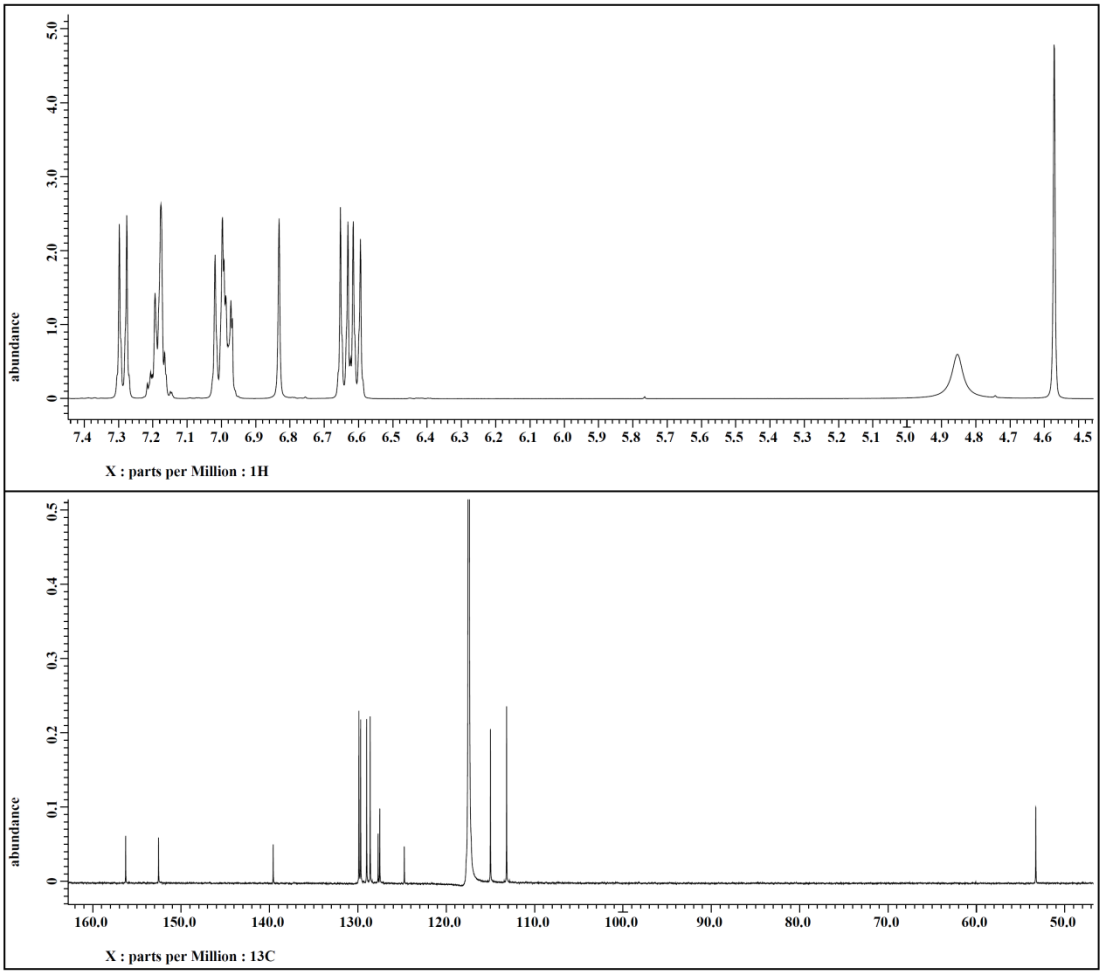

***N*-(2-(1*H*-Indol-3-yl)ethyl)-4-aminobenzenesulfonamide (1.67)**. Purification was done via flash column chromatography using 50% ethyl acetate in hexane. Yield (56.8 mg, 41%).

^{1}H NMR (400 MHz, Methanol-d_4): δ 7.48 (d, *J* = 8.7 Hz, 2H; Ar-H), 7.37 (d, *J* = 7.8 Hz, 1H; Ar-H), 7.27 (d, *J* = 7.8 Hz, 1H; Ar-H), 7.03 (t, *J* = 7.3 Hz, 1H; Ar-H), 6.95 (s, 1H; Ar-H), 6.93 (t, *J* = 7.8 Hz, 1H; Ar-H), 6.64 (d, *J* = 8.7 Hz, 2H; Ar-H), 3.05 (dd, *J* = 7.3, 7.8 Hz, 2H; N-CH_2), 2.82 (dd, *J* = 7.3, 7.8 Hz, 2H; Ar-CH_2).

^{13}C NMR (100 MHz, Methanol-d_4): δ 152.7, 136.7, 128.6 (2C), 127.2, 126.2, 122.2, 121.0, 118.3, 117.8, 113.1 (2C), 111.4, 110.9, 43.6, 25.4.

HRMS (ESI, m/z): Calculated for $C_{16}H_{18}N_3O_2S$ $[M + H]^+$ 316.1114; found 316.1106 (2.6 ppm).

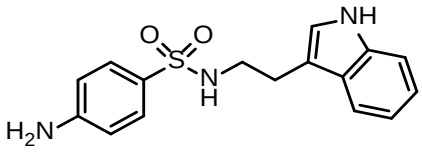

Figure 1.33 ^{1}H and ^{13}C NMR spectra of compound **1.67** [400 MHz for ^{1}H and 100 MHz for ^{13}C, Methanol-d_4].

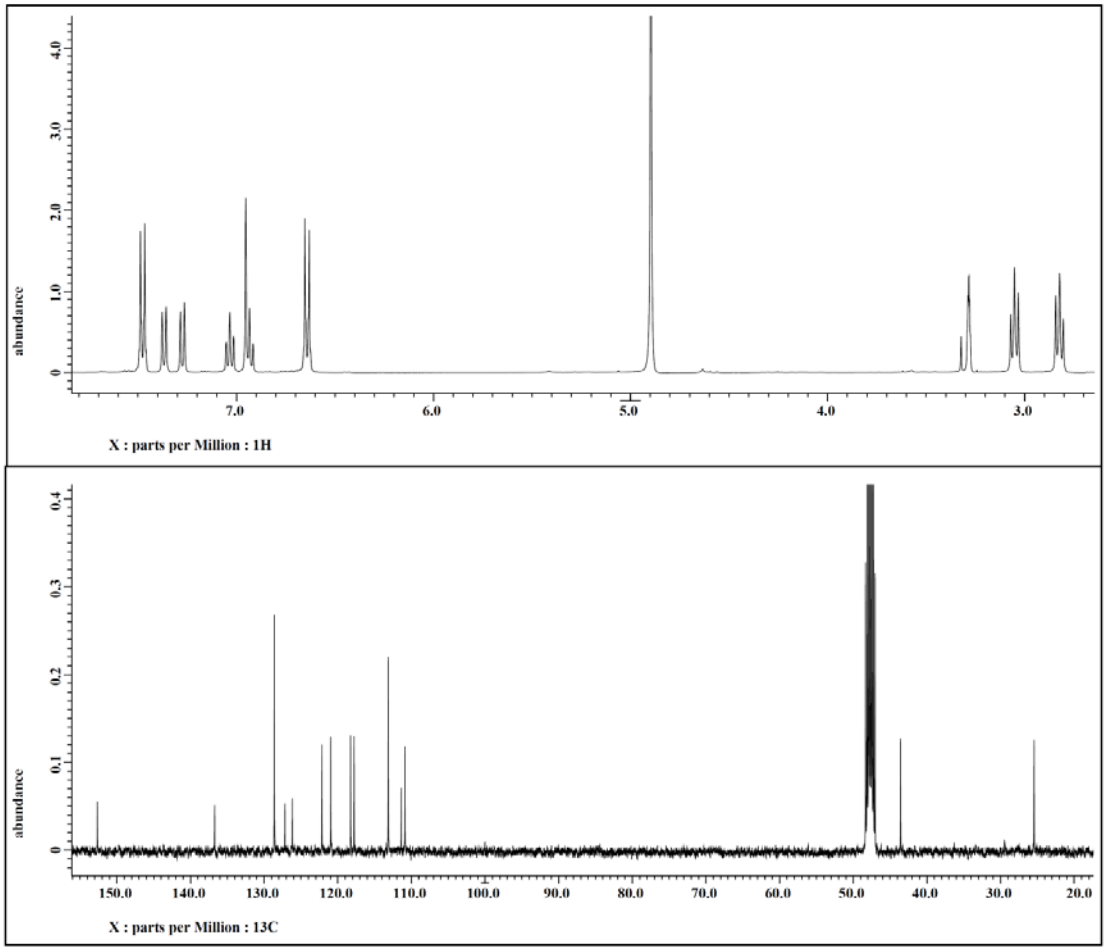

4-Amino-*N*-(2-hydroxyethyl)benzenesulfonamide (1.68). Purification was done via recrystallization using a mixture of ethyl acetate in hexane. Yield (118 mg, 34%).

^{1}H NMR (500 MHz, Methanol-d_4) δ: δ 7.51 (d, *J* = 8.6 Hz, 2H; Ar-H), 6.68 (d, *J* = 8.6 Hz, 2H; Ar-H), 3.51 (t, *J* = 5.7 Hz, 2H; O-CH_2), 2.87 (t, *J* = 5.7 Hz, 2H; N-CH_2).

^{13}C NMR (125 MHz, Methanol-d_4): δ 152.8, 128.6 (2C), 125.9, 113.1 (2C), 60.5, 44.8.

HRMS (ESI, m/z): Calculated for $C_8H_{13}N_2O_3S$ $[M + H]^+$ 217.0641; found 217.0637 (2.0 ppm).

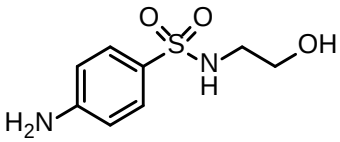

Figure 1.34 ^{1}H and ^{13}C NMR spectra of compound **1.68** [500 MHz for ^{1}H and 125 MHz for ^{13}C, Methanol-d_4].

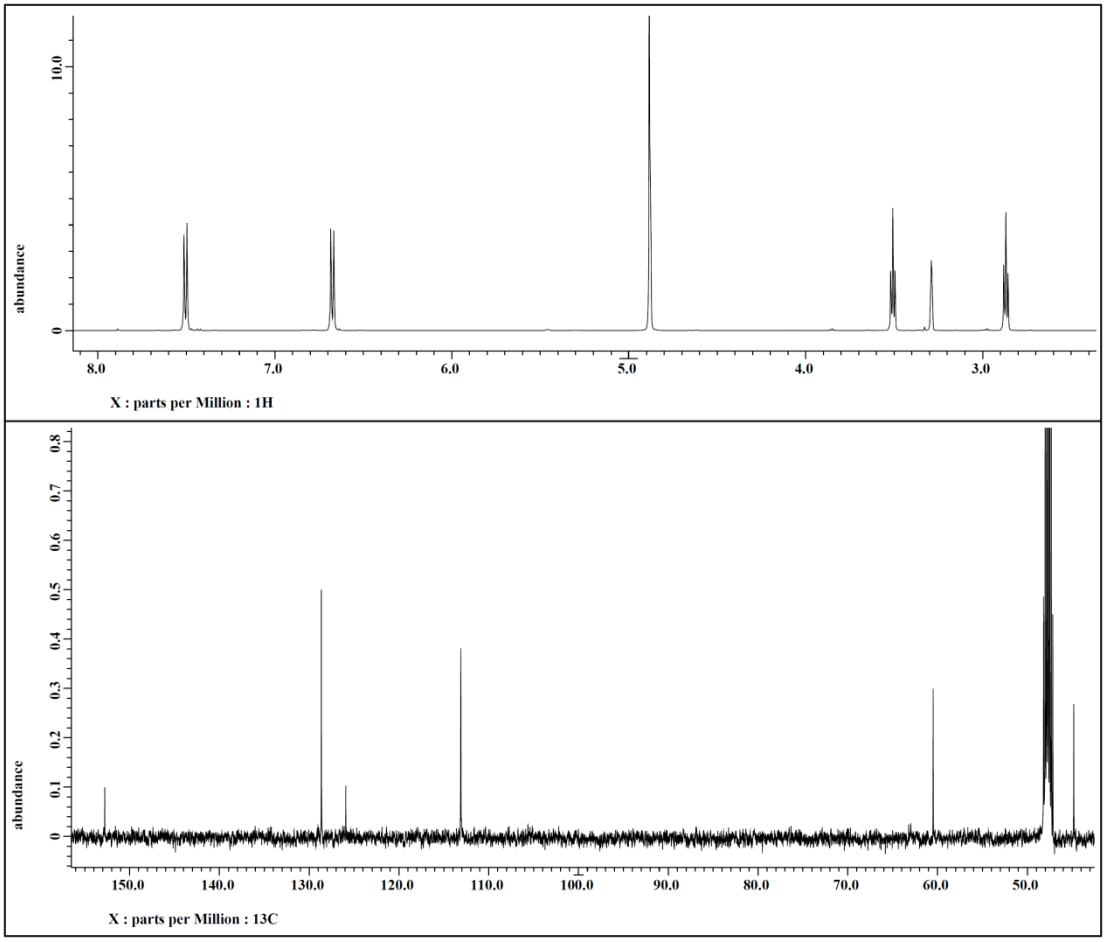

4-Amino-*N*-(2,3-dihydroxypropyl)benzenesulfonamide (1.69). Purification was done via flash column chromatography using 100% ethyl acetate. Yield (47 mg, 92%). ^{1}H NMR matched that previously reported.[35]

^{1}H NMR (500 MHz, Methanol-d_4): δ 7.51 (d, *J* = 8.6 Hz, 2H; Ar-H), 6.68 (d, *J* = 8.6 Hz, 2H; Ar-H), 3.62 (p, *J* = 5.2 Hz, 1H; CHO), 3.48 (dd, *J* = 4.6, 11.5 Hz, 1H; O-CH_2), 3.43 (dd, *J* = 4.6, 11.5 Hz, 1H; O-CH_2), 2.91 (dd, *J* = 5.2, 13.2 Hz, 1H; N-CH_2), 2.74 (dd, *J* = 5.2, 13.2 Hz, 1H; N-CH_2).

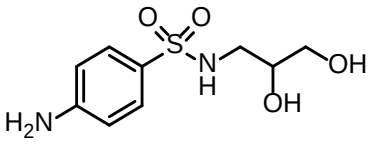

Figure 1.35 ^{1}H and ^{13}C NMR spectra of compound **1.69** [500 MHz, Methanol-d_4]

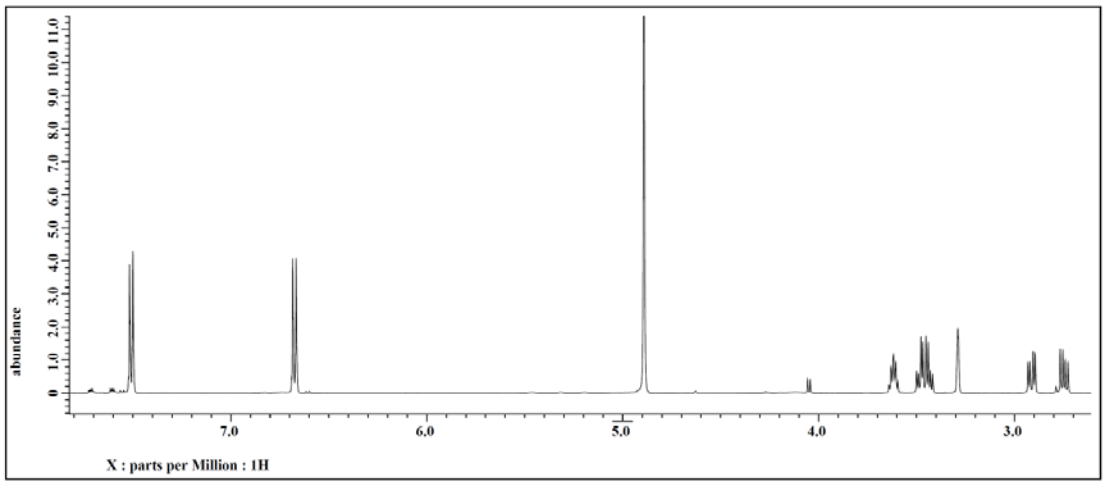

1.4.5 Synthesis of 6-(2-((*tert*-Butyldimethylsilyl)oxy)methyl)-2-naphthoic acid (1.41) and 6-(2-((*tert*-Butyldimethylsilyl)oxy)ethyl)-2-naphthoic acid (1.42).

(6-Bromonaphthalen-2-yl)methanol (1.35).[23]

Methyl 6-bromo-2-naphthoate (**1.34**) (1.5 g, 5.66 mmol) was dissolved in anhydrous THF and cooled to -40 $^{\circ}$C in CH_3CN/dry ice bath. DIBAL-H (17 mL, 17 mmol) was added drop wise and the mixture left stirring at ambient temperature for 8 hours. The mixture was then quenched using a saturated solution of NH_4Cl (15 mL) followed by extraction with CH_3Cl (100 mL x 2). The organic layers were combined, extracted with H_2O (100 mLx1), dried using anhydrous Na_2SO_4 and the solvent evaporated. Yield (1.194 g, 90%). ^{1}H NMR matched that previously reported.[37]

^{1}H NMR (500 MHz, Acetone-d_6) δ 8.07 (d, *J* = 1.7 Hz, 1H; Ar-H), 7.84-7.79 (m, 3H; Ar-H), 7.57-7.52 (m, 2H; Ar-H), 4.77 (s, 2H; O-CH_2), 4.85 (bs, 1H; O-H).

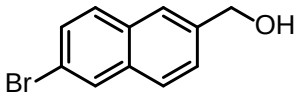

Figure 1.36 ^{1}H NMR spectrum of compound **1.35** [500 MHz, Acetone-d_6].

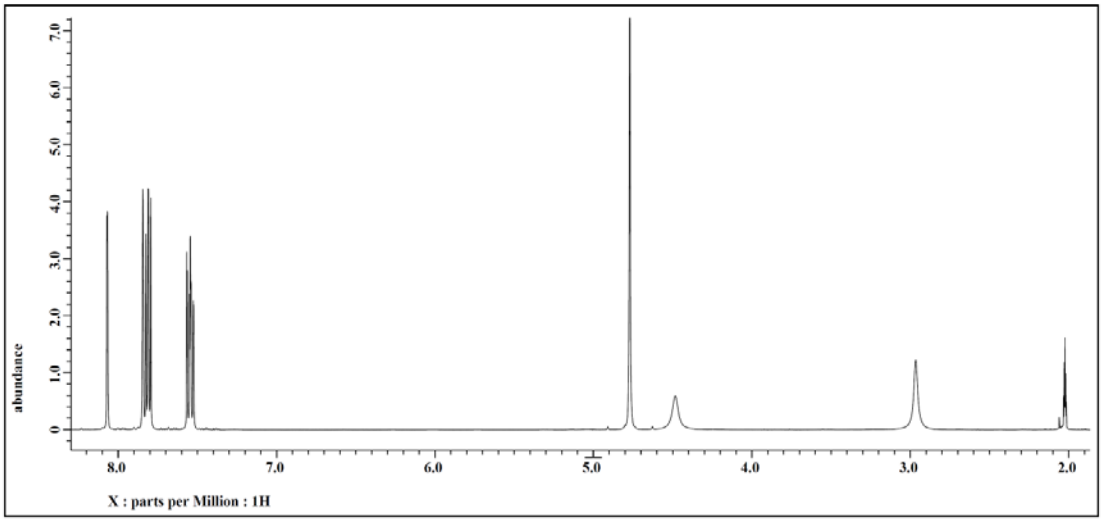

6-Bromo-2-naphthaldehyde (1.36).[38] DMSO (2.9 mL, 41.2 mmol) was added drop-wise to a solution of oxalyl chloride (1.77 mL, 20.58 mmol) in CH_2Cl_2 (65 mL) at -78 °C. A solution of (6-bromonaphthalen-2-yl)methanol (**1.35**) (1.22 g, 5.14 mmol) in CH_2Cl_2 (12 mL) was then added drop-wise and the mixture stirred for 15 minutes. Triethylamine (12.9 mL, 0.926 mmol) was then added to mixture drop-wise followed by H_2O (5 mL) after 15 minutes. The mixture was diluted with EtOAc (100 mL) and extracted with 20 $KHSO_3$ (100 mLx2) and brine (100 mL). The organic layer was dried and condensed under reduced pressure. Yield (724 mg, 60%). ^{1}H NMR matched that previously reported.[39]

^{1}H NMR (500 MHz, Acetone-d_6): δ 10.16 (s, 1H; O=CH), 8.52 (s, 1H; Ar-H), 8.24 (d, *J* = 2.3 Hz, 1H; Ar-H), 8.08 (d, *J* = 8.6 Hz, 1H; Ar-H), 8.02 (d, *J* = 8.6 Hz, 1H; Ar-H), 7.96 (dd, *J* = 1.2, 8.6 Hz, 1H; Ar-H), 7.74 (dd, *J* = 1.7, 8.6 Hz, 1H; Ar-H).

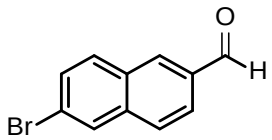

Figure 1.37 ^{1}H NMR spectrum of compound **1.36** [500 MHz, Acetone-d_6].

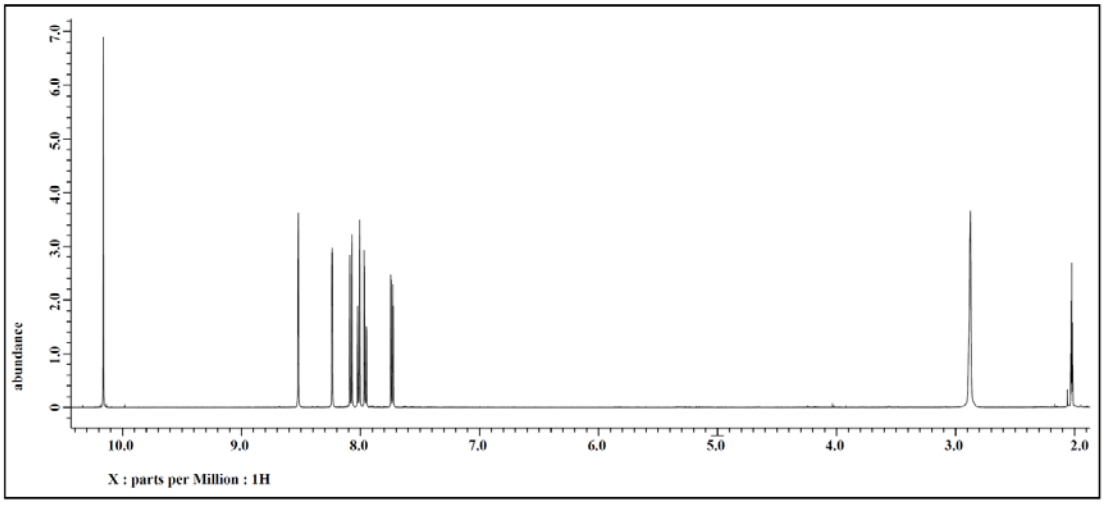

2-Bromo-6-vinylnaphthalene (1.37).[25] Sodium hydride (0.299 g, 12.46 mmol) was added to a suspension of 6-bromo-2-naphthaldehyde (**1.36**) (0.586 g, 2.49 mmol) and triphenylphosphonium iodide (1.61 g, 3.99 mmol) in anhydrous THF (30 mL) and the mixture stirred for 25 hours. The mixture was diluted with $CHCl_3$ (30 mL) and extracted with brine (100 mL x 3). The organic layer was dried using anhydrous Na_2SO_4 and condensed under reduced pressure. The solid residue was purified via flash column chromatography (5% Ethyl acetate/Hexane) to afford the desired product. Yield (377 mg, 65%). ^{1}H NMR matched that previously reported.[40]

^{1}H NMR (400 MHz, Chloroform-d_3): δ 7.95 (d, *J* = 1.8 Hz, 1H; Ar-H), 7.70-7.63 (m, 4H; Ar-H), 7.52 (dd, *J* = 2.3, 8.7 Hz, 1H; Ar-H), 6.84 (dd, *J* = 11.0, 17.9 Hz, 1H; Ar-CH=C), 5.86 (d, *J* = 17.9 Hz, 1H; C=CH_2), 5.36 (d, *J* = 11.0 Hz, 1H; C=CH_2).

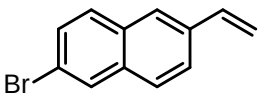

Figure 1.38 ^{1}H NMR spectrum of compound **1.37** [400 MHz, Chloroform-d_3].

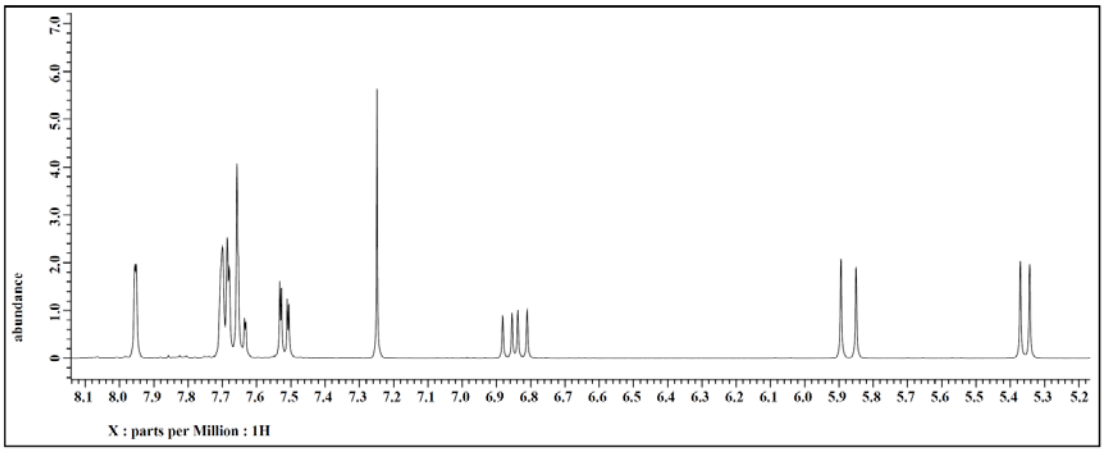

2-(6-Bromonaphthalen-2-yl)ethan-1-ol (1.38).[26] 2-Bromo-6-vinylnaphthalene (**1.37**) (200 mg, 0.858 mmol) was added to a cooled solution of BH_3.THF (0.64 mL, 0.64 mmol) in anhydrous THF (4 mL) and the mixture stirred for 2 hours at ambient temperature. NaOH (3M, 0.52 mL) followed by 30% H_2O_2 (0.17 mL) were added and the mixture stirred for additional 2 hours. The mixture was then diluted with EtOAc (20 mL), extracted with H_2O and brine (20 mL x 2), dried over anhydrous Na_2SO_4) and condensed under reduced pressure. The solid residue was purified via flash column chromatography (0-60% EtOAc/Hexane) to afford the desired product. Yield (98 mg, 46%). ^{1}H NMR matched that previously reported.[37]

^{1}H NMR (500 MHz, Chloroform-d_3): δ 7.97 (d, *J* =1.8 Hz, 1H; Ar-H), 7.70 (d, *J* = 8.6 Hz, 1H; Ar-H), 7.65 (d, *J* = 8.7 Hz, 1H; Ar-H), 7.64 (s, 1H; Ar-H), 7.52 (dd, *J* = 2.3, 8.6 Hz, 1H; Ar-H), 7.38 (dd, *J* = 1.7, 8.6 Hz, 1H; Ar-H), 3.94 (t, *J* = 6.3 Hz, 2H; O-CH_2), 3.00 (t, *J* = 6.3 Hz, 2H; Ar-CH_2).

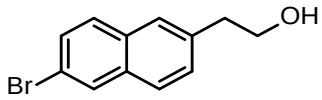

Figure 1.39 ^{1}H NMR spectrum of compound **1.38** [500 MHz, Chloroform-d_3].

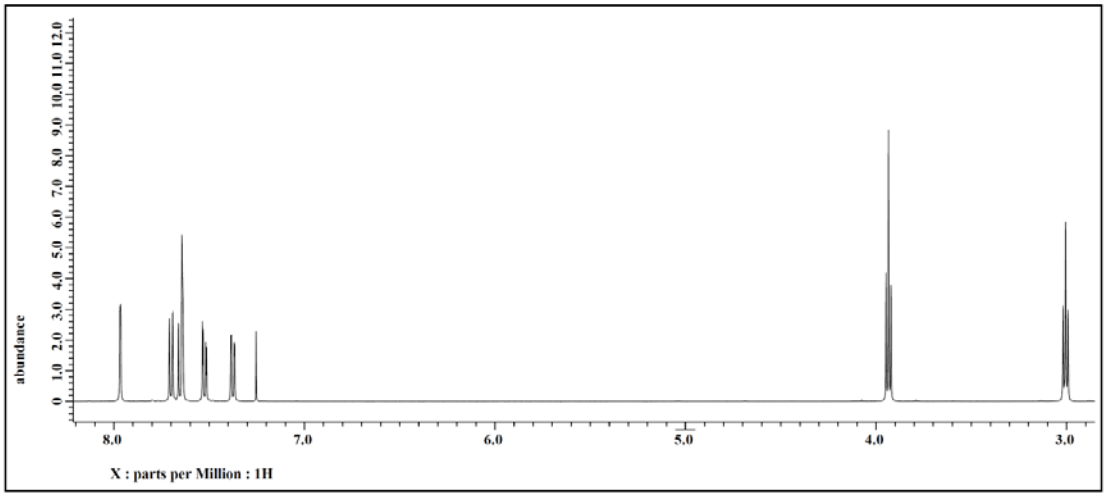

((6-bromonaphthalen-2-yl)methoxy)(*tert*-butyl)dimethylsilane (1.39).[27] *tert*-Butyldimethylsilyl chloride (100 mg, 0.42 mmol), 4-dimethylaminopyridine (12.9 mg, 0.11 mmol), and trimethylamine (0.22 mL, 0.55 mmol) were added to a solution of 2-(6-bromonaphthalen-2-yl)methanol (100 mg, 0.42 mmol) in CH_2Cl_2 (5 mL) and stirred at room temperature for 25 hours. The mixture was then diluted with CH_2Cl_2 (10 mL), extracted with a saturated solution of NH_4Cl (15 mLx2). The organic layer was dried using anhydrous sodium sulfate and condensed under reduced pressure. The solid residue was purified via flash column chromatography (0-5% EtOAc/Hexane) to afford the desired product. Yield (125 mg, 84%). ^{1}H NMR matched that previously reported.[41]

^{1}H NMR (500 MHz, Chloroform-d_3): δ 7.97 (s, 1H; Ar-H), 7.74 (s, 1H; Ar-H), 7.70 (t, *J* = 8.2 Hz, 2H; Ar-H), 7.52 (dd, *J* = 1.8, 8.7 Hz, 1H; Ar-H), 7.44 (d, *J* = 8.2 Hz, 1H; Ar-H), 4.87 (s, 2H; O-CH_2), 0.97 (s, 9H, Si-$C(CH_3)_3$), 0.13 (s, 6H; $Si(CH_3)_2$).

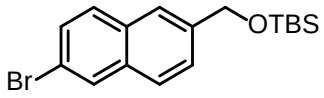

Figure 1.40 ^{1}H NMR spectrum of compound **1.39** [500 MHz, Chloroform-d_3].

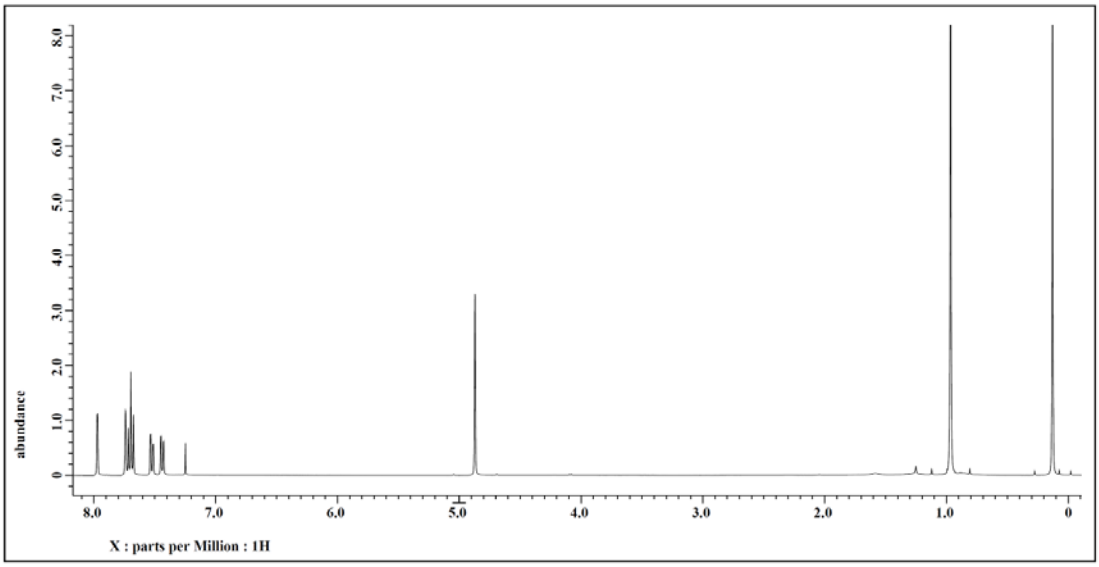

(2-(6-Bromonaphthalen-2-yl)ethoxy)(*tert*-butyl)dimethylsilane (1.40).[27] *tert*-butyldimethylsilyl chloride (57.6 mg, 0.38 mmol), 4-dimethylaminopyridine (9.7 mg, 0.08 mmol), and trimethylamine (58 µL, 0.414 mmol) were added to a solution of 2-(6-bromonaphthalen-2-yl)ethanol **1.5** (80.0 mg, 0.32 mmol) in CH_2Cl_2 (4 mL) and stirred at room temperature for 25 hours. The mixture was then diluted with CH_2Cl_2 (10 mL, extracted with a saturated solution of NH_4Cl (15 mLx2). The organic layer was dried using anhydrous sodium sulfate and condensed under reduced pressure. The solid residue was purified via flash column chromatography (0-5% EtOAc/Hexane) to afford the desired product. Yield (62 mg, 53%). ^{1}H NMR matched that previously reported.[42]

^{1}H NMR (500 MHz, Chloroform-d_3): δ 7.96 (d, *J* =1.7 Hz, 1H; Ar-H), 7.67 (d, *J* = 8.6 Hz, 1H; Ar-H), 7.64 (d, *J* = 8.6 Hz, 1H; Ar-H), 7.62 (s, 1H; Ar-H), 7.51 (dd, *J* = 2.3, 8.6 Hz, 1H; Ar-H), 7.37 (dd, *J* = 1.7, 8.6 Hz, 1H; Ar-H), 3.87 (t, *J* = 6.9 Hz, 2H; O-CH_2), 2.96 (t, *J* = 6.9 Hz, 2H; Ar-CH_2), 0.85 (s, 9H, Si-C(CH_3)$_3$), -0.05 (s, 6H; Si(CH_3)$_2$).

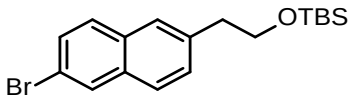

Figure 1.41 ^{1}H NMR spectrum of compound **1.40** [500 MHz, Chloroform-d_3].

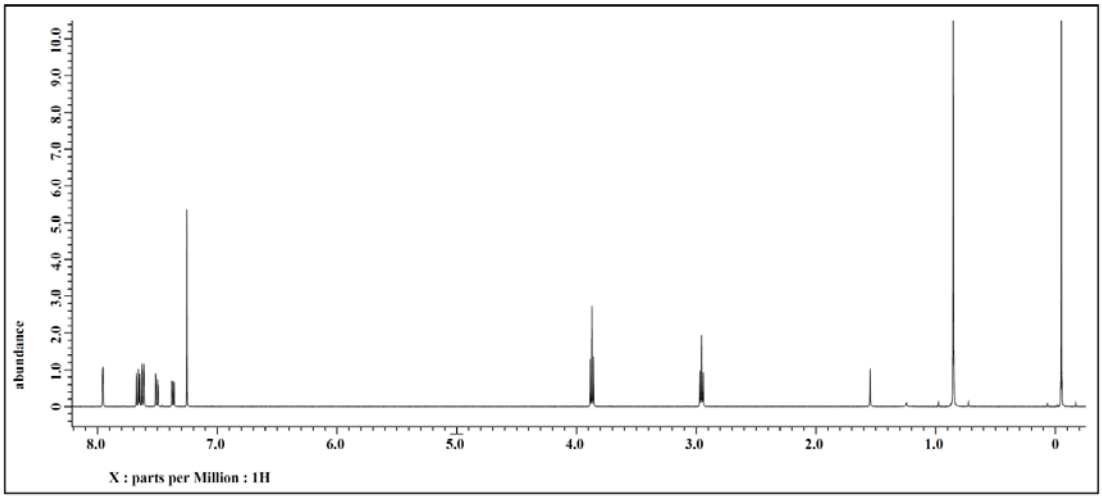

6-(2-((*tert*-butyldimethylsilyl)oxy)methyl**)-2-naphthoic acid (1.41)**.[28] A solution of (2-(6-Bromonaphthalen-2-yl)methoxy)(*tert*-butyl)dimethylsilane (**1.39**) (100 mg, 0.29 mmol) in anhydrous THF (10 mL) was cooled to -78 °C was added drop-wise to a previously cooled *n*-butyllithium (0.12 mL, 0.30 mmol) and the mixture stirred for 3 hours. The mixture was purged with CO_2 gas at -78 °C for half an hour then allowed to warm to room temperature. The mixture was then acidified with 1 M HCl, extracted with ethyl acetate (20 mL x 2) and the organic layer dried over anhydrous Na_2SO_4 and condensed under reduced pressure. Purification was done via flash column chromatography using 20% ethyl acetate in hexane. Yield (17.0 mg, 19%). ^{1}H NMR matched that previously reported.[43]

^{1}H NMR (500 MHz, Chloroform-d_3): δ 8.67 (bs, 1H; Ar-H), 8.10 (dd, *J* = 1.7, 8.6 Hz, 1H; Ar-H), 7.94 (d, *J* = 8.6 Hz, 1H; Ar-H), 7.89 (d, *J* = 8.6 Hz, 1H; Ar-H), 7.84 (s, 1H; Ar-H), 7.50 (dd, *J* = 1.2, 8.6 Hz, 1H; Ar-H), 4.93 (s, 2H; O-CH_2), 0.98 (s, 9H, Si-$C(CH_3)_3$), 0.14 (s, 6H; $Si(CH_3)_2$).

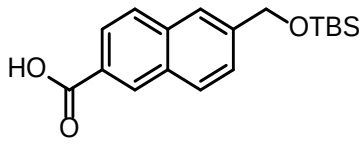

Figure 1.42 ^{1}H NMR spectrum of compound **1.41** [500 MHz, Chloroform-d_3].

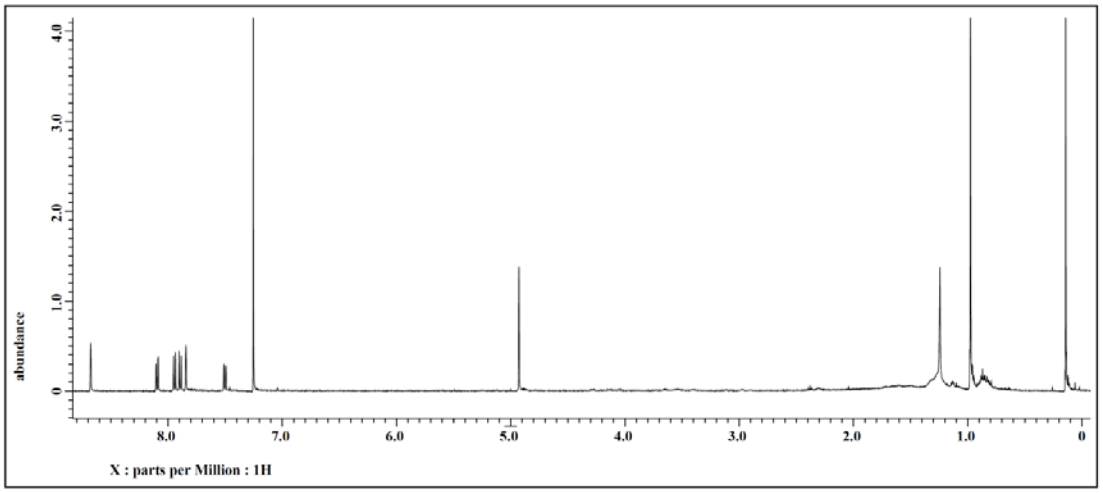

6-(2-((*tert*-butyldimethylsilyl)oxy)ethyl)-2-naphthoic acid (1.42).[28] A solution of (2-(6-Bromonaphthalen-2-yl)ethoxy)(*tert*-butyl)dimethylsilane (**1.40**) (61.9 mg, 0.17 mmol) in anhydrous THF (4 mL) was cooled to -40 °C was added drop-wise to a previously cooled *n*-butyllithium (0.25 mL, 0.25 mmol) and the mixture stirred for 3 hours. The mixture was purged with CO_2 gas at -40 °C for half an hour then allowed to warm to room temperature. The mixture was then acidified with 1 M HCl, extracted with brine (20 mL x 2) and the organic layer dried over anhydrous Na_2SO_4 and condensed under reduced pressure. Purification was done via flash column chromatography using 50% v/v ethyl acetate in hexane. Yield (29.7mg, 53%).

^{1}H NMR (500 MHz, Chloroform-d_3): δ 8.67 (bs, 1H; Ar-H), 8.09 (dd, *J* = 1.7, 8.6 Hz, 1H; Ar-H), 7.90 (d, *J* = 8.6 Hz, 1H; Ar-H), 7.84 (d, *J* = 8.6 Hz, 1H; Ar-H), 7.72 (s, 1H; Ar-H), 7.45 (dd, *J* = 1.7, 8.6 Hz, 1H; Ar-H), 3.91 (t, *J* = 6.9 Hz, 2H; O-CH_2), 3.01 (t, *J* = 6.9 Hz, 2H; Ar-CH_2), 1.25 (s, 9H, Si-C(CH_3)$_3$), 0.86 (s, 6H; Si(CH_3)$_2$).

^{13}C NMR (100 MHz, Methanol-d_4): δ 169.3, 139.9, 135.7, 131.4, 130.4, 128.7, 128.5, 127.9, 127.3, 127.2, 125.2, 63.9, 39.3, 25.0, -6.7.

HRMS (ESI, m/z): Calculated for $C_{19}H_{27}O_3Si$ $[M + H]^+$ 331.1724; found 331.1720 (1.2 ppm).

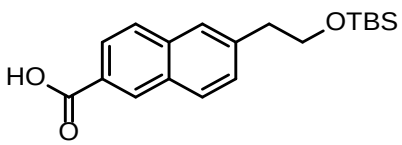

Figure 1.43 ^{1}H and ^{13}C NMR spectra of compound **1.42** [500 MHz for ^{1}H, Chloroform-d_3 and 100 MHz for ^{13}C, Methanol-d_4].

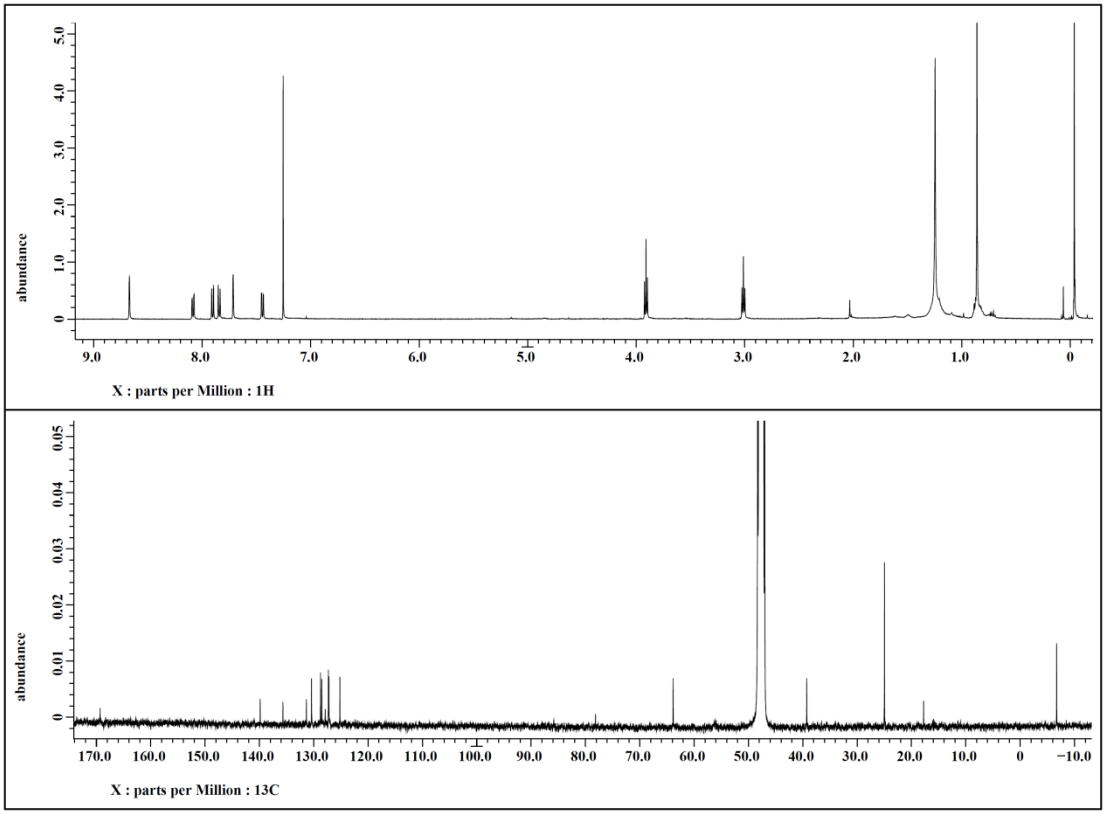

6-Bromo-2-naphthoic acid (1.43).[44] Potassium hydroxide (127 mg, 2.26 mmol) was added to a suspension of methyl 6-bromo-2-naphthoate (200 mg, 0.75 mmol) in methanol (50 mL) and the mixture heated at 50 °C for 48 hours. The solvent was evaporated and the residue diluted with water (30 mL), acidified with HCl (1M) and the extracted with ethyl acetate (30 mL x 2). The combined organic layers were dried with anhydrous magnesium sulfate and the solvent evaporated under reduced pressure. The crude product was purified via recrystallization using ethyl acetate to give the product as white crystals (105 mg, yield 56%). ^{1}H NMR matched that previously reported.[45]

^{1}H NMR: (400 MHz, Methanol-d_4): δ 8.58 (s, 1H; Ar-H), 8.14 (s, 1H; Ar-H), 8.06 (dd, *J* = 1.8, 8.7 Hz, 1H; Ar-H), 7.92 (d, *J* = 8.7 Hz, 1H; Ar-H), 7.87 (d, *J* = 8.7 Hz, 1H; Ar-H), 7.64 (dd, *J* = 1.8, 8.7 Hz, 1H; Ar-H).

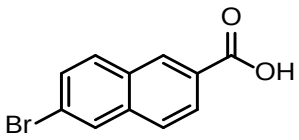

Figure 1.44 ^{1}H NMR spectrum of compound **1.43** [400 MHz, Methanol-d_4].

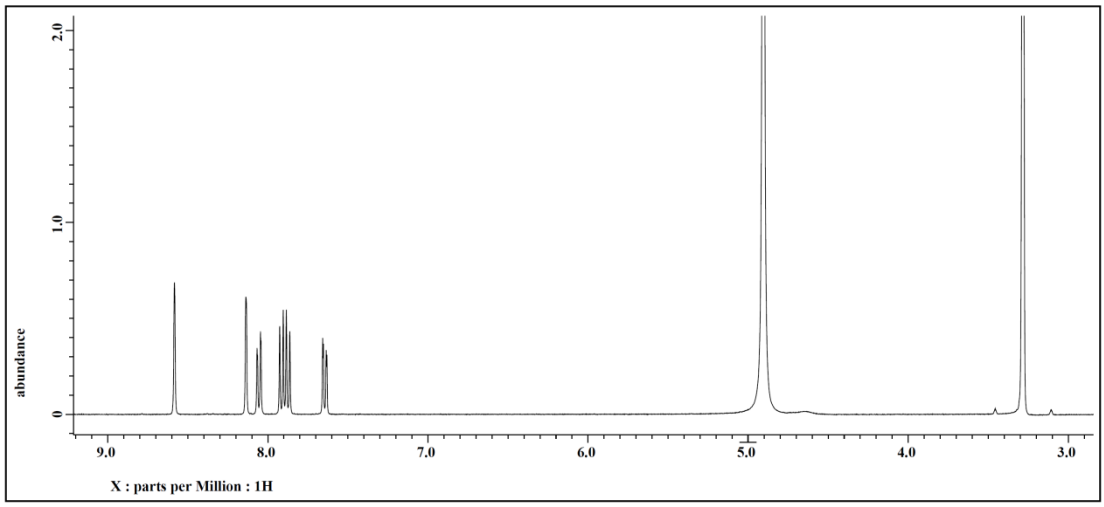

1.4.6 Synthesis of N-((4-(N-methyl-N-phenylsulfamoyl)phenyl)carbamothioyl)acrylamide (1.70).

KSCN (48 mg, 0.50 mmol)) was added to a cooled solution of acryloyl chloride (0.02 mL, 0.25 mmol) in anhydrous acetonitrile (1mL) and the reaction was allowed to stir for 4 hours at room temperature. The solid KCl was removed through filtration and aniline **2** (65 mg, 0.25mmol), dissolved in acetonitrile (1 mL), was added drop wise to the filtrate and the mixture stirred for 24 hours and the solvent evaporated. The crude product was purified via frit column chromatography using 50% ethyl acetate in hexane to give a white solid (44 mg, yield 47%).

^{1}H NMR (500 MHz, Chloroform-d_3): δ 12.83 (s, 1H; N-H), 8.76 (s, 1H; N-H), 7.90 (d, *J* = 8.4 Hz, 2H; Ar-H), 7.56 (d, *J* = 8.4 Hz, 2H; Ar-H), 7.32-7.27 (m, 3H; Ar-H), 7.10 (d, *J* = 8.4 Hz, 2H; Ar-H), 6.60 (d, *J* = 16.8 Hz, 1H; C=CH_2), 6.20 (dd, *J* = 10.7, 16.8 Hz, 1H; C=CH), 6.04 (d, *J* = 10.7 Hz, 1H; C=CH_2), 3.19 (s, 3H; N-CH_3).

^{13}C NMR: (125 MHz, Chloroform-d_3): δ 178.0, 165.1, 141.5, 141.4, 133.8, 133.2, 129.1 (2C), 128.9, 128.8 (2C), 127.6, 126.8 (2C), 122.9 (2C), 38.3.

HRMS (ESI, m/z): calculated for $C_{17}H_{18}N_3O_3S_2$ $[M + H]^+$ 376.0784; found 376.0778 (1.6 ppm).

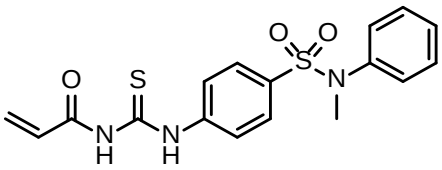

Figure 1.45 ^{1}H and ^{13}C NMR spectra of compound **1.70** [500 MHz for ^{1}H, and 100 MHz for ^{13}C, Chloroform-d_3].

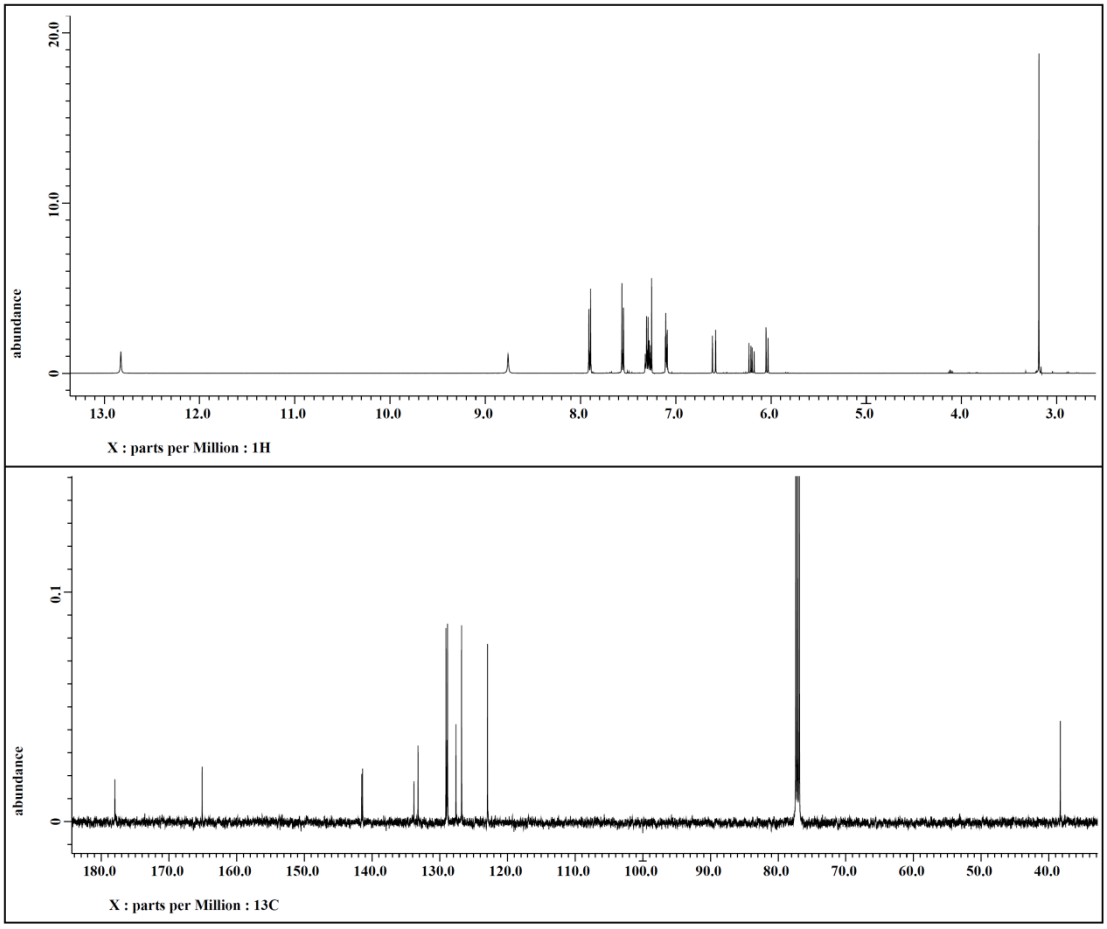

1.4.7 General Procedure for the synthesis of thiourea compounds (1.2, 1.10-1.16, 1.75-1.87).

The carboxylic acid **1.41-1.39**, **1.70-1.72** (1 eq.) was refluxed with thionyl chloride (120 eq.) and the mixture heated under reflux for 3 hours. The solution was cooled to room temperature and concentrated under reduced pressure. The residue was further dried via high vacuum and used in the proceeding reaction without further purification. KSCN (1-2 eq.) was added to the solution of crude acyl chloride in anhydrous acetonitrile (0.5

M) and the reaction was allowed to stir for 4 hours at room temperature. The solid KCl was removed through filtration and the aniline **1.57**-**1.68** (1 eq.), dissolved in acetonitrile (0.1 M), was added drop wise to the filtrate and the mixture stirred for 24 hours.[21] The product either precipitated and needed no further purification, recrystallized using the appropriate mixture of solvents or purified via flash column chromatography or preparative HPLC.

(*E*)-3-(2-Methoxyphenyl)-*N*-((4-(*N*-methyl-*N*-phenylsulfamoyl)phenyl)carbamothioyl)acrylamide (1.2). The product precipitated as a pure yellow solid. Yield (25 mg, 46%).

^{1}H NMR (500 MHz, Acetone-d_6): δ 8.05 (d, *J* = 15.5 Hz, 1 H, Ar-CH=), 7.95 (d, *J* = 8.6, 2H, Ar-H), 7.56 (d, *J* = 8.6, 2H, Ar-H), 7.49 (dd, *J* = 1.7, 8.0 Hz, 1H, Ar-H), 7.42 (dd, *J* = 1.7, 8.0 Hz, 1H, Ar-H), 7.30 (m, 3H, Ar-H), 7.12 (s, 1 H, Ar-H), 7.10 (d, *J* = 7.5 Hz, 1 H, Ar-H), 7.00 (t, *J* = 7.5 Hz, 1 H, Ar-H), 6.96 (d, *J* = 8.6 Hz, 1 H, Ar-H), 6.66 (d, *J* = 15.5 Hz, 1 H, C=CHCO), 3.19 (s, 3H; N-CH_3), 3.94 (s, 3H; O-CH_3).

^{13}C NMR (125 MHz, DMSO-d_6): δ 179.4, 167.4, 158.9, 142.6, 141.6, 140.8, 133.3, 133.1, 129.8, 129.5 (2C), 128.8 (2C), 127.8, 126.8 (2C), 123.9 (2C), 122.9, 121.4, 120.5, 112.5, 56.2, 38.5.

HRMS (ESI, m/z): Calculated for $C_{24}H_{24}N_3O_4S_2$ $[M + H]^+$ 482.1203; found 482.1184 (3.9 ppm).

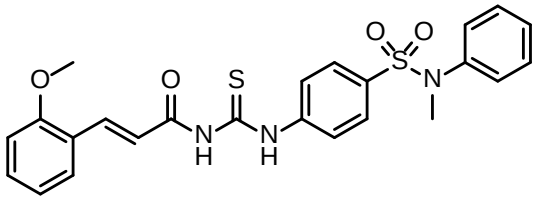

Figure 1.46 ^{1}H and ^{13}C NMR spectra of compound **1.2** [500 MHz for ^{1}H, Acetone-d_6 and 100 MHz for ^{13}C, DMSO-d_6].

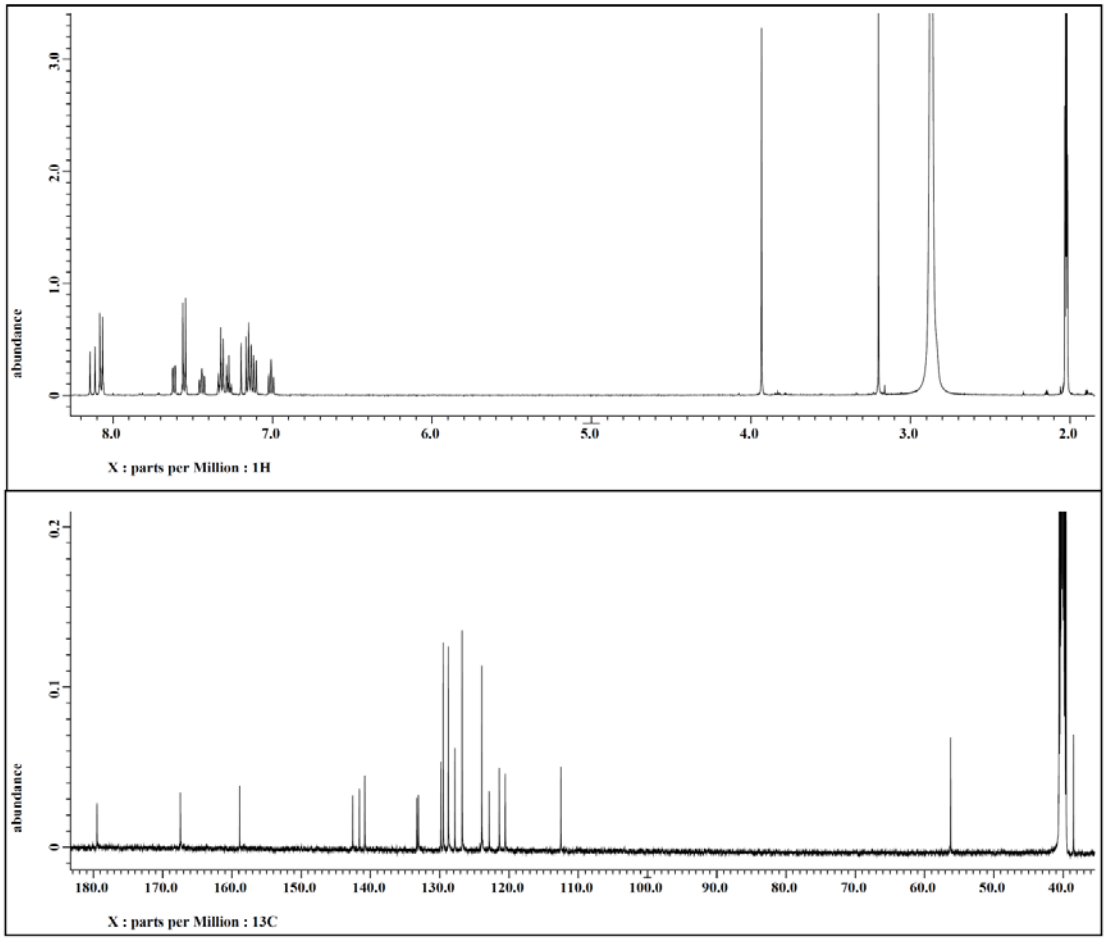

***N*-((4-(*N*-methyl-*N*-phenylsulfamoyl)phenyl)carbamothioyl)quinoline-3-carboxamide (1.10)**. The product precipitated as a pure yellow solid. Yield (59 mg, 65%).

^{1}H NMR (500 MHz, Acetone-d_6): δ 9.40 (d, *J* = 2.3 Hz, 1H; Ar-H), 9.23 (s, 1H; Ar-H), 8.26 (d, *J* = 8.6Hz, 1H; Ar-H), 8.22 (d, *J* = 8.0 Hz, 1H; Ar-H), 8.10 (dd, *J* = 6.3, 8.6 Hz, 2H; Ar-H), 8.01 (d, *J* = 7.7 Hz, 1H; Ar-H), 7.80 (d, *J* = 7.5 Hz, 1H; Ar-H), 7.59 (d, *J* = 8.9 Hz, 2H; Ar-H), 7.35-7.27 (m, 3H; Ar-H), 7.15 (dd, *J* = 1.7, 8.3 Hz, 2H; Ar-H), 3.22 (s, 3H; N-CH_3).

^{13}C NMR (100 MHz, DMSO-d_6): δ 179.6, 167.4, 149.6, 149.5, 142.7, 141.6, 138.6, 133.5, 132.8, 130.2, 129.5 (2C), 129.3, 128.8 (2c), 128.3, 127.8, 126.8 (2C), 126.5, 125.6, 124.3 (2C), 38.5.

HRMS (ESI, m/z): calculated for $C_{24}H_{21}N_4O_3S_2$ $[M + H]^+$ 477.1050; found 477.1030 (4.1 ppm).

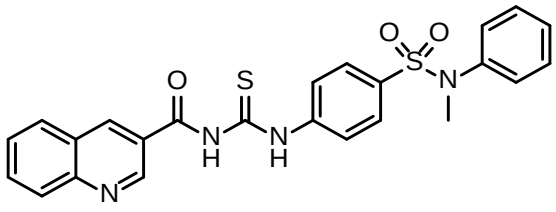

Figure 1.47 ^{1}H and ^{13}C NMR spectra of compound **1.10** [500 MHz for ^{1}H, Acetone-d_6 and 100 MHz for ^{13}C, DMSO-d_6].

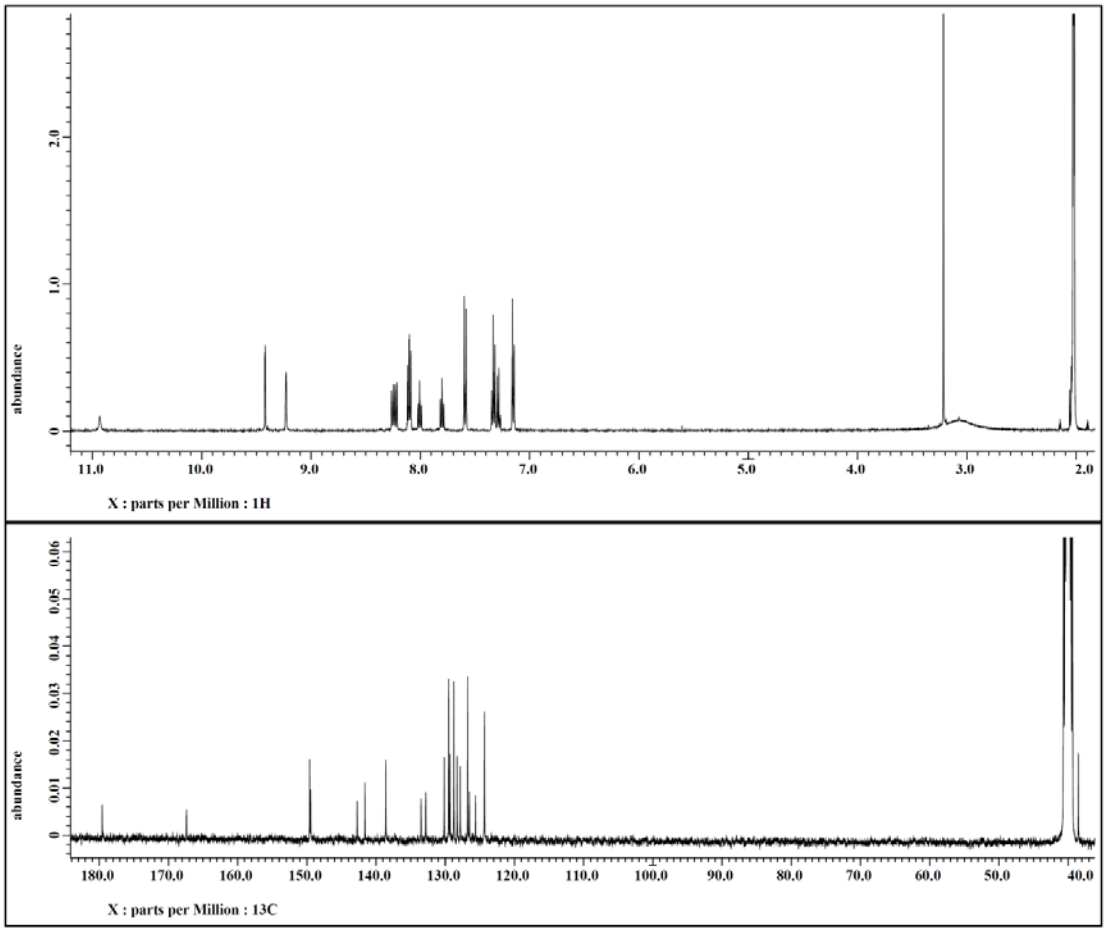

***N*-((4-(*N*-Methyl-*N*-phenylsulfamoyl)phenyl)carbamothioyl)quinoline-7-carboxamide (1.11)**. Purification was done via recrystallization using a mixture of chloroform and hexane. Yield (8.0 mg, 11%).

^{1}H NMR (500 MHz, Acetone-d_6): δ 9.02 (dd, *J* = 1.7, 4.0 Hz, 1H; Ar-H), 8.76 (s, 1H; Ar-H), 8.44 (dd, *J* = 1.2, 8.6 Hz, 1H; Ar-H), 8.14 (s, 2H), 8.11 (d, *J* = 8.6 Hz, 2H; Ar-H), 7.66 (dd, *J* = 4.0, 8.6 Hz, 1H; Ar-H), 7.59 (d, *J* = 8.9 Hz, 2H; Ar-H), 7.35-7.27 (m, 3H; Ar-H), 7.15 (d, *J* = 8.0 Hz, 2H; Ar-H), 3.22 (s, 3H; N-CH_3).

^{13}C NMR (125 MHz, DMSO-d_6): δ. 179.0, 168.2, 152.1, 147.4, 142.4, 141.8, 135.9, 133.7, 132.8, 130.9, 130.7, 129.0, 128.9 (2C), 128.6 (2C), 127.3, 126.6 (2C), 124.8, 123.6, 123.2, 37.7.

HRMS (ESI, m/z): Calculated for $C_{24}H_{21}N_4O_3S_2$ $[M + H]^+$ 477.1050; found 477.1030 (4.1 ppm).

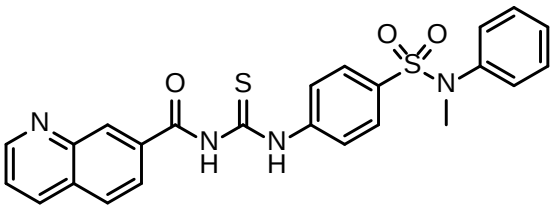

Figure 1.48 ^{1}H and ^{13}C NMR spectra of compound **1.11** [500 MHz for ^{1}H, Acetone-d_6 and 100 MHz for ^{13}C, DMSO-d_6].

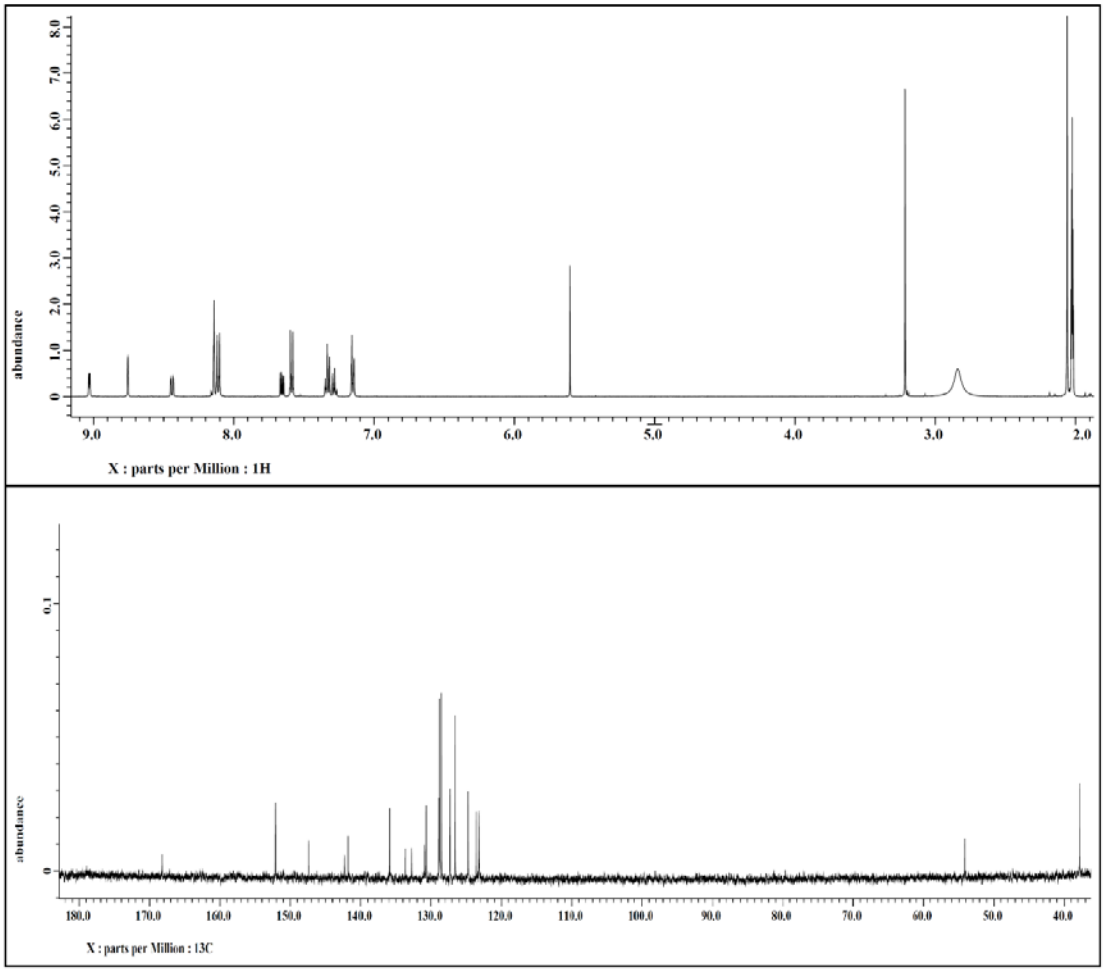

6-(2-Hydroxyethyl)-*N*-((4-(*N*-methyl-*N*-phenylsulfamoyl)phenyl)carbamothioyl)-2-naphthamide (1.12). The residue was purified by preparative HPLC using a Phenomenex Gemini-NX column C18 (250 x 21.20 mm, 110 A, 5 μm spherical particle size). The column was perfused at a flow rate of 21.24 mL/min with a linear gradient from 60% (CH_3CN-H_2O) to 80% over 15 min. The compound eluted at 12.5 min. Yield (7.4 mg, 6%).

^{1}H NMR (500 MHz, Chloroform-d_3): δ 9.26 (s, 1H; N-H), 8.40 (s, 1H; Ar-H), 7.98-7.92 (m, 4H; Ar-H), 7.87 (dd, *J* = 1.4, 8.7 Hz, 1H; Ar-H), 7.57 (d, *J* = 8.7 Hz, 2H; Ar-H), 7.51 (dd, *J* = 1.8, 8.2 Hz, 1H; Ar-H), 7.33-7.27 (m, 3H; Ar-H), 7.10 (dd, *J* = 1.8, 6.9 Hz, 2H; Ar-H), 3.99 (t, *J* = 6.4 Hz, 2H; O-CH_2), 3.19 (s, 3H; N-CH_3), 3.08 (t, *J* = 6.4 Hz, 2H; Ar-CH_2).

^{13}C NMR (100 MHz, Chloroform-d_3): δ 178.1, 167.3, 141.7, 141.4, 140.5, 136.0, 133.8, 131.3, 129.7, 129.4, 129.2, 129.1 (2C), 129.0, 128.9 (2C), 127.7, 127.6, 126.8 (2C), 123.2, 123.0 (2C), 63.3, 39.5, 38.3.

HRMS (ESI, m/z): Calculated for $C_{27}H_{26}N_3O_4S_2$ $[M + H]^+$ 520.1359; found 520.1339 (3.9 ppm).

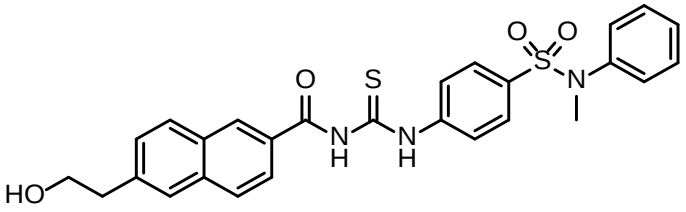

Figure 1.49 ^{1}H and ^{13}C NMR spectra of compound **1.12** [500 MHz for ^{1}H and 100 MHz for ^{13}C, Chloroform-d_3].

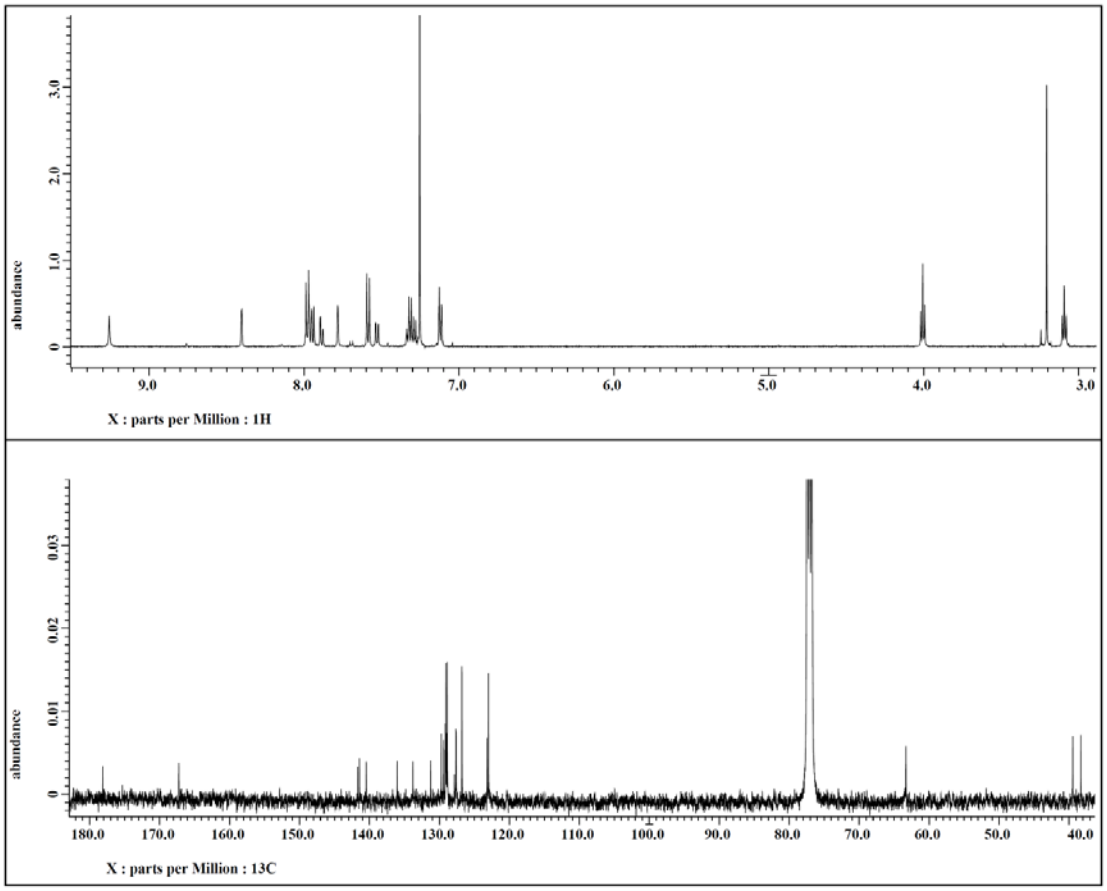

(*E*)-*N*-((4-(*N*-(2-Hydroxyethyl)-*N*-phenylsulfamoyl)phenyl)carbamothioyl)-3-(2-methoxyphenyl)acrylamide (1.13). The product precipitated as a yellow solid. Yield (58%).

^{1}H NMR (500 MHz, Acetone-d_6): δ 10.54 (s, 1H; N-H), 8.13 (d, *J* = 15.8 Hz, 1H; Ar-CH=C), 8.08 (d, *J* = 8.6 Hz, 2H; Ar-H), 7.64-7.61 (m, 3H; Ar-H), 7.44 (d, *J* = 7.7 Hz, 1H; Ar-H), 7.35-7.29 (m, 3H; Ar-H), 7.19 (d, *J* = 15.8 Hz, 1H; CH=CO), 7.14-7.10 (m, 3H; Ar-H), 7.01 (t, *J* = 7.5 Hz, 1H; Ar-H), 3.94 (s, 3H; O-CH_3), 3.83 (t, *J* = 5.7 Hz, 1H; O-H), 3.73 (t, *J* = 6.3 Hz, 2H, N-CH_2), 3.54 (q, *J* = 6.0 Hz, 2H; O-CH_2).

^{13}C NMR (125 MHz, Acetone-d_6) δ 179.2, 167.3, 159.0, 142.3, 141.3, 139.9, 135.5, 132.6, 129.5, 129.1 (2C), 129.0 (2C), 128.4 (2C), 127.9, 122.8 (2C), 120.9 (2C), 119.5, 111.7 (2C), 59.6, 55.3, 53.2.

HRMS (ESI, m/z): Calculated for $C_{25}H_{26}N_3O_5S_2$ $[M + H]^+$ 512.1308; found 512.1287 (4.2 ppm).

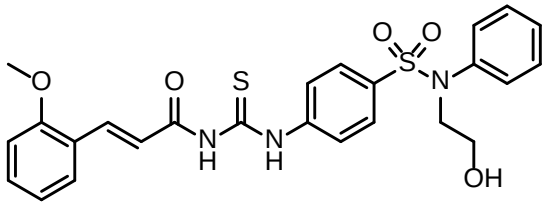

Figure 1.50 ^{1}H and ^{13}C NMR spectra of compound **1.13** [500 MHz for ^{1}H and 125 MHz for ^{13}C, Acetone-d_6].

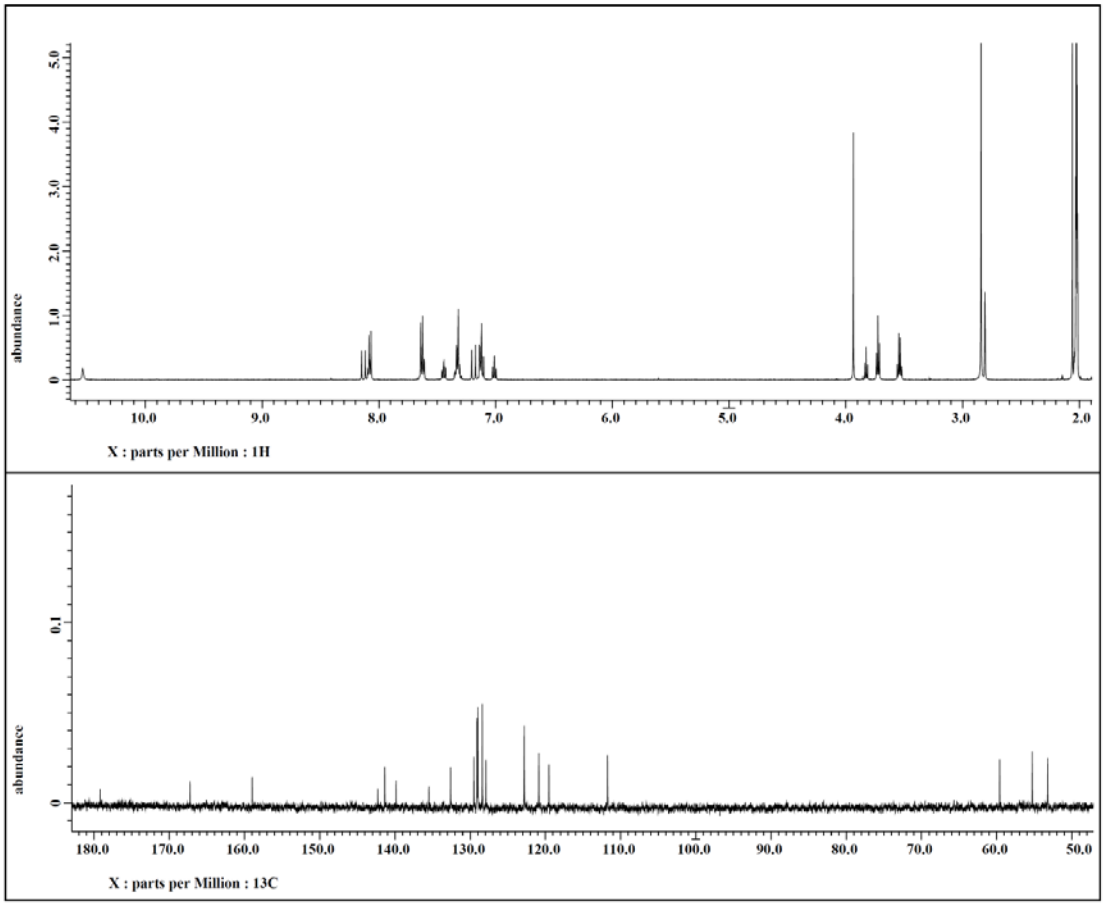

(*E*)-3-(2-Methoxyphenyl)-*N*-((4-(*N*-methyl-*N*-(pyridin-4-yl)sulfamoyl)phenyl)carbamothioyl)acrylamide (1.14). Purification was done via recrystallization using Methanol. Yield (12 mg, 15%).

^{1}H NMR (500 MHz, Chloroform-d_3): δ 8.78 (s, 1H; N-H), 8.53 (dd, *J* = 1.7, 4.6 Hz, 2H; Ar-H), 8.06 (d, *J* = 15.8 Hz, 1H; Ar-CH=C), 7.97 (d, *J* = 8.9 Hz, 2H; Ar-H), 7.60 (d, *J* = 8.6 Hz, 2H; Ar-H), 7.49 (dd, *J* = 1.7, 7.5 Hz, 1H; Ar-H), 7.43 (dd, *J* = 1.7, 7.7 Hz, 1H; Ar-H), 7.18 (dd, *J* = 1.7, 4.7 Hz, 2H; Ar-H), 7.00 (t, *J* = 7.5 Hz, 1H; Ar-H), 6.96 (d, 8.6 Hz, 1H; Ar-H), 6.65 (d, *J* = 15.8 Hz, 1H; C=CH-CO), 3.93 (s, 3H; N-CH_3).

^{13}C NMR (125 MHz, Chloroform-d_3): δ 178.5, 166.8, 159.2, 150.7 (2C), 148.8, 143.5, 142.4, 133.2, 132.9, 130.9, 128.4 (2C), 123.1 (2C), 122.4, 121.0, 118.6, 118.3 (2C), 111.4, 55.7, 36.7.

HRMS (ESI, m/z): Calculated for $C_{23}H_{23}N_4O_4S_2$ $[M + H]^+$ 483.1155; found 483.1134 (4.4 ppm).

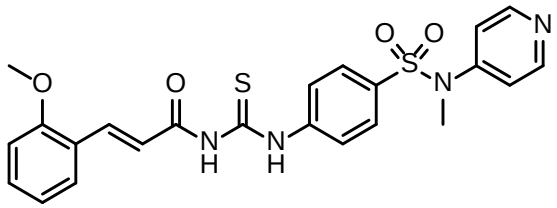

Figure 1.51 ^{1}H and ^{13}C NMR spectra of compound **1.14** [500 MHz for ^{1}H and 125 MHz for ^{13}C, Chloroform-d3].

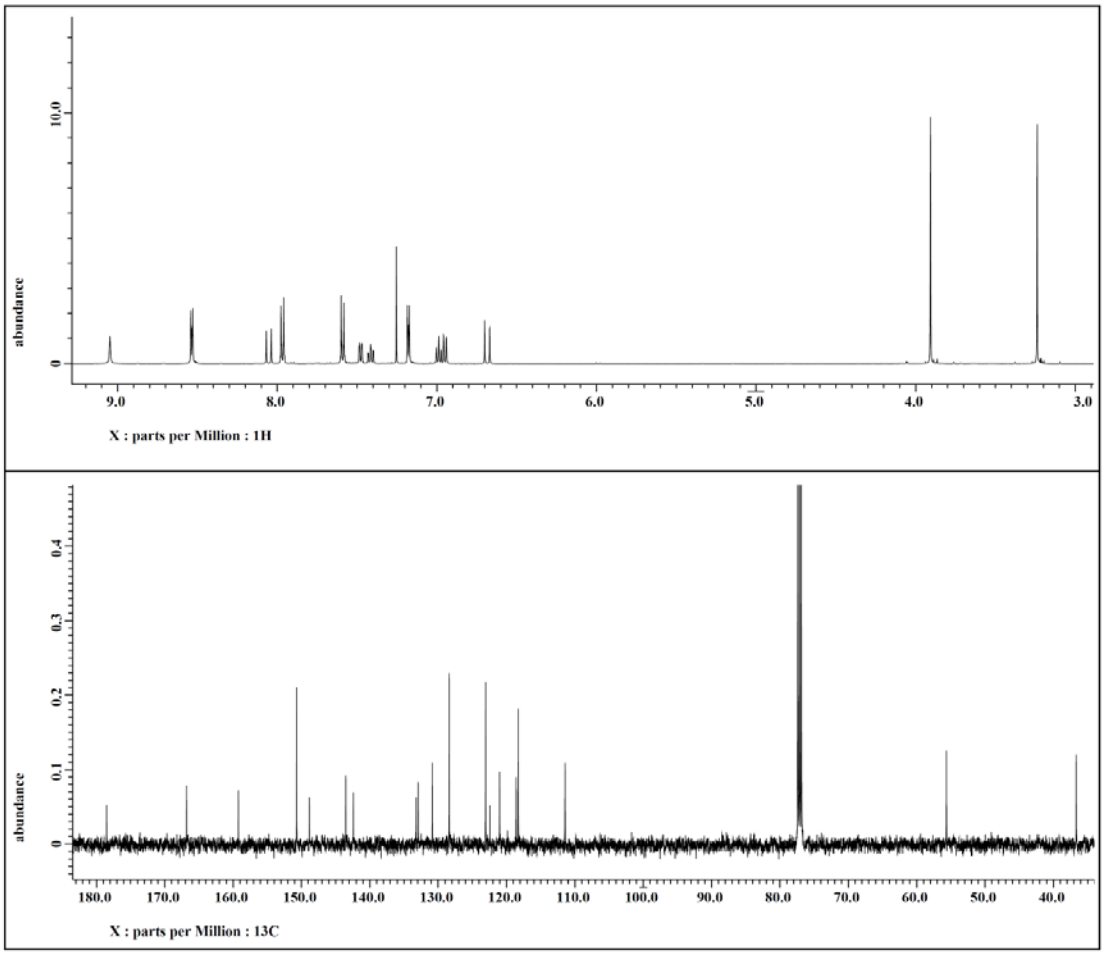

(*E*)-*N*-((4-(*N*-((5-(Hydroxymethyl)furan-2-yl)methyl)-*N*-phenylsulfamoyl)phenyl)carbamothioyl)-3-(2-methoxyphenyl)acrylamide (1.15). The product precipitated as a yellow solid. Yield (98 mg, 61%).

^{1}H NMR (500 MHz, Acetone-d_6): δ 8.14 (d, *J* = 15.8 Hz, 1 H; Ar-CH=C), 8.08 (d, *J* = 8.9 Hz, 2H; Ar-H), 7.66 (d, *J* = 8.6 Hz, 2H; Ar-H), 7.62 (dd, *J* = 1.7, 7.7 Hz, 2H; Ar-H), 7.45 (dt, J_t = 1.7, J_d = 7.7 Hz, 1H; Ar-H), 7.28-7.25 (m, 3H; Ar-H), 7.19 (d, *J* = 15.5 Hz, 1H; C=CHCO), 7.11 (d, *J* = 8.6 Hz, 1H; Ar-H), 7.07-7.05 (m, 2H; Ar-H), 7.01 (t, *J* = 7.5 Hz, 1H; Ar-H), 6.05 (d, *J* = 3.2 Hz, 1H; Fu-H), 6.02 (d, *J* = 3.2 Hz, 1H; Fu-H), 4.84 (s, 2H; O-CH_2), 4.39 (s, 2H; N-CH_2), 3.94 (s, 3H; O-CH_3).

^{13}C NMR (125 MHz, Acetone-d_6): δ 179.2, 167.3, 159.0, 155.9, 149.0, 142.3, 141.4 (2C), 139.2, 135.7, 132.6, 129.5, 129.1 (2C), 128.9 (2C), 128.5 (2C), 128.0, 122.8 (2C), 120.9, 119.5, 111.7, 110.3, 107.4, 56.4, 55.3, 47.8.

HRMS (ESI, m/z): Calculated for $C_{29}H_{28}N_3O_6S_2$ $[M + H]^+$ 578.1414; found 578.1395 (3.3 ppm).

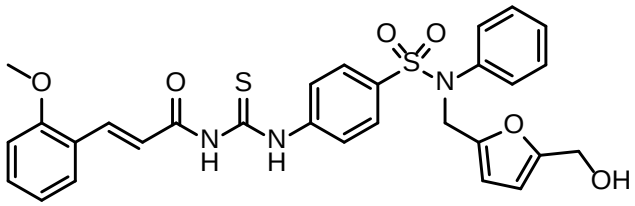

Figure 1.52 ^{1}H and ^{13}C NMR spectra of compound **1.15** [500 MHz for ^{1}H and 125 MHz for ^{13}C, Acetone-d_6].

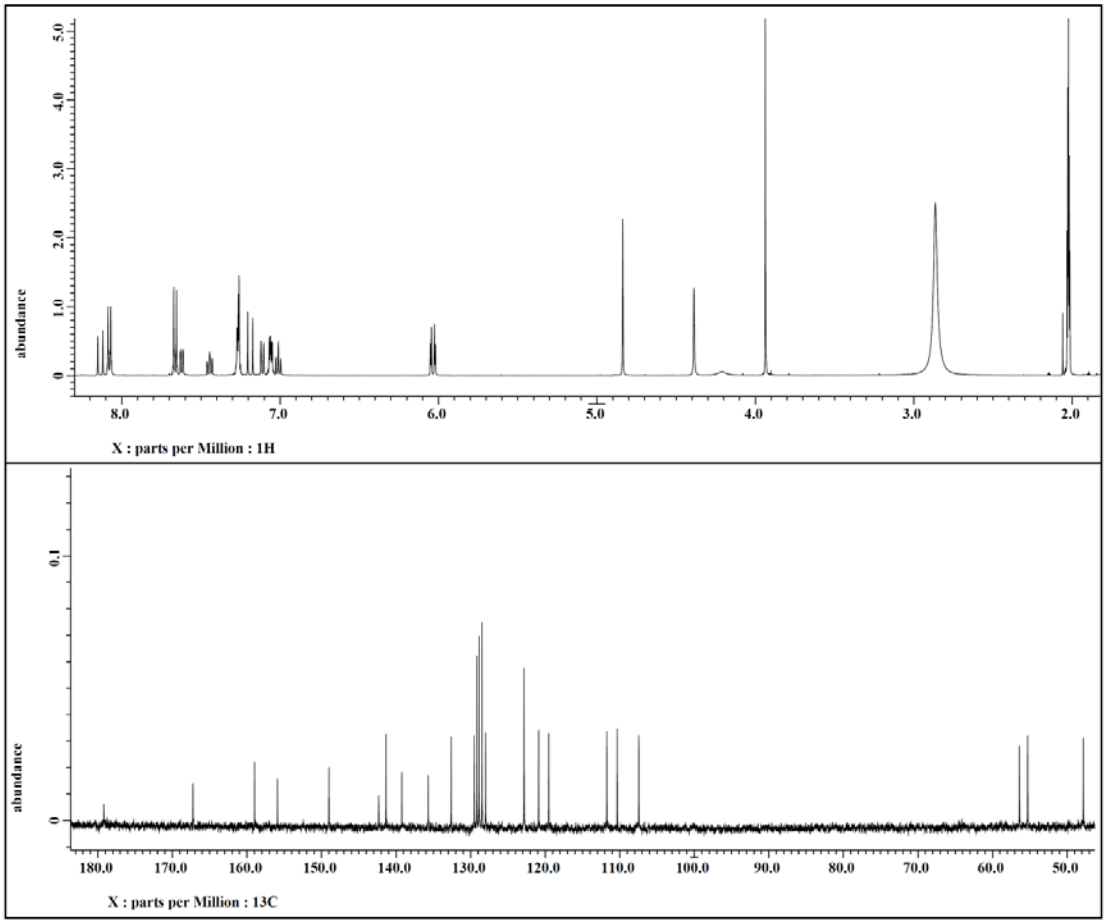

(*E*)-3-(2-Methoxyphenyl)-*N*-((4-(*N*-phenylsulfamoyl)phenyl)carbamothioyl)acrylamide (1.16). The product precipitated as a yellow solid. Yield (21 mg, 38%).

^{1}H NMR (500 MHz, Acetone-d_6): δ 8.10 (d, *J* = 15.8 Hz, 1H; Ar-CH=C), 8.02 (d, *J* = 8.6 Hz, 2H;Ar-H), 7.80 (d, *J* = 8.6 Hz, 2H; Ar-H), 7.59 (dd, *J* = 1.7, 7.7 Hz, 2H; Ar-H), 7.42 (d, *J* = 8.1 Hz, 1H; Ar-H), 7.25-7.20 (m, 3H; Ar-H), 7.15 (d, *J* = 15.8 Hz, 1H; CH=CO), 7.08 (d, *J* = 8.1 Hz, 1H; Ar-H), 7.07-7.03 (m, 2H; Ar-H), 7.01 (t, *J* = 7.5 Hz, 1H; Ar-H), 3.91 (s, 3H; O-CH_3).

^{13}C NMR (125 MHz, Acetone-d_6): δ 179.2, 167.2, 159.0, 142.3, 141.3, 137.9, 136.7, 132.6, 129.5, 129.2 (2C), 127.9 (2C), 124.6, 122.9 (2C), 122.8, 120.9 (2C), 119.5, 111.7 (2C), 55.3.

HRMS (ESI, m/z): Calculated for $C_{23}H_{22}N_3O_4S_2$ $[M + H]^+$ 468.1046; found 468.1028 (3.9 ppm).

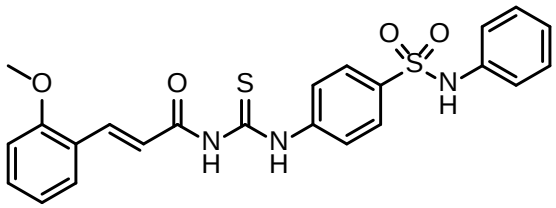

Figure 1.53 ^{1}H and ^{13}C NMR spectra of compound **1.16** [500 MHz for ^{1}H and 125 MHz for ^{13}C, Acetone-d_6].

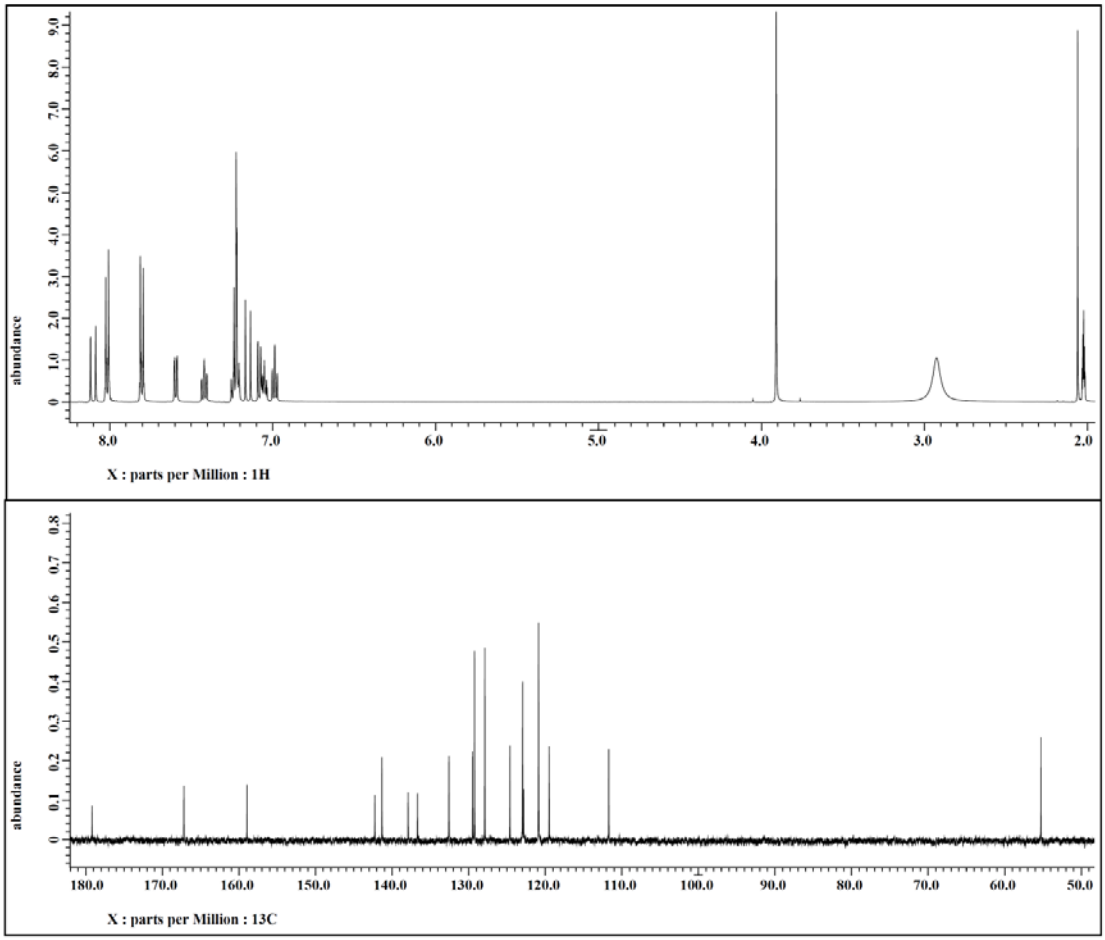

6-(Hydroxymethyl)-*N*-((4-(*N*-methyl-*N*-phenylsulfamoyl)phenyl)carbamothioyl)-2-naphthamide (1.75). The product precipitated as a yellow solid. Yield (13.25 mg, 48%).

^{1}H NMR (500 MHz, Chloroform-d_3): δ 9.26 (s, 1H; N-H), 8.40 (s, 1H; Ar-H), 7.98-7.92 (m, 4H; Ar-H), 7.87 (dd, *J* = 1.4, 8.7 Hz, 1H; Ar-H), 7.57 (d, *J* = 8.7 Hz, 2H; Ar-H), 7.51 (dd, *J* = 1.8, 8.2 Hz, 1H; Ar-H), 7.33-7.27 (m, 3H; Ar-H), 7.10 (dd, *J* = 1.8, 6.9 Hz, 2H; Ar-H), 3.99 (t, *J* = 6.4 Hz, 2H; O-CH_2), 3.19 (s, 3H; N-CH_3), 3.08 (t, *J* = 6.4 Hz, 2H; Ar-CH_2).

^{13}C NMR (100 MHz, Chloroform-d_3): δ 178.1, 167.3, 141.7, 141.4, 140.5, 136.0, 133.8, 131.3, 129.7, 129.4, 129.2, 129.1 (2C), 129.0, 128.9 (2C), 127.7, 127.6, 126.8 (2C), 123.2, 123.0 (2C), 63.3, 39.5, 38.3.

HRMS (ESI, m/z): Calculated for $C_{26}H_{24}N_3O_4S_2$ $[M + H]^+$ 506.1203; found 506.1186 (3.3 ppm).

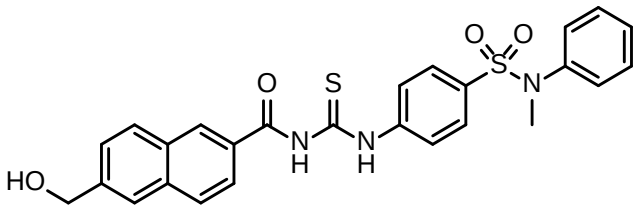

Figure 1.54 ^{1}H and ^{13}C NMR spectra of compound **1.75** [500 MHz for ^{1}H and 100 MHz for ^{13}C, Chloroform-d_3].

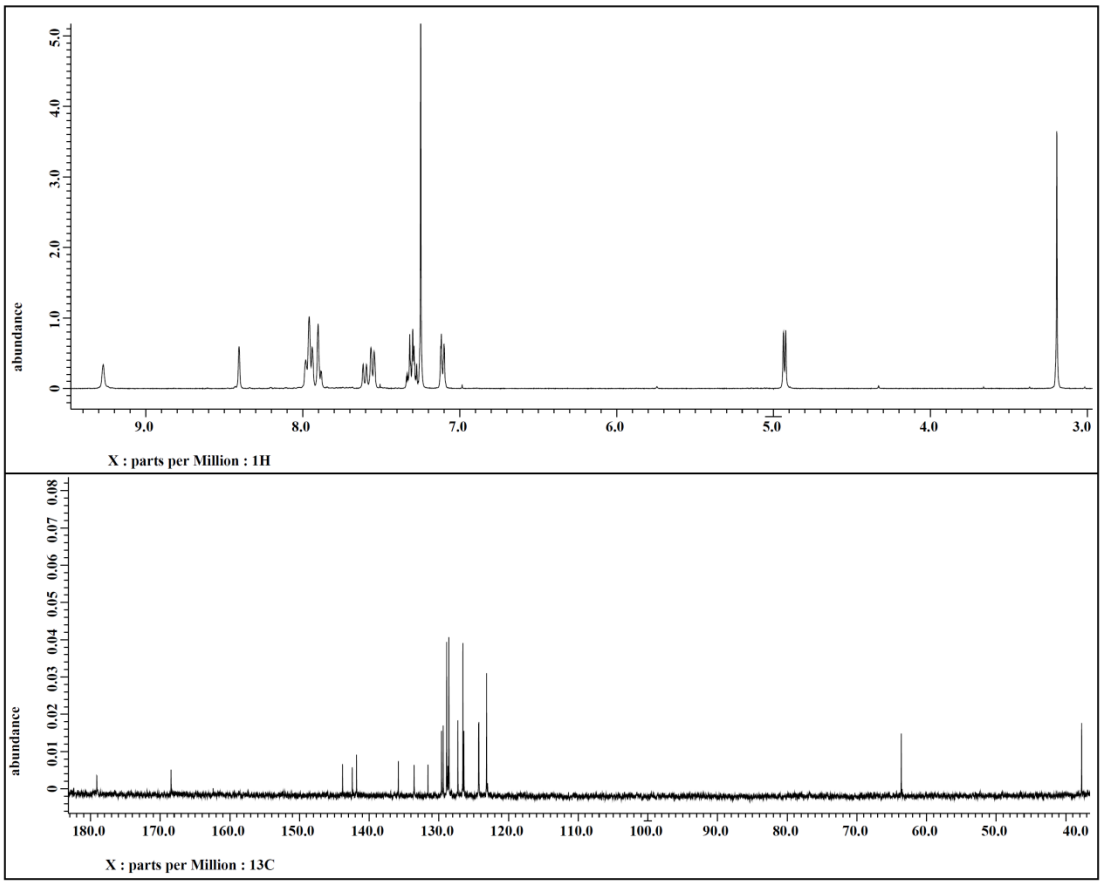

***N*-((4-(N-(2-Hydroxyethyl)-*N*-phenylsulfamoyl)phenyl)carbamothioyl)quinoline-7-carboxamide (1.76)**. The product precipitated as a yellow solid. Yield (55%).

^{1}H NMR (500 MHz, Chloroform-d_3): δ 9.42 (s, 1H; N-H), 9.07 (dd, *J* = 1.7, 4.0 Hz, 1H; Ar-H), 8.68 (s, 1H; Ar-H), 8.27 (dd, *J* = 1.2, 8.6 Hz, 1H; Ar-H), 8.05-8.02 (m, 2H; Ar-H), 8.00 (d, *J* = 9.2 Hz, 2H; Ar-H), 7.66 (d, *J* = 9.2 Hz, 2H; Ar-H), 7.59 (dd, *J* = 4.0, 8.0 Hz, 1H; Ar-H), 7.37-7.32 (m, 3H; Ar-H), 7.11-7.09 (m, 2H; Ar-H), 3.75 (m, 2H; O-CH_2), 3.68 (m, 2H; N-CH_2).

^{13}C NMR (125 MHz, Chloroform-d_3): δ 177.9, 166.7, 152.4, 147.4, 141.7, 139.3, 136.1, 135.4, 132.0, 131.2, 120.0, 129.6, 129.5 (2C), 129.0 (2C), 128.7 (2C), 128.6, 124.1, 123.8, 123.2 (2C), 60.5, 53.7.

HRMS (ESI, m/z): Calculated for $C_{25}H_{23}N_4O_4S_2$ $[M + H]^+$ 507.1155; found 507.1145 (2.0 ppm).

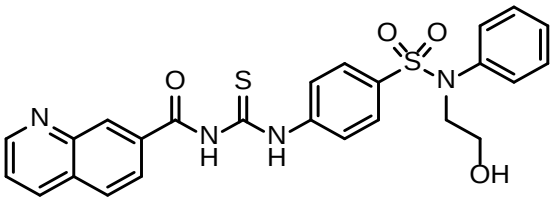

Figure 1.55 ^{1}H and ^{13}C NMR spectra of compound **1.76** [500 MHz for ^{1}H and 125 MHz for ^{13}C, Chloroform-d_3].

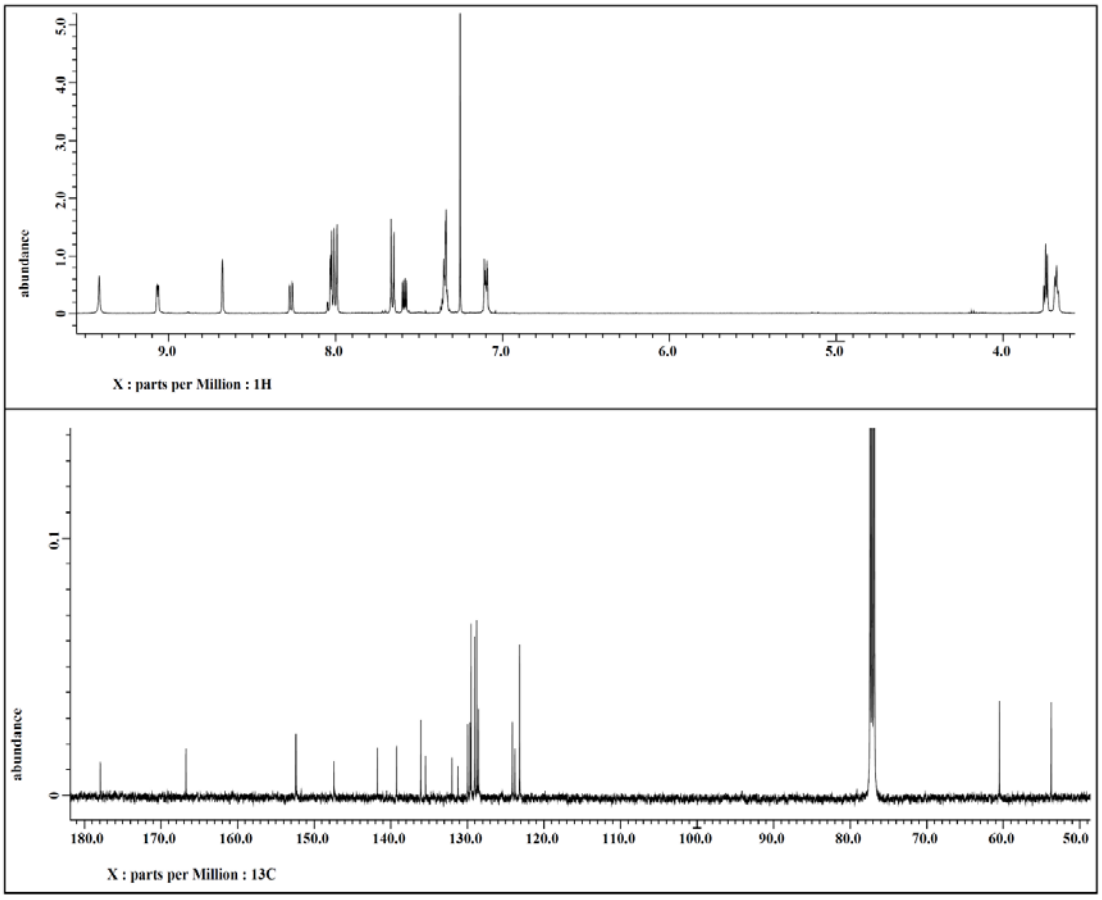

(*E*)-3-(2-Methoxyphenyl)-*N*-((4-(N-phenyl-*N*-(pyridin-4 ylmethyl)sulfamoyl)phenyl)carbamothioyl)acrylamide (1.77). The product precipitated as a yellow solid. Yield (16.5 mg, 28%).

^{1}H NMR (500 MHz, Chloroform-d_3): δ 8.69 (s, 1H, N-H), 8.53 (d, *J* = 6.0 Hz, 2H; Ar-H), 8.07 (d, *J* = 15.5 Hz, 1H; Ar-CH=C), 8.00 (d, *J* = 8.6 Hz, 2H; Ar-H), 7.64 (d, *J* = 8.6 Hz, 2H; Ar-H), 7.59 (dd, *J* = 1.7, 8.0 Hz, 2H; Ar-H), 7.43 (dt, J_t = 1.7, J_d = 8.0 Hz, 1H; Ar-H), 7.38 (d, *J* = 4.0 Hz, 2H; Ar-H), 7.28-7.26 (m, 3H; Ar-H), 7.04-7.00 (m, 3H; Ar-H), 6.97 (d, *J* = 8.0 Hz, 1H; Ar-H), 6.66 (d, *J* = 15.5 Hz, 1H; CH=CO), 4.80 (s, 2H; N-CH_2), 3.95 (s, 3H; O-CH_3).

^{13}C NMR (125 MHz, Chloroform-d_3): δ 178.4, 166.7, 159.3, 149.5, 146.1, 143.6, 142.1, 138.6, 134.9, 132.9, 130.9, 129.4 (2C), 128.7 (2C), 128.5, 123.4, 123.1 (2C), 122.4, 121.0, 118.6, 11.5, 55.7, 53.9.

HRMS (ESI, m/z): Calculated for $C_{29}H_{27}N_4O_4S_2$ $[M + H]^+$ 559.1396; found 559.1446.

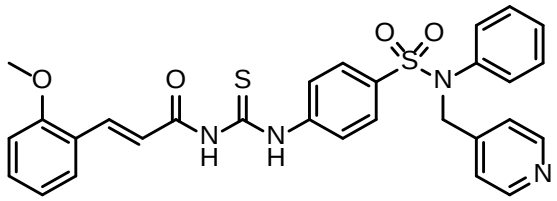

Figure 1.56 ^{1}H and ^{13}C NMR spectra of compound **1.77** [500 MHz for ^{1}H and 125 MHz for ^{13}C, Chloroform-d_3].

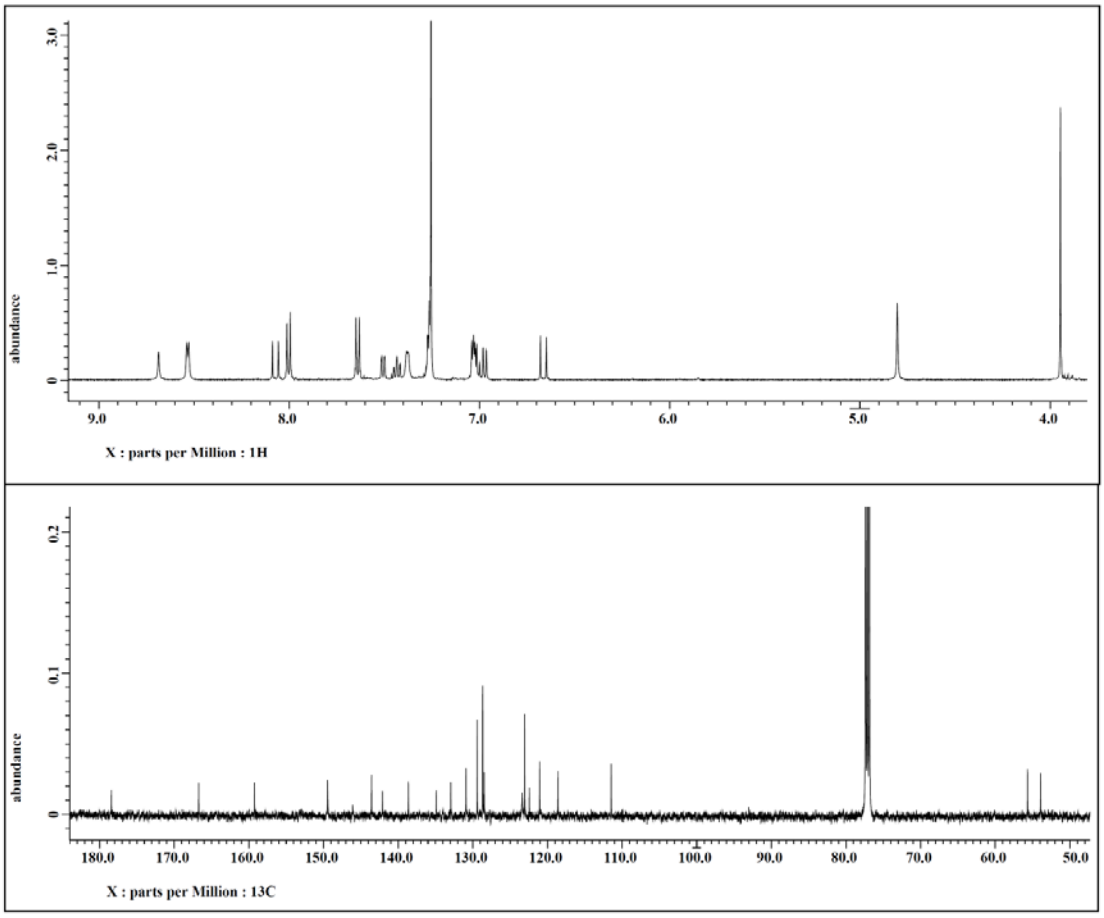

***N*-((4-(*N*-((5-(Hydroxymethyl)furan-2-yl)methyl)-*N*-phenylsulfamoyl)phenyl)carbamothioyl)quinoline-7-carboxamide (1.78)**. The product precipitated as yellow solid. Yield (45 mg, 34%).

^{1}H NMR (500 MHz, DMSO-d_6): δ 12.04 (s, 1H; N-H), 9.02 (dd, *J* = 1.4, 4.1 Hz, 1H; Ar-H), 8.64 (s, 1H; Ar-H), 8.46 (d, *J* = 8.2 Hz, 1H; Ar-H), 8.11 (d, *J* = 8.7 Hz, 1H; Ar-H), 8.04 (dd, *J* = 1.7, 8.7 Hz, 1H; Ar-H), 7.99 (d, *J* = 8.7 Hz, 2H; Ar-H) 7.66 (dd, *J* = 4.1, 8.2 Hz, 1H; Ar-H), 7.62 (d, *J* = 8.7 Hz, 2H; Ar-H), 7.27-7.25 (m, 3H; Ar-H), 7.00 (dd, *J* = 2.3, 7.8 Hz, 2H; Ar-H), 6.04 (d, *J* = 3.2 Hz, 1H; Fur-H), 6.00 (d, *J* = 3.2 Hz, 1H; Fur-H), 5.17 (t, *J* = 6.0 Hz, 1H; O-H), 4.78 (s, 2H; N-CH_2), 4.24 (d, *J* = 6.0, 2H; O-CH_2).

^{13}C NMR (125 MHz, Chloroform-d_3): δ 179.6, 168.2, 156.1, 152.1, 148.8, 142.7, 139.0, 137.4, 135.4, 133.7, 130.8, 130.4, 129.4 (2C), 129.2, 129.1 (2C), 128.7 (2C), 128.7 (2C), 128.5, 126.0, 124.3, 124.1, 110.8, 108.0, 56.1, 48.0.

HRMS (ESI, m/z): Calculated for $C_{29}H_{25}N_4O_5S_2$ $[M + H]^+$ 573.1261; found 573.1243 (3.1 ppm).

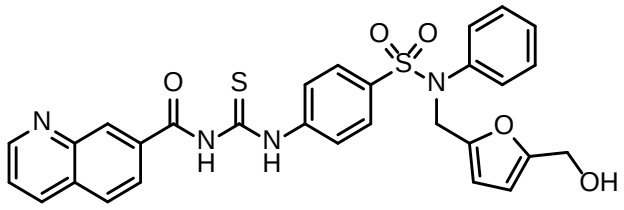

Figure 1.57 ^{1}H and ^{13}C NMR spectra of compound **1.78** [500 MHz for ^{1}H, DMSO-d_6 and 125 MHz for ^{13}C, Chloroform-d_3].

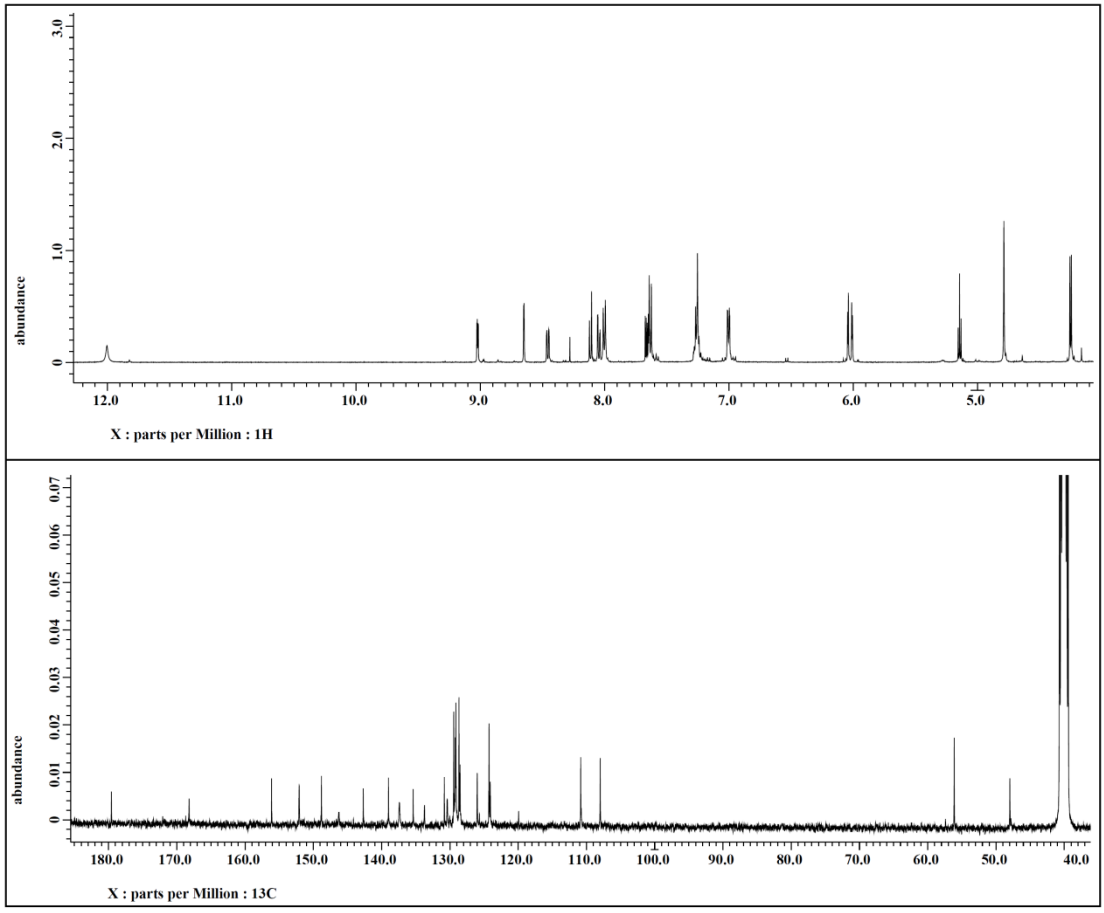

(*E*)-*N*-((4-(*N*-(2-Hydroxybenzyl)-*N*-phenylsulfamoyl)phenyl)carbamothioyl)-3-(2-methoxyphenyl)acrylamide (1.79). The product precipitated as a yellow solid. Yield (39 mg, 48%).

^{1}H NMR (400 MHz, Chloroform-d_3): δ 8.62 (s, 1H, N-H), 8.07 (d, *J* = 15.6 Hz, 1H; Ar-CH=C), 8.03 (d, *J* = 8.7 Hz, 2H; Ar-H), 7.73 (d, *J* = 8.7 Hz, 2H; Ar-H), 7.50 (d, *J* = 8.0 Hz, 1H; Ar-H), 7.43 (t, *J* = 8.0 Hz, 1H; Ar-H), 7.27 (d, *J* = 2.3 Hz, 2H; Ar-H), 7.17-7.12 (m, 1H; Ar-H), 7.02 (d, *J* = 7.8 Hz, 1H; Ar-H), 6.99-6.96 (m, 3H; Ar-H), 6.90 (d, *J* = 7.3 Hz, 2H; Ar-H), 6.65 (d, *J* = 15.6 Hz, 1H; CH=CO), 6.63 (d, *J* = 4.6 Hz, 2H; Ar-H), 4.71 (s, 2H; N-CH_2), 3.95 (s, 3H; O-CH_3).

^{13}C NMR (100 MHz, Acetone-d_6): δ 179.2, 167.3, 159.0, 155.0, 142.4, 141.4, 139.5, 135.3, 132.6, 129.9, 129.5, 128.8 (2C), 128.7 (2C), 128.6, 128.5 (2C), 127.6, 122.9 (2C), 122.9, 122.4, 119.5, 119.5, 115.2, 111.7, 55.3, 48.7.

HRMS (ESI, m/z): Calculated for $C_{30}H_{28}N_3O_5S_2$ $[M + H]^+$ 574.1465; found 574.1449 (2.8 ppm).

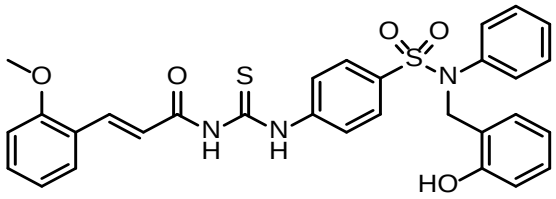

Figure 1.58 ^{1}H and ^{13}C NMR spectra of compound **1.79** [400 MHz for ^{1}H, Chloroform-d_3 and 100 MHz for ^{13}C, Acetone-d_6].

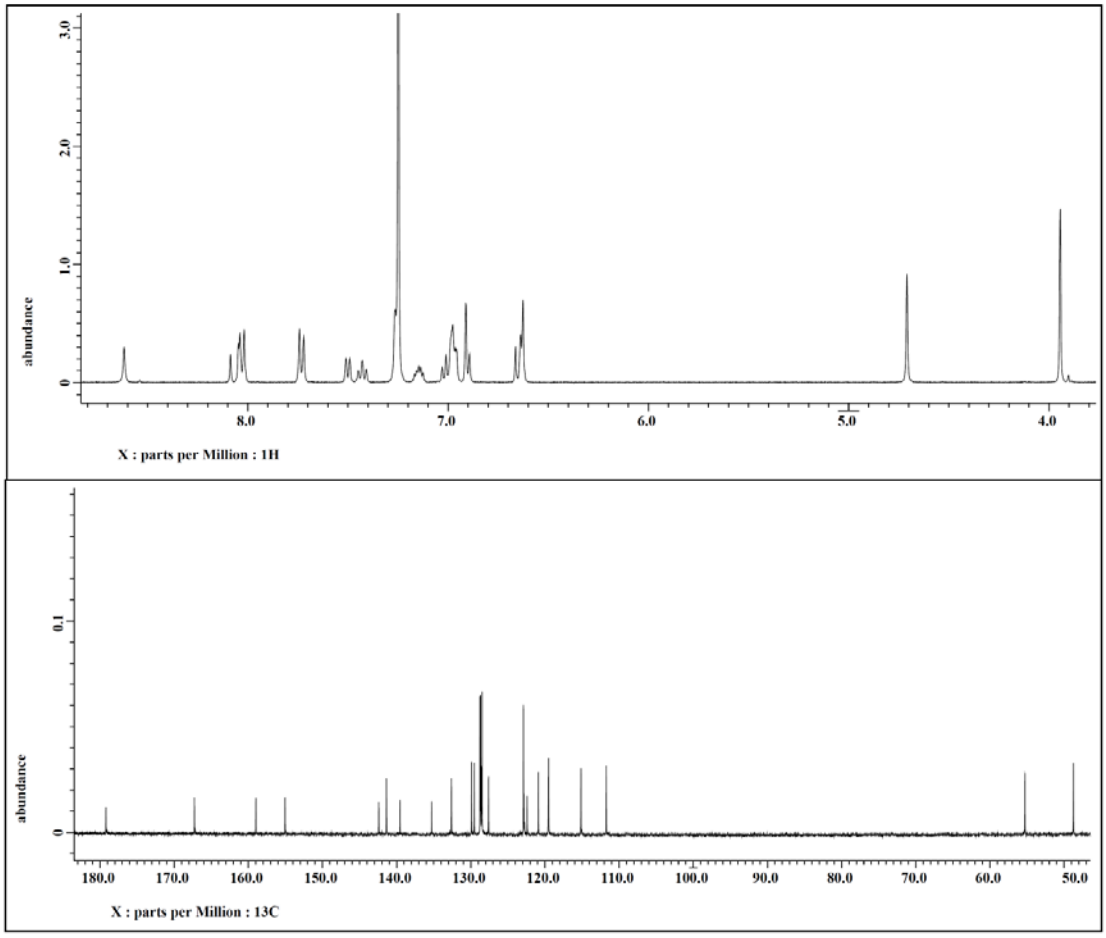

(*E*)-*N*-((4-(*N*-(3-Hydroxybenzyl)-*N*-phenylsulfamoyl)phenyl)carbamothioyl)-3-(2-methoxyphenyl)acrylamide (1.80). The product precipitated as a yellow solid. Yield (32 mg, 44%).

^{1}H NMR (400 MHz, Chloroform-d_3): δ 8.62 (s, 1H, N-H), 8.06 (d, *J* = 15.6 Hz, 1H; Ar-CH=C), 7.97 (d, *J* = 8.7 Hz, 2H; Ar-H), 7.67 (d, *J* = 8.7 Hz, 2H; Ar-H), 7.50 (dd, *J* = 1.8, 8.0 Hz, 1H; Ar-H), 7.43 (t, *J* = 8.0 Hz, 1H; Ar-H), 7.22 (dd, *J* = 1.8, 5.0 Hz, 2H; Ar-H), 7.07 (t, *J* = 7.8 Hz, 1H; Ar-H), 7.03-6.96 (m, 4H; Ar-H), 6.75-6.72 (m, 2H; Ar-H), 6.67-6.65 (m, 1H; Ar-H), 6.64 (d, *J* = 15.6 Hz, 1H; CH=CO), 4.70 (s, 1H; O-H), 4.68 (s, 2H; N-CH_2), 3.94 (s, 3H; O-CH_3).

^{13}C NMR (100 MHz, Acetone-d_6): δ 179.2, 167.3, 159.0, 157.5, 142.4, 141.4, 139.3, 138.2, 135.4, 132.6, 129.5, 129.4, 128.9 (2C), 128.8 (2C), 128.4 (2C), 127.7, 122.9 (2C), 122.8, 120.9, 119.5, 119.4, 115.2, 114.5, 111.7, 55.3, 54.1.

HRMS (ESI, m/z): Calculated for $C_{30}H_{28}N_3O_5S_2$ $[M + H]^+$ 574.1465; found 574.1438 (4.7 ppm).

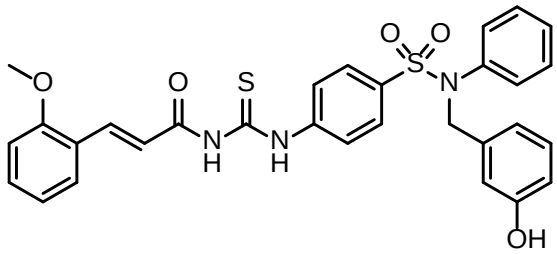

Figure 1.59 ^{1}H and ^{13}C NMR spectra of compound **1.80** [400 MHz for ^{1}H, Chloroform-d_3 and 100 MHz for ^{13}C, Acetone-d_6].

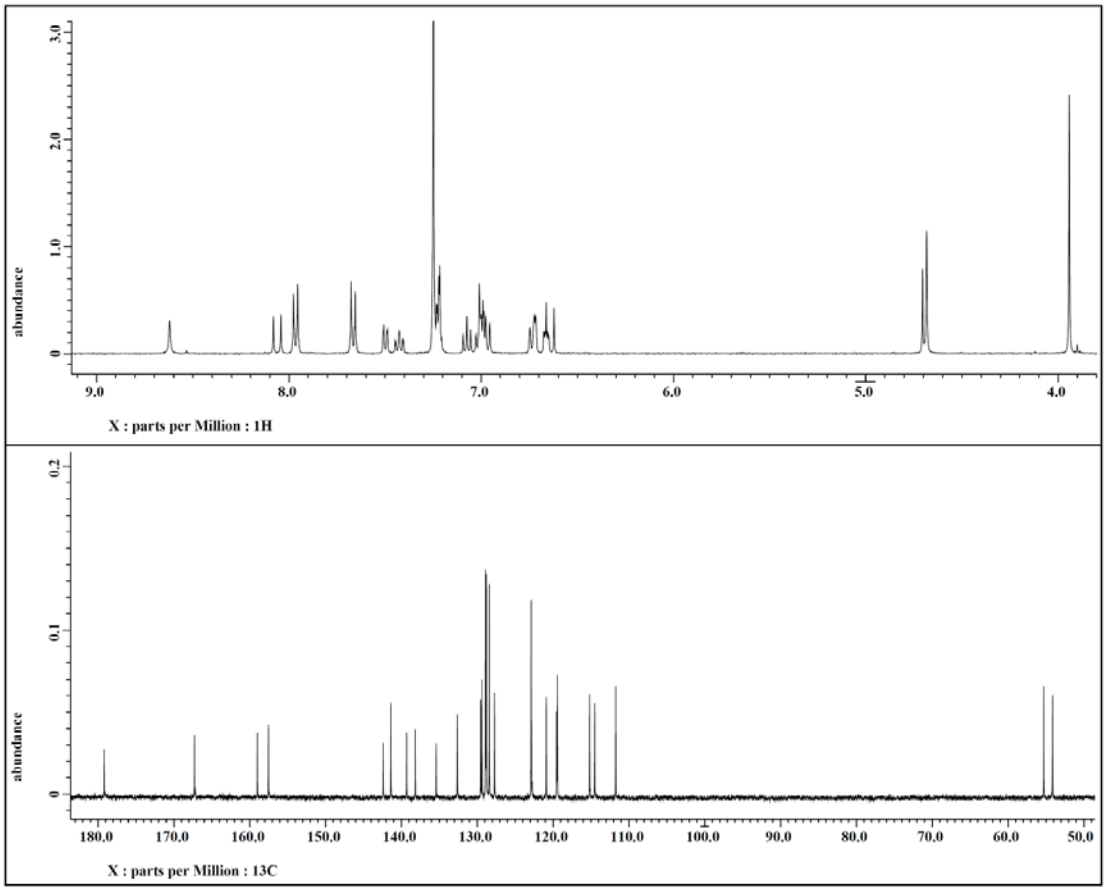

(*E*)-*N*-((4-(*N*-(4-Hydroxybenzyl)-*N*-phenylsulfamoyl)phenyl)carbamothioyl)-3-(2-methoxyphenyl)acrylamide (1.81). The product precipitated as a yellow solid. Yield (104 mg, 54%).

^{1}H NMR (400 MHz, DMSO-d_6): δ 11.76 (s, 1H; N-H), 9.31 (s, 1H; N-H), 7.99 (d, *J* = 8.70 Hz, 2H; Ar-H), 7.94 (d, *J* = 16.0 Hz, 1H; Ar-CH=C), 7.63 (d, *J* = 8.7 Hz, 2H; Ar-H), 7.54 (dd, *J* = 1.4, 7.8 Hz, 1H; Ar-H), 7.44 (dd, *J* = 7.3, 7.8 Hz, 1Hz; Ar-H), 7.23-7.09 (m, 6H; Ar-H), 7.03 (d, *J* = 7.3 Hz, 1H; Ar-H), 6.99-6.95 (m, 5H; Ar-H), 6.56 (d, *J* = 8.2 Hz, 2H; Ar-H), 4.64 (s, 2H; N-CH_2), 3.87 (s, 3H; O-CH_3).

^{13}C NMR (125 MHz, $CDCl_3$): δ 178.1, 167.3, 142.3, 141.6, 141.4, 135.9, 133.7, 131.8, 129.8, 129.5, 129.1 (2C), 129.0, 128.8 (2C), 128.2, 127.6, 126.8 (2C), 125.1, 123.3, 122.9 (2C), 65.0, 38.3.

HRMS (ESI, m/z): Calculated for $C_{30}H_{28}N_3O_5S_2$ $[M + H]^+$ 574.1465; found 574.1452 (2.2 ppm).

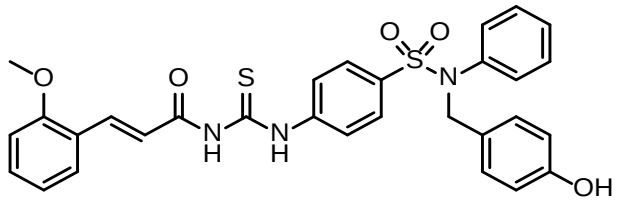

Figure 1.60 ^{1}H and ^{13}C NMR spectra of compound **1.81** [400 MHz for ^{1}H, Chloroform-d_3 and 100 MHz for ^{13}C, Acetone-d_6].

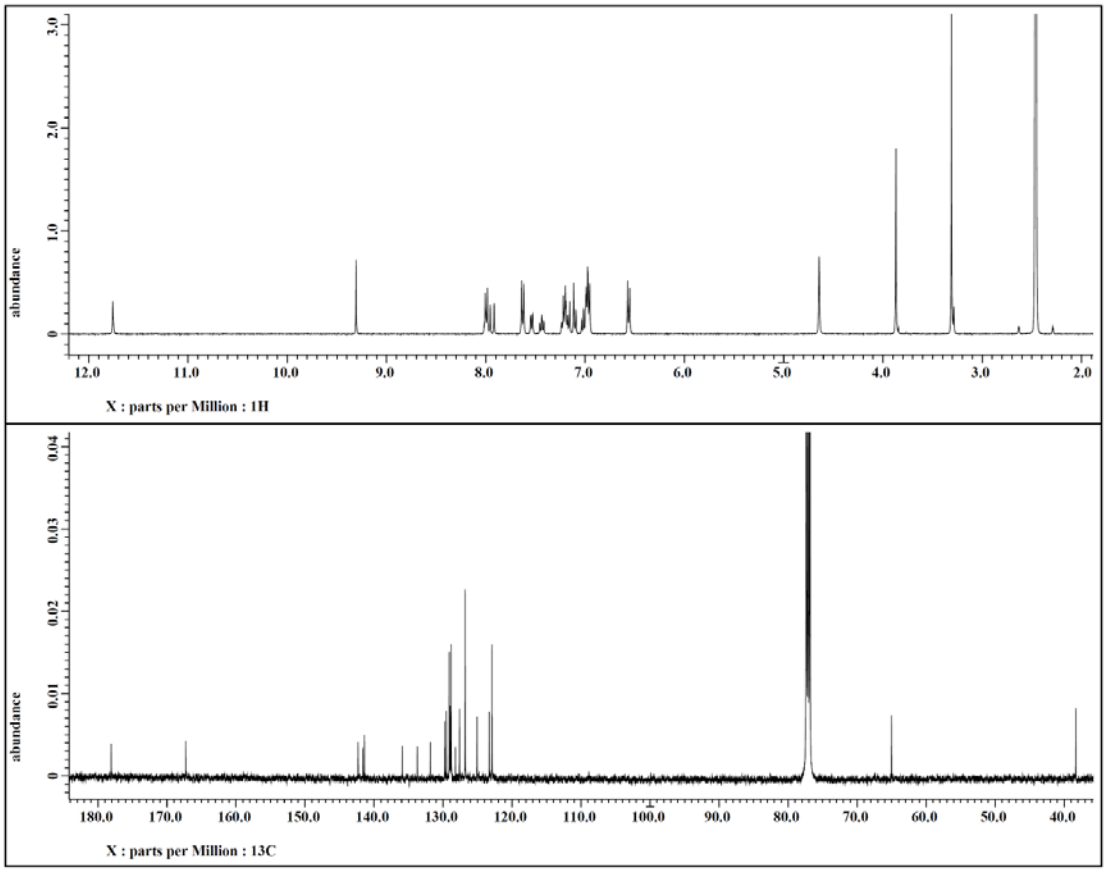

(*E*)-*N*-((4-(*N*-(2-Hydroxyethyl)sulfamoyl)phenyl)carbamothioyl)-3-(2-methoxyphenyl)acrylamide (1.83).

^{1}H NMR (500 MHz, DMSO-d_6): δ 12.95 (s, 1H; N-H), 11.70 (s, 1H; N-H), 7.95-7.92 (m, 3H; Ar-H), 7.79 (d, J = 9.2 Hz, 2H; Ar-H), 7.59 (t, J = 6.1 Hz, 1H; Ar-H), 7.54 (dd, J = 1.5, 7.6 Hz, 1H; Ar-H), 7.43 (dt, J_d = 1.5 , J_t = 7.6 Hz, 1H; Ar-H), 7.13 (d, J = 16.1 Hz, 1H; Ar-CH=C), 7.10 (d, J = 7.6 Hz, 1H; Ar-H), 7.02 (t, J = 7.6 Hz, 1H; Ar-H), 4.66 (t, J = 6.1 Hz, 1H; O-H), 3.87 (s, 3H; O-CH_3), 3.35 (q, J = 6.1 Hz, 2H; O-CH_2), 2.78 (q, J = 6.1 Hz, 2H; N-CH_2).

^{13}C NMR (125 MHz, DMSO-d_6): δ 179.7, 167.4, 158.9, 141.7, 140.7, 138.0, 133.0, 129.8, 127.7 (2C), 124.6 (2C), 122.8, 121.5, 120.6, 112.4, 60.5, 56.2, 45.6.

HRMS (ESI, m/z): Calculated for $C_{19}H_{22}N_3O_5S_2$ $[M + H]^+$ 436.0995; found 574.1452 (1.7 ppm).

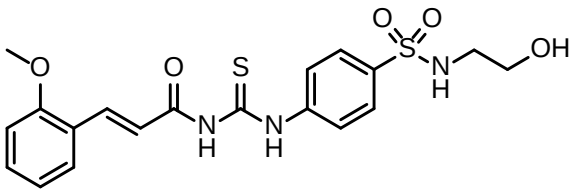

Figure 1.61 ^{1}H and ^{13}C NMR spectra of compound **1.83** [500 MHz for ^{1}H and 100 MHz for ^{13}C, DMSO-d_6].

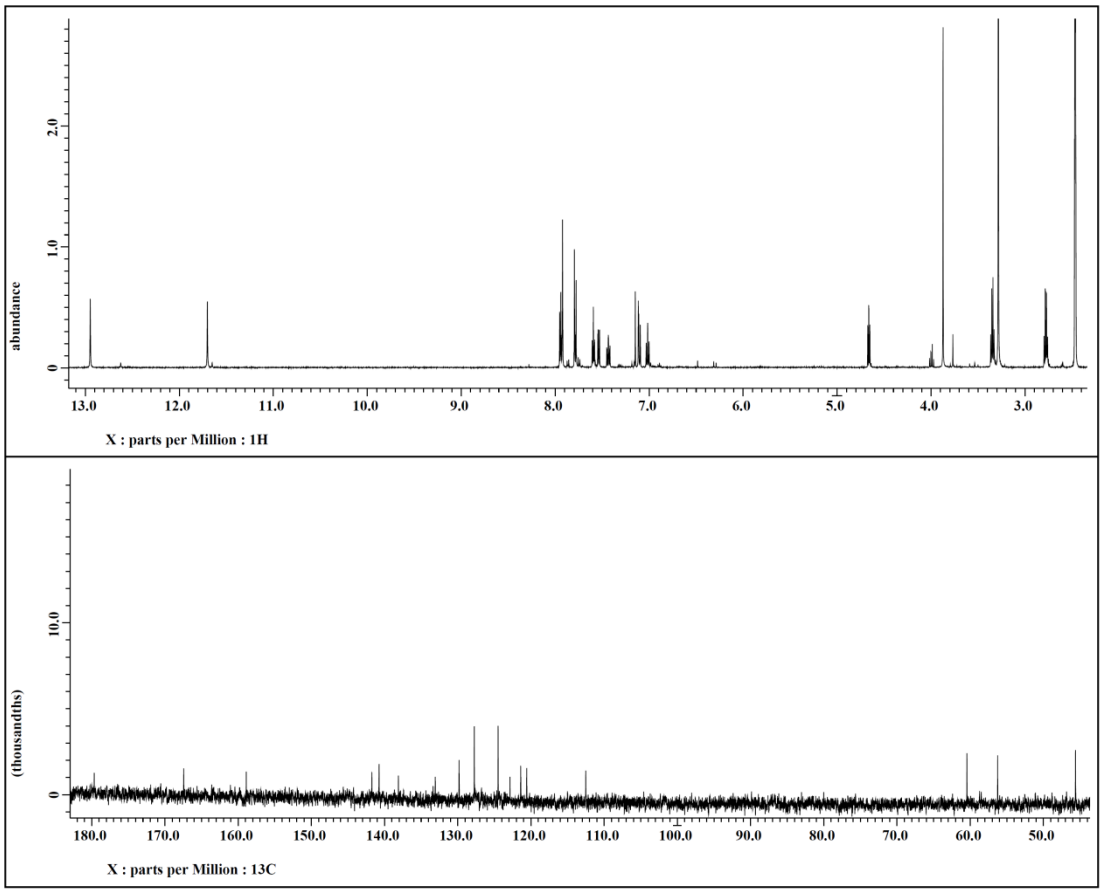

(*E*)-*N*-((4-(*N*-(2,3-Dihydroxypropyl)sulfamoyl)phenyl)carbamothioyl)-3-(2-methoxyphenyl)acrylamide (1.84). The product precipitated as a yellow solid. Yield (77 mg, 59%).

^{1}H NMR (400 MHz, DMSO-d_6): δ 12.95 (s, 1H; N-H), 11.73 (s, 1H; N-H), 7.95-7.91 (m, 3H; Ar-CH=C and Ar-H), 7.78 (d, J = 8.7 Hz, 2H; Ar-H), 7.58-7.52 (m, 2H; Ar-H), 7.43 (t, J = 7.3 Hz, 2H; Ar-H), 7.13 (d, J = 15.6 Hz, 1H; C=CH), 7.10 (d, J = 8.7 Hz, 1H; Ar-H), 7.01 (t, J = 7.3 Hz, 1H; Ar-H), 4.77 (d, J = 5.0 Hz, 1H; O-H), 4.53 (t, J = 6.0 Hz, 1H; O-H), 3.86 (s, 3H; O-CH_3), 3.43 (dq, J_d = 6.9, J_q = 5.5 Hz, 1H; O-CH), 3.23 (m, 2H; O-CH_2-), 2.85 (m, 1H; N-CH_2), 2.57 (m, 1H; N-CH_2).

^{13}C NMR (125 MHz, DMSO-d_3): δ 179.6, 167.4, 158.9, 141.7, 140.8, 138.0, 133.1, 129.9, 127.8 (2C), 124.5 (2C), 122.8, 121.4, 120.5, 112.5, 70.9, 64.0, 56.2, 46.6.

HRMS (ESI, m/z): Calculated for $C_{20}H_{24}N_3O_6S_2$ $[M + H]^+$ 466.1101; found 466.1088 (2.8 ppm).

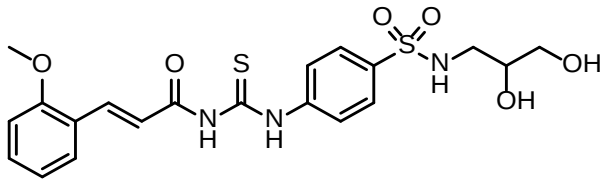

Figure 1.62 ^{1}H and ^{13}C NMR spectra of compound **1.84** [400 MHz for ^{1}H and 125 MHz for ^{13}C, DMSO-d_6].

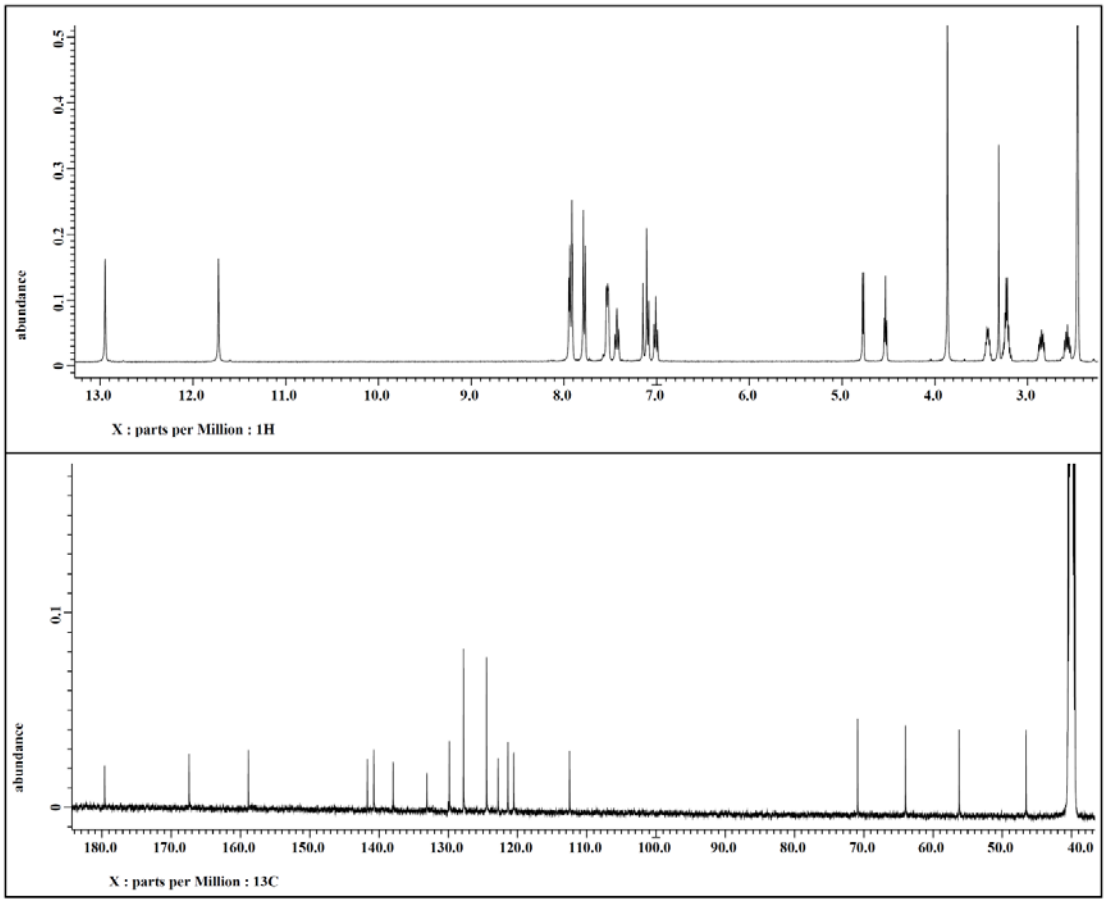

(*E*)-*N*-((4-(*N*-(3,4-Dimethylisoxazol-5-yl)sulfamoyl)phenyl)carbamothioyl)-3-(2-methoxyphenyl)acrylamide (1.85). Yellow precipitate. Yield (63%).

^{1}H NMR (400 MHz, Chloroform-d_3): δ 8.69 (s, 1H; N-H), 8.05 (d, *J* = 15.6 Hz, 1H; Ar-CH=C), 8.02 (d, *J* = 8.7 Hz, 2H; Ar-H), 7.83 (d, *J* = 8.7 Hz, 2H; Ar-H), 7.49 (d, *J* = 7.6 Hz, 1H; Ar-H), 7.42 (dt, J_d = 1.4, J_t = 8.0 Hz, 1H; Ar-H), 7.00 (t, *J* = 7.3 Hz, 1H; Ar-H), 6.96 (d, *J* = 8.4 Hz, 1H; Ar-H), 6.65 (d, *J* = 15.6 Hz, 1H; C=CHCO), 6.63 (bs, 1H; SO_2N-H), 3.93 (s, 3H; O-CH_3), 2.19 (s, 3H; Ar-CH_3), 1.92 (s, 3H; Ar-CH_3).

^{13}C NMR (125 MHz, Chloroform-d_3): δ 179.4, 167.2, 161.6, 159.0, 155.4, 142.8, 141.4, 137.0, 132.6, 129.5, 127.9, 123.3, 123.2, 122.8, 120.9, 119.5, 11.7, 106.5, 55.3, 9.9, 5.7.

HRMS (ESI, m/z): Calculated for $C_{22}H_{23}N_4O_5S_2$ $[M + H]^+$ 487.1104; found 487.1088 (3.4 ppm).

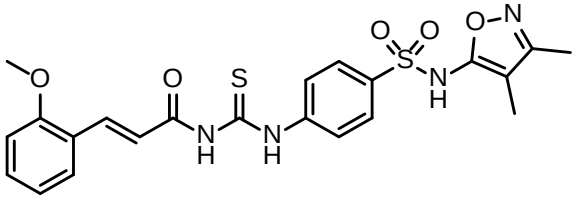

Figure 1.63 ^{1}H and ^{13}C NMR spectra of compound **1.85** [400 MHz for ^{1}H and 125 MHz for ^{13}C, Chloroform-d_3].

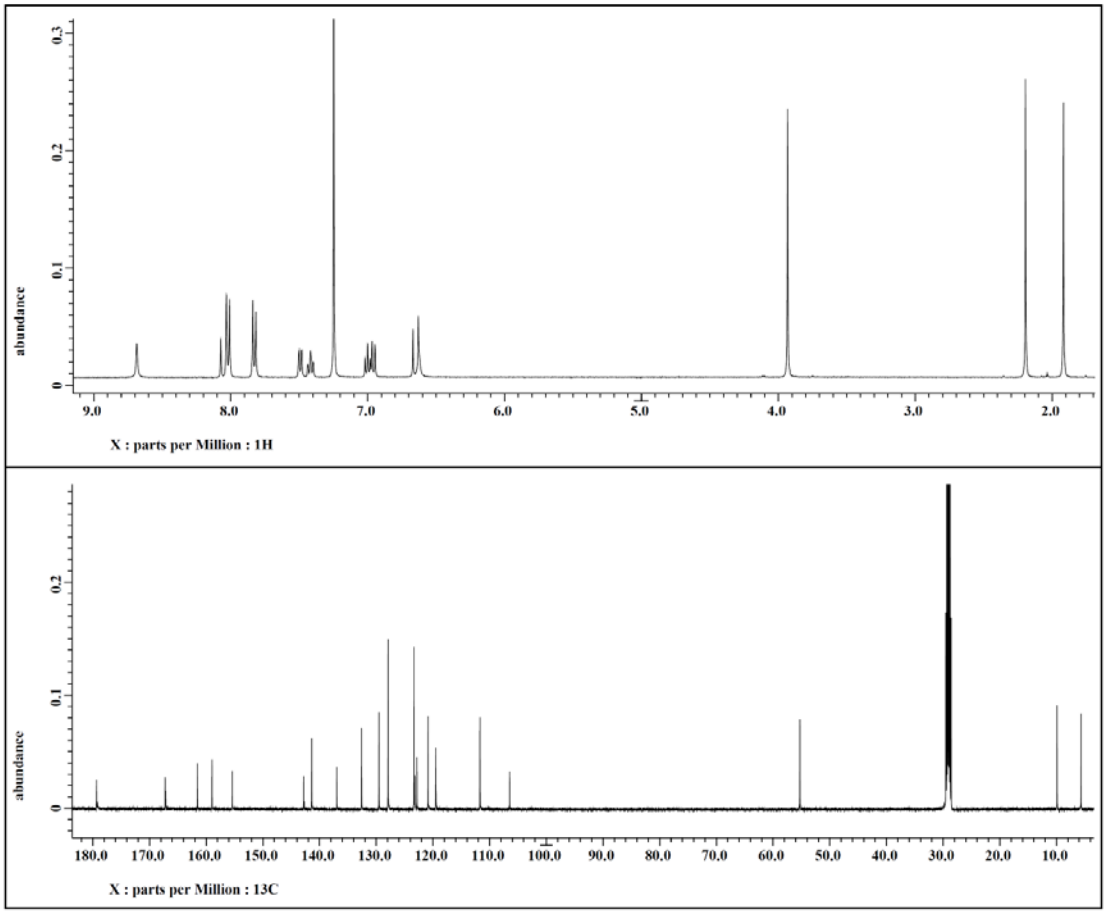

***N*-((4-(*N*-phenyl-*N*-(Pyridin-4-ylmethyl)sulfamoyl)phenyl)carbamothioyl)quinoline-7-carboxamide (1.86)**. The product precipitated as a yellow solid. Yield (80 mg, 63%).

^{1}H NMR (500 MHz, DMSO-d_6): δ 12.74 (s, 1H; N-H), 12.02 (s, 1H; N-H), 9.02 (dd, 1.5, 4.6 Hz, 1H; Ar-H), 8.65 (s, 1H; Ar-H), 8.46 (d, *J* = 8.4 Hz, 1H; Ar-H), 8.43 (d, *J* = 6.1 Hz, 2H; Ar-H), 8.12 (d, *J* = 8.4 Hz, 1H; Ar-H), 8.05 (d, *J* = 8.4 Hz, 3H; Ar-H), 7.69-7.65 (m, 3H; Ar-H), 7.29 (d, *J* = 5.4 Hz, 2H; Ar-H), 7.26 (d, *J* = 7.6 Hz, 2H; Ar-H), 7.23-7.20 (m, 1H; Ar-H), 7.11 (d, *J* = 6.9 Hz, 2H; Ar-H), 4.87 (s, 2H; N-CH_2)

^{13}C NMR (125 MHz, DMSO-d_6): δ 179.6, 168.3, 152.5 (2C), 150.1 (2C), 147.1, 146.2, 142.9, 139.1, 136.5, 134.7, 133.4, 131.1, 130.8, 129.6 (2C), 129.1, 128.8 (2C), 128.7 (2C), 128.5, 125.7, 124.4, 124.1, 123.4 (2C), 53.2.

HRMS (ESI, m/z): Calculated for $C_{29}H_{24}N_5O_3S_2$ $[M + H]^+$ 554.1315; found 554.1298 (3.1 ppm).

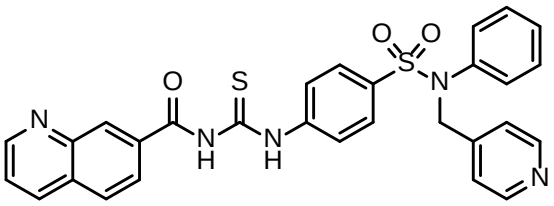

Figure 1.64 ^{1}H and ^{13}C NMR spectra of compound **1.86** [500 MHz for ^{1}H and 125 MHz for ^{13}C, DMSO-d_6].

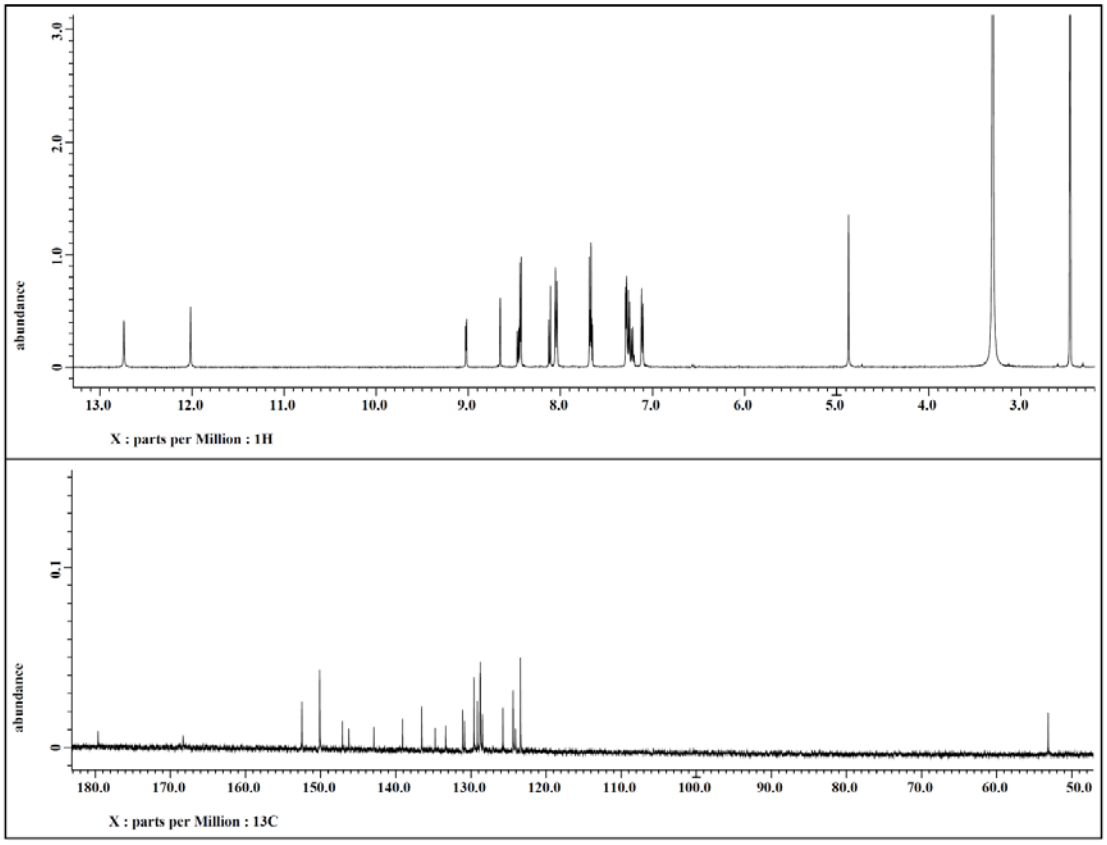

***N*-((4-(*N*-(4-Hydroxybenzyl)-*N*-phenylsulfamoyl)phenyl)carbamothioyl)quinoline-7-carboxamide (1.87)**. The product precipitated as a yellow solid. Yield (42.5 mg, 29%).

^{1}H NMR (400 MHz, DMSO-d_6): δ 12.73 (s, 1H; N-H), 12.04 (s, 1H; N-H), 9.13 (bs, 1H; O-H), 9.03 (dd, *J* = 1.8, 4.1 Hz, 1H; Ar-H), 8.65 (s, 1H; Ar-H), 8.48 (d, *J* = 7.8 Hz, 1H; Ar-H), 8.12 (d, *J* = 8.2 Hz, 1H; Ar-H), 8.07-8.01 (m, 3H; Ar-H), 7.69-7.64 (m, 3H; Ar-H), 7.24-7.16 (m, 3H; Ar-H), 6.99-6.96 (m, 4H; Ar-H), 6.56 (d, *J* = 8.2 Hz, 2H; Ar-H), 4.65 (s, 2H, N-CH_2).

^{13}C NMR (125 MHz, Chloroform-d_3): δ 179.5, 157.4, 152.2, 147.1, 142.6, 139.1, 136.7, 135.5, 133.4, 131.1, 130.8, 130.1 (2C), 129.3 (2C), 129.1 (2C), 128.6 (2C), 128.2, 126.6, 125.7, 124.4 (2C), 124.0, 115.6, 53.8.

HRMS (ESI, m/z): Calculated for $C_{30}H_{25}N_4O_4S_2$ $[M + H]^+$ 569.1312; found 569.1295 (2.9 ppm).

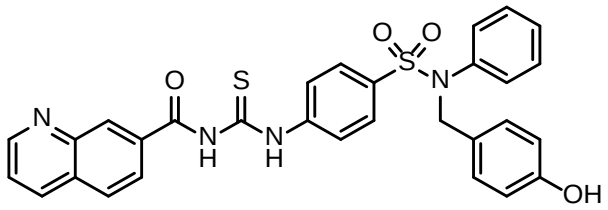

Figure 1.65 ^{1}H and ^{13}C NMR spectra of compound **1.87** [400 MHz for ^{1}H, DMSO-d_6, and 125 MHz for ^{13}C, Chloroform-d_3].

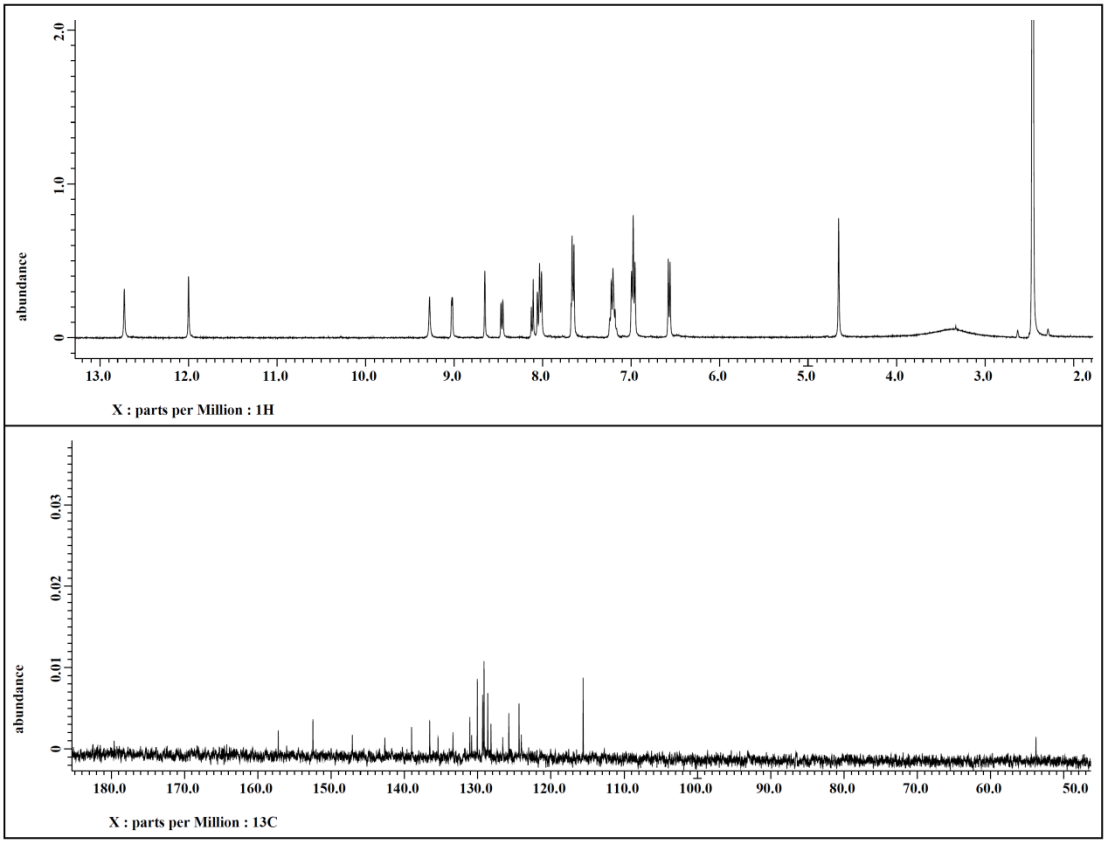

1.5 References

1 Sawzdargo, M.; Nguyen, T.; Lee, D. K.; Lynch, K. R.; Cheng, R.; Heng, H. H.; George, S. R.; O'Dowd, B. F., Identification and cloning of three novel human G protein-coupled receptor genes GPR52, PsiGPR53 and GPR55: GPR55 is extensively expressed in human brain. *Molecular Brain Research* **1999,** *64* (2), 193-198.

2 Whyte, L. S.; Ryberg, E.; Sims, N. A.; Ridge, S. A.; Mackie, K.; Greasley, P. J.; Ross, R. A.; Rogers, M. J., The putative cannabinoid receptor GPR55 affects osteoclast function in vitro and bone mass in vivo. *Proceedings of the National Academy of Sciences of the United States of America* **2009,** *106* (38), 16511-16516.

3 Balenga, N. A.; Aflaki, E.; Kargl, J.; Platzer, W.; Schroder, R.; Blattermann, S.; Kostenis, E.; Brown, A. J.; Heinemann, A.; Waldhoer, M., GPR55 regulates cannabinoid 2 receptor-mediated responses in human neutrophils. *Cell Research* **2011,** *21* (10), 1452-1469.

4 Ryberg, E.; Larsson, N.; Sjogren, S.; Hjorth, S.; Hermansson, N. O.; Leonova, J.; Elebring, T.; Nilsson, K.; Drmota, T.; Greasley, P. J., The orphan receptor GPR55 is a novel cannabinoid receptor. *British Journal of Pharmacology* **2007,** *152* (7), 1092-10101.

5 Staton, P. C.; Hatcher, J. P.; Walker, D. J.; Morrison, A. D.; Shapland, E. M.; Hughes, J. P.; Chong, E.; Mander, P. K.; Green, P. J.; Billinton, A.; Fulleylove, M.; Lancaster, H. C.; Smith, J. C.; Bailey, L. T.; Wise, A.; Brown, A. J.; Richardson, J. C.; Chessell, I. P., The putative cannabinoid receptor GPR55 plays a role in mechanical hyperalgesia associated with inflammatory and neuropathic pain. *Pain* **2008,** *139* (1), 225-36.

6 Andradas, C.; Caffarel, M. M.; Perez-Gomez, E.; Salazar, M.; Lorente, M.; Velasco, G.; Guzman, M.; Sanchez, C., The orphan G protein-coupled receptor GPR55 promotes cancer cell proliferation via ERK. *Oncogene* **2011,** *30* (2), 245-52.

7 Li, K.; Fichna, J.; Schicho, R.; Saur, D.; Bashashati, M.; Mackie, K.; Li, Y.; Zimmer, A.; Goke, B.; Sharkey, K. A.; Storr, M., A role for O-1602 and G protein-

coupled receptor GPR55 in the control of colonic motility in mice. *Neuropharmacology* **2013,** *71*, 255-263.

8 Kargl, J.; Brown, A. J.; Andersen, L.; Dorn, G.; Schicho, R.; Waldhoer, M.; Heinemann, A., A selective antagonist reveals a potential role of g protein-coupled receptor 55 in platelet and endothelial cell function. *Journal of Pharmacology and Experimental Therapeutics* **2013,** *346* (1), 54-66.

9 Pineiro, R.; Maffucci, T.; Falasca, M., The putative cannabinoid receptor GPR55 defines a novel autocrine loop in cancer cell proliferation. *Oncogene* **2011,** *30* (2), 142-152.

10 Zhang, X.; Maor, Y.; Wang, J. F.; Kunos, G.; Groopman, J. E., Endocannabinoid-like N-arachidonoyl serine is a novel pro-angiogenic mediator. *British journal of pharmacology* **2010,** *160* (7), 1583-1594.

11 Baker, D.; Pryce, G.; Davies, W. L.; Hiley, C. R., In silico patent searching reveals a new cannabinoid receptor. *Trends in Pharmacological Sciences* **2006,** *27* (1), 1-4.

12 Yin, H.; Chu, A.; Li, W.; Wang, B.; Shelton, F.; Otero, F.; Nguyen, D. G.; Caldwell, J. S.; Chen, Y. A., Lipid G protein-coupled receptor ligand identification using beta-arrestin PathHunter assay. *The Journal of Biological Chemistry* **2009,** *284* (18), 12328-12338.

13 Brown, A. J., Novel cannabinoid receptors. *British Journal of Pharmacology* **2007,** *152* (5), 567-575.

14 Kapur, A.; Zhao, P.; Sharir, H.; Bai, Y.; Caron, M. G.; Barak, L. S.; Abood, M. E., Atypical responsiveness of the orphan receptor GPR55 to cannabinoid ligands. *The Journal of Biological Chemistry* **2009,** *284* (43), 29817-29827.

15 Lauckner, J. E.; Jensen, J. B.; Chen, H. Y.; Lu, H. C.; Hille, B.; Mackie, K., GPR55 is a cannabinoid receptor that increases intracellular calcium and inhibits M current. *Proceedings of the National Academy of Sciences of the United States of America* **2008,** *105* (7), 2699-2704.

16 Maguire, J. J.; Kuc, R. E.; Davenport, A. P., Radioligand binding assays and their analysis. *Methods in Molecular Biology* **2012,** *897*, 31-77.

17 Cherezov, V.; Rosenbaum, D. M.; Hanson, M. A.; Rasmussen, S. G.; Thian, F. S.; Kobilka, T. S.; Choi, H. J.; Kuhn, P.; Weis, W. I.; Kobilka, B. K.; Stevens, R. C., High-resolution crystal structure of an engineered human beta2-adrenergic G protein-coupled receptor. *Science* **2007,** *318* (5854), 1258-1265.

18 Kotsikorou, E.; Madrigal, K. E.; Hurst, D. P.; Sharir, H.; Lynch, D. L.; Heynen-Genel, S.; Milan, L. B.; Chung, T. D.; Seltzman, H. H.; Bai, Y.; Caron, M. G.; Barak, L.; Abood, M. E.; Reggio, P. H., Identification of the GPR55 agonist binding site using a novel set of high-potency GPR55 selective ligands. *Biochemistry* **2011,** *50* (25), 5633-2647.

19 Pagliero, R. J.; Lusvarghi, S.; Pierini, A. B.; Brun, R.; Mazzieri, M. R., Synthesis, stereoelectronic characterization and antiparasitic activity of new 1-benzenesulfonyl-2-methyl-1,2,3,4-tetrahydroquinolines. *Bioorganic & Medicinal Chemistry* **2010,** *18* (1), 142-150.

20 Ansari, M. H.; Ahmada, M.; Dicke, K. A., Synthesis of 2-(p-aminobenzyl) derivatives of 1,4,7-triazacyclononane-N,N′,N″-triacetic acid (NOTA) and 1,4,7,10-tetraazacyclododecane-N,N′,N″,N‴-tetraacetic acid (DOTA): macrocyclic bifunctional chelating agents useful for antibodies labeling. *Bioorganic & Medicinal Chemistry Letters* **1993,** *3* (6), 1067-1070.

21 Liu, Y.; Meng, L.; Lu, X.; Zhang, L.; He, Y., Thermo and pH sensitive fluorescent polymer sensor for metal cations in aqueous solution. *Polymers for Advanced Technologies* **2008,** *19* (2), 137-143.

22 Dickson, S. J.; Paterson, M. J.; Willans, C. E.; Anderson, K. M.; Steed, J. W., Anion binding and luminescent sensing using cationic ruthenium(II) aminopyridine complexes. *Chemistry* **2008,** *14* (24), 7296-7305.

23 Nicolaou, K. C.; Xu, J. Y.; Kim, S.; Pfefferkorn, J.; Ohshima, T.; Vourloumis, D.; Hosokawa, S., Total synthesis of sarcodictyins A and B. *Journal of the American Chemical Society* **1998,** *120* (34), 8661-8673.

24 Highet, R. J.; Wildman, W. C., Solid Manganese Dioxide as an Oxidizing Agent. *Journal of the American Chemical Society* **1955,** *77* (16), 4399-4401.

25 Cho, S. J.; Jensen, N. H.; Kurome, T.; Kadari, S.; Manzano, M. L.; Malberg, J. E.; Caldarone, B.; Roth, B. L.; Kozikowski, A. P., Selective 5-Hydroxytryptamine 2C Receptor Agonists Derived from the Lead Compound Tranylcypromine: Identification of Drugs with Antidepressant-Like Action. *Journal of Medicinal Chemistry* **2009,** *52* (7), 1885-1902.

26 Todd, R. C.; Hossain, M. M.; Josyula, K. V.; Gao, P.; Kuo, J.; Tan, C. T., New amine-stabilized deuterated borane–tetrahydrofuran complex (BD3–THF): convenient reagent for deuterium incorporations. *Tetrahedron Letters* **2007,** *48* (13), 2335-2337.

27 Goldstein, D. M.; Alfredson, T.; Bertrand, J.; Browner, M. F.; Clifford, K.; Dalrymple, S. A.; Dunn, J.; Freire-Moar, J.; Harris, S.; Labadie, S. S.; La Fargue, J.; Lapierre, J. M.; Larrabee, S.; Li, F. J.; Papp, E.; McWeeney, D.; Ramesha, C.; Roberts, R.; Rotstein, D.; San Pablo, B.; Sjogren, E. B.; So, O. Y.; Talamas, F. X.; Tao, W.; Trejo, A.; Villasenor, A.; Welch, M.; Welch, T.; Weller, P.; Whiteley, P. E.; Young, K.; Zipfel, S., Discovery of S-[5-amino-1-(4-fluorophenyl)-1H-pyrazol-4-yl]-[3-(2,3-dihydroxypropoxy)phenyl]methanone (RO3201195), an orally bioavailable and highly selective inhibitor of p38 map kinase. *Journal of Medicinal Chemistry* **2006,** *49* (5), 1562-1575.

28 Willis, P. G.; Pavlova, O. A.; Chefer, S. I.; Vaupel, D. B.; Mukhin, A. G.; Horti, A. G., Synthesis and structure-activity relationship of a novel series of aminoalkylindoles with potential for imaging the neuronal cannabinoid receptor by positron emission tomography. *Journal of Medicinal Chemistry* **2005,** *48* (18), 5813-5822.

29 Ferguson, S. S.; Caron, M. G., Green fluorescent protein-tagged beta-arrestin translocation as a measure of G protein-coupled receptor activation. *Methods Mol Biol* **2004,** *237*, 121-126.

30 Kouznetsov, V.; Rodriguez, W.; Stashenko, E.; Ochoa, C.; Vega, C.; Rolon, M.; Pereira, D. M.; Escario, J. A.; Barrio, A. G., Transformation of Schiff bases derived from alpha-naphthaldehyde. Synthesis, spectral data and biological activity of new-3-aryl-2-(alpha-naphtyl)-4-thiazolidinones and N-aryl-N-[1-(alpha-naphthyl)but-3-enyl]amines. *Journal of Heterocyclic Chemistry* **2004,** *41* (6), 995-999.

31 Huang, Y.-B.; Yi, W.-B.; Cai, C., An efficient, recoverable fluorous organocatalyst for direct reductive amination of aldehydes. *Journal of Fluorine Chemistry* **2010,** *131* (8), 879-882.

32 Armani, E.; Amari, G.; Riccaboni, M.; Rizzi, A.; Baker-Glenn, C.; Blackaby, W.; Van de Poel, H.; Whittaker, B. Phenylethylpyridine derivatives as PDE4-inhibitors. WO/2014/086852 2014.

33 Sreedhar, B.; Rawat, V. S., Mild and Efficient PtO2-Catalyzed One-Pot Reductive Mono-N-alkylation of Nitroarenes. *Synthetic Communications* **2012,** *42* (17), 2490-2502.

34 Zheng, X.; Oda, H.; Takamatsu, K.; Sugimoto, Y.; Tai, A.; Akaho, E.; Ali, H. I.; Oshiki, T.; Kakuta, H.; Sasaki, K., Analgesic agents without gastric damage: Design and synthesis of structurally simple benzenesulfonanilide-type cyclooxygenase-1-selective inhibitors. *Bioorganic & Medicinal Chemistry* **2007,** *15* (2), 1014-1021.

35 Bombrun, A.; Schwarz, M.; Crosignani, S.; Covini, D.; Marin, D. 6-amino-pyrimidine-4-carboxamide derivatives and related compounds which bind to the sphingosine 1-phosphate (s1p) receptor for the treatment of multiple sclerosis. WO2008EP59933 20080729 2009.

36 Zheng, X. X.; Oda, H.; Takamatsu, K.; Sugimoto, Y.; Tai, A.; Akaho, E.; Ali, H. I.; Oshiki, T.; Kakuta, H.; Sasaki, K., Analgesic agents without gastric damage: Design and synthesis of structurally simple benzenesulfonanilide-type cyclooxygenase-1-selective inhibitors (vol 15, pg 1014, 2007). *Bioorganic & Medicinal Chemistry* **2007,** *15* (9), 3299-3300.

37 Pu, Y.-M.; Ku, Y.-Y.; Grieme, T.; Black, L. A.; Bhatia, A. V.; Cowart, M., An Expedient and Multikilogram Synthesis of a Naphthalenoid H3 Antagonist. *Organic Process Research & Development* **2007,** *11* (6), 1004-1009.

38 Sleebs, B. E.; Nguyen, N. H.; Hughes, A. B., Diastereoselective synthesis of cyclic beta(2,3)-amino acids utilizing 4-substituted-1,3-oxazinan-6-ones. *Tetrahedron* **2013,** *69* (30), 6275-6284.

39 Granzhan, A.; Teulade-Fichou, M.-P., Synthesis of mono- and bibrachial naphthalene-based macrocycles with pyrene or ferrocene units for anion detection. *Tetrahedron* **2009,** *65* (7), 1349-1360.

40 Ku, Y.-Y.; Grieme, T.; Pu, Y.-M.; Bhatia, A. V., A Highly Efficient Synthesis of a Naphthalenoid Histamine-3 Antagonist. *Advanced Synthesis & Catalysis* **2009,** *351* (11-12), 2024-2030.

41 Gillig, J. R.; Kinnick, M. D.; Morin, J. M. J.; Navarro, M. A. Novel mch receptor antagonists. WO2004US32314 20041021 2006.

42 McPherson, J.; Edmunds, T.; Zhou, Q. Antibody-based therapeutics with enhanced adcc activity. US20060551679 20061020 2007.

43 de Groot, F. M. H.; Loos, W. J.; Koekkoek, R.; van Berkom, L. W. A.; Busscher, G. F.; Seelen, A. E.; Albrecht, C.; de Bruijn, P.; Scheeren, H. W., Elongated Multiple Electronic Cascade and Cyclization Spacer Systems in Activatible Anticancer Prodrugs for Enhanced Drug Release. *The Journal of Organic Chemistry* **2001,** *66* (26), 8815-8830.

44 Milanese, A.; Gorincioi, E.; Rajabi, M.; Vistoli, G.; Santaniello, E., New synthesis of 6[3-(1-adamantyl)-4-methoxyphenyl]-2-naphthoic acid and evaluation of the influence of adamantyl group on the DNA binding of a naphthoic retinoid. *Bioorganic Chemistry* **2011,** *39* (4), 151-158.

45 Venkatraj, M.; Messagie, J.; Joossens, J.; Lambeir, A.-M.; Haemers, A.; Van der Veken, P.; Augustyns, K., Synthesis and evaluation of non-basic inhibitors of urokinase-type plasminogen activator (uPA). *Bioorganic & Medicinal Chemistry* **2012,** *20* (4), 1557-1568.

CHAPTER II

ISOLATION, SEMISYNTHESIS, COVALENT DOCKING AND TRANSFORMING GROWTH FACTOR BETA-ACTIVATED KINASE 1 (TAK1)-INHIBITORY ACTIVITIES OF (5Z)-7-OXOZEAENOL ANALOGUES

2.1 Introduction

Transforming growth factor-β-activated kinase 1 (TAK-1) is a member of the serine/threonine mitogen-activated protein kinase kinase kinase (MAP3K) family.[1] A wide range of extracellular stimuli, such as proinflammatory interleukins, activate the intracellular TAK-1 via membrane-bound receptors.[2] Turning on the upstream key signaling enzyme results in subsequent phosphorylation of specific MAP2Ks and MAPKs which, in turn, activates a number of transcription factors including AP-1 and NF-κB.[3] These DNA-binding proteins are known to regulate inflammatory responses and apoptosis. Inhibition of upstream kinases such as MAP3Ks has an advantage over inhibiting downstream signaling molecules, mostly due to the former being more stimuli-specific.[4] Indeed, it has been shown that inhibiting TAK-1/NF-κB signaling pathway, using either TAK-1 inhibitors or via silencing its expression, promotes apoptosis in colon cancer,[5] suppresses renal cell carcinoma survival,[6] inhibits proliferation of LPS-induced human hepatocellular carcinoma,[7] and reverses chemo resistance of pancreatic cancer.[8]

In 1978, Ellestad *et al*. isolated (5*Z*)-7-oxozeaenol (**2.1**) (Figure 2.1), a β-resorcylic acid lactone, from an unidentified fungus[9] and in 2003 it was found that **2.1** was a potent

inhibitor of TAK-1 with an IC_{50} of 8.1 nM.[10]Similar to almost all other kinase inhibitors,[11] (5*Z*)-7-oxozeaenol is a competitive ATP ligand that binds covalently to its target.[10] This irreversible interaction was determined when the covalently-bound ligand was cocrystalized with TAK-1.[12] The surging interest in discovering and developing small molecule covalent inhibitors stems from the fact that these ligands would have increased selectivity to their targets and therefore less intense side effects, resulting from dose reduction of the candidate drug to achieve therapeutic effects.[13] Selectivity of covalent inhibitors between kinases is difficult to achieve because the target is the ATP-binding pocket which is highly conserved.[14] However, the selectivity profile improves when moving from biochemical to cell-based kinase screening. There was a promising degree of selectivity for (5*Z*)-7-oxozeaenol since a 1 μM concentration exhibited at least 50% inhibition for only 12 of the 85 kinases tested by Wu *et al*, while, in cell lines, the TAK-1 signaling pathway was demonstrated to be most sensitive to the macrolide inhibitor.[12] Due to the selective and potent activity with this medicinally important receptor, it was decided that (5*Z*)-oxozeaenol was worth further analysis.

Figure 2.1 Structures of isolated resorcylic acid lactones from different fungal strains.

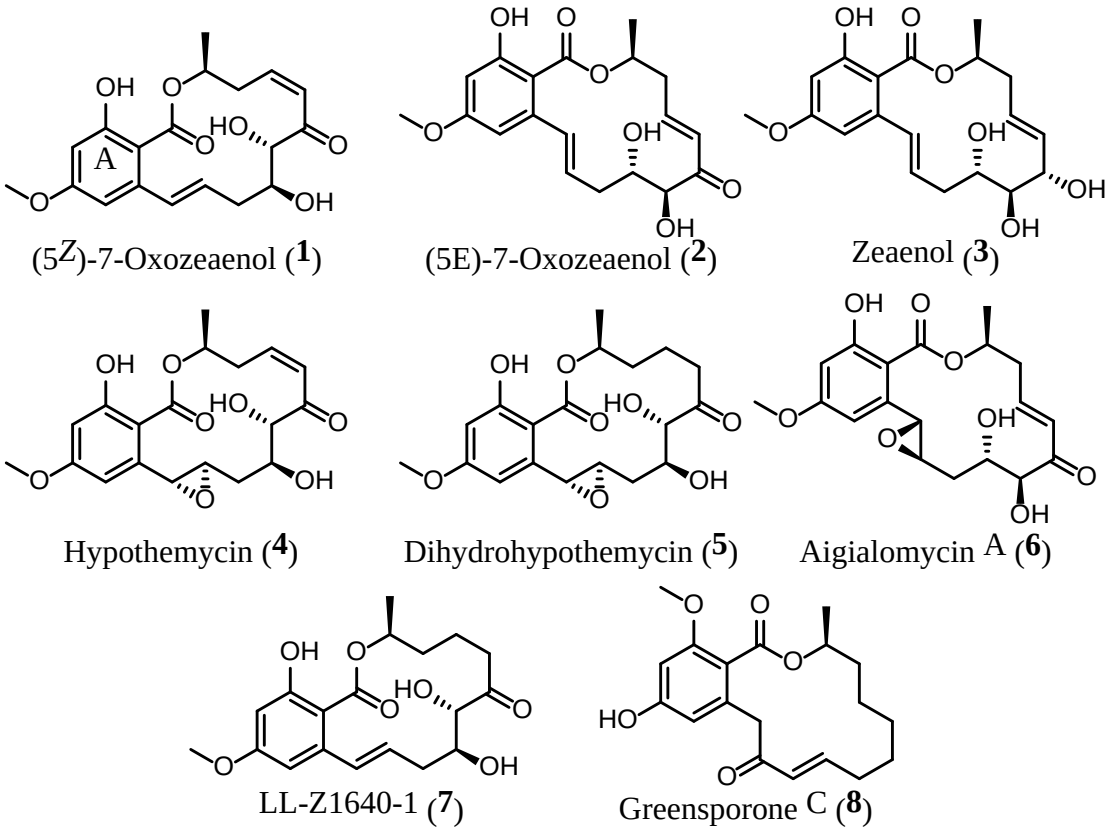

In the current work, we studied analogues of (5*Z*)-7-oxozeaenol that were obtained by way of semi synthesis or isolation from fungi. Fortunately, filamentous fungus MSX 63935 is a prolific producer of **2.1**, reproducibly biosynthesizing over 800 mg per a single solid-based culture grown in a 2.8 L Fernbach flask.[15] Analogues of (5*Z*)-7-oxozeaenol were concomitantly isolated from this fungus and other strains[16] and analyzed for their activities. Semisynthetic analogues were prepared using (5*Z*)-7-oxozeaenol as the starting material. Bioassay and covalent docking of the synthesized and isolated analogues were carried out to correlate, at a molecular level, structural changes with

variations in inhibitory activity. These data are presented to establish initial structure-activity relationships for (5*Z*)-7-oxozeaenol's TAK-1 activity.

2.2 Results and Discussion

2.2.1 Isolation of (5*Z*)-7-oxozeaenol (2.1) and related secondary metabolites

The lead compound in this study, (5*Z*)-7-oxozeaenol (**2.1**), and six related analogues (Figure 2.1) were isolated from solid-phase cultures of MSX 63935 as previously described in detail.[15] The decision of choosing **2.1** as the lead for further diversification was primarily due to the greater potency in inhibiting NF-κB (11 nM).[15] Fortuitously, the relative amount of cis-enone **2.1** was much higher in the extract compared to all other metabolites.[15]

2.2.2 Synthesis of (5*Z*)-7-oxozeaenol analogues

For treatment of inflammation and cancer, (5*Z*)-7-oxozeaenol (**2.1**) is a potent inhibitor of the kinase target TAK-1; however, its progress in the clinic has been stalled largely due to instability in plasma.[17] Thus, there is an opportunity to diversify this scaffold to generate analogues with improved activity and/or improved pharmaceutical properties. It is our understanding, based on some of the products obtained, that cis-enone **2.1** is sensitive to both acidic and basic conditions. These conditions, in any reaction, resulted in isomerization, elimination, or intramolecular cyclization products.

2.1.1.1 Methylation of ring A-phenolic hydroxyl

The free phenol was the first appealing position to diversify. The main reason for methylating the phenol was to verify the prior hypothesis that the phenol hydrogen bonds to the carbonyl of nearby residue Pro160.[12] The use of diazomethane[18] or iodomethane

with sodium hydride[19] did not result in the methylation of the alcohol, at carbon 17, as indicated by ^{1}H NMR spectroscopy. Instead, the macrolactone **2.1** either decomposed or was unreactive under those conditions. The hydroxyl hydrogen is strongly chelated to the nearby ester carbonyl oxygen, as can be inferred from the strong sharp peak at 12 ppm in ^{1}H NMR spectrum of **2.1**. The use of potassium carbonate[20] or tetrabutylammonium hydroxide[21] in DMF produced a reaction, but only elimination instead of substitution (Scheme 2.1). Dienoates **2.9** and **2.10** suggest that the strong bases deprotonated one of the hydrogens on carbon 3 and led to elimination of the ester attached to carbon 3 (Scheme 2.1). Under these more forcing conditions, the phenolic hydroxyl group was found to react with excess iodomethane. The stereochemical configurations of compounds **2.9** and **2.10** were assigned as (3*E*,5*Z*) based on the coupling constants between the protons at C3/C4 and C5/C6 (i.e. 13.8 Hz and 11.5 Hz, respectively).

Scheme 2.1 Synthesis of compounds **1.9**-**1.16**. Reagents and conditions a) K_2CO_3, DMF, CH_3I or Bu_4NOH, DMF, CH_3I, r.t; b) 6 eq. Selectfluor®, CH_3CN; c) NBS, $CHCl_3$; d) Dimethoxy propane, 0.2 eq. *p*-TSA; e) Dimethoxy propane, 2 mg *p*-TSA.

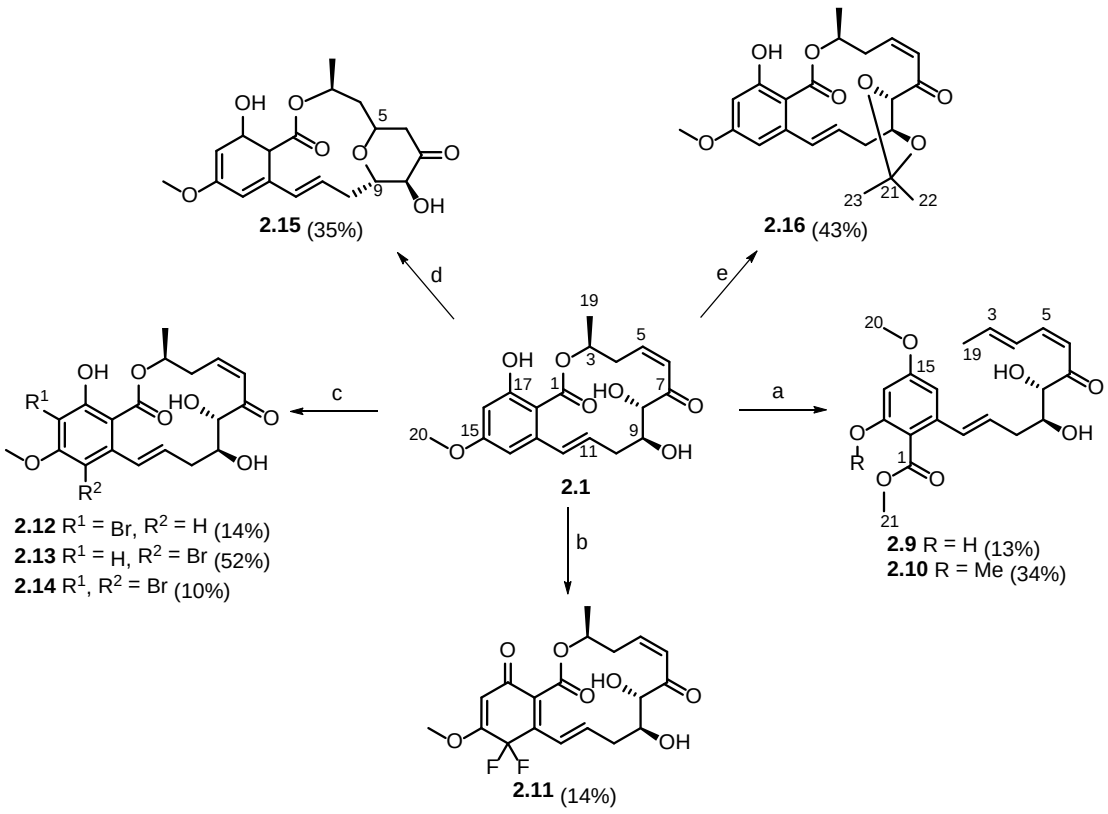

2.1.1.2 Fluorination of ring A

There has been an increased interest in introducing fluorine atoms into drug candidates for the enhanced pharmaokinetics and pharmacodynamics that this atom provides. More than 25% of marketed drugs have at least fluorine atom in their structures.[22] The small size and large electronegativity of this heteroatom often leads to an increase in drug potency and half-life due to decreased metabolism. In light of these advantages, fluorination was attempted. The reagent of choice for this reaction was the electrophilic Selectfluor® which usually has high levels of reactivity and selectivity.[23]

Fluorination using fluorine radicals would probably not be as selective due to competition from the double bond at carbons 11 and 12 of the macrocycle. Surprisingly, the product obtained was a result of difluorination at carbon 14 (Scheme 2.1). A reasonable explanation for disubstitution at the more sterically accessible carbon is the strong activation of the nucleophilic aromatic ring by the two electron-donating oxygens at carbons 15 and 17. Attempts to synthesize the monofluorinated compound led only to reduced yields of the difluorinated product.

2.1.1.3 Bromination of ring A

In a separate attempt to introduce fluorine into the molecule, trifluoromethylation was carried out. Unexpectedly, the major product obtained when using sodium trifluoromethane sulfinate, copper (II) trifluoromethane sulfonate and hydrogen peroxide[24] resulted in the formation of bromide **2.12** (Scheme 2.1). It is surmised that the trace impurities of a bromine-containing contaminant, as suggested by mass analysis of sodium trifluoromethane sulfinate, was the source of reactive bromine (Figure 2.2). Interestingly, when arene **2.1** was treated with NBS, bromination at the other position (i.e. C14), and at both positions occurred (Scheme 2.1).[25]

Figure 2.2 (A) (+)-ESI TIC of Sodium trifluoromethanesulfinate. (B) UPLC-PDA chromatogram. (C) m/z spectrum.

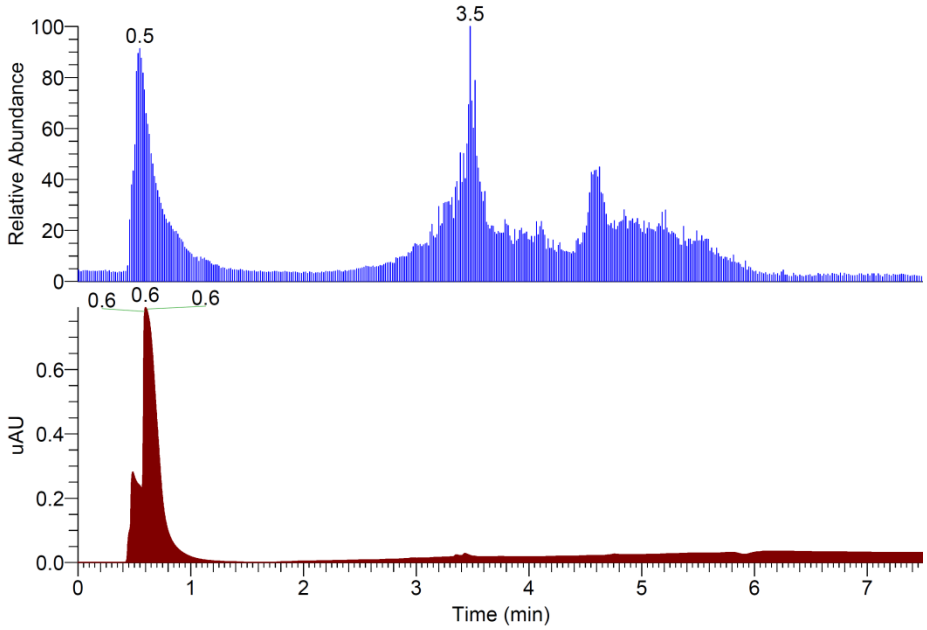

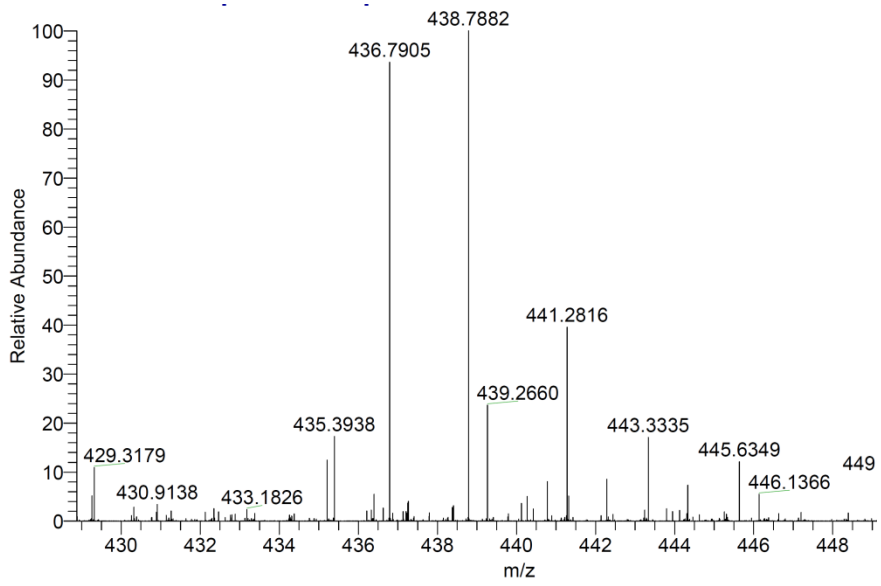

2.1.1.4 Synthesis of (5*Z*)-7-oxozeaenol acetonide

To investigate the importance of the free hydroxyl groups at carbons 8 and 9 for activity, acetonide formation was targeted. The use of acetone with dimethyl sulfoxide[26] was not successful to prepare the target product, however, dimethoxypropane with catalytic amounts of *p*-toluenesulfonic acid was successful if only few crystals[9] of the acid were used. Larger amounts than only a few crystals[27] activated the carbonyl at carbon 7 and facilitated intramolecular conjugate addition of the oxygen at carbon 9 to give pyranone **2.15** (Scheme 2.1).

2.1.1.5 Attempts to synthesize open-ring 2.17, 5, 6-epoxy 2.18, thionoester 2.19, desmethyl 2.20 and lactam 2.21 derivatives of (5*Z*)-7-oxozeaenol.

Saponification of **2.1** (Scheme 2.2) to acquire the acyclic derivative **2.17** was attempted using sodium hydroxide in dimethyl sulfoxide or water[28] or LiOH in a mixture of tetrahydrofuran and water.[29] The strong basic conditions led only to degradation of **2.1** as indicated by ^{1}H NMR analysis of the crude reaction mixture.

Scheme 2.2 Attempted synthesis of 5(*Z*)-7-oxozeanol derivatives **2.17**-**2.21**. Reagents and conditions: a) NaOH, DMSO or H_2O; b) LiOH, THF/H_2O; c) *t*-BuOOH, *t*-BuOOK, THF; d) Lawesson reagent, Toluene, 120 °C; e) BBr_3, CH_2Cl_2, -78 °C; f) i) RN_3, catalyst ii) PPh_3 iii. NHS, DCC.

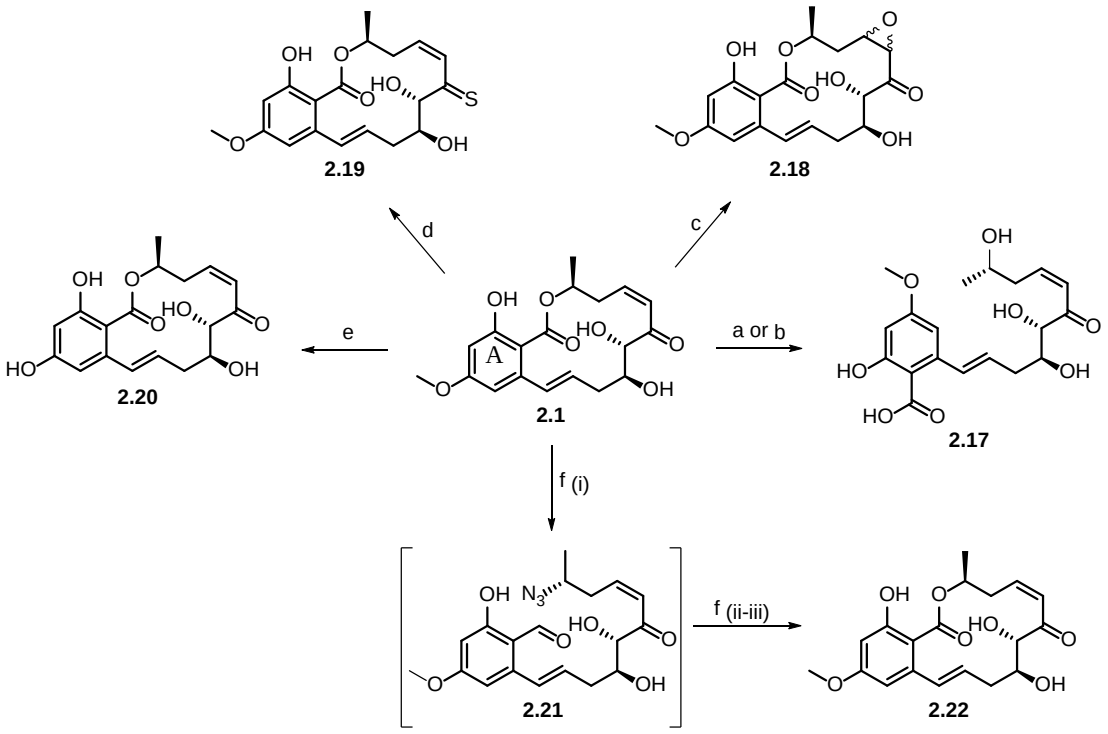

Decreasing the alkylating potency of the michael acceptor in **2.1** will potentially increase its selectively to react with Cys174 sulfur in the enzyme-binding pocket due to proximity. For that reason, conversion of the 5, 6-enone in **2.1** to the corresponding 5, 6-epoxy derivative **2.18** was attempted (Scheme 2.2). Yet, the use of the conventional nucleophilic peroxides, such as cumene hydroperoxide and hydrogen peroxide, in the presence of *tert*-butoxide[30] did not result in any change as indicated by ^{1}H NMR analysis. Thiation of the 5, 6-enone in **2.1**, using Lawesson reagent in toluene,[31] to give **2.19** (Scheme 2.2) was attempted to investigate the biological effects of increasing the michael

acceptor reactivity upon substituting the carbonyl oxygen in **2.1** with the less electronegative sulfur.[32] The product obtained is presumed, based on ^{1}H NMR analysis of the purified product, to be a dimer of **2.1** and Lawesson reagent monomer. Due to the instability of the isolated major product, which hindered complete data collection and definite structural identification, alongside its unexciting nature, it was decided that the product was unworthy of any further investigation.

Demethylation of ring A methoxy group in **2.1**, to give the desmethyl derivative **2.20** (Scheme 2.2), will be crucial in investigating the effect on activity upon increasing hydrogen bonding likelihood at that position with the nearby Tyr106. However, the reagent of choice; tribromoborane (BBr_3) resulted only in isomerization of the (5*Z*)-enone to the corresponding (5*E*)-enone **2.2**.

The primary reason for the instability of (5*Z*)-7-oxozeaenol **2.1** in plasma is due to macro lactone ring opening via esterases.[17] Thus, conversion to the lactam derivative **2.21** was attempted. The seemingly most applicable method was via opening the 14-membered ring via azide intermediate **2.21** formation[33] followed by Staudinger mild reduction to the amine and *in situ* intramolecular lactam formation **2.22** catalyzed by the use of *N*-hydroxy succinmide NHS and dicyclohexylcarbodiimide DCC[34] (Scheme 2.2). Sodium azide NaN_3 or trimethylsilyl azide $TMSN_3$ were used as the azide sources without or with variant catalysts to prepare the azide intermediate **2.21** (Table 2.2). Yet, the products obtained were due to either ester elimination (i.e. entry 1) or 5, 6-enone isomerization (i.e. entry 2). $SnCl_4$, $BF_3.Et_2O$ and Cu(dppe)(OAc_2) catalysts led to decomposition of **2.1** (i.e. entries 2, 7-8).

Table 2.1 Attempts to synthesize the azide intermediate **2.21**.

Entry	Azide source	Catalyst	Result
1	NaN_3	------	Elimination
2	NaN_3	$Cu(dppe)(OAc_2)$	Decomposition
3	$TMSN_3$	$FeCl_3$	No Change
4	$TMSN_3$	$CeCl_3$	Isomerization
5	$TMSN_3$	$AlCl_3$	No Change
6	$TMSN_3$	$TiCl_4$	No Change
7	$TMSN_3$	$SnCl_4$	Decomposition
8	$TMSN_3$	$BF3.O(C_2H_5)_2$	Decomposition

2.2.3 Biological testing

Few isolated RALs **2.2**-**2.8** (Figure 2.1) and the semi synthesized analogues **2.10**-**2.16** were evaluated for their *in vitro* TAK-1 inhibitory activities (Table 2.2). Compound **2.9** was not tested due to its short-term stability as indicated by the sub 90% purity, detected by UPLC, following prep HPLC purification. The Michael acceptor is, as expected, a crucial part for the inhibitory activity of this group of compounds; loss of this functionality, involved in the covalent bond formation, whether through reduction of the

double bond or reduction of the carbonyl, leads to loss of activity as seen with zeaenol (**2.3**), LL-Z164-1 (**2.7**), dihydrohypothemycin (**2.5)**, and pyranone **2.15**. Not only is the enone presence crucial to the pharmacophore structure, the position matters also since shifting the enone from carbons 5-7 to carbons 9-11, as in greensborone C (**2.8B** diminishes activity. Additionally, isomerization of the enone double bond from a *Z* to an *E* configuration significantly reduces activity. This effect can be seen by comparing two different pairs of isomers, namely; (5*Z*)-7-oxozeaenol (**2.1**) versus (5*E*)-7-oxozeaenol (**2.2**) and hypothemycin (**2.4**) versus aigialomycin A (**2.6**).

Table 2.2 IC_{50}'s, docking scores and 95% confidence intervals of isolated and semi synthesized RALs.

Compound	Docking Score	IC_{50} (μM)	95% Confidence Intervals
1	-12.9	0.011	0.009-0.015
4	-12.0	0.033	0.024-0.045
11	-12.9	0.077	0.047-0.125
13	-10.2	0.36	0.271-0.746
16	-10.8	0.38	0.220-0.655
6	N/A[b]	0.99	NA

Table 2.2 IC_{50}'s, docking scores and 95% confidence intervals of isolated and semi synthesized RALs.

2	-11.5	1.3	0.932-1.780
12	-10.0	2.6	2.206-3.150
7	N/A[b]	2.6	2.206-3.150
14	-6.8	8.9	2188-3914
3	N/A[b]	10	8.168-12.441
5	N/A[b]	>30	NA
8	-8.4	>30	NA
10	-6.4	>30	NA
15	N/A[b]	>30	NA

[a] The compounds are arranged in a descending order in regards to their inhibitory concentrations.
[b] Compounds were not docked due to lacking the Michael acceptor functionality

By comparing (5*Z*)-7-oxozeaenol (**2.1**) and hypothemycin (**2.4**), it can be inferred that epoxidation of the double bond on carbons 11 and 12 does not change the inhibitory activity. As mentioned by Chen *et al*., the hydroxyl group located at carbon 9 binds to the enzyme via formation of a hydrogen bond with the backbone carbonyl of Pro160.[12] As

expected, blocking this interaction, as seen in acetonide **2.16**, reduced the activity by more than 30 folds. The inability of compound **2.10** to inhibit TAK-1 indicates that the macrocycle is important for activity, probably due to the rigidity it provides to correctly position the Michael acceptor close to the nucleophilic cysteine residue. The only semi synthesized analogue that was found to be statistically equipotent to **2.1** is the difluoro (5*Z*)-7-oxozeaenol (**2.11**). The relative potency of compound **2.11** indicates that the aromatic ring is not crucial for binding. This observation with TAK1 is unprecedented.

The crystal structure of **2.1** bound to TAK-1 indicates insufficient space to accommodate substituting the proton on carbon 16 with bromine. Thus, as expected, the 16-Bromo analogue **2.12** was significantly less active. The better activity of **2.13** relative to **2.12** indicates that the binding pocket is more tolerant in accommodating the large bromine atom when installed in position 14 yet **2.13** was still significantly less active than the parent ligand **2.1** .The added clashes of having two bromine atoms at positions 14 and 16, renders the dibromo analogue **2.14** the least active.

2.2.4 Covalent docking

2.2.4.1 Ligand preparation

Prior to docking, ligands having the Michael acceptor moiety were examined using Spartan (Wavefunction, Inc.). The structures of those ligands were first subjected to conformational searches using semi empirical molecular mechanics. The resulting conformers, ranging from 100-600, were further optimized using Hartree-Fock implementing the 6–31G* and 6-311G basis sets. The theoretical global minimum energy conformation was chosen to be docked into the crystal structure.

2.2.4.2 Covalent docking

The prepared ligands were docked using the Chen *et al*.[12] reported crystal structure (PDB 4GS6). The crystal structure was first prepared using protein preparation wizard (Maestro) and the prepared ligands were docked using covalent docking implemented in (Maestro).

To validate the accuracy of the calculations performed in regards to our work, (5*Z*)-7-oxozeaenol **2.1** was the first ligand to be docked. The best docking orientation, as judged by the docking score, was further subjected to protein refinement using prime implemented in Maestro followed by covalent docking of the minimization outputs. RMSD of the docking output superimposed to the crystal structure was found to be 0.0984 $^{\circ}$A (Figure 2.3). The configuration of the β carbon for the best-scored docking output is *R*. The geometry shown in the crystal structure is that of a sp^2 carbon. It is assumed that the geometry of carbons 5 and 6 in the crystal structure are incorrectly assigned since both of these carbons should be sp^3 hybridized after addition of the cysteine. It is therefore not clear which model, *R* or *S* truly fits better for the preferred ligand binding geometry, but the R diastereomer is more consistent with the data.

Figure 2.3 (A) Superimposed covalent docking output pose (Purple) with the cocrystalized (5*Z*)-7-oxozeaenol (cayan). Parts of the enzyme's residues (D175, F176 and G177), in the binding pocket, were deleted for clarification.

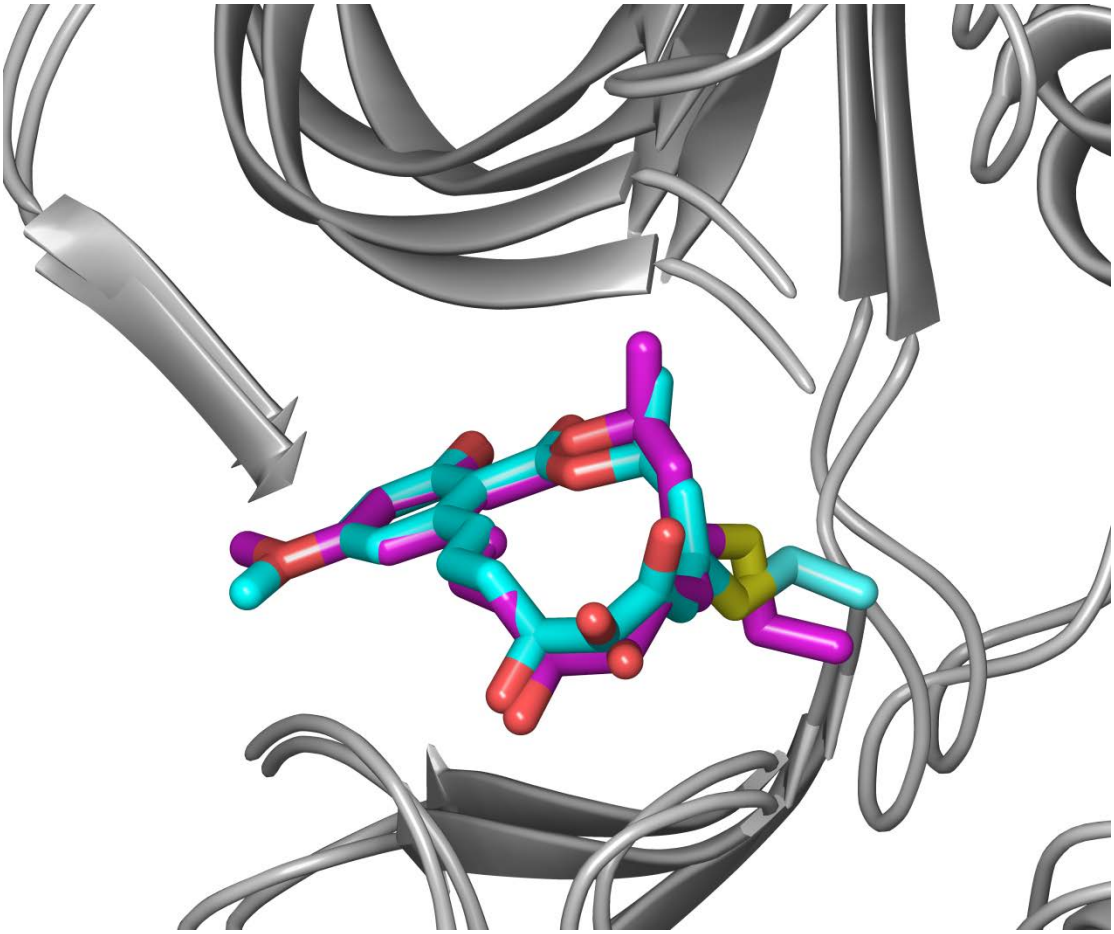

Similar to the parent ligand, semi synthesized and isolated RALs, bearing an enone, were also docked covalently in the same previously described manner (Table 2.1). The scores obtained appear to be in an acceptable alignment with the experimental data. Distinct gaps are observed between compounds having inhibitory concentrations in the nM range, low μM range, and inactive compounds. Analogues having low nM inhibitory concentration had docking scores of -12 to -12.9 Kcal/mol. A range of -10 to -11.5

Kcal/mol was representative of analogues with 0.4-2.6 μM range of activities. As for inactive compounds, they had considerably lower docking scores as compared with the active compounds. In general, scoring based on the implemented covalent docking-prime minimization-covalent docking method proves to be considerably accurate in distinguisihing between active and inactive analogues.

2.3 Experimental

Unless otherwise stated, all reactions were carried out under an atmosphere of dry nitrogen in dried glassware. Indicated reaction temperatures refer to those of the reaction bath, while room temperature (rt) is noted as 25 °C. All solvents and reagents were obtained from commercial sources and were used as received. Analytical thin layer chromatography (TLC) was performed on silica gel 60 F254 precoated plates (0.25 mm) from Merck. Visualization was accomplished by irradiation under a 254 nm UV lamp. Silicycle silica gel 230−400 (particle size 40−63 μm) mesh was used for all flash column chromatography. The crude extract and reaction products were purified by reverse phase chromatography, which was performed using a Varian purification system employing a Phenomenex Gemini-NX, (5 μm, C18, 110A, AX. 250 × 21.20 mm) or a Phenomenex Kinete, (2.6 μm C18 100 Å, 30 x 2.1 mm). The mobile phase was a mixture of acetonitrile or and H_2O containing 0.1% formic acid. ^{1}H NMR spectra were recorded on a Jeol ECA 500 MHz spectrometer or a Jeol ECS 400 MHz spectrometer in the solvent indicated. All ^{1}H NMR experiments are reported in δ units, parts per million (ppm) downfield of TMS , and were measured relative to the signals for chloroform (7.26 ppm), methanol (3.31 ppm), acetone (2.05 ppm) and dimethyl sulfoxide (2.50 ppm). All ^{13}C

NMR spectra were reported in ppm relative to the signals for chloroform (77 ppm), methanol (49 ppm), acetone (29.8 ppm) and dimethyl sulfoxide (39.5 ppm) with ^{1}H decoupled observation. Data for ^{1}H NMR are reported as follows: chemical shift (δ ppm), multiplicity (s = singlet, d = doublet, t = triplet, q = quartet, quint = quintet, sext = sextet, sept = septet, m = multiplet), integration and coupling constant (Hz), whereas ^{13}C NMR analyses were reported in terms of chemical shift. High resolution mass spectra (HRMS) were performed on a Thermo Fisher Scientific UPLC/LTQ Orbitrap XL system.

2.3.1 Isolation of (5Z)-7-oxozeaenol

The purification of (5*Z*)-7-oxozeaenol (**2.1**) from solid phase cultures of MSX 63935 has been described.[15] Briefly, 800 mg of the extract was dissolved in 2 mL of DMSO and purified via 10 separate injections by preparative HPLC using a gradient that initiated with 35:65 (CH_3CN/H_2O) and increased linearly to 45:55 over 40 min. Compound **2.1** and LL-Z164-1 **2.7** eluted together from 16 to 20 min. The isolated mixture of (5*Z*)-7-oxozeaenol **2.1** and LL-Z164-1 **2.7** was subjected to an additional round of preparative HPLC under the same conditions to yield 206 mg (26%) of pure (>95%, Figure 2.4) (5*Z*)-7-oxozeaenol.

Figure 2.4 UPLC chromatograms of compounds **2.1**, **2.10**-**2.16** (λ 254 nm), demonstrating >97% purity for compounds **2.1**, **2.10**, **2.12**-**2.16**. All data were acquired via an Acquity UPLC system with a Phenomenex Kinetex C18 (1.3 µm; 50 × 2.1 mm) column and a CH_3CN/H_2O gradient that increased linearly from 20 to 100% CH_3CN over 1.2 min.

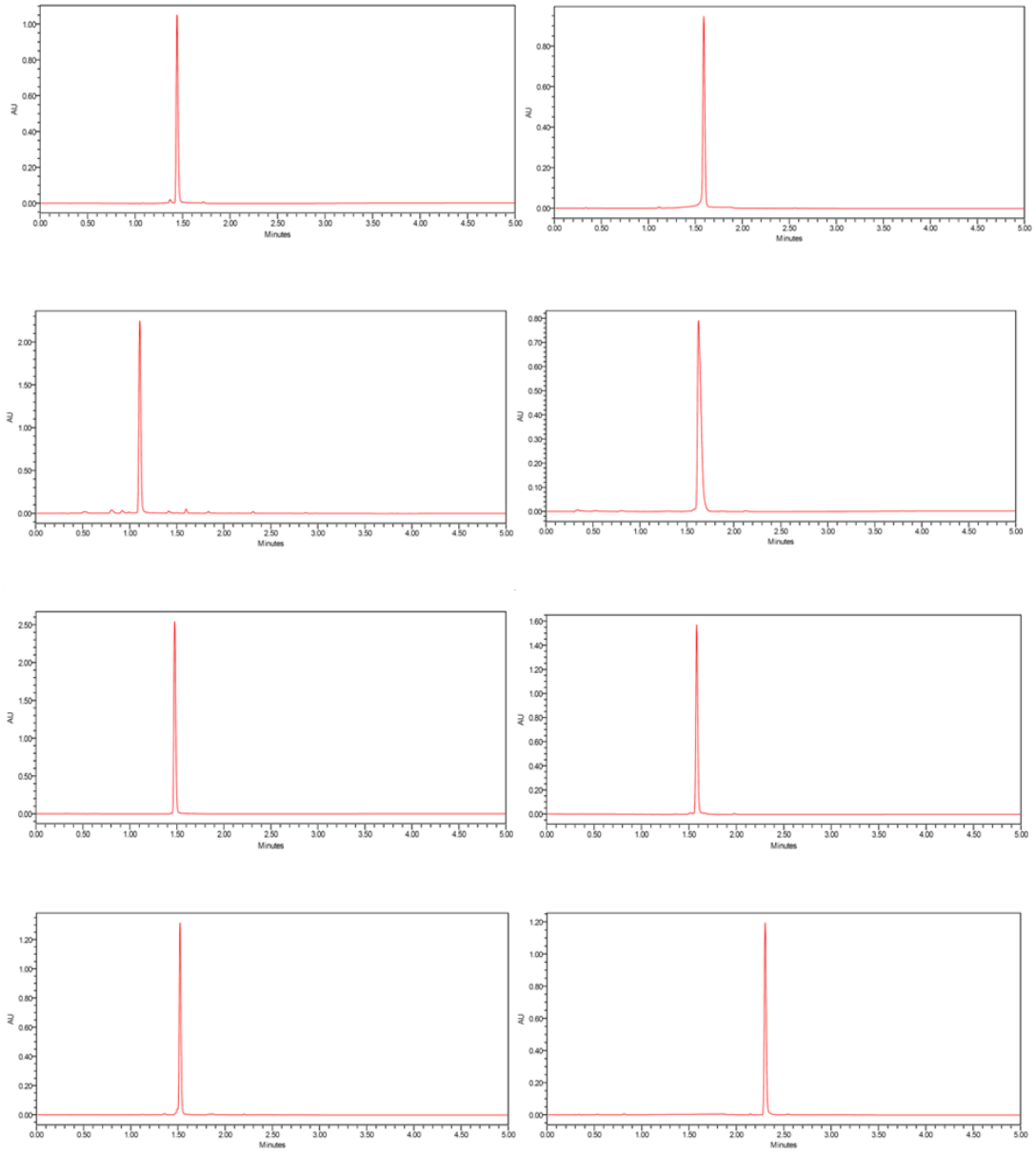

2.3.2 Synthesis of (5Z)-7-oxozeaenol analogues 2.9-2.16

Methyl 2-((1*E*,4*S*,5*S*,7*Z*,9*Z*)-4,5-dihydroxy-6-oxoundeca-1,7,9-trien-1-yl)-6-hydroxy-4-methoxybenzoate (2.9).[20]

Potassium carbonate (38.1 mg, 0.28 mmol) was added to a solution of (5*Z*)-7-oxozeaenol (**2.1)** (50 mg, 0.14 mmol) in DMF (2 mL) and stirred for an hour. Iodomethane (10 μL, 0.16 mmol) was then added and the mixture stirred for 4 hours. It was diluted with water (20 mL) and acidified with 1M HCl, until a pH of 2, followed by extraction with $CHCl_3$ (20 mLx3). The combined organic layers were dried using anhydrous sodium sulfate and the solvent evaporated. The residue was purified by preparative HPLC using a Phenomenex Gemini-NX column C18 (250 x 21.20 mm, 110 A, 5 μm spherical particle size). The column was perfused at a flow rate of 21.24 mL/min with 70% of (water, 0.1% FA) and 30% of CH_3CN over 80 min. The compound eluted at ~ 70 min. Yield (6.6 mg, 13%).

^{1}H NMR (500 MHz, Chloroform-d_3): δ 11.56 (s, 1H; 17-OH), 7.43 (dd, J = 11.5, 13.8, 1H; 4-H), 6.98 (d, J = 15.5 Hz, 1H; 12-H), 6.57 (dd, J = 11.2, 11.5 Hz, 1H; 5-H), 6.37 (d, J = 2.9 Hz, 1H; 16-H), 6.25 (dq, J_d = 13.8, J_q 6.9 Hz, 1H; 3-H), 6.41 (d, J = 2.9 Hz, 1H; 14-H), 6.08 (d, J = 11.5 Hz, 1H; 6-H), 5.84 (dt, J_d = 15.5, J_t = 7.5 Hz, 1H; 11-H), 4.37 (bs, 1H; 8-H), 3.95 (ddd, J = 4.6, 8.0, 8.2 Hz, 1H; 9-H), 3.91 (s, 3H; 21-H), 3.80 (s, 3H; 20-H), 2.33-2.40 (m, 2H; 10-H), 1.90 (d, J = 6.9, 3H; 19-H).

^{13}C NMR (125 MHz, Chloroform-d_3): δ 198.9, 171.5, 164.9, 164.2, 146.7, 145.2, 142.8, 135.2, 129.3, 127.5, 117.9, 108.5, 103.7, 100.0, 79.4, 72.2, 55.5, 52.3, 35.7, 19.0.

HRMS (ESI, m/z): Calculated for $C_{20}H_{25}O_7$ $[M + H]^+$ 377.1595; found 377.1589 (1.5 ppm).

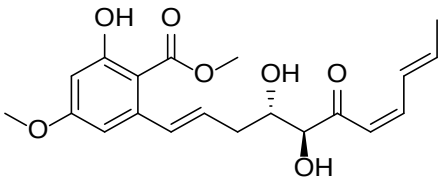

Figure 2.5 ^{1}H and ^{13}C NMR spectra of compound **2.9** [500 MHz for ^{1}H and 125 MHz for ^{13}C, Chloroform-d_3].

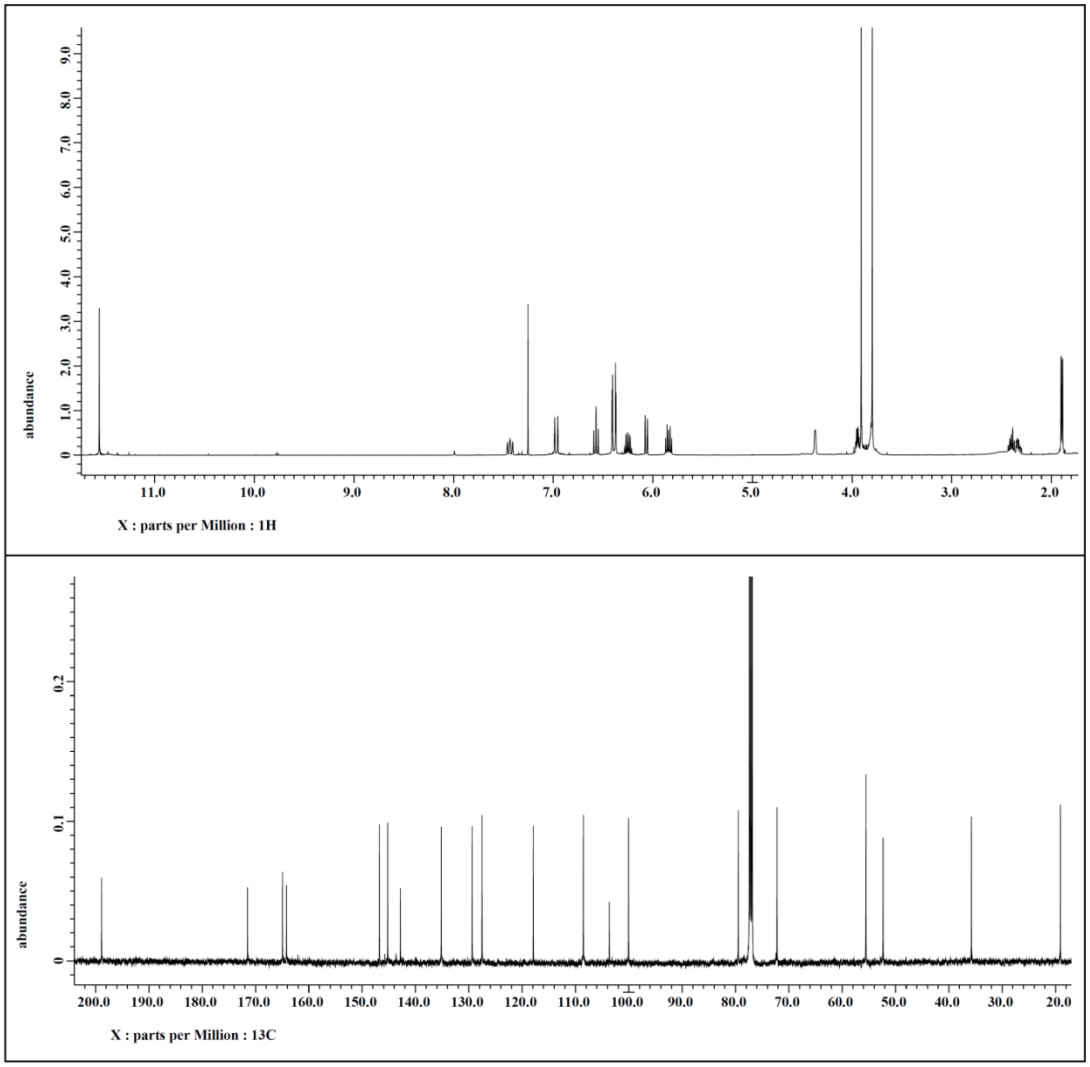

Figure 2.6 Major COSY (▬) and HMBC (blue arrows) correlations of compound **2.9.**

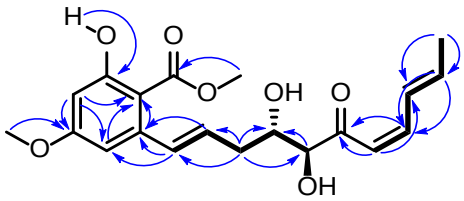

Methyl 2-((1*E*,4*S*,5*S*,7*Z*,9*Z*)-4,5-dihydroxy-6-oxoundeca-1,7,9-trien-1-yl)-4,6-dimethoxybenzoate (2.10).[20] Same as procedure described for synthesis of compound **2.9**. The compound eluted at ~ 46 min. UPLC was used to evaluate the purity using a gradient solvent system that initiated with 20:80 $CH_3CN{-}H_2O$ to 100% CH_3CN over 4.5 min; it was > 97% pure (Figure 2.4). Yield (18.0 mg, 34%).

^{1}H NMR (500 MHz, Chloroform-d_3): δ 7.43 (dd, J = 11.5, 14.9 Hz, 1H; 4-H), 6.57 (d, J = 11.5 Hz, 1H; 5-H), 6.54 (d, J = 2.3 Hz, 1H; 14-H), 6.40 (d, J = 15.8 Hz, 1H; 12-H), 6.34 (d, J = 2.3 Hz, 1H; 16-H), 6.24 (dq, J_d = 14.9, J_q = 6.9 Hz, 1H; 3-H), 6.13 (dt, J_d = 15.8, J_t = 7.5 Hz, 1H; 11-H), 6.04 (d, J = 11.5 Hz, 1H; 6-H), 4.35 (d, J = 4.0 Hz, 1H; 8-H), 3.95 (m, 1H; 9-H), 3.87 (s, 3H; 21-H), 3.80 (s, 3H; 22-H), 3.78 (s, 3H; 20-H), 2.38 (m, 1H; 10-H), 2.26 (ddd, J = 4.0, 7.4, 14.3 Hz, 1H; 10-H), 1.89 (d, J = 6.9 Hz, 3H; 19-H).

^{13}C NMR (125 MHz, Chloroform-d_3): δ 198.8, 168.7, 161.6, 158.2, 146.9, 145.2, 137.8, 130.5, 129.4, 129.3, 117.9, 115.3, 101.8, 97.9, 79.4, 72.4, 56.1, 55.5, 52.5, 35.9, 19.1.

HRMS (ESI, m/z): Calculated for $C_{21}H_{27}O_7$ $[M + H]^+$ 391.1751; found 391.1745 (1.6 ppm).

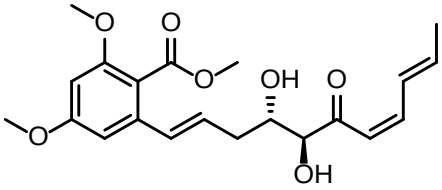

Figure 2.7 ^{1}H and ^{13}C NMR spectra of compound **2.10** [500 MHz for ^{1}H and 125 MHz for ^{13}C, Chloroform-d_3].

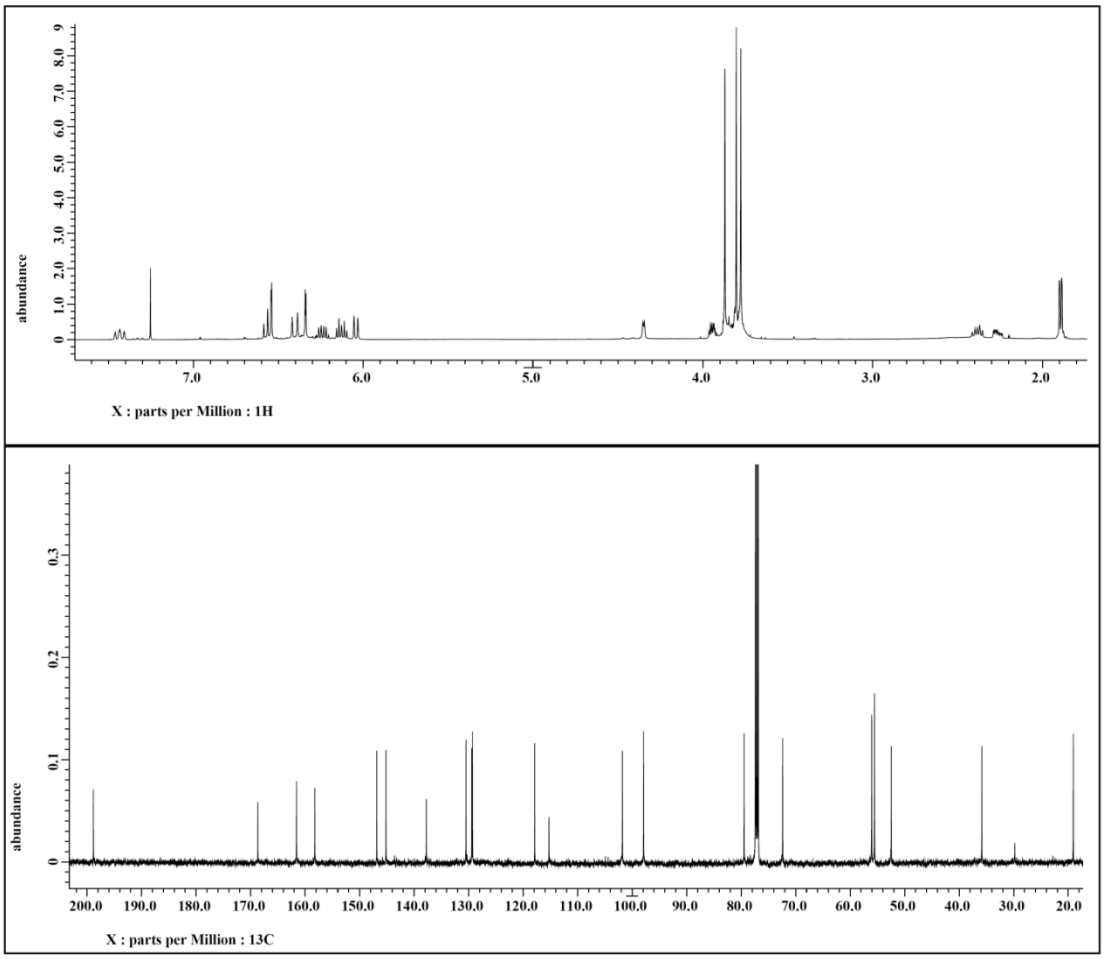

Figure 2.8 Major COSY (━) and HMBC (blue arrows) correlations of compound **2.10.**

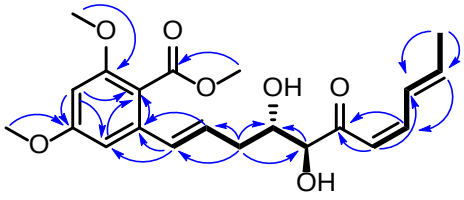

(3*S*,5*Z*,8*S*,9*S*,11*E*)-13,13-Difluoro-8,9-dihydroxy-14-methoxy-3-methyl-3,4,9,10-tetrahydro-1*H* benzo[*c*][1]oxacyclotetradecine-1,7,16(8*H*,13*H*)-trione (2.11).[23]

Selectfluor® (177 mg, 0.50 mmol) was added to a solution of (5*Z*)-7-oxozeaenol (**2.1**) (30 mg, 0.083 mmol) in CH_3CN (3 mL) and the mixture stirred for 3 hrs. The solvent was evaporated and the residue was purified by preparative HPLC using a Phenomenex Gemini-NX column C18 (250 x 21.20 mm, 110 A, 5 µm spherical particle size). The column was perfused at a flow rate of 21.24 mL/min with 60% (water, 0.1% TFA), and 40% of MeOH over 40 min. The compound eluted at ~ 30 min. UPLC was used to evaluate the purity using a gradient solvent system that initiated with 20:80 $CH_3CN{-}H_2O$ to 100% CH_3CN over 4.5 min; it was > 97% pure based on the ELSD detector (Figure 2.9). Yield (27 mg, 14%).

Figure 2.9 UPLC chromatogram of compound **2.11** (ELDS), demonstrating >98% purity. All data were acquired via an Acquity UPLC system with a Phenomenex Kinetex C18 (1.3 µm; 50 × 2.1 mm) column and a CH_3CN/H_2O gradient that increased linearly from 20 to 100% CH_3CN over 1.2 min.

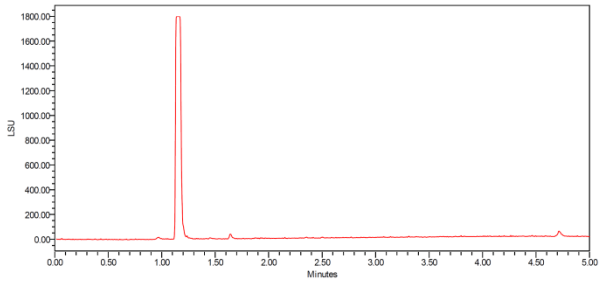

^{1}H NR (500 MHz, Chloroform-d_3): δ 6.63 (dt, J_d = 11.5, J_t = 4 Hz, 1H; 5H), 6.35 (m, 1H; 11-H), 6.31 (d, J = 11.5 Hz, 1H; 6-H), 6.07 (d, J = 15.5 Hz, 1H; 12-H), 5.58 (t, J =

2.3 Hz, 1H; 16-H), 5.43 (dq, J_d = 10.3 Hz, J_d = 6.3 Hz, 1H; 3-H), 4.47 (bs, 1H; 8-H), 4.11 (m, 1H; 9-H), 3.85 (s, 3H; 20-H), 3.80 (m, 1H; 3-H), 2.57 (ddd, *J* = 6.9, 8.0, 15.5 Hz, 1H; 10-H), 2.46 (d, 16.0 Hz, 1H; 4-H), 2.37 (dd, *J* = 5.2, 15.5 Hz, 1H; 10-H), 1.41 (d, *J* = 6.3 Hz, 3H; 19-H).

^{13}C NMR (125 MHz, Chloroform-d_3): δ 198.3, 181.4, 164.2, 163.1 (t, *J* = 24 Hz, 1C; 15-C), 150.4, 140.3, 138.3 (t, *J* = 25 Hz, 1C; 13-C), 130.3 (t, *J* = 6 Hz, 1H; 18-C), 123.1, 122.7, 109.0 (t, *J* = 241.5 Hz, 1C; 14-C), 102.3 (t, *J* = 4 Hz, 1H; 16-C), 80.7, 73.8, 72.6, 57.0, 38.1, 37.2, 21.4.

^{19}F NMR (376 MHz, Chloroform-d_3): δ -103.30 (d, *J* = 355.2 Hz, 1F), -104.31 (d, *J* = 355.2 Hz, 1F) (Figure 2.8).

HRMS (ESI, m/z): Calculated for $C_{19}H_{21}F_2O_7$ $[M + H]^+$ 399.1250; found 399.1242 (2.0 ppm).

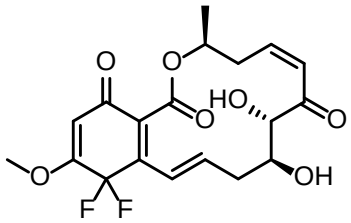

Figure 2.10 ^{1}H and ^{13}C NMR spectra of compound **2.11** [500 MHz for ^{1}H and 125 MHz for ^{13}C, Chloroform-d_3].

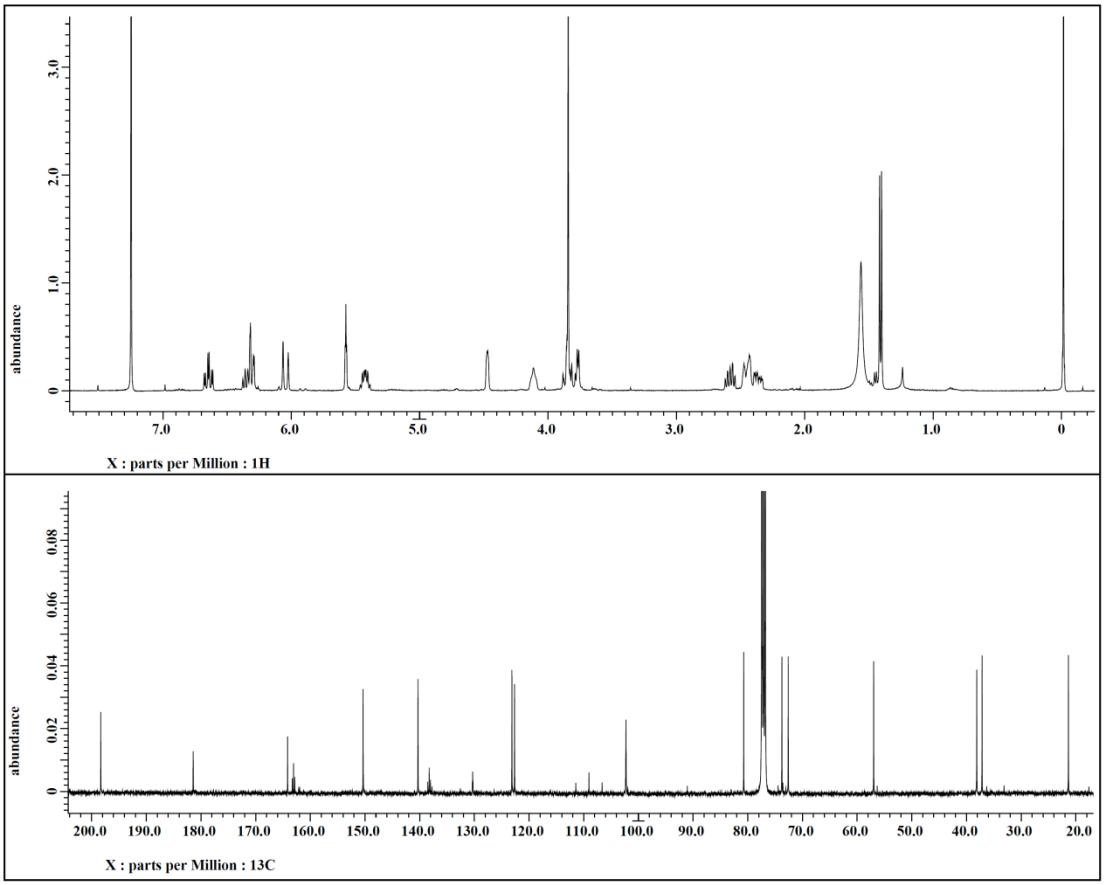

Figure 2.11 ^{19}F NMR spectra of compound **2.11** [376 MHz, Chloroform-d_3].

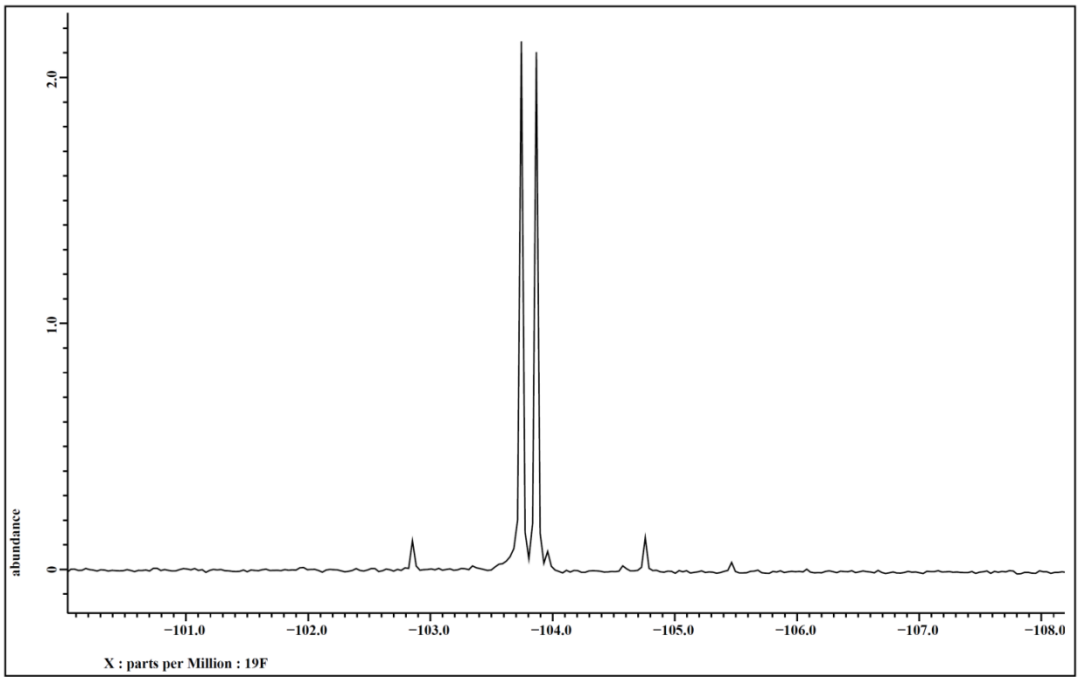

Figure 2.12 Major COSY (▬) and HMBC (blue arrows) correlations of compound **2.11.**

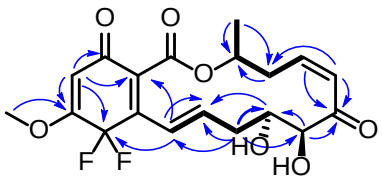

(3*S*,5*Z*,8*S*,9*S*,11*E*)-15-Bromo-8,9,16-trihydroxy-14-methoxy-3-methyl-3,4,9,10-tetrahydro-1*H*-benzo[*c*][1]oxacyclotetradecine-1,7(8*H*)-dione (2.12).[25] *N*-Bromosuccinimide (7.4 mg, 0.04 mmol) was added to a solution of (5*Z*)-7-oxozeaenol (**2.1**) (15 mg, 0.04 mmol) in $CHCl_3$ (1 mL) and the mixture stirred for 4 hours and the solvent evaporated. The residue was purified by preparative HPLC using a Phenomenex Gemini-NX column C18 (250 x 21.20 mm, 110 A, 5 μm spherical particle size). The column was perfused at a flow rate of 21.24 mL/min with a linear gradient from 40% (CH_3CN-H_2O) to 50% over 15 min. The compound eluted at 18.5 min. UPLC was used to evaluate the purity using a gradient solvent system that initiated with 20:80 CH_3CN−H_2O to 100% CH_3CN over 4.5 min; it was >97% pure (Figure 2.4). Yield (1.76 mg, 14%).

^{1}H NMR (500 MHz, Chloroform-d_3): δ 12.79 (s, 1H; 17-OH), 6.88 (d, J = 15.3 Hz, 1H; 12-H), 6.42 (s, 1H; 14-H), 6.34 (dd, J = 3, 11.5 Hz, 1H; 6-H), 6.22 (dt, J_d = 11.5, J_t = 3 Hz, 1H; 5-H), 6.03 (ddd, J = 4.6, 10.7, 15.3 Hz, 1H; 11-H), 5.26 (dq, J_d = 6.1, J_q = 8.5 Hz, 1H; 3-H), 4.53 (dd, J = 2.3, 5.4 Hz, 1H; 8-H), 4.00 (bs, 1H; 9-H), 3.95 (s, 3H; 20-H), 3.57 (ddd, J = 5.4, 10.7, 11.5 Hz, 1H; 4-H), 2.53 (dd, J = 2.3, 17.6 Hz, 1H; 4-H), 2.23-2.11 (m, 2H; 10-H), 1.48 (d, J = 6.1 Hz, 3H; 19-H).

^{13}C NMR (100 MHz, Chloroform-d_3): δ 199.0, 171.1, 161.4, 160.4, 147.6, 142.3, 132.9, 131.1, 125.3, 104.8, 103.7, 99.1, 80.9, 74.6, 73.6, 56.5, 37.5, 37.1, 20.8.

HRMS (ESI, m/z): Calculated for $C_{19}H_{22}{}^{79}BrO_7$ $[M + H]^+$ 441.0543; found 441.0546 (0.6 ppm), Calculated for $C_{19}H_{22}{}^{81}BrO_7$ $[M + H]^+$ 443.0523; found 443.0521 (0.4 ppm).

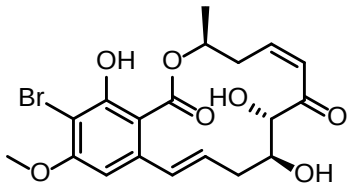

Figure 2.13 ^{1}H and ^{13}C NMR spectra of compound **2.12** [500 MHz for ^{1}H and 100 MHz for ^{13}C, Chloroform-d_3].

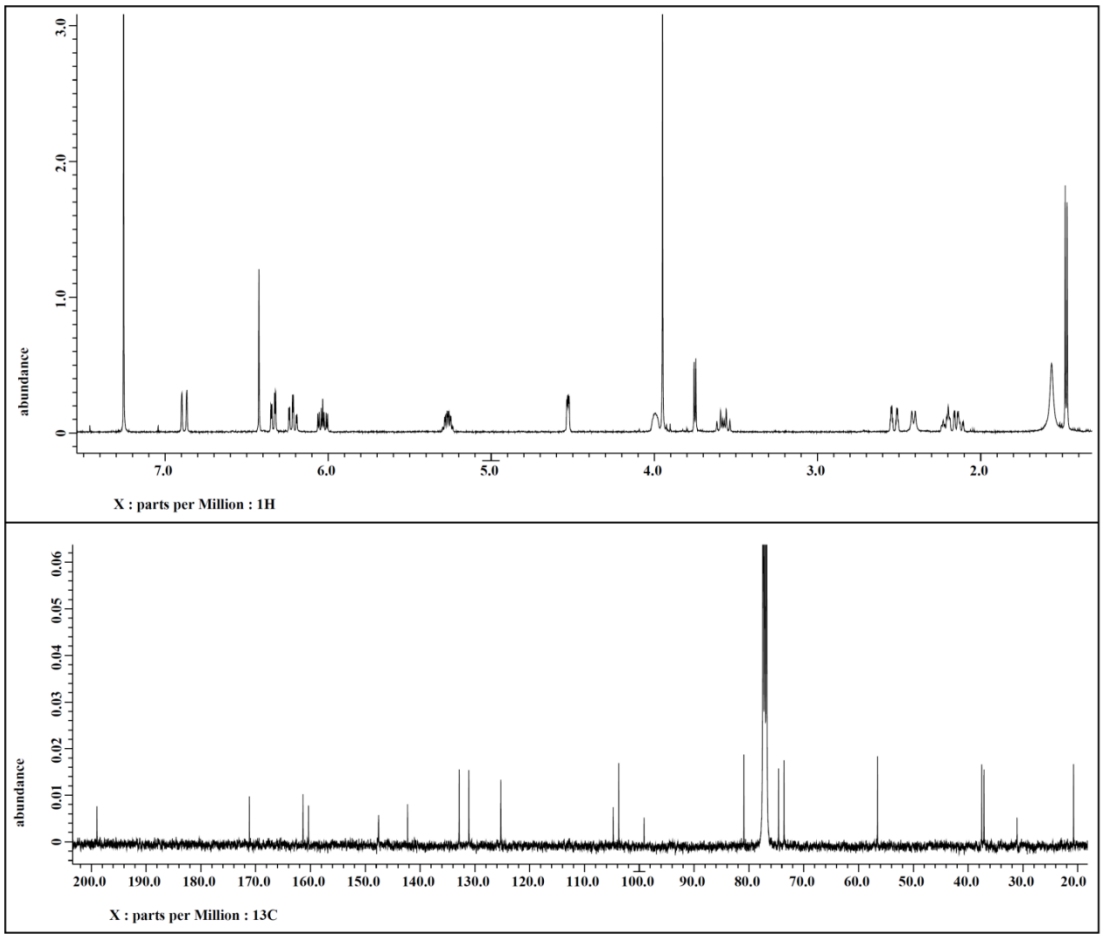

Figure 2.14 Major COSY (━) and HMBC (blue arrows) correlations of compound **2.12.**

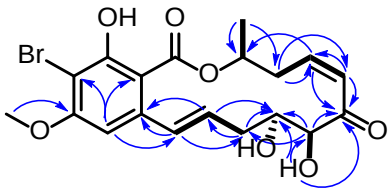

(3*S*,5*Z*,8*S*,9S,11*E*)-13-Bromo-8,9,16-trihydroxy-14-methoxy-3-methyl-3,4,9,10-tetrahydro-1*H*-benzo[*c*][1]oxacyclotetradecine-1,7(8*H*)-dione[25] **(2.13)**. Same as procedure described for synthesis of compound **2.12**. The compound eluted at 14.5 min. UPLC was used to evaluate the purity using a gradient solvent system that initiated with 20:80 $CH_3CN{-}H_2O$ to 100% CH_3CN over 4.5 min; it was >97% pure (Figure 2.4). Yield (6.36 mg, 52%).

^{1}H NMR (500 MHz, Chloroform-d_3): δ 12.12 (s, 1H; 17-OH), 6.43 (s, 1H; 16-H), 6.39 (dd, *J* = 2.0, 15.3 Hz, 1H; 12-H), 6.31 (dd, *J* = 2.9, 11.5 Hz, 1H; 6-H), 6.18 (ddd, *J* = 2.9, 10.9, 11.5 Hz, 1H; 5-H), 5.72 (ddd, *J* = 3.2, 10.3, 16.0 Hz, 1H; 11-H), 5.40 (dq, *Jd* = 8.5, *Jq* = 6.1 Hz, 1H; 3-H), 4.55 (bs, 1H; 8-H), 3.95 (bs, 1H; 9-H), 3.89 (s, 3H; 20-H), 3.74 (d, *J* = 4.0 Hz, 1H; 8-OH), 3.35 (ddd, *J* = 5.4, 10.9 Hz, 1H; 4-H), 2.51 (dd, *J* = 2.3, 17.2 Hz, 1H; 4-H), 2.33 (dd, *J* = 2.3, 16.6 Hz, 1H; 10-H), 2.10 (ddd, *J* = 2.9, 10.3, 16.6 Hz, 1H; 10-H), 1.46 (d, *J* = 6.1 Hz, 3H; 19-H).

^{13}C NMR (125 MHz, Chloroform-d_3): δ 199.4, 170.9, 164.4, 161.1, 146.6, 142.2, 133.9, 129.6, 125.6, 105.8, 105.4, 99.5, 81.0, 73.8, 73.1, 56.7, 37.0, 36.8, 21.0.

HRMS (ESI, m/z): Calculated for $C_{19}H_{22}{}^{79}BrO_7$ $[M + H]^+$ 441.0543; found 441.0546 (0.6 ppm), Calculated for $C_{19}H_{22}{}^{81}BrO_7$ $[M + H]^+$ 443.0523; found 443.0522 (0.2 ppm).

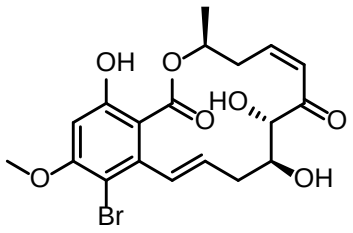

Figure 2.13 ^{1}H and ^{13}C NMR spectra of compound **2.13** [500 MHz for ^{1}H and 125 MHz for ^{13}C, Chloroform-d_3].

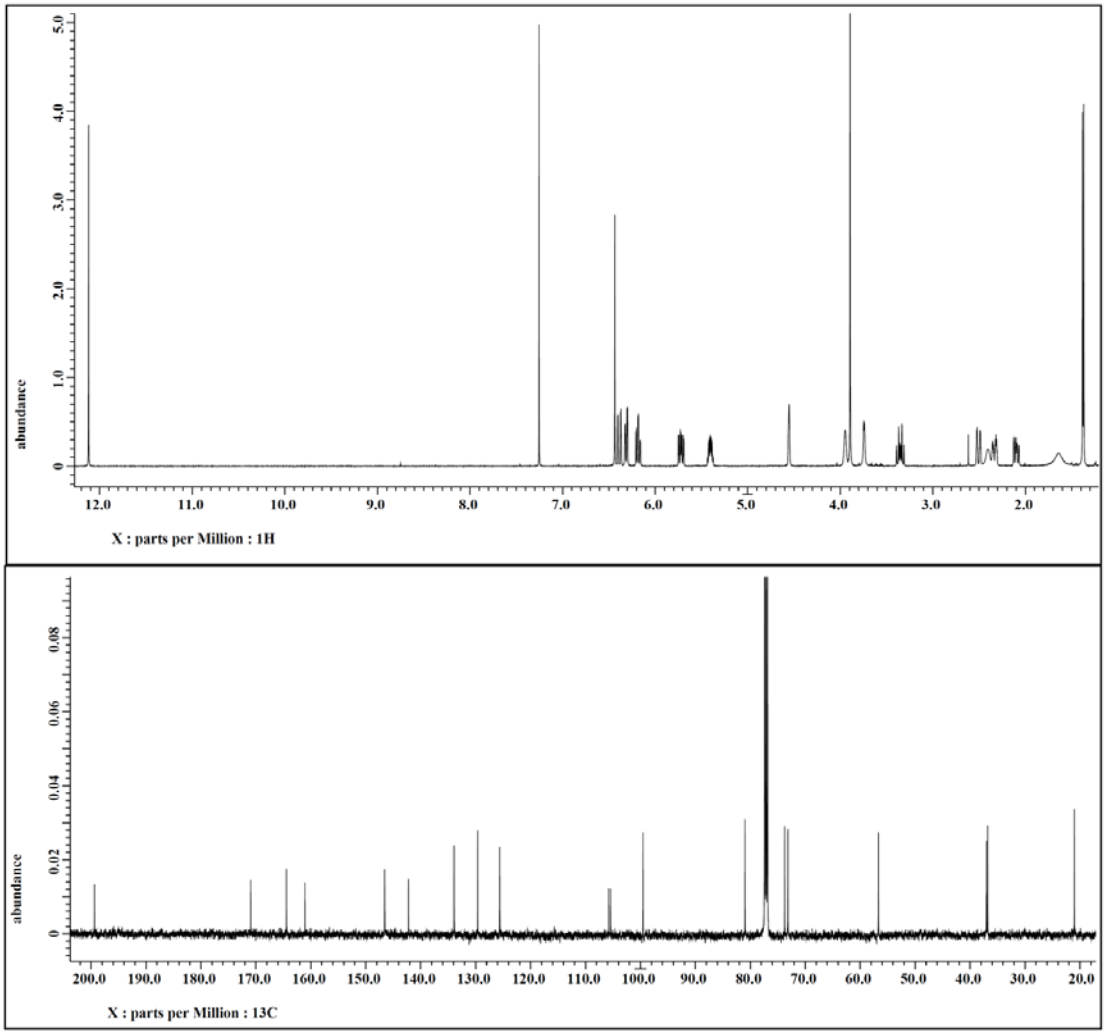

Figure 2.14 Major COSY (—) and HMBC (blue arrows) correlations of compound **2.13**.

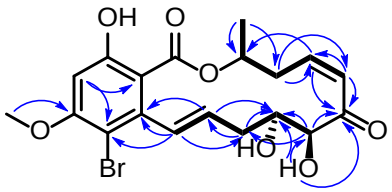

(3*S*,5*Z*,8*S*,9*S*,11*E*)-13,15-Dibromo-8,9,16-trihydroxy-14methoxy-3-methyl-3,4,9,10-tetrahydro-1*H*-benzo[*c*][1]oxacyclotetradecine-1,7(8*H*)-dione (2.14).[25] Same as procedure described for synthesis of compound **2.12**. The compound eluted at 21 min. UPLC was used to evaluate the purity using a gradient solvent system that initiated with 20:80 $CH_3CN{-}H_2O$ to 100% CH_3CN over 4.5 min; it was >97% pure (Figure 2.4). Yield (1.42 mg, 10%).

^{1}H NMR (500 MHz, Chloroform-d_3): δ 12.46 (s, 1H; 17-OH), 6.37 (d, J = 16.0 Hz, 1H; 12-H), 6.32 (dd, J = 2.9, 11.5 Hz, 1H; 6-H), 6.20 (ddd, J = 2.9, 10.9, 11.5 Hz, 1H; 5-H), 5.72 (ddd, J = 3.4, 10.3, 16.0 Hz, 1H; 11-H), 5.47 (dq, J_d = 6.3, J_d = 11.5 Hz, 1H; 3-H), 4.55 (dd, J = 2.3, 5.2, 1H; 8-H), 4.55 (dd, J = 2.3, 5.2 Hz, 1H; 8-H), 3.95 (bs, 1H; 9-H), 3.90 (s, 3H; 20-H), 3.72 (d, J = 5.2 Hz, 1H; 8-OH), 3.40 (ddd, J = 10.9, 11.2, 11.5 Hz, 1H; 4-H), 2.53 (ddd, J = 2.3, 2.9, 17.5, Hz, 1H; 4-H), 2.33 (m, H; 10-H), 2.13 (ddd, J = 2.3, 10.3, 16.6, Hz, 1H; 10-H), 1.39 (d, J = 6.3 Hz, 3H; 19-H).

^{13}C NMR (100 MHz, Chloroform-d_3): δ 199.2, 170.5, 160.0, 159.6, 146.4, 141.3, 134.6, 129.1, 125.1, 104.7, 103.6, 99.0, 80.9, 74.8, 73.0, 60.6, 37.0, 36.8, 21.

HRMS (ESI, m/z): Calculated for $C_{19}H_{21}{}^{79}Br_2O_7$ $[M + H]^+$ 518.9648; found 518.9633 (3.0 ppm), Calculated for $C_{19}H_{21}{}^{79}Br\,{}^{81}BrO_7$ $[M + H]^+$ 520.9628; found 520.9613 (2.9 ppm), Calculated for $C_{19}H_{21}{}^{81}Br_2O_7$ $[M + H]^+$ 522.9608; found 522.9593 (2.8 ppm).

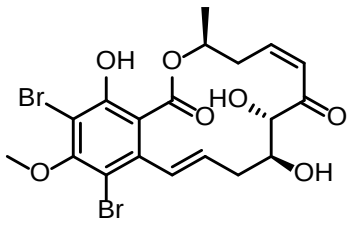

Figure 2.15 ^{1}H and ^{13}C NMR spectra of compound **2.14** [500 MHz for ^{1}H and 100 MHz for ^{13}C, Chloroform-d_3].

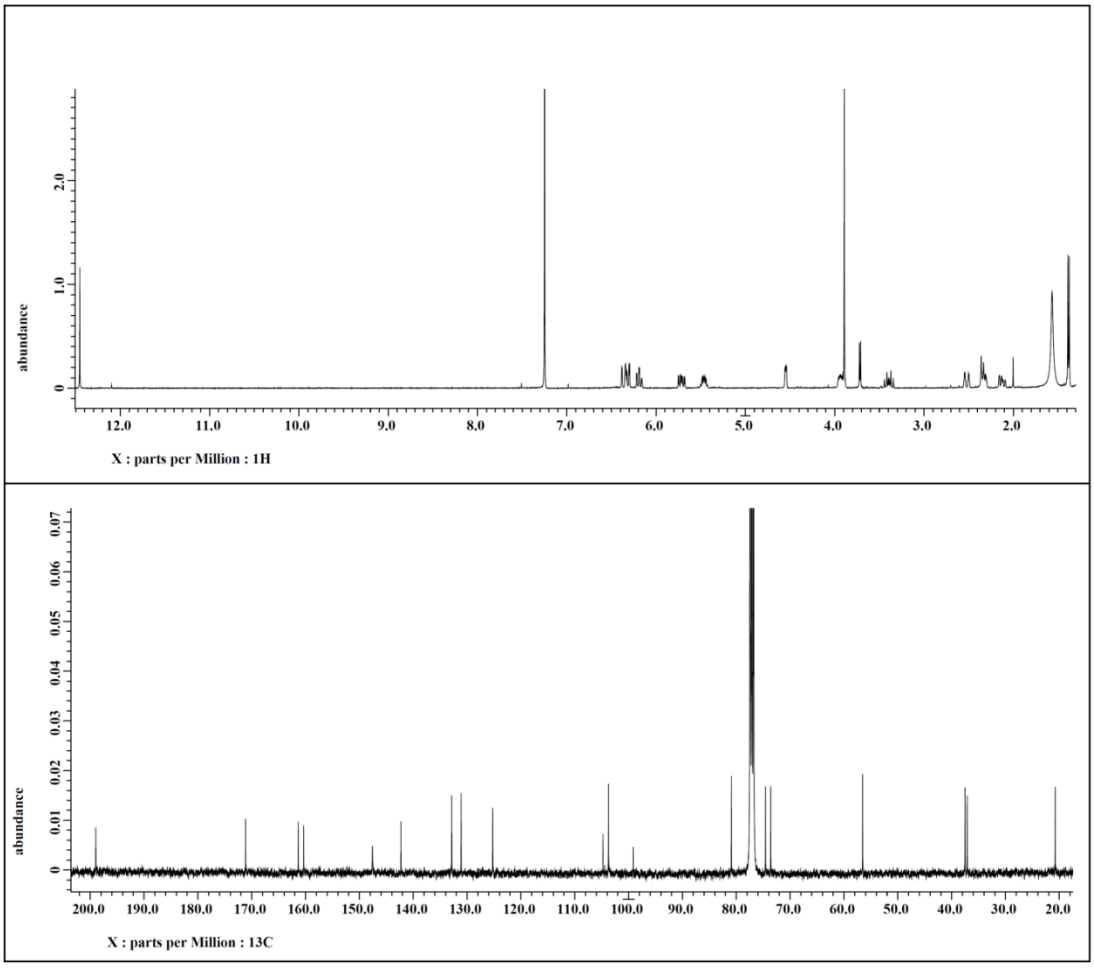

Figure 2.16 Major COSY (━) and HMBC (blue arrows) correlations of compound **2.14**.

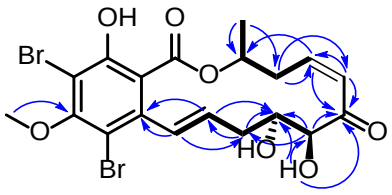

(12S,13S,8S,E)-13,53-Dihydroxy-55-methoxy-8-methyl13,14,15,16-tetrahydro-12H-7-oxa-1(2,6)-pyrana-5(1,2) benzenacyclononaphan-3-ene-14,6-dione (2.15).[27] *p*-Toluenesulfonic acid (7.9 mg, 0.041 mmol) were added to a solution of (5Z)-7-oxozeaenol (**2.1**) (15.0 mg, 0.041 mmol) in CH_2Cl_2 (2 mL) and the mixture stirred overnight. It was extracted with 10% $NaHCO_3$ (2mL), the organic layer dried and the solvent evaporated. The residue was purified by preparative HPLC using a Phenomenex Gemini-NX column C18 (250 x 21.20 mm, 110 A, 5 μm spherical particle size). The column was perfused at a flow rate of 21.24 mL/min with (water, 0.1% TFA), and a linear gradient from 40% to 50% of CH_3CN over 30 min. The compound eluted at 28.5 min. UPLC was used to evaluate the purity using a gradient solvent system that initiated with 20:80 $CH_3CN{-}H_2O$ to 100% CH_3CN over 4.5 min; it was >97% pure (Figure 2.4). Yield (5.2 mg, 35%).

^{1}H NMR (400 MHz, Chloroform-d_3): δ 11.19 (s, 1H; 17-OH), 7.13 (d, J = 16.0 Hz, 1H; 12-H), 6.36 (d, J = 2.8 Hz, 1H; 16-H), 6.33 (d, 2.8 Hz, 1H; 14-H), 5.83 (ddd, J = 6.4, 6.9, 16.0 Hz, 1H; 11-H), 5.16 (dq, J = 3.2, 6.4 Hz, 1H; 3-H), 4.64 (m, 1H; 5-H), 4.11 (dd, J = 4.1, 9.6 Hz, 1H; 8-H), 3.85 (ddd, J = 2.8, 8.2, 10.1 Hz, 1H; 9-H), 3.80 (s, 3H; 20-H), 3.55 (d, J = 4.1 Hz, 1H; 8-OH), 2.89 (dd, J = 6.9, 15.1 Hz, 1H; 6-H), 2.72 (dd, J = 7.0, 14.5 Hz, 1H; 10-H), 2.48 (dd, J = 3.7, 15.1 Hz, 1H; 6-OH), 2.41 (m, 1H; 10-H), 2.21 (ddd, J = 4.1, 6.6, 8.2 Hz, 1H; 4-H), 1.56 (m, 1H; 4-H), 1.41 (d, J = 6.0 Hz, 1H;19-H).

^{13}C NMR (100 MHz, Chloroform-d_3): δ 207.6, 171.2, 164.3, 164.1, 143.7, 135.7, 125.7, 107.5, 105.1, 99.8, 77.7, 76.2, 73.6, 72.4, 55.5, 46.2, 37.2, 33.3, 21.7.

HRMS (ESI, m/z): Calculated for $C_{19}H_{23}O_7$ $[M + H]^+$ 363.1438; found 363.1433 (1.5 ppm).

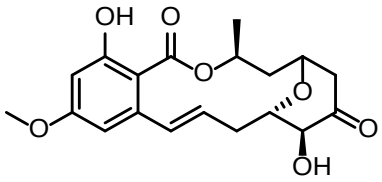

Figure 2.17 ^1H and ^{13}C NMR spectra of compound **2.15** [400 MHz for ^1H and 100 MHz for ^{13}C, Chloroform-d_3].

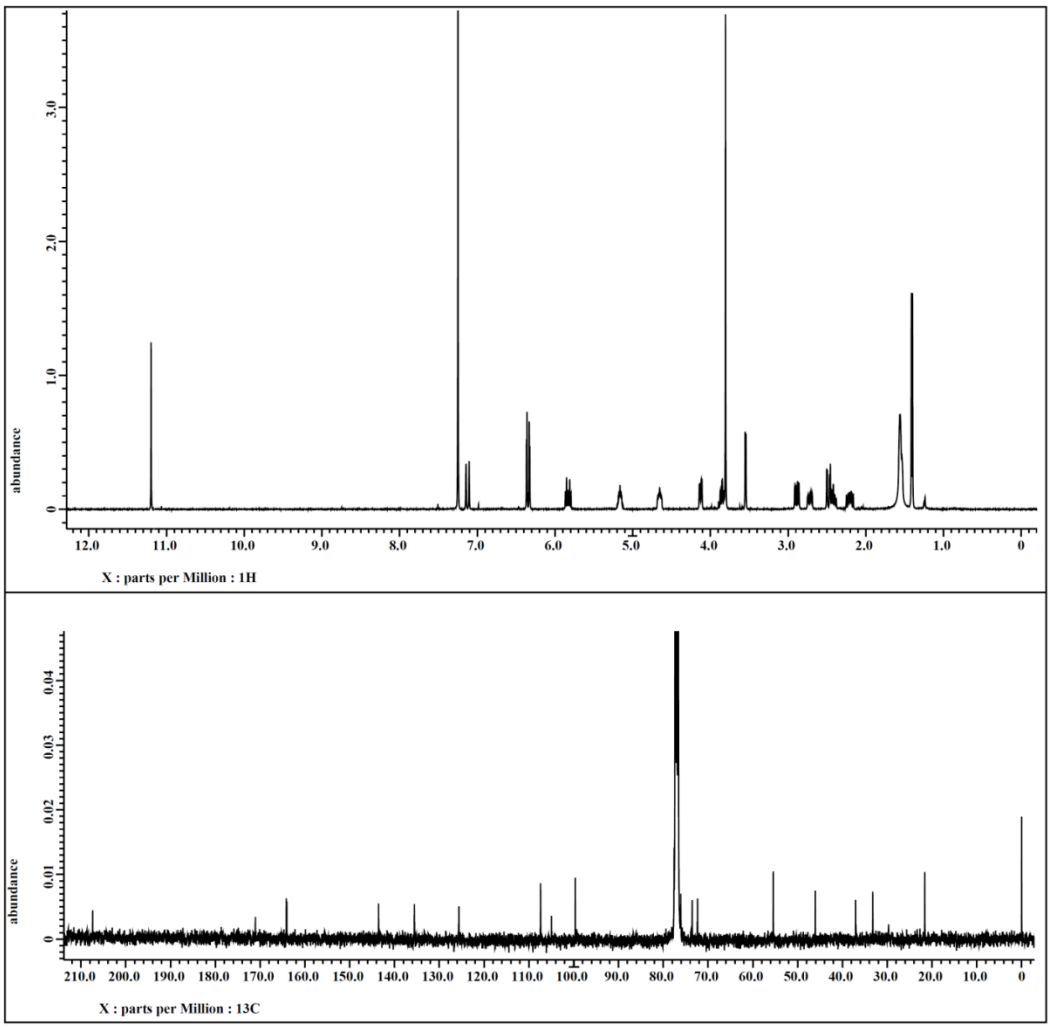

Figure 2.18 Major COSY (—) and HMBC (blue arrows) correlations of compound **2.15.**

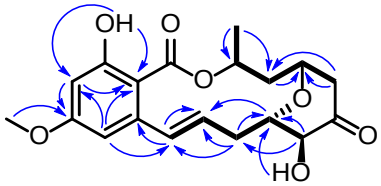

(3a*S*,5*Z*,8*S*,15*E*,17a*S*)-11-Hydroxy-13-methoxy-2,2,8-trimethyl-7,8,17,17a-tetrahydro-4*H*-benzo[*c*][1,3]dioxolo[4,5-*h*][1]oxacyclotetradecine-4,10(3a*H*)-dione (**2.16**).[9] *p*-Toluenesulfonic acid (2 mg, 0.0116 mmol, 9 mol %) was added to a suspension of (5*Z*)-7-oxozeaenol (**2.1**) (50.0 mg, 0.138 mmol) in dimethoxypropane (3 mL) and the mixture stirred for an hour. Dimethoxypropane was evaporated and the residue dissolved in $CHCl_3$ (20 mL) and extracted with 10% aqueous $NaHCO_3$ (10 mL). The organic layer was dried over anhydrous magnesium sulfate and the solvent evaporated. The residue was purified by preparative HPLC using a Phenomenex Gemini-NX C18 column (250 x 21.20 mm, 110 A, 5 μm spherical particle size). The column was perfused at a flow rate of 21.24 mL/min with (water, 0.1% TFA), and a linear gradient from 60% to 70% of (CH_3CN) over 15 min. The compound eluted at 16.5 min. UPLC was used to establish purity using a gradient solvent system that initiated with 20:80 CH_3CN/H_2O to 100% CH_3CN over 4.5 min; it was >97% pure (Figure 2.3). Yield (23.6 mg, 43%).

^{1}H NMR (500 MHz, Chloroform-d_3): δ 12.07 (s, 1H; 17-OH), 6.93 (d, J = 15.1 Hz, 1H; 12-H), 6.36 (s, 2H; 14-H and 16-H), 5.69 (m, 1H; 11-H), 5.37 (bs, 1H; 3-H), 4.58 (m, 1H; 8-H), 4.55 (m, 1H; 9-H), 3.79 (s, 3H; 20-H), 2.63 (m, 2H; 3-H), 1.57 (s, 3H; 21-H), 1.47 (d, J = 6.4 Hz, 3H; 19-H). 1.38 (s, 3H; 22-H).

^{13}C NMR (100 MHz, Chloroform-d_3): δ 196.5 (m, 7-C=O), 171.1, 165.6, 163.9, 146.3 (m; 5-C), 142.6, 133.6, 127.1 (m; 6-C), 126.6, 110.0, 108.9, 103.6, 100.1, 81.7 (m; 8-C), 77.2, 72.9 (m; 3-C), 55.4, 35.8, 27.0, 25.2 (m; $(CH_3)_2$), 19.9 (m; 19-C).

HRMS (ESI, m/z): Calculated for $C_{22}H_{27}O_7$ $[M + H]^+$ 403.1751; found 403.1749 (0.6 ppm).

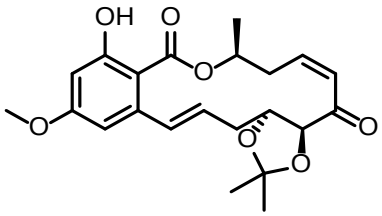

Figure 2.19 ^1H and ^{13}C NMR spectra of compound **2.16** [500 MHz for ^1H and 100 MHz for ^{13}C, Chloroform-d_3].

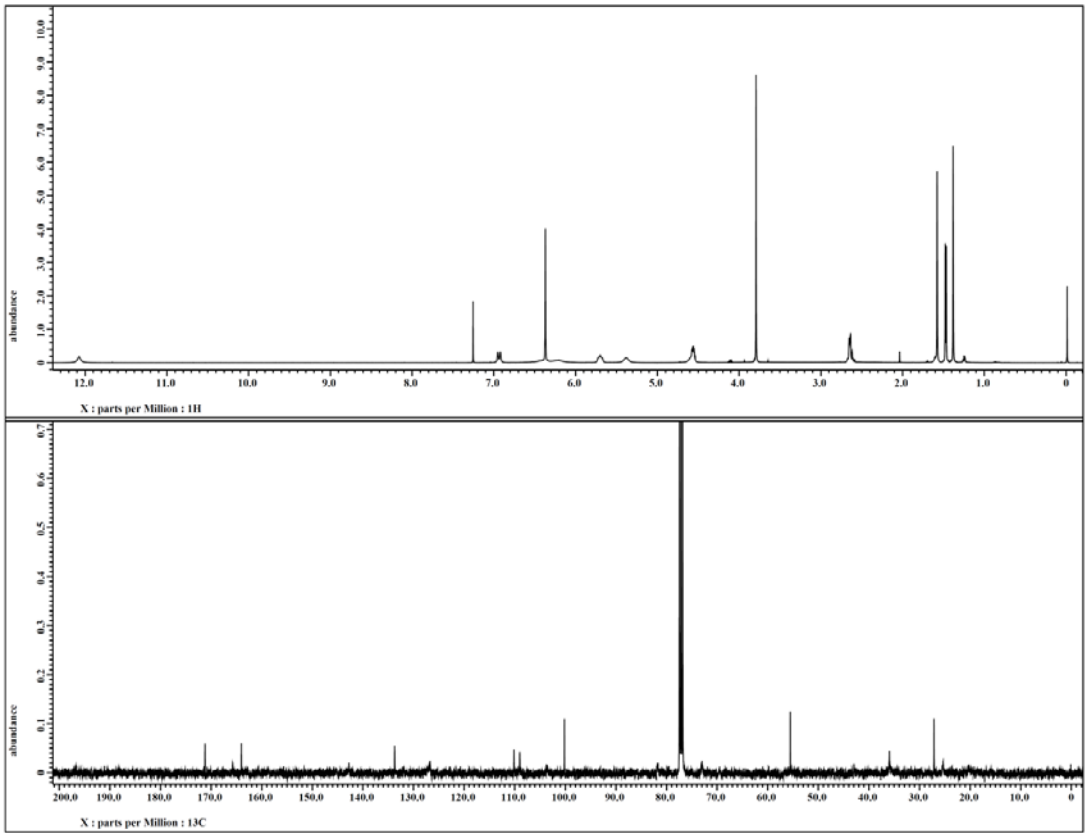

Figure 2.20 Major COSY (▬) correlations for compound **2.16**.

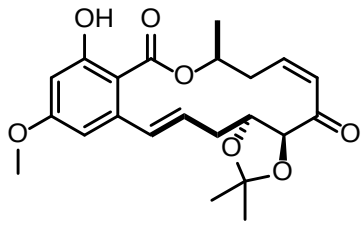

2.3.3 Computational calculations and covalent docking

2.3.3.1 Ligand preparation

All calculations were carried out using SPARTAN'08 for Linux. Initial conformational analyses were carried out on each ligand using a Monte-Carlo molecular mechanics conformational search using the RM1/semi-empirical force field at the ground state. All resulting conformations with E_{rel} less than 20 kcal/mol, relative to the lowest-energy conformation, were then modeled using Hartree-Fock with the 6-31G* basis set in the gas phase. The resulting global minimum was exported to maestro as mol.2 file and subjected to covalent docking.

2.3.3.2 Covalent Docking

Prior to covalent docking, the crystal structure (PDB ID: 4GS6) was prepared using protein preparation wizard, implemented in Maestro, where only hydrogens were added to all atoms and bond orders were assigned. The covalent linkage between the cocrystallized (5*Z*)-7-oxozeaenol TAK-1 enzyme was broken, the ligand deleted and the bare enzyme used as the binding protein for docking. Covalent docking, implemented in Glide, was used to evaluate the relative binding affinities of the various ligands tested. The reaction type chosen was Michael addition where amino acid Cycteine 174 was

identified as the reactive reside. The grid box was determined as the centroid of residues cysteine 174, valine 42 and alanine 46. Cysteine 174 was not chosen as the sole determinant of the grid box because it is impeded at the back of the binding pocket thus will not result in spanning the biding site efficiently. Many residue combinations were screened and the aforementioned collection was representative of a box holding all atoms of the co-crystalized (5*Z*)-7-oxozeaenol in the original crystal structure.

2.3.3.3 Prime minimization

The initial covalent docking output with the highest score for each docked ligand was minimized using prime, implemented in Maestro. All atoms including those of the enzyme and the ligand were minimized using VSGB solvation model. The number of iterations implemented for the automatic method of minimization was 8 and the steps per iteration were 200. The covalent linkage between the docked ligand and the enzyme, in the prime minimization output, was broken and the minimized ligand was covalently docked in the minimized enzyme.

2.3.3.4 TaK1-TaB1 (Transforming Growth Factor-β Activated Linase-1/TAK-1 Binding Protein 1) Inhibitor Assays

The assay was performed using Kinase–Glo Plus luminescence kinase assay kit (Promega). It measures kinase activity by quantitating the amount of ATP remaining in solution following a kinase reaction. The luminescent signal from the assay is correlated with the amount of ATP present and is inversely correlated with the amount of kinase activity. Compounds (1–14) were diluted in 10% DMSO and 5 µL of the dilution was added to a 50 µL reaction so that the final concentration of DMSO is 1% in all of

reactions. The compounds were preincubated with the enzyme in a reaction mixture for 10 min at room temperature. The enzymatic reactions were initiated by adding ATP (20 μM at final) and conducted for 40 min at 30 °C. The 50 μL reaction mixture contained 40 mM Tris, pH 7.4, 10 mM MgCl2, 0.1 mg/mL BSA, 1 mM DTT, 0.2 mg/mL MBP substrate, 20 μM ATP and Tak1–TAB1. After the enzymatic reaction, 50 μL of Kinase–Glo Plus Luminescence kinase assay solution (Promega) was added to each reaction, and the plate was incubated for 20 min at room temperature. Luminescence signal was measured using a BioTek Synergy 2 microplate reader. Tak1–TAB1 activity assays were performed in duplicate at each concentration. The luminescence data were analyzed using the computer software, Graphpad Prism. The difference between luminescence intensities in the absence of Tak1–TAB1 (Lut) and in the presence of Tak1–TAB1 (Luc) was defined as 100% activity (Lut – Luc). Using luminescence signal (Lu) in the presence of the compound, % activity was calculated as: % activity = [(Lut – Lu)/(Lut – Luc)]×100%, where Lu= the luminescence intensity in the presence of the compound. The values of % activity versus a series of compound concentrations were then plotted using non–linear regression analysis of Sigmoidal dose–response curve generated with the equation Y=B+(T–B)/1+10((LogEC50–X)×Hill Slope), where Y = percent activity, B = minimum percent activity, T = maximum percent activity, X = logarithm of compound and Hill Slope = slope factor or Hill coefficient. The IC50 values were determined by the concentration causing a half–maximal percent activity. 5Z–7–oxozeaenol was used as a positive control and showed an IC50 value of 21 nM.

2.4 Conclusion

The importance of TAK-1as a potential target for treating cancer yet the lack of clinical candidacy of its most active inhibitor (5*Z*)-7-Oxozeaenol **2.1** stimulated its derivatization via semisynthesis. Seven Analogues were prepared and tested for their TAK-1 inhibitory activity along with other structurally-related isolated secondary metabolites. The reported activities reconfirmed the necessity of having the Michael acceptor and defined part of the scope of allowed structural changes. The implemented covalent docking-prime minimization method of the enone-bearing analogues, in hand, showed an acceptable level of accuracy in terms of predicting activity.

2.5 References

1 Yamaguchi, K.; Shirakabe, K.; Shibuya, H.; Irie, K.; Oishi, I.; Ueno, N.; Taniguchi, T.; Nishida, E.; Matsumoto, K., Identification of a member of the MAPKKK family as a potential mediator of TGF-beta signal transduction. *Science* **1995,** *270* (5244), 2008-2011.

2 Schuman, J.; Chen, Y.; Podd, A.; Yu, M.; Liu, H.-H.; Wen, R.; Chen, Z. J.; Wang, D., A critical role of TAK1 in B-cell receptor–mediated nuclear factor κB activation. *Blood* **2009,** *113* (19), 4566-4574.

3 Ninomiya-Tsuji, J.; Kishimoto, K.; Hiyama, A.; Inoue, J.; Cao, Z.; Matsumoto, K., The kinase TAK1 can activate the NIK-I kappaB as well as the MAP kinase cascade in the IL-1 signalling pathway. *Nature* **1999,** *398* (6724), 252-256.

4 Johnson, G. L.; Dohlman, H. G.; Graves, L. M., MAPK kinase kinases (MKKKs) as a target class for small-molecule inhibition to modulate signaling networks and gene expression. *Current Opinion in Chemical Biology* **2005,** *9* (3), 325-331.

5 Singh, A.; Sweeney, M. F.; Yu, M.; Burger, A.; Greninger, P.; Benes, C.; Haber, D. A.; Settleman, J., TAK1 inhibition promotes apoptosis in KRAS-dependent colon cancers. *Cell* **2012,** *148* (4), 639-650.

6 Meng, F.; Li, Y.; Tian, X.; Fu, L.; Yin, Y.; Sui, C.; Ma, P.; Jiang, Y., Identification of TGF-beta-activated kinase 1 as a possible novel target for renal cell carcinoma intervention. *Biochemical and Biophysical Research Communications* **2014,** *453* (1), 106-111.

7 Wang, Y.; Tu, Q.; Yan, W.; Xiao, D.; Zeng, Z.; Ouyang, Y.; Huang, L.; Cai, J.; Zeng, X.; Chen, Y. J.; Liu, A., CXC195 suppresses proliferation and inflammatory response in LPS-induced human hepatocellular carcinoma cells via regulating TLR4-MyD88-TAK1-mediated NF-kappaB and MAPK pathway. *Biochemical and Biophysical Research Communication* **2014,** *456* (1), 373–379.

8 Melisi, D.; Xia, Q.; Paradiso, G.; Ling, J.; Moccia, T.; Carbone, C.; Budillon, A.; Abbruzzese, J. L.; Chiao, P. J., Modulation of pancreatic cancer chemoresistance by inhibition of TAK1. *J Natl Cancer Inst* **2011,** *103* (15), 1190-1204.

9 Ellestad, G. A.; Lovell, F. M.; Perkinson, N. A.; Hargreaves, R. T.; McGahren, W. J., New zearalenone related macrolides and isocoumarins from an unidentified fungus. *The Journal of Organic Chemistry* **1978,** *43* (12), 2339-2343.

10 Ninomiya-Tsuji, J.; Kajino, T.; Ono, K.; Ohtomo, T.; Matsumoto, M.; Shiina, M.; Mihara, M.; Tsuchiya, M.; Matsumoto, K., A resorcylic acid lactone, 5Z-7-oxozeaenol, prevents inflammation by inhibiting the catalytic activity of TAK1 MAPK kinase kinase. *The Journal of Biological Chemistry* **2003,** *278* (20), 18485-18490.

11 Zhang, J.; Yang, P. L.; Gray, N. S., Targeting cancer with small molecule kinase inhibitors. *Nature Reviews. Cancer* **2009,** *9* (1), 28-39.

12 Wu, J.; Powell, F.; Larsen, N. A.; Lai, Z.; Byth, K. F.; Read, J.; Gu, R. F.; Roth, M.; Toader, D.; Saeh, J. C.; Chen, H., Mechanism and in vitro pharmacology of TAK1 inhibition by (5Z)-7-Oxozeaenol. *ACS Chemical Biology* **2013,** *8* (3), 643-650.

13 Singh, J.; Petter, R. C.; Baillie, T. A.; Whitty, A., The resurgence of covalent drugs. *Nature Reviews. Drug Discovery* **2011,** *10* (4), 307-317.

14 Kilty, I.; Green, M. P.; Bell, A. S.; Brown, D. G.; Dodd, P. G.; Hewson, C.; Hughes, S. J.; Phillips, C.; Ryckmans, T.; Smith, R. T.; van Hoorn, W. P.; Cohen, P.; Jones, L. H., TAK1 inhibition in the DFG-out conformation. *Chemical Biology & Drug Design* **2013,** *82* (5), 500-505.

15 Ayers, S.; Graf, T. N.; Adcock, A. F.; Kroll, D. J.; Matthew, S.; Carcache de Blanco, E. J.; Shen, Q.; Swanson, S. M.; Wani, M. C.; Pearce, C. J.; Oberlies, N. H., Resorcylic Acid Lactones with Cytotoxic and NF-κB Inhibitory Activities and Their Structure–Activity Relationships. *Journal of Natural Products* **2011,** *74* (5), 1126-1131.

16 El-Elimat, T.; Raja, H. A.; Day, C. S.; Chen, W. L.; Swanson, S. M.; Oberlies, N. H., Greensporones: resorcylic acid lactones from an aquatic Halenospora sp. *Journal of Natural Products* **2014,** *77* (9), 2088-2098.

17 Goto, M.; Chow, J.; Muramoto, K.; Chiba, K.; Yamamoto, S.; Fujita, M.; Obaishi, H.; Tai, K.; Mizui, Y.; Tanaka, I.; Young, D.; Yang, H.; Wang, Y. J.; Shirota, H.; Gusovsky, F., E6201 [(3S,4R,5Z,8S,9S,11E)-14-(ethylamino)-8, 9,16-trihydroxy-3,4-dimethyl-3,4,9,19-tetrahydro-1H-2-benzoxacyclotetradecine-1,7 (8H)-dione], a novel kinase inhibitor of mitogen-activated protein kinase/extracellular signal-regulated kinase kinase (MEK)-1 and MEK kinase-1: in vitro characterization of its anti-inflammatory and antihyperproliferative activities. *The Journal of pharmacology and experimental therapeutics* **2009,** *331* (2), 485-495.

18 Wu, H.; Thatcher, L. N.; Bernard, D.; Parrish, D. A.; Deschamps, J. R.; Rice, K. C.; MacKerell, A. D.; Coop, A., Position of Coordination of the Lithium Ion Determines the Regioselectivity of Demethylations of 3,4-Dimethoxymorphinans with L-Selectride. *Organic Letters* **2005,** *7* (13), 2531-2534.

19 Pinkerton, A., B.;; Vernier, J.-M.; Cube, R., V.; ; Hutchinson, J., H.; ; Huang, D.; Bonnefous, C.; Govak, S., P.; ; Kamenecka, T. Heterocyclic acetophenone potentiators of metabotropic glutamate receptors. WO2005US26425 20050726, 2006.

20 Dean, M. A.; Hitchcock, S. R., Synthesis and application of oxadiazines as chiral ligands for the enantioselective addition of diethylzinc to aldehydes. *Tetrahedron: Asymmetry* **2010,** *21* (20), 2471-2478.

21 Zea-Ponce, Y.; Mavel, S.; Assaad, T.; Kruse, S. E.; Parsons, S. M.; Emond, P.; Chalon, S.; Giboureau, N.; Kassiou, M.; Guilloteau, D., Synthesis and in vitro evaluation of new benzovesamicol analogues as potential imaging probes for the vesicular acetylcholine transporter. *Bioorganic & Medicinal Chemistry* **2005,** *13* (3), 745-753.

22 Wang, J.; Sánchez-Roselló, M.; Aceña, J. L.; del Pozo, C.; Sorochinsky, A. E.; Fustero, S.; Soloshonok, V. A.; Liu, H., Fluorine in Pharmaceutical Industry: Fluorine-Containing Drugs Introduced to the Market in the Last Decade (2001–2011). *Chemical Reviews* **2013,** *114* (4), 2432-2506.

23 Woodhead, A. J.; Angove, H.; Carr, M. G.; Chessari, G.; Congreve, M.; Coyle, J. E.; Cosme, J.; Graham, B.; Day, P. J.; Downham, R.; Fazal, L.; Feltell, R.; Figueroa, E.; Frederickson, M.; Lewis, J.; McMenamin, R.; Murray, C. W.; O'Brien, M. A.; Parra, L.; Patel, S.; Phillips, T.; Rees, D. C.; Rich, S.; Smith, D.-M.; Trewartha, G.; Vinkovic, M.; Williams, B.; Woolford, A. J. A., Discovery of (2,4-Dihydroxy-5-isopropylphenyl)-[5-(4-methylpiperazin-1-ylmethyl)-1,3-dihydroisoindol-2-yl]methanone (AT13387), a Novel Inhibitor of the Molecular Chaperone Hsp90 by Fragment Based Drug Design. *Journal of Medicinal Chemistry* **2010,** *53* (16), 5956-5969.

24 Langlois, B. R.; Laurent, E.; Roidot, N., Trifluoromethylation of aromatic compounds with sodium trifluoromethanesulfinate under oxidative conditions. *Tetrahedron Letters* **1991,** *32* (51), 7525-7528.

25 Dijkstra, P. J.; Den Hertog, H. J.; Van Steen, B. J.; Zijlstra, S.; Skowronska-Ptasinska, M.; Reinhoudt, D. N.; Van Eerden, J.; Harkema, S., Use of pyrylium synthons in the synthesis of hemispherands with modified cavities. X-ray structures of the 21-hemispherand and a pyrido hemispherand. *The Journal of Organic Chemistry* **1987,** *52* (12), 2433-2442.

26 Xu, J.; Chen, A.; Go, M.-L.; Nacro, K.; Liu, B.; Chai, C. L. L., Exploring Aigialomycin D and Its Analogues as Protein Kinase Inhibitors for Cancer Targets. *ACS Medicinal Chemistry Letters* **2011,** *2* (9), 662-666.

27 Schmidt, B.; Staude, L.; Kelling, A.; Schilde, U., A Cross-Metathesis–Conjugate Addition Route to Enantiopure γ-Butyrolactams and γ-Lactones from a C2-Symmetric Precursor. *European Journal of Organic Chemistry* **2011,** *2011* (9), 1721-1727.

28 Zhao, G.; Yang, C.; Li, B.; Xia, W., A new phenylethyl alkyl amide from the Ambrostoma quadriimpressum Motschulsky. *Beilstein Journal of Organic Chemistry* **2011,** *7*, 1342-1346.

29 Yadav, J. S.; Rao, K. V. R.; Ravindar, K.; Reddy, B. V. S., Total Synthesis of (+)-Bourgeanic Acid Utilizing Desymmetrization Strategy. *European Journal of Organic Chemistry* **2011,** *2011* (1), 58-61.

30 Švenda, J.; Myers, A. G., Anti-Selective Epoxidation of Methyl α-Methylene-β-tert-butyldimethylsilyloxycarboxylate Esters. Evidence for Stereospecific Oxygen Atom Transfer in a Nucleophilic Epoxidation Process. *Organic Letters* **2009,** *11* (11), 2437-2440.

31 Pratt, N. E.; Albizati, K. F., The effect of .beta.-dialkylamino substitution on ketone enolization. *The Journal of Organic Chemistry* **1990,** *55* (2), 770-773.

32 Krstić, N. M.; Bjelaković, M. S.; Dabović, M. M.; Pavlović, V. D., Thionation of Some α,β-Unsaturated Steroidal Ketones. *Molecules* **2010,** *15* (5), 3462-3477.

33 Armstrong, A.; Geldart, S. P.; Jenner, C. R.; Scutt, J. N., Organocatalytic Synthesis of β-Alkylaspartates via β-Lactone Ring Opening. *The Journal of Organic Chemistry* **2007,** *72* (21), 8091-8094.

34 Borzilleri, R. M.; Zheng, X.; Schmidt, R. J.; Johnson, J. A.; Kim, S.-H.; DiMarco, J. D.; Fairchild, C. R.; Gougoutas, J. Z.; Lee, F. Y. F.; Long, B. H.; Vite, G. D., A Novel Application of a Pd(0)-Catalyzed Nucleophilic Substitution Reaction to the Regio- and Stereoselective Synthesis of Lactam Analogues of the Epothilone Natural Products. *Journal of the American Chemical Society* **2000,** *122* (37), 8890-8897.